# *Temporal and spatial variability of phytoplankton fluxes in the Australian and New Zealand Sectors of the Southern Ocean*

Jessica Verity Wilks

(BSc majoring in plant biology, Hons (1st Class) in diatom sedimentology)
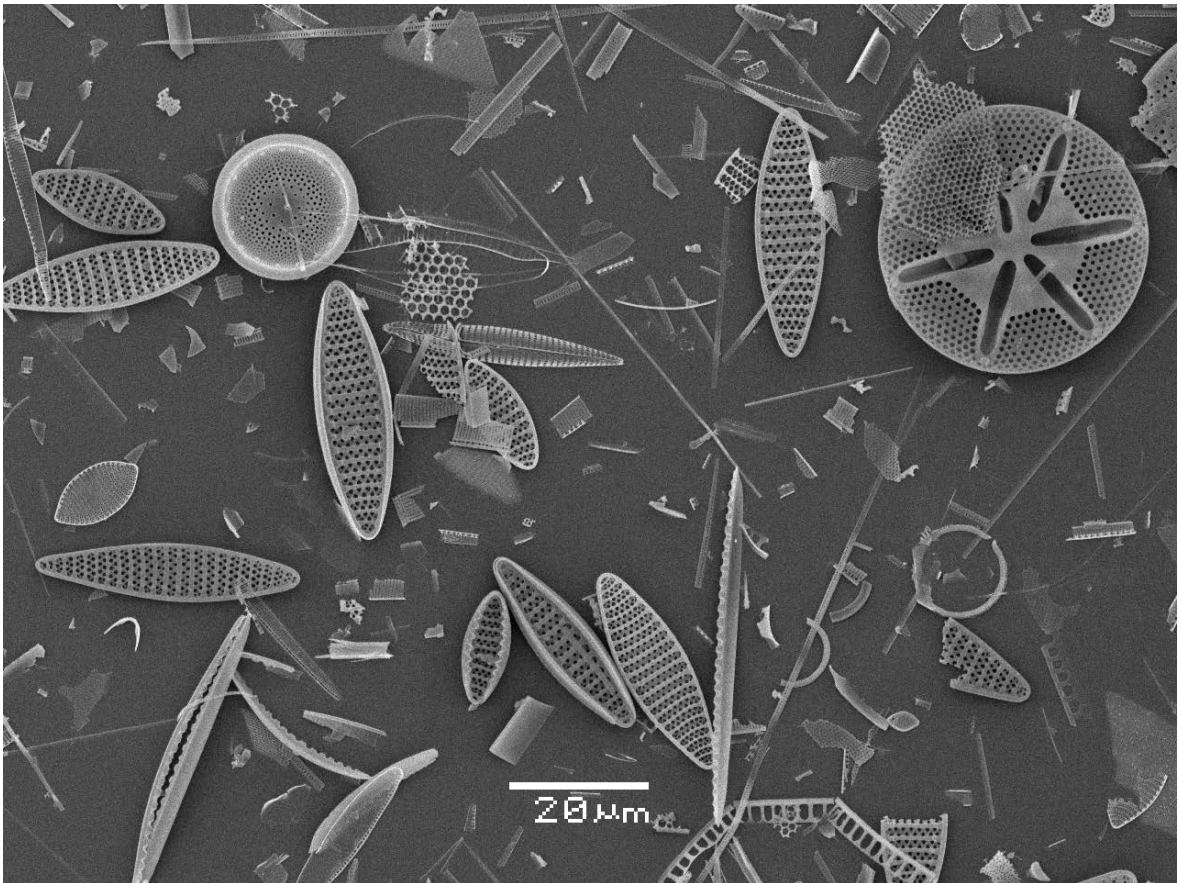
A thesis in fulfilment of the requirements for the degree of

Doctor of Philosophy

MACQUARIE
University

For Trev and Francis.
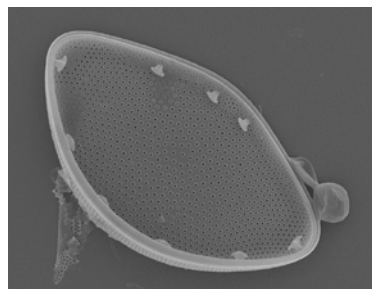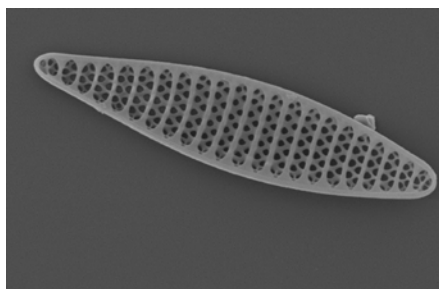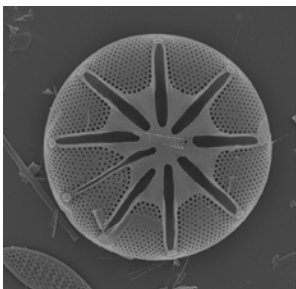
Table of contents

List of Figures

Appendix One

List of Tables

Thesis abstract

Phytoplankton are key to global carbon cycling, and critical to understanding a changing climate. Phytoplankton such as diatoms remove CO_2 from the atmosphere via photosynthesis, of which one fifth is exported to the deep ocean in a process termed the "Biological Pump". In opposition to the Biological Pump, the "Carbonate Counter-Pump" releases CO_2, driven by calcifying phytoplankton such as coccolithophores. Thus carbon export depends upon phytoplankton community composition, quantified with sediment traps, which preserve a time series of sinking particles. Sediment trap deployments are patchy in the Subantarctic and Subtropics and little work has been done quantifying the phytoplankton. This thesis quantified assemblages and flux of diatoms and coccolithophores from Australian and New Zealand deployments, were not previously well characterized, and discusses their role in export.

Subantarctic Australian traps captured among the highest coccolith fluxes of the southern hemisphere, while diatoms were the main silica-exporters. Species-level phytoplankton seasonal ecological succession was also reported for the first time in the Australian region. Scanning Electron Microscopy culminated in a taxonomic study describing the poorly-known diatom genus *Shionodiscus*, improving our understanding of key Australian taxa.

In Subantarctic New Zealand, a 48-day "pulse" bloom of *Pseudo-nitzschia* diatoms comprised 98% of annual diatom flux. New Zealand Subtropical traps exhibited strong coastal and benthic phytoplankton input, providing evidence for significant particle advection as a result of local oceanography, the Wairarapa Eddy system. Finally, diatom and coccolith fluxes from 46 sediment trap deployments were mapped from the Subtropics to Antarctica, revealing a broad trend of increasing diatom flux from 30° S to the coast of Antarctica, which will potentially inform future trapping efforts. Records of phytoplankton seasonality and abundance are key to understanding the physical and chemical drivers of regional differences in the Biological Pump, and how carbon cycling may experience regional change in the future, under future climate change. The work undertaken for this thesis provides a valuable record against which future studies may compare, and makes a compelling argument for the continuation of sediment trap studies.

Statement of Originality

This thesis is my own work, and has not previously been submitted for a degree or diploma in any university. The thesis contains no material previously published or written by another person except where due reference is made in the thesis itself. Where collaboration was undertaken on research or publications, this is indicated in the Statement of Co-authorship.

(Signed)_____   Date: _____
                                                  14/12/2018

Jessica V. Wilks

Statement of Co-authorship

The majority of the work in this thesis was carried out by myself, Jessica Verity Wilks. The contributions of co-authors in the multi-author chapters are outlined below.

Chapter Two

This chapter used sediment trap material provided by Prof. Thomas Trull and Mr. Steven Bray, who were responsible for the bulk compound analyses. All steps from sample cleaning and processing, slide-making, microscopy, identification of diatoms and calculation of diatom fluxes was undertaken by myself. Dr. Andrés Rigual-Hernández undertook the coccolith slide-making and counting, but conversion to fluxes and ecological interpretations were my own. Statistical analyses between biogeochemical fluxes, diatom and coccolith fluxes, and their interpretation and discussion were my work. Assc. Prof Leanne Armand provided literature on diatom taxonomy, as well as guidance on statistics. I undertook the writing, with the help of some editorial suggestions from the co-authors, and advice from Andrés and Prof. José-Abel Flores-Villarejo on coccolithophore ecology.

Chapter Three

This chapter used the sediment trap material collected by Dr. Scott Nodder. As above, sample processing, cleaning, microscopy, statistical analyses and flux calculations were my own. Dr. Andrés Rigual-Hernández undertook the coccolith slide-making and counting, but conversion to fluxes, statistical analyses, and interpretations were my own. 95% of the writing was done by me, with co-authors providing suggestions on re-emphasising key findings during the review process, and suggestions on figure presentation. The other co-authors provided feedback to guide this publication through the writing process.

Chapter Four

The collection of publications, extraction from data, plotting of data, statistical analyses and interpretation was my own work. Dr. Andrés Rigual-Hernández and Assc. Prof Leanne Armand gave guidance on the objective and direction of the paper, as well as input on data presentation and scope, and some editorial suggestions.

Chapter Five

This chapter used the same sediment trap material as Chapter Two. It was a joint publication between myself and Assc. Prof. Leanne Armand. All microscopy, analysis and microphotography was undertaken by me. Leanne provided invaluable taxonomic expertise, as well as taxonomic sources not part of the library collections. I wrote the manuscript, with editorial suggestions from Leanne.

Acknowledgments

This thesis could not have come to completion without the support of many colleagues, friends and family, and neither would my sanity, or last vestiges thereof, have remained.

Firstly to my family, particularly my mother Sarah Wilks, the first Dr. Wilks in the family, who has always encouraged me to pursue my calling in biology. Just having someone who I knew would understand the myriad emotions endured during this process was a deep comfort; the victories small and large, the frustrations and joys of research, all these could be shared with her. When I could not conceive of continuing, she gave me all I needed: a warm home and love.

To my supervisors; I began as a diatom enthusiast with little direction, and became a researcher with great confidence in my ability. Leanne Armand, my primary supervisor for the bulk of my candidature, you always had my future in mind, even when I did not. It is thanks to your drive to publish that I submit this thesis with two publications and one manuscript in press. You have always been exceptionally patient and practical through all weather, and shared with me your love of diatoms, and for this I give you my deepest thanks.

Andrés Rigual-Hernández, I could not ask for a supervisor more generous with their time. You have always done your very best to remain involved with this project, even on the other side of the world. This thesis could not have come together without your optimistic and unstinting support, and when I was in need of morale, you never let me down. Thank you.

Glenn Brock and Matt Kosnik, you became my supervisors during the most stressful year of any thesis, when what I needed was not direction so much as a positive outlook. You both generously offered me a can-do attitude, practical support and advice during my writing stage, for which I am immensely grateful.

To Scott Nodder, who allowed me to visit his lab twice over the course of my candidature, you were an excellent host and I have thoroughly enjoyed working with you. I extend additional thanks to the microscopy unit staff at Macquarie, particularly Nicole Vella and Sue Lindsay. I thank Macquarie University for funding this thesis via a MQRES scholarship, as well as award of Postgraduate Award Funding. Sincere thanks to three Examiners, Helen Bostock, Elisa Malinverno and Sophie Leterme, for their excellent and thorough comments, with which this thesis was greatly improved.

Finally, I wish to acknowledge the person who unknowingly set me on this course. Gustaaf Hallegraeff, my lecturer at the University of Tasmania, instilled in me a lifelong adoration of diatoms. It was in the space of one lecture that I decided I would go into diatom research. I will never forget how you said several times in that lecture with such vigor; "Diatoms are the grasses of the sea!"

Chapter One

General introduction
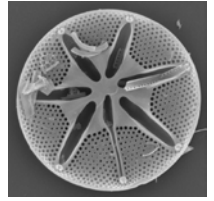
1. The oceanic carbon cycle

The ocean contains approximately 50 times more carbon than the atmosphere, and 20 times as much as the terrestrial biosphere (Sigman & Haug 2003). As carbon dioxide (CO_2) is released by heterotrophic respiration and anthropogenic processes (burning of fossil fuels), much of it dissolves into the ocean. Once dissolved, CO_2 reacts with water to form carbonic acid, and eventually bicarbonate, releasing hydrogen ions, and causing the water to become more acidic (Equation 1). During the two centuries since the Industrial Revolution, oceanic pH has fallen by 0.1 units, becoming ~30% more acidic (Ciais et al. 2013). Anthropogenic CO_2 production has increased in this time, and is accelerating (IPCC synthesis report 2014). Increasing atmospheric CO_2 uptake by the ocean, accompanying increases in acidification, and interplay with other climate-change related effects such as warming, is likely to affect the functioning of marine ecosystems in unexpected ways (Deppeler and Davidson 2017).

Equation 1. $CO_2 + H_2O \rightarrow 2HCO^{3-} + H^+$
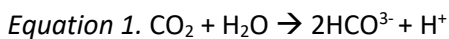
The Southern Ocean is the water mass encircling Antarctica from ~40° S, and is bounded on the north by the Subtropical Front, the meeting place of subtropical and subantarctic water masses (Arndt et al. 2013). Approximately 40% of anthropogenic CO_2 absorption occurs in the Southern Ocean from 30° S (Frölicher et al. 2015). Palaeontological data from ice cores indicate that past shifts in atmospheric CO_2 have been associated with changes in climate (Petit et al. 1999; Pearson and Palmer 2000). The Southern Ocean has apparently regulated these events in the past via CO_2 uptake or outgassing (Rosenthal et al. 2000; Gottschalk et al. 2016; Ronge et al. 2018), and continues to influence global climate and carbon cycling (Toggweiler et al. 2006).

1.1 Oceanic carbon cycling mechanisms

Carbon cycling within the ocean is driven by both biological and physical processes. The combined biological processes are referred to as the "Biological Pump" (Fig 1), and are related largely to the phytoplankton- a diverse, polyphyletic group of mainly single-celled photosynthesizing organisms, spanning four kingdoms and eight phyla. Phytoplankton take up CO_2 via photosynthesis, turning it into carbon biomass (primary production). Due to their vast numbers, phytoplankton are responsible for half of global carbon fixation (Falkowski and Knoll 2007). Most phytoplankton biomass produced in the ocean's photic zone is consumed by zooplankton or remineralised by microbes, becoming Dissolved Inorganic Carbon (DIC), which accumulates in the deep ocean reservoir (Gottschalk et al. 2016). In fact over 90% of global inorganic carbon is stored within the ocean (Sigman and Boyle 2000). A small fraction of biological carbon will escape these fates and

sink to the deep ocean layers in the form of Particulate Organic Carbon (POC) (Falkowski et al. 2003; Honjo et al. 2008).
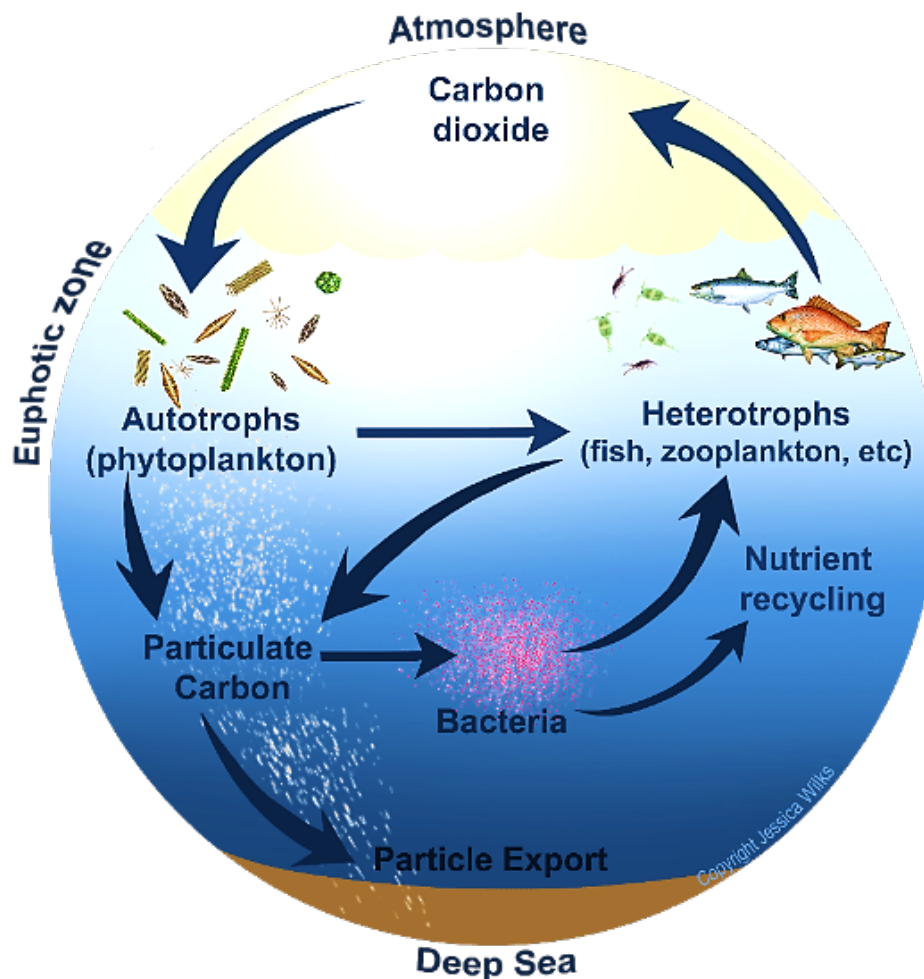
Figure 1. Schematic of the biological pump, showing the flow of carbon in the ocean from atmosphere to primary production, followed by heterotroph consumption and bacterial recycling (respiratory processes), and/or export to the deep sea (sequestration).

Individual phytoplankton cells sink slowly, increasing the likelihood that an individual cell will be remineralised in the water column (Alldredge & Gotschalk, 1989). Thus most POC export occurs in the form of aggregates, which fall more quickly, often over 100m d^{-1} or more (Smetacek, 1985; Alldredge & Gotschalk, 1989), and thus have a higher chance of reaching the depths undissolved and intact. Aggregates may be formed by the entanglement of cells during dense blooms, the adhesion of particles due to phytoplankton mucous production (de la Roche, 2003; Amin et al., 2012), or commonly in the form of zooplankton faecal pellets (De La Rocha and Passow 2007).

The physical processes of carbon cycling are referred to as the Solubility Pump, which describes the transport of CO_2 in dissolved form from the atmosphere to the ocean interior, and relies upon the physical properties of ocean water that affect solubility and diffusion, such as temperature

(Volk and Hoffert, 1985). Carbon exported to the deep ocean is considered isolated (sequestered) from the active carbon cycle, and may remain so for decades or millennia (Honjo et al. 2008). Eventually, carbon stored by the ocean is cycled back to surface waters via upwelling (Anderson et al. 2009), where it is either recycled in the euphotic zone, or "outgassed" as CO_2 into the atmosphere. The process of upwelling of CO_2-rich waters to the surface, followed by the outgassing as a result of thermohaline circulation (Ducklow et al. 2001) to the atmosphere falls under the combined physical processes of the Solubility Pump (Volk and Hoffert, 1985).

In opposition to the biological and solubility pumps, the carbonate counter pump increases dissolved CO_2 in surface waters via the formation of calcium carbonate by organisms such as coccolithophores and foraminifera (Equation 2; Smith and Key 1975; Frankignoulle et al. 1994). The counter pump results in the formation of Particulate Inorganic Carbon (PIC) in the form of calcium carbonate. The balance of the biological and carbonate counter pumps determines the net direction of carbon movement (Riebesell et al. 2009), quantified using the "Rain Ratio", or the ratio of POC:PIC.

Equation 2. $Ca^{2+} + 2HCO_3^{-} \leftrightarrow CaCO_3 + CO_2 + H_2O$
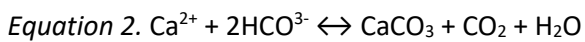
The strength of the biological and carbonate pumps is largely determined by variability in phytoplankton community structure (see section 2), while the solubility pump is affected by variability in physical properties of the ocean, so that while some regions of the ocean are considered carbon sinks, others are considered carbon sources (outgassing) (Balch 2018). Typically, regions of upwelling that bring deep waters to the surface are carbon sources, such as in the Antarctic Divergence Zone of the Antarctic Circumpolar Current (ACC) (Hayakawa et al. 2012).

The Southern Ocean has been alternately a carbon sink and source throughout geological time, due to a complex interplay of factors. Changes in wind, and the resulting increased upwelling has been suggested as a mechanism for increased atmospheric CO_2 in the deglacial period (Anderson et al. 2009). However many factors are likely responsible for changing sinks and sources of CO_2 in the Southern Ocean in the past, including sea ice retreat (Stephens and Keeling 2000), and variability in algal production and consequently in marine calcium carbonate production (Sigman and Boyle 2000). The Southern Ocean is presently considered a net carbon sink for 0.2-0.9 Pg carbon per year (Hanson 2001), but even regionally, the strength of upwelling is seasonal (Hayakawa et al. 2012). Recently, the strength of the Southern Ocean carbon sink has fluctuated, with evidence to suggest a trend of weakening between 1980 and 2000 (Lenton et al. 2013), although the sink is believed to have strengthened since (Landschützer et al. 2015). Because of the

volume of carbon stored by the Southern Ocean, its future as a carbon sink will be relevant as atmospheric CO_2 continues to increase.

2. Roles of diatoms and coccolithophores in carbon cycling

Phytoplankton export approximately 16 gigatons of carbon to the deep ocean each year (Falkowski et al. 1998). In the Southern Ocean phytoplankton growth is highly seasonal (Harrison et al. 2018) and often patchy (Smith and Nelson 1986; Weber and El-Sayed 1987; Little et al. 2018), so the quantity of carbon export varies both spatially and seasonally (Schlitzer 2000). How different phytoplankton groups will respond to increasing atmospheric and oceanic CO_2 levels is unclear, and remains the subject of ongoing study (Kaufman et al. 2017). The opposing influences of the biological and carbonate counter pumps is well illustrated by two abundant phytoplankton groups: diatoms and coccolithophores, respectively.

Diatoms are unicellular photosynthetic eukaryotes (Phylum Bacillariophyta) found in all aquatic ecosystems, and even in moist terrestrial environments. They range in size from approximately 10 - 200μm, and may exist in the water column individually, in chains and/or in colonies. They are taxonomically the most diverse of the phytoplankton (Harper et al. 2012), and during the last 100 million years, the most abundant (Armbrust 2009). Diatoms account for as much global carbon fixation as all terrestrial rainforests combined (Nelson et al. 1995; Field et al. 1998).

Diatoms are most recognisable for their siliceous shell (frustule), which afford them their distinctive and diverse shapes. The silica frustule is highly ornate, and is one of the main taxonomic features used to differentiate species (Kooistra et al. 2007). The tough, often spined frustules have roles in anti-herbivory, pathogen resistance, and buoyancy in the water column (Hamm and Smetacek 2007). The ruggedness of the frustules means that diatoms can be well preserved in the sediment, providing us a record of past climates which is used extensively in modelling and palaeoreconstruction in marine, estuarine and polar environments (Takahashi 1994; Crosta et al. 2004; de Vernal et al. 2013; Chiba et al. 2016; Taffs et al. 2017). Because the silica frustule does not contain calcium carbonate, diatoms do not contribute to the carbonate counter pump, but to the biological pump. Diatoms tend to increase in abundance south of the Polar Front (~60° S), the mixing point of subantarctic and Antarctic waters, facilitated by high silicate concentrations (Bostock et al. 2013).

Coccolithophores are marine unicellular autotrophs (Phylum Haptophyta, class Prymnesiophyceae) that usually exist as single cells. They are characterised by their overlapping calcium carbonate scales, or coccoliths. The morphology and crystallography of the coccoliths is the main taxonomic feature used to differentiate species of coccolithophores (Hagino and Young

2015). Like diatoms, coccolithophores are important carbon fixers, but with a more complex effect on carbon export. While the construction of coccoliths releases CO_2 into the water (via the carbonate counter pump), the incorporation of the relatively heavy coccoliths into particles increases sinking speed (ballasting), thus expediting carbon export (Klaas and Archer 2002; Weber et al. 2016). In this way, coccolithophores contribute to both the biological and carbonate counter pumps, particularly the ubiquitous *Emiliania huxleyi*, the most abundant coccolithophore globally, and capable of exporting large quantities of carbon, such that a bloom of *E. huxleyi* may still result in net carbon export (Winter et al. 2014).

In the past, the dominant paradigm held that large diatoms accounted for the bulk of carbon export to depth (Martin 1990; Moore et al. 2001). In recent years this paradigm has been questioned, and it is now suggested that high organic carbon export regimes are characterised by small cells and high abundances of calcium-carbonate producers such as coccolithophores (Lam et al. 2011; Maiti et al. 2013; Leblanc et al. 2018). Further, the quality and quantity of exported materials may depend on the specific diatom assemblage composition and diversity, life histories, nutrient status and the size classes of species present (Mouw et al. 2016; Tréguer et al. 2018). The carbonate production of coccolithophores is also species-specific: for example *Coccolithus pelagicus* produce 30 to 80 times more calcium carbonate than *Emiliania huxleyi* (Daniels et al. 2016)*,* although the latter is the most common and abundant coccolithophore in the global ocean. Since different taxa may contribute differently to carbon export, traditional taxonomic work remain valuable to studies of carbon fluxes. Now, and in future oceans, knowledge of diatom and coccolithophore assemblage composition will be of great interest and importance in determining the efficiency and changeability of the biological pump.

3. Quantifying carbon export- sediment traps

Critical to the study of export production was the development and use of time-series of sediment traps beginning in the 1980s (Honjo and Doherty 1988; Honjo et al. 2008). Using sediment traps, researchers can quantify the volume and spatial variability of POC and PIC export as well as other components of fluxes such as biogenic silica (BSi) – the silica produced by organisms such as diatoms and radiolarians. These data may give insights into the type of export system in which the trap was moored. For example, if the ratio of BSi:PIC is less than 1, the region would be considered part of the "carbonate ocean", i.e., export mainly composed of calcium carbonate, while a value >1 would suggest a "silicate ocean" region (Honjo et al. 2008). Sediment traps also provide highly valuable data for developing understanding of the contribution of different phytoplankton taxa to global carbon export, as the assemblages of captures species may be analysed from sediment trap records, along with their seasonal abundances.

Sediment traps are receptacles that may be moored, free floating, or surface-tethered, and capture particulate matter settling from the surface ocean (Fig. 2). Though they have been in use (in a simple form) since the 1970s, modern sediment traps can be deployed for a year or longer, often comprising several capture receptacles that are programmed to open for pre-determined time increments of several days to a month, and capture a time-series of export.
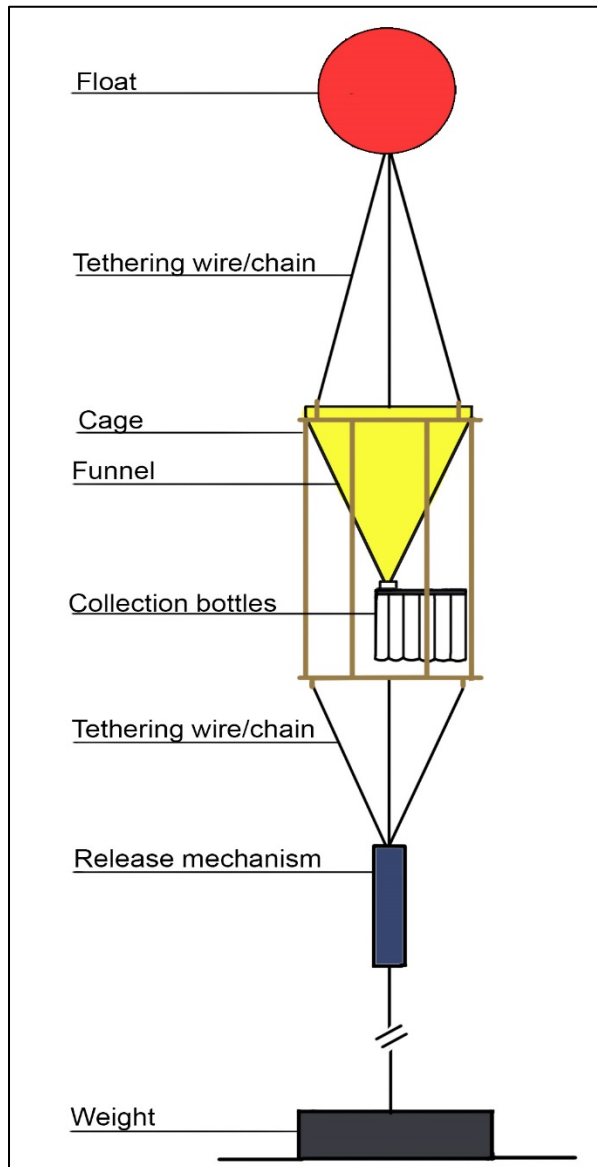
Figure 2. Diagram of a generic conical aperture moored sediment trap setup. Sediment trap deployments may often include current speed, tilt, pressure and temperature sensors on the mooring line.

Sediment traps have been critical to our understanding of the spatial and temporal variability of surface production and export (Honjo and Doherty 1988; Honjo et al. 2008; Maiti et al. 2013). In 1984, the Joint Global Ocean Flux Study (JGOFS) was initiated in order to identify the best way to employ sediment traps to their full advantage, and to make advancements in our understanding

of oceanic carbon fluxes. The work resulting from JGOFS researchers set the scene for modern sediment trap research, and created a scaffold of understanding of oceanic particle fluxes, upon which researchers continue to build (Fasham et al. 2001). It is increasingly understood that export is influenced not only by the volume of production at the surface, but by various transformative processes that occur in the water column, and even interactions between phytoplankton, zooplankton and their symbionts (Foster and Zehr 2006; Amin et al. 2012). Sediment traps studies indicate that particle export is greatest at high latitudes, such as the Southern Ocean, where remineralization of particles by microbes is slower due to lower temperatures, and particle sinking rates are higher due to ballasting by heavy phytoplankton (e.g. coccolithophores, particularly north of the Polar Front) (Weber et al. 2016).

Considerable uncertainty exists about the relationship between surface production and export at high latitudes, such as in the Southern Ocean (Maiti et al. 2013), and how climate change may affect export. While rising oceanic CO_2 intuitively should promote phytoplankton growth, increasing sea temperature is expected to shift phytoplankton towards smaller size classes, causing decreased particle export efficiency (Cram et al. 2017). However, this too is contentious, with other studies suggesting that small plankton size classes are the most important exporters anyway (Maiti et al. 2013, Richardson 2018). Further, the effects on increasing ocean acidification on phytoplankton are complex; calcifying groups such as coccolithophores may experience altered growth rates and reduced calcification (Feng et al. 2016), with flow-on effects on the oceanic carbon cycle (Law et al. 2017). However, the effect on growth and photosynthesis may be species-specific (Langer et al 2006), resulting in changes to community assemblages.

Despite the complexity of the various effects of climate change on phytoplankton, it is generally accepted that the size structure and community composition of phytoplankton is likely to have great bearing on the efficiency of the biological pump in the Southern Ocean and globally (Mouw et al. 2016; Weber et al. 2016; Tréguer et al. 2018). Understanding phytoplankton communities will be of vital significance to determining flux controls, and how they may change under future climate change (Laurenceau et al. 2015).

3.1 Phytoplankton fluxes from sediment traps

Globally, few studies report both diatom and coccolith fluxes from the same sediment traps deployments. These reports are mainly from the Northern Hemisphere, with deployments spanning the Norwegian-Greenland Sea (Samtleben et al. 1995), Mediterranean (Bárcena et al. 2004; Hernández-Almeida et al. 2011; Rigual-Hernández et al. 2013; Malinverno et al. 2014), Atlantic (Abrantes et al. 2002; Fischer et al. 2016), temperate to subarctic North Pacific oceans

(Takahashi et al. 2002; De Bernardi et al. 2005) and off Northwest Africa (Köbrich and Baumann 2009). Sediment trap studies that quantify coccolith flux are particularly rare and are largely restricted to the Northern Hemisphere e.g. (Broerse et al. 2000; Ziveri et al. 2000; Romero et al. 2002; González et al. 2004; Ziveri et al. 2007). In the Southern Hemisphere, the only publications that reported both diatom and coccolith fluxes from the same deployment are in the Benguela Upwelling System (~30°S) (Romero et al. 2002).

3.2 The focal sector- Australia and New Zealand

Considering the importance of understanding the relative contribution of different phytoplankton groups to carbon export at regional and global levels, the relative dearth of attempts to characterise the flux of diatoms and coccoliths in the Southern Hemisphere is of concern. One of the best-sampled regions of the Southern Ocean is the Australian and New Zealand sector. In the Australian and New Zealand sectors, ~44 moorings have been deployed with sediment traps since the 1970s (Fig. 2; Table 1 Chapter 4). Many of these trap deployments have yielded diatom flux data for an annual series (indicated with white rings in Fig. 3, references in Chapter 4). However, prior to this thesis, none of these trapping efforts published coccolith fluxes, let alone both diatom and coccolith fluxes from the same deployment.

Despite the lack of published fluxes, both diatom and coccolithophore living assemblages are well documented in the Australian and New Zealand sector (Malinverno et al. 2015; Davies et al. 2017), making these sectors ideal for studying surface to deep ocean export processes. Further, geological, palaeobiological and geochemical evidence indicates that the Australian/New Zealand sector has alternately been both a carbon source and sink to the atmosphere over the last 30,000 years due to physical changes in winds, circulation of water masses and upwelling of sequestered carbon (Anderson et al. 2009; Bostock et al. 2013). Given the potential significance of this sector to carbon sequestration, and the existing good spatial coverage of sediment traps, the Australian and New Zealand sector is considered an excellent candidate for spatial and temporal comparisons of sediment trap-derived flux data.
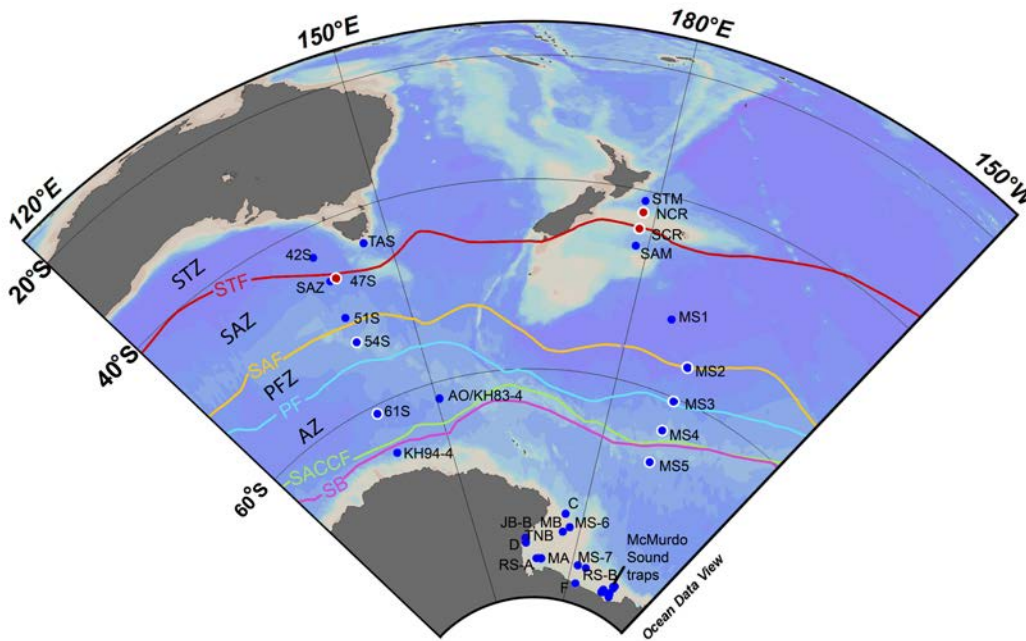
Figure 3. Map of sediment trap moorings of the Australian and New Zealand sector from the subtropics to Antarctica. Sediment trap moorings are indicated with blue circles. Red circles represent the study locations in this thesis. Ocean fronts defined in Orsi et al. (1995); STF = Subtropical Front, STZ = Subtropical Zone, SAF = Subantarctic Front, SAZ = Subantarctic Zone, PF= Polar Front, PFZ = Polar Frontal Zone, SACCF= South Antarctic Circumpolar Current Front, AZ = Antarctic Zone, SB= Southern Boundary (of the ACC). Trap identifiers given in Chapter Five. Map created with Ocean Data View, available http://odv.awi.de (Schlitzer 2016)

In the Australian and New Zealand sectors, maximum winter sea ice does not extend north of ~60° S, and does not influence the trap sites in this thesis (World Ocean Atlas 2009 data, Locarnini et al., 2010). The Australian sector site (47° S) and the New Zealand sector site SCR (see Fig. 3) occupy a similar latitude, but due to local oceanography, different hydrological conditions affect each trap site. In this sector the key phytoplankton nutrient iron is relatively high north of the STF, while nitrate is higher to the south (Fig. 4). The 47° S site, sitting south of the STF, is lower in both nitrate and iron than its New Zealand counterpart, and as such differences in phytoplankton assemblages are expected. Further, the sites are influenced by different conditions in the surface layer of the ocean-the mixed layer, in which temperature, salinity and nutrients are considered homogenous. For a particle to be exported, it must leave the mixed layer. The degree of stratification of the water column can significantly affect phytoplankton productivity, as it affects light levels to which the phytoplankton are exposed, and nutrient supply via upwelling (Gran and Braarud 1935).
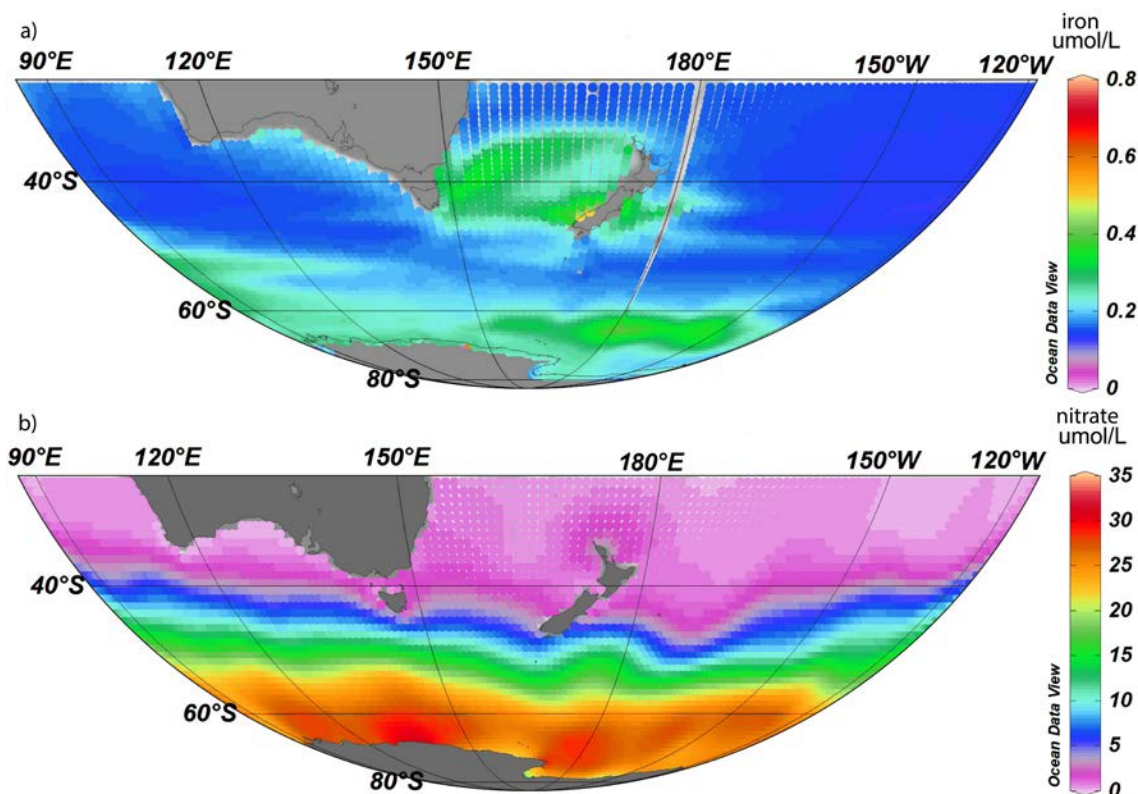
Figure 4. Map of a) iron, and b) nitrate concentrations in the Australian and New Zealand regions. Data from Goddard Earth Sciences Data and Information Services Centre (GES DISC). Plotted using Ocean Data View 4, available at http://odv.awi.de (Schlitzer 2006).

In terms of phytoplankton communities, some taxa will be adapted to living in deeper mixed layers than others (Balch et al. 2018). In the SAZ south of Australia, summer mixed layer depths are between 75-100 m, while in winter depths reach 400+ m (Rintoul and Trull 2001). These fairly deep mixed layers present the challenge of light limitation to phytoplankton in this region, even in summer when the mixed layer is shallower (Rintoul and Trull 2001), and possibly favouring low-light adapted taxa. In the New Zealand sector, mixed layer depths are generally shallower than in the Australian sector (Dong et al. 2008). In the region of the Chatham Rise, Dong et al. (2008) report mixed layers north of the Chatham Rise between 220 m (August) and ~30 m (December/January), consistent with maximum depth determined by Sutton (2001) of roughly 200 m in winter. At SCR, maximum winter mixed layer depth is about 117 m, while the minimum is 20 m (Dong et al. 2008, Chapter 3 Supplementary Figure 1).

3.2.1 Oceanography of the Australian sector

The uppermost margin of the Southern Ocean is the Subtropical Front (STF), which is the boundary between the warmer, saltier Subtropical waters and the cooler, fresher Antarctic waters. In the Australian Sector, the STF presently occurs at a steady 44.5° S - 45.6° S (Orsi et al. 1995). The

Australian sediment trap mooring is located just within the Subantarctic Zone (SAZ), just south of Tasmania (Fig. 5), and considered representative of the SAZ between 90° E and 145° E (Trull et al. 2001a). The trap site is largely influenced by the Leeuwin current, which travels eastward along the Great Australian Bight, deflecting southwards towards the Tasmanian shelf, and becoming the Zeehan current (Baines et al. 1983), which may carry shelf material to the trap site at 47°S. Westward water flow originating from the east of Australia (the East Australian Current, EAC) has also been observed passing south of Tasmania (Herraiz-Borreguero and Rintoul 2011), with the potential to carry warm, saline EAC waters to near the trap site.
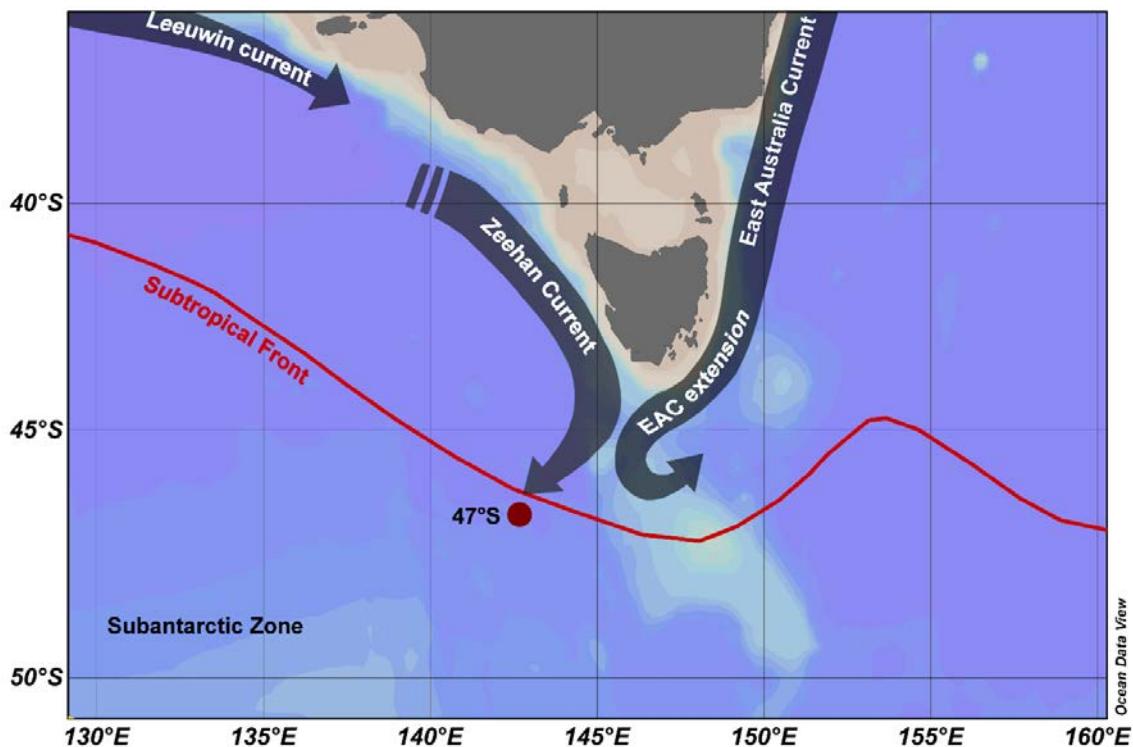
Figure 5. Australian sector local oceanography showing current systems. Summer extension of the East Australian Current (EAC) shown, as per Cresswell (2000). The SAZ Project site at 47 °S is indicated with a red circle. Plotted using Ocean Data View 4, available at http://odv.awi.de (Schlitzer 2006).

3.2.2 Oceanography of the New Zealand sector

The eastern margin of New Zealand is bathed in both Subtropical and Subantarctic surface waters, separated by the STF at roughly 43° S (Heath 1985). The STF follows the southern flank of the Chatham Rise, an ~1500 km long undersea rise extending due east from the north-eastern coast of the South Island at 250-350 m depth (Sutton 2001; Chiswell et al. 2015) (Fig. 6).
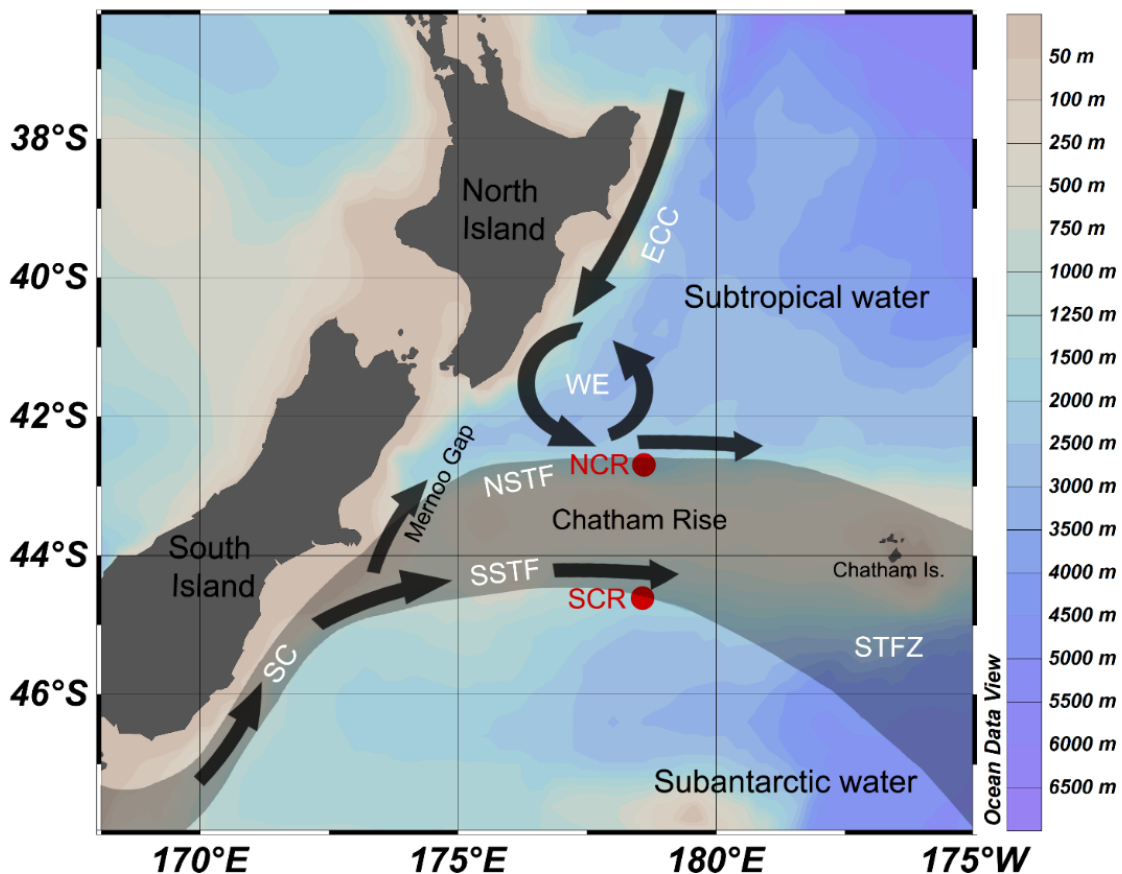
Figure 6. Schematic of New Zealand region showing generalized oceanographic features influencing the mooring sites, and front positions (after Sutton 2001, Fig. 1). Abbreviations: East Cape Current, ECC; Wairarapa Eddy, WE; Southland Current, SC; North Subtropical Front, NSTF; South Subtropical Front, SSTF; Subtropical Frontal Zone, STFZ (gray region); North Chatham Rise, NCR; South Chatham Rise, SCR. Plotted using Ocean Data View 4, available at http://odv.awi.de (Schlitzer 2006).

As elsewhere in the Southern Ocean, a northern and southern subtropical front can be distinguished in the New Zealand region (NSTF and SSTF; (Belkin et al. 1988; Belkin and Gordon 1996), Fig. 6). The New Zealand trap sites sit north and south of the Chatham Rise (NCR and SCR, respectively). The mixing of iron-rich, nitrate-poor subtropical waters with nitrate-rich subantarctic waters over the Chatham Rise creates a unique, high-productivity region (Bradford-Grieve et al. 1997; Boyd et al. 1999). Thus, while NCR and SCR are believed to be sampling primarily from subtropical and subantarctic waters, respectively, both sites exhibit elevated productivity typical of the STF.

3.3 Knowledge gaps in phytoplankton export

Despite significant efforts and funding associated with Australian/New Zealand sector sediment trap deployments over the last ~20 years, prior to this thesis, there were no deployments for which diatom and coccolith fluxes had been characterised. The rarity of sediment trap studies calculating phytoplankton flux assemblages in the Southern Ocean is attributable to the cost of trap deployment, geographic isolation, and lack of taxonomic expertise. Diatoms do not conform well to traditional definitions of species because of high numbers of intermediate forms, cryptic taxa, and seasonal morphological variants (Guiry 2012). Coccolithophores also show pseudo-cryptic speciation indicating that there are perhaps more coccolithophore species than are presently recognised (Hagino and Young 2015). Presently, the taxonomy of both diatoms and coccolithophores is in a "transitional" stage whereby most taxonomists use morphological characteristics in identification, but increasingly genetic analysis are challenging phylogenies. However, specimens from sediment trap samples are typically too old and degraded for genetic analyses, so traditional morphologically-based taxonomy remains of great value.

Knowledge of the spatial and seasonal contribution of different phytoplankton taxa to export is crucial, particularly in light of climate change. Rising temperatures, ocean acidification, and changes to nutrient availability are predicted to drastically affect phytoplankton assemblages (Hopkinson et al. 2011; Feng et al. 2017) and hence, potentially, export flux and carbon sequestration (Lam et al. 2011).

4. Thesis objectives and structure

In this thesis, archival sediment trap material from three mooring locations in the Australian and New Zealand Sectors was analysed for diatom and coccolithophore species composition and flux for an annual cycle. The seasonality of diatom and coccolithophore assemblages was documented for the three trap sites in order to identify patterns of ecological succession. The trap deployments analysed were located south of Tasmania (46° 46' S, 142° 4' E; 2003-2004), and at two sites east of New Zealand, north and south of the Chatham Rise (44° 37' S 178°37' E, and 42° 42' S 178°38' E, respectively; 1996-1997) (indicated with stars in Fig. 3). The three deployment sites for which sediment trap material was analysed in this thesis are, at the time of writing, the only sites in the Australian/New Zealand sector for which both diatom and coccolith fluxes have been quantified to species level for an entire annual cycle.

The aims of this thesis were:

1. To characterise the diversity, abundance and seasonality of two major phytoplankton groups, diatoms and coccolithophores, from sediment trap records in two hydrologically distinct regions of the Southern Ocean (Chapters Two and Three),

2. To place these findings into the wider context of Southern Hemisphere sediment trap research, with commentary on the state of the field and the limitations of the medium (Chapter Four).

3. To provide a description and guide to the identity of the poorly-known diatom genus *Shionodiscus* from the Australian sector, with a clarification of its taxonomic status (Chapter Five),

Several chapters of this thesis have been published, and are included in their published format with the permission of the copyright holders. Detailed methodology for each chapter is provided in Supplementary Information 1. The thesis objectives are addressed in each chapter as follows:

Chapter Two (Wilks et al. 2017)

Wilks JV, Rigual-Hernández AS, Trull TW, Bray SG, Flores J-A, Armand LK (2017) Biogeochemical flux and phytoplankton succession: A year-long sediment trap record in the Australian sector of the Subantarctic Zone. Deep Sea Research Part I: Oceanographic Research Papers **121**:143-159.

This chapter is included in its published format, available at https://doi.org/10.1016/j.dsr.2017.01.001.

This chapter used sediment trap material from a year-long deployment south of Tasmania, at 500 and 2000 m depths. Diatom and coccolith total and species fluxes were calculated for the entire annual record, in addition to bulk compound fluxes calculated by researchers at the University of Tasmania. The ecology and seasonal succession of diatoms and coccolithophores was determined, as well as their individual significance to carbon and other fluxes in this region. This paper represented the first annual record of seasonal coccolith flux and assemblages in the Tasmanian region, as well as the first diatom record at 500 m depth, and just below the mixed layer.

Chapter Three (Wilks et al.; in review)

Titled: "Diatom and coccolithophore flux assemblages from the Subtropical Frontal region, east of New Zealand."

This chapter employed the same methodology as Chapter Two, whereby diatom and coccolith fluxes were characterised at two sites and two depths (300 m and 1000 m). These two sites

represented unique hydrological zones north and south of the Subtropical Front, where Subtropical waters meet the Subantarctic. This chapter's data was generated from archival trap material as an addition to the biogeochemical fluxes already published by Nodder and Northcote (2001), in order to complete the picture of particle flux in these records. This represents the first record of diatom and coccolith fluxes and assemblages for an annual record in this region, and allows for contrast of the export regimes and community structures at each site. Further, the analysis of assemblages allowed us to identify some of the complex particle sources at each trap site, and captured a potentially significant carbon-exporting, sporadic flux event of the diatom *Pseudo-nitzschia.*

Chapter Four (Wilks and Armand 2017)

Titled: "Reviews and syntheses: diatom and coccolith fluxes from temperate to polar Southern Hemisphere sediment traps."

From Chapters Two and Three, it became apparent that broad-scale comparisons of sediment trap phytoplankton fluxes would be of great value in determining regions potentially significant to the global carbon cycle. A review of this type was lacking in the Southern Hemisphere. Chapter Five of this thesis is a meta-analysis/systematic review of 76 publications since 1977, spanning 126 mooring sites from 30° S to the Antarctic coast. Diatom flux data were available for 44 trap deployments, while coccolith fluxes existed for six. Given the range of methodologies employed and data presentation methods, flux calculations were standardised and mapped for the first time in this region. In doing so, some broad-scale patterns of diatom flux became clear. In addition to mapping, several environmental parameters, known to influence diatom flux magnitudes, were chosen to create a simple model identifying the key predictors of diatom flux. The model revealed that nitrate concentration, above all others, is key in determining the magnitudes of diatom fluxes in this region.

Chapter Five

Wilks JV, Armand LK (2017) Diversity and taxonomic identification of *Shionodiscus* spp. in the Australian sector of the Subantarctic Zone. Diatom Research **32**:295-307

This is the author's accepted manuscript of an article published as the version of record in Diatom Research © International Society for Diatom Research https://doi.org/10.1080/0269249X.2017.1365015.

During diatom taxonomic analyses of Chapter Two, some taxa were encountered that were believed to be different species, but which could not be distinguished using light microscopy. Chapter Four used Scanning Electron Microscopy (SEM) to differentiate these taxa, revealing that

Shionodiscus spp. may be more significant in Australian waters than would be determined using light microscopy alone. Using cell measurements, new taxonomic descriptions and a key were constructed for Australian sector *Shionodiscus* spp. diatoms. Traditional diatom taxonomy will always have a place in sediment trap research, or other fields in which DNA may not be preserved in samples, making molecular taxonomy infeasible. Further, taxonomic studies are valuable to palaeobiological studies, where past climatic conditions may be reconstructed from preserved species assemblages.

Supplementary Information 1

Detailed methodology
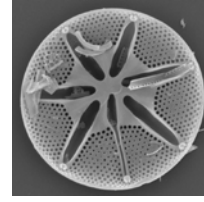
Methodologies are discussed in respective chapters, so to avoid repetition, a brief account is below.

S1. Deployments and trap processing

S1.1 The SAZ Project sediment trap deployments- Chapter Two

The Tasmanian sediment trap samples used in this project were obtained as part of the work undertaken during the multidisciplinary Subantarctic Zone (SAZ) Project, which began in 1997 (Bray et al. 2000). McLane^{TM} PARFLUX sediment traps were deployed in the Subantarctic Zone (46°46'S, 140° E) from Sept. 2003 to Oct. 2004, at 500 m and 2000 m depths. Details on deployment methodology is given in Bray et al. (2000); Trull et al. (2001a); Trull et al. (2001b). Taxonomic data for Chapter Four was also derived from these sediment traps.

After retrieval, samples were sieved through a 1 mm sieve cloth, then split with McLane rotary splitter into ten 50 ml centrifuge tubes. Chapter Two used a 1/10 fraction, and the remaining nine fractions were analysed for total mass, inorganic carbon, biogenic silica, other elements, and presence of other organisms captured such as foraminifera and large planktonic swimmers such as copepods and pteropods. 10 ml from the fraction allocated to this study was used for coccolith fluxes and assemblage analysis at the Universidad de Salamanca, Spain.

S1.2 The NIWA sediment trap deployments- Chapter Three

The New Zealand sediment trap samples were obtained with a McLane^{TM} PARFLUX 7G-21 time-incremental sediment trap, deployed for one continuous year at two locations on either side of the Chatham Rise ridge between 1996 and 1997. The North Chatham Rise (NCR) trap was deployed on the northern flank of the Chatham Rise (42°42'S 178°38'E) from early September 1996 to May 1997, and the South Chatham Rise (SCR) trap was deployed on the southern flank (44°37'S 178°37'E) from May 1996 to May 1997. Traps were deployed at 300 and 1000 m depths at both sites, in water 1500 m deep.

After retrieval, subsamples were taken from each 250 mL sample bottle for nutrient analyses. The remaining material was sieved through a 1 mm mesh to remove swimmers, and split using a McLane^{TM} wet-splitter. Several fractions were used in determining biogeochemical fluxes, which are presented and discussed in Nodder and Northcote (2001). This study used one 1/16th split from each trap depth at each site. Of the 1/16th split, 10 mL was set aside for coccolith analysis (1/80th of original sample). The remaining portion was cleaned for diatom counting.

S2. Sample preparation and analysis

S2.1 Sample cleaning for diatom analysis

Sample cleaning followed the same methodology for Chapters Two and Three for the diatom flux analyses. The subsamples removed for coccolith fluxes were not processed in this way. Diatom samples were cleaned of organic material and carbonates, leaving just siliceous material (diatoms, silcoflagellates and radiolarians). Samples were transferred to glass beakers, and 50 ml of saturated potassium permanganate was added, then left overnight to react. The next day, in a water bath at 95°C, 50 ml 1M HCL was added to samples and left for 30 minutes or until bubbling had stopped. Following this, 50 ml of hydrogen peroxide was added and left again until the reaction had completed, and the samples became clear. Distilled water was added to bring beakers to approximately the same volume, and then left overnight. The following day the supernatant was again removed and the pellet transferred to centrifuge tubes. Tubes were topped up to 45 ml with distilled water. In some of the New Zealand samples, the samples were very high in carbonates and did not clear after one round of cleaning. In these cases, after the first round of acid and peroxide had been added, the samples were allowed to settle and then the supernatant was removed, and the acid and peroxide steps repeated.

To bring the pH to neutral for long-term storage, samples were spun for 8 minutes at 2000 rpm in the centrifuge, then the supernatant removed, and the sample topped up to 45 ml again with distilled water and mixed. This process was repeated 7 or 8 times until the samples tested neutral with pH test strips. The final sample pellet was transferred to a small Nalgene™ 60ml plastic archive bottle and topped up to 50 ml with distilled water. A broken 22 x 22 mm glass coverslip was added to the archive bottles to increase silica saturation inside the bottles. Although the solubility of silicates in distilled water is very low, the presence of excess silicate in the form of the glass cover slip minimises the possibility of diatom dissolution.

S2.2 Slide preparation

Preparation of slides for microscopic analysis was the same for Chapters Two and Three. Three slides per sample were prepared using a modified form of the random settling method (Flores & Sierro, 1997), while coccolithophore slides were made true to the latter author's directions. For diatoms, two glass coverslips were placed in the bottom of a 30 ml glass petri dish, and the dish was mostly filled with distilled water. During early stages of slide processing, a solution of gelatin in distilled water (0.09 g L^{-1}) was used as a medium instead of distilled water, to reduce surface tension and promote the even distribution of diatom frustules on the coverslip. However, gelatin

solution and distilled water methods were compared, giving identical results, so distilled water was chosen to prepare all slides.

A known fraction of the diatom suspension was pipetted into the petri dish containing the distilled water, with a zigzagging motion so as to distribute the sample throughout the dish. Then with the pipette, the solution was sucked in and out repeatedly in a zigzagging motion across the dish from left to right, then from top to bottom. This created turbulence inside the dish, ensuring even distribution of frustules onto the coverslip. The petri dishes were left covered overnight until the sediment solution had settled, and then a single strip of filter paper (~1cm wide) was placed into each petri dish to allow the water to quickly evaporate. Once dry, each coverslip was evenly coated with diatom frustules. The coverslips were glued to glass slides using UV-activated, optical grade Nalgene™ glue.

For Scanning Electron Microscopy (SEM) analysis in Chapter Four, smaller, round coverslips designed for use with SEM "stubs" were coated with the diatom suspension the same way as above, and then gold-coated.

S2.3 Diatom taxonomy and counting protocols

The counting procedure used followed that published by Schrader and Gersonde (1978). Slides were viewed under phase contrast on a DIC phase Olympus BH-2 compound microscope at 1000x magnification. Counting was undertaken along three transects on each slide. All diatoms within the field of view along each transect were visually identified to species or genus level and counted. This method was employed for all three slides for each sample, until 300 individual diatoms had been counted. 300 cells has been determined as the minimum threshold at which error stabilizes between replicate counts of the same sample, and a good balance is achieved between time taken and breadth of coverage of rare species (Boden 1991).

Diatom identification followed modern taxonomy as per Tomas (1997). During diatom counts, other siliceous organisms (silicoflagellates and radiolarians) were also counted, but not identified. Diatoms were identified to species level, except when not possible due to degradation or when frustules were covered in debris. When more than half of a frustule was present, it was counted as one. For long pennate taxa such as *Thalassiothrix*, which are rarely found intact, one end of the frustule was counted as ½. Species that could not be identified to species level were grouped by genus (e.g. *Pseudo-nitzschia*, and some *Shionodiscus* and *Navicula* spp.). *Chaetoceros* spores and vegetative cells were grouped thus. If the genus could not be determined, cells were counted as unknown centric or unknown pennate. Frustules of less than 15 μm, and also unidentifiable were called either centric or pennate <15 μm.

For the Tasmanian traps, coccoliths were counted at both 500 and 2000 m depths, while for the New Zealand traps, only the 300 m traps were counted due to time constraints. 300 coccoliths per sample were counted and identified under 1000x magnification using a LEICA DMRXE polarized light microscope, following the procedure of diatoms. Identification of coccolithophore taxa followed Young et al. (2003; 2014). Identification was to species level where possible, but additional groupings were used to capture unknown *Gephyrocapsa* spp., and *Gephyrocapsa* spp. <3 μm. *Oolithotus* spp., *Pontosphaera* spp., and *Syracosphaera* spp. were not identified past genus level.

S2.4 Flux calculations

For all trap samples, flux of diatoms and coccoliths was calculated for every cup interval, and transformed into both fluxes $m^{-2}\,d^{-1}$ and fluxes $m^{-2}\,year^{-1}$ using the equation of Sancetta and Calvert (1988):

$$Valve\ or\ coccolith\ flux\ m^{-2}\,d^{-1}\ = \left(\frac{N.\left(\frac{A}{a}\right).\left(\frac{V}{v}\right)}{D.T} \right)$$

where *N* is the number of specimens counted, *A* is the area of the petri dish upon which the slide was made, *a* is the area of the slide counted, *V* is the volume of the diluted initial sample before splitting, *v* is the volume of the split of each cup, *D* is the number of days of trap deployment, and *T* is the area of the sediment trap opening in m^2. For the flux calculations for both diatoms and coccoliths, a modifier was applied after flux was calculated to compensate for the fact that a 10 mL subsample was removed for the calcareous phytoplankton (i.e. that the diatom fluxes were calculated based on ~80% of a whole sample, while the coccolith fluxes were calculated using 20%).

S2.5 Environmental data collection and statistical analyses

Chapters Two and Three of this thesis dealt with seasonal phytoplankton fluxes, and similar statistical methods were employed, which are described in the relevant chapters. For each set of deployments, diatom or coccolith fluxes were log_{10} transformed. Environmental parameters were gathered in order to relate flux seasonality to physical processes at each site. For Chapter Two, Photosynthetically Active Radiation (PAR), chlorophyll-*a* concentration (Chl-*a*) and Sea Surface Temperature (SST) data for the trap deployment period (Aug. 2003 - Oct. 2004) were obtained from the Goddard Earth Sciences Data and Information Services Centre (GES DISC) for the area 48° 30' 0'' S - 46° 30' 0'' S x 130° 0' 0'' E - 150° 0' 0'' E. In Chapter Three (New Zealand traps), ten-year monthly average NASA Ocean Biogeochemical Model (NOBM) Photosynthetically Active Radiation

(PAR; 2000 to 2010, 9 km resolution) and Chlorophyll-*a* concentration (Chl-*a*; 2002 to 2012, 4 km resolution) was obtained from the Goddard Earth Sciences Data and Information Services Centre (GES DISC) for 0.5 decimal degrees around each study site at NCR and SCR. Advanced Very High Resolution Radiometer (AVHRR) Sea Surface Temperature (SST; 9 km resolution) data were obtained from a publication on the same trap deployments (King and Howard 2001).

Chapters Two and Three employed Canonical Correspondence Analysis (CCA) to visually represent the relationships between species fluxes and environmental parameters, and were undertaken using PAST software (Hammer et al. 2001). CCA identifies the most significant drivers of variation in a dataset, then plots data points (here species and environmental data) in a 2-dimensional matrix, with the most significant driver on one axis, and the second most significant on another. Environmental data are displayed as "vectors" (lines), with species data points close to vectors indicating a stronger influence of that environmental variable on that species. CCA represents a way to extract patterns from seemingly complex datasets when more "robust" statistical methods are not possible, due to the limitations of replicates in sediment trap studies.

In Chapter Four, environmental data were also gathered to create a linear model attempting to identify which variables best predicted diatom flux from sediment trap records. Eight environmental variables were selected: phosphate, nitrate, silicate, iron, Sea Surface Temperature, % annual sea ice cover, Chlorophyll-*a* concentration, and Particulate Inorganic Carbon as possible drivers of diatom flux. Phosphate, nitrate, silicate and SST were accessed from the World Ocean Atlas 2009, from the National Centres for Environmental Information (accessible at https://www.nodc.noaa.gov/OC5/WOA09/pr_woa09.html). Time-averaged (2009-2014) mean Chl-*a* (4km resolution, MODIS-Aqua satellite), time-averaged (2009-2014) mean iron (0.67 x 1.25° resolution, NOBM model), time-averaged (2009-2014) PIC concentration (4km resolution, MODIS-Aqua satellite), and time-averaged (2009-2014) mean % annual sea ice cover (NOBM model) was obtained from the via the Goddard Earth Sciences Data and Information Services Centre (GES DISC) for the region 25° S to the pole (accessible at https://giovanni.gsfc.nasa.gov). Statistical analyses in Chapter Four were undertaken in R Studio. A linear model was fitted for $\log_{10}$ maximum diatom flux against the chosen variables, using the lm function in R. Then, the predictive value of each variable was tested using the step function (backwards and forwards). Analyses were conducted in R v. 3.5.0 (R Core Team 2018). Silicate was $\log_{10}$ transformed to improve linearity of data points.

References

Abrantes F, Meggers H, Nave S, Bollman J, Palma S, Sprengel C, Henderiks J, Spies A, Salgueiro E, Moita T, Neuer S (2002) Fluxes of micro-organisms along a productivity gradient in the Canary Islands region (29°N): implications for paleoreconstructions. Deep Sea Research Part II: Topical Studies in Oceanography **49**:3599-3629. doi:https://doi.org/10.1016/S0967-0645(02)00100-5

Amin SA, Parker MS, Armbrust EV (2012) Interactions between diatoms and bacteria. Microbiology and Molecular Biology Reviews **76**:667-684.

Anderson R, Ali S, Bradtmiller L, Nielsen S, Fleisher M, Anderson B, Burckle L (2009) Wind-driven upwelling in the Southern Ocean and the deglacial rise in atmospheric CO2. Science **323**:1443-1448.

Armbrust EV (2009) The life of diatoms in the world's oceans. Nature **459**:185-192.

Arndt JE, Schenke HW, Jakobsson M, Nitsche FO, Buys G, Goleby B, Rebesco M, Bohoyo F, Hong J, Black J (2013) The International Bathymetric Chart of the Southern Ocean (IBCSO) Version 1.0–A new bathymetric compilation covering circum‐Antarctic waters. Geophysical Research Letters **40**:3111-3117

Baines P, Edwards R, Fandry C (1983) Observations of a new baroclinic current along the western continental slope of Bass Strait. Marine and Freshwater Research **34**:155-157.

Balch WM (2018) The Ecology, Biogeochemistry, and Optical Properties of Coccolithophores. Annual review of marine science **10**:71-98.

Bárcena M, Flores J, Sierro F, Pérez-Folgado M, Fabres J, Calafat A, Canals M (2004) Planktonic response to main oceanographic changes in the Alboran Sea (Western Mediterranean) as documented in sediment traps and surface sediments. Marine Micropaleontology **53**:423-445.

Belkin IM, Gordon AL (1996) Southern Ocean fronts from the Greenwich meridian to Tasmania. Journal of Geophysical Research: Oceans **101**:3675-3696.

Belkin, IM (1988) Main hydrological features of the central South Pacific. In: ME Vinogradov, MV Flint (eds) Pacific Subantarctic Ecosystems. Nauka, Moscow, pp 21–28.

Boden P (1991) Reproducibility in the random settling method for quantitative diatom analysis. Micropaleontology:313-319

Bostock HC, Barrows TT, Carter L, Chase Z, Cortese G, Dunbar G, Ellwood M, Hayward B, Howard W, Neil H (2013) A review of the Australian–New Zealand sector of the Southern Ocean over the last 30 ka (Aus-INTIMATE project). Quaternary Science Reviews **74**:35-57.

Bostock HC, Hayward BW, Neil HL, Sabaa AT, Scott GH (2015) Changes in the position of the Subtropical Front south of New Zealand since the last glacial period. Paleoceanography 30:824-844. doi:10.1002/2014PA002652

Boyd P, LaRoche J, Gall M, Frew R, McKay RML (1999) Role of iron, light, and silicate in controlling algal biomass in subantarctic waters SE of New Zealand. Journal of Geophysical Research: Oceans **104**:13395-13408. doi:10.1029/1999JC900009

Bradford-Grieve J, Chang F, Gall M, Pickmere S, Richards F (1997) Size‐fractionated phytoplankton standing stocks and primary production during austral winter and spring 1993 in the Subtropical Convergence region near New Zealand. New Zealand journal of marine and freshwater research **31**:201-224.

Bray S, Trull T, Manganini S, Antarctic C (2000) SAZ project moored sediment traps: results of the 1997-1998 deployments. Antarctic CRC

Broerse AT, Ziveri P, van Hinte JE, Honjo S (2000) Coccolithophore export production, species composition, and coccolith-CaCO 3 fluxes in the NE Atlantic (34° N21° W and 48° N21° W). Deep Sea Research Part II: Topical Studies in Oceanography **47**:1877-1905.

Burckle LH (1984) Diatom distribution and paleoceanographic reconstruction in the Southern Ocean — Present and last glacial maximum. Marine Micropaleontology **9**:241-261. doi:10.1016/0377-8398(84)90015-X

Chiba T, Sugihara S, Matsushima Y, Arai Y, Endo K (2016) Reconstruction of Holocene relative sea-level change and residual uplift in the Lake Inba area, Japan. Palaeogeography, Palaeoclimatology, Palaeoecology **441**:982-996. doi:http://dx.doi.org/10.1016/j.palaeo.2015.10.042

Chiswell SM, Bostock HC, Sutton PJH, Williams MJM (2015) Physical oceanography of the deep seas around New Zealand: a review. New Zealand Journal of Marine and Freshwater Research **49**:286-317. doi:10.1080/00288330.2014.992918

Ciais P, Sabine C, Bala G, Bopp L, Brovkin V, Canadell J, Chhabra A, DeFries R, Galloway J, Heimann M, et al. (2013) Carbon and other biogeochemical cycles. In: Stocker TF, Qin D, Plattner GK, Tignor M, Allen SK, Boschung J, Nauels A, Xia Y, Bex V, Midgley PM, editors. Climate change 2013: the physical science basis. Contribution of working group I to the fifth

assessment report of the Intergovernmental Panel on Climate Change. Cambridge (UK): Cambridge University Press. p. 465–570.

Cram JA, Weber T, Leung SW, McDonnell AM, Liang JH, Deutsch C (2017) The role of particle size, ballast, temperature, and oxygen in the sinking flux to the deep sea. Global Biogeochemical Cycles **32**:858-876.

Crosta X, Sturm A, Armand L, Pichon J-J (2004) Late Quaternary sea ice history in the Indian sector of the Southern Ocean as recorded by diatom assemblages. Marine Micropaleontology **50**:209-223. doi:http://dx.doi.org/10.1016/S0377-8398(03)00072-0

Daniels CJ, Poulton AJ, Young JR, Esposito M, Humphreys MP, Ribas-Ribas M, Tynan E, Tyrrell T (2016) Species-specific calcite production reveals Coccolithus pelagicus as the key calcifier in the Arctic Ocean. Marine Ecology Progress Series **555**:29-47.

Davies CH, Coughlan A, Hallegraeff G, Ajani P, Armbrecht L, Atkins N, Bonham P, Brett S, Brinkman R, Burford M (2017) A database of marine phytoplankton abundance, biomass and species composition in Australian waters. Scientific data **4**:170042.

De Bernardi B, Ziveri P, Erba E, Thunell RC (2005) Coccolithophore export production during the 1997–1998 El Niño event in Santa Barbara Basin (California). Marine Micropaleontology **55**:107-125. doi:https://doi.org/10.1016/j.marmicro.2005.02.003

De La Rocha CL, Passow U (2007) Factors influencing the sinking of POC and the efficiency of the biological carbon pump. Deep Sea Research Part II: Topical Studies in Oceanography **54**:639-658. doi:https://doi.org/10.1016/j.dsr2.2007.01.004

de Vernal A, Gersonde R, Goosse H, Seidenkrantz M-S, Wolff EW (2013) Sea ice in the paleoclimate system: the challenge of reconstructing sea ice from proxies – an introduction. Quaternary Science Reviews **79**:1-8. doi:http://dx.doi.org/10.1016/j.quascirev.2013.08.009

Deppeler SL, Davidson AT (2017) Southern Ocean phytoplankton in a changing climate. Frontiers in Marine Science **4**:40.

Dong S, Sprintall J, Gille ST, Talley L (2008) Southern Ocean mixed-layer depth from Argo float profiles. Journal of Geophysical Research: Oceans **113**. doi:doi:10.1029/2006JC004051

Ducklow HW, Steinberg DK, Buesseler KO (2001) Upper ocean carbon export and the biological pump. Oceanography Washington DC Oceanography Society- **14**:50-58.

Dutkiewicz A, O'Callaghan S, Müller R (2016) Controls on the distribution of deep‐sea sediments. Geochemistry, Geophysics, Geosystems **17**:3075-3098.

Falkowski PG, Barber RT, Smetacek V (1998) Biogeochemical Controls and Feedbacks on Ocean Primary Production. Science **281**:200-206. doi:10.1126/science.281.5374.200

Falkowski PG, Knoll AH (2007) CHAPTER 1 - An Introduction to Primary Producers in the Sea: Who They Are, What They Do, and When They Evolved. In: Evolution of Primary Producers in the Sea. Academic Press, Burlington, pp 1-6.

Falkowski PG, Laws EA, Barber RT, Murray JW (2003) Phytoplankton and their role in primary, new, and export production. In: Ocean biogeochemistry. Springer, Berlin, pp 99-121

Fasham MJ, Baliño BM, Bowles MC, Anderson R, Archer D, Bathmann U, Boyd P, Buesseler K, Burkill P, Bychkov A (2001) A new vision of ocean biogeochemistry after a decade of the Joint Global Ocean Flux Study (JGOFS). AMBIO: A Journal of the Human Environment **10**:4-31.

Feng Y, Roleda MY, Armstrong E, Boyd PW, Hurd CL (2017) Environmental controls on the growth, photosynthetic and calcification rates of a Southern Hemisphere strain of the coccolithophore Emiliania huxleyi. Limnology and Oceanography **62**:519-540.

Field CB, Behrenfeld MJ, Randerson JT, Falkowski P (1998) Primary Production of the Biosphere: Integrating Terrestrial and Oceanic Components. Science **281**:237-240. doi:10.1126/science.281.5374.237

Fischer G, Karstensen J, Romero O, Baumann K-H, Donner B, Hefter J, Mollenhauer G, Iversen M, Fiedler B, Monteiro I (2016) Bathypelagic particle flux signatures from a suboxic eddy in the oligotrophic tropical North Atlantic: production, sedimentation and preservation. Biogeosciences **13**:3203-3223.

Foster RA, Zehr JP (2006) Characterization of diatom–cyanobacteria symbioses on the basis of nifH, hetR and 16S rRNA sequences. Environmental Microbiology **8**:1913-1925.

Frankignoulle M, Canon C, Gattuso JP (1994) Marine calcification as a source of carbon dioxide: Positive feedback of increasing atmospheric CO2. Limnology and Oceanography **39**:458-462

Frölicher TL, Sarmiento JL, Paynter DJ, Dunne JP, Krasting JP, Winton M (2015) Dominance of the Southern Ocean in anthropogenic carbon and heat uptake in CMIP5 models. Journal of Climate **28**:862-886.

González HE, Hebbeln D, Iriarte JL, Marchant M (2004) Downward fluxes of faecal material and microplankton at 2300m depth in the oceanic area off Coquimbo (30 S), Chile, during 1993–1995. Deep Sea Research Part II: Topical Studies in Oceanography **51**:2457-2474.

Gottschalk J, Skinner LC, Lippold J, Vogel H, Frank N, Jaccard SL, Waelbroeck C (2016) Biological and physical controls in the Southern Ocean on past millennial-scale atmospheric CO2 changes. Nature Communications **7**:11539. doi:10.1038/ncomms11539 https://www.nature.com/articles/ncomms11539#supplementary-information

Gran HH, Braarud T (1935) A Quantitative Study of the Phytoplankton in the Bay of Fundy and the Gulf of Maine (including Observations on Hydrography, Chemistry and Turbidity). Journal of the Biological Board of Canada 1:279-467. doi:10.1139/f35-012

Guiry MD (2012) HOW MANY SPECIES OF ALGAE ARE THERE? Journal of Phycology **48**:1057-1063. doi:10.1111/j.1529-8817.2012.01222.x

Hagino K, Young JR (2015) Biology and paleontology of Coccolithophores (Haptophytes). In: al. Oe (ed) Marine Protists. Springer, pp 311-330.

Hamm C, Smetacek V (2007) CHAPTER 14 - Armor: Why, When, and How A2 - Falkowski, Paul G. In: Knoll AH (ed) Evolution of Primary Producers in the Sea. Academic Press, Burlington, pp 311-332.

Hanson RB (2001) Introduction to the Joint Global Ocean Flux Study (JGOFS). Ambio **10**:3-31.

Harper M, Cassie Cooper V, Chang FH, Nelson W, Broady P (2012) Phylum Ochrophyta: brown and golden-brown algae, diatoms, silicoflagellates, and kin. New Zealand inventory of biodiversity. Volume Three. Kingdoms Bacteria, Protozoa, Chromista, Plantae, Fungi. Canterbury University Press, Christchurch:114-163.

Harrison CS, Long MC, Lovenduski NS, Moore JK (2018) Mesoscale Effects on Carbon Export: A Global Perspective. Global Biogeochemical Cycles **32**:680-703. doi:10.1002/2017GB005751

Hayakawa H, Shibuya K, Aoyama Y, Nogi Y, Doi K (2012) Ocean bottom pressure variability in the Antarctic Divergence Zone off Lützow-Holm Bay, East Antarctica. Deep Sea Research Part I: Oceanographic Research Papers **60**:22-31. doi:https://doi.org/10.1016/j.dsr.2011.09.005

Heath RA (1985) A review of the physical oceanography of the seas around New Zealand — 1982. New Zealand Journal of Marine and Freshwater Research **19**:79-124. doi:10.1080/00288330.1985.9516077

Hernández-Almeida I, Bárcena MA, Flores JA, Sierro FJ, Sanchez-Vidal A, Calafat A (2011) Microplankton response to environmental conditions in the Alboran Sea (Western Mediterranean): One year sediment trap record. Marine Micropaleontology **78**:14-24. doi:https://doi.org/10.1016/j.marmicro.2010.09.005

Herraiz-Borreguero L, Rintoul SR (2011) Regional circulation and its impact on upper ocean variability south of Tasmania. Deep Sea Research Part II: Topical Studies in Oceanography **58**:2071-2081. doi:http://dx.doi.org/10.1016/j.dsr2.2011.05.022

Honjo S, Doherty KW (1988) Large aperture time-series sediment traps; design objectives, construction and application. Deep Sea Research Part A. Oceanographic Research Papers **35**:133-149. doi:http://dx.doi.org/10.1016/0198-0149(88)90062-3

Honjo S, Manganini SJ, Krishfield RA, Francois R (2008) Particulate organic carbon fluxes to the ocean interior and factors controlling the biological pump: A synthesis of global sediment trap programs since 1983. Progress in Oceanography **76**:217-285.

IPCC (2014) Climate change 2014: synthesis report. Contribution of Working Groups I, II and III to the Fifth Assessment Report of the Intergovernmental Panel on Climate Change. IPCC, Geneva.

Kaufman DE, Friedrichs MAM, Smith WO, Hofmann EE, Dinniman MS, Hemmings JCP (2017) Climate change impacts on southern Ross Sea phytoplankton composition, productivity, and export. Journal of Geophysical Research: Oceans **122**:2339-2359. doi:10.1002/2016JC012514

Klaas C, Archer DE (2002) Association of sinking organic matter with various types of mineral ballast in the deep sea: Implications for the rain ratio. Global Biogeochemical Cycles **16**:1116.

King AL, Howard WR (2001) Seasonality of foraminiferal flux in sediment traps at Chatham Rise, SW Pacific: implications for paleotemperature estimates. Deep Sea Research Part I: Oceanographic Research Papers **48**:1687-1708

Köbrich M, Baumann K (2009) Coccolithophore flux in a sediment trap off Cape Blanc (NW-Africa). Journal of Nannoplankton Research **30**:83-96.

Kooistra WHCF, Gersonde R, Medlin LK, Mann DG (2007) CHAPTER 11 - The Origin and Evolution of the Diatoms: Their Adaptation to a Planktonic Existence A2 - Falkowski, Paul G. In: Knoll AH (ed) Evolution of Primary Producers in the Sea. Academic Press, Burlington, pp 207-249.

Lam PJ, Doney SC, Bishop JK (2011) The dynamic ocean biological pump: Insights from a global compilation of particulate organic carbon, CaCO3, and opal concentration profiles from the mesopelagic. Global Biogeochemical Cycles **25**:GB3009. doi:10.1029/2010GB003868.

Landschützer P, Gruber N, Haumann FA, Rödenbeck C, Bakker DCE, van Heuven S, Hoppema M, Metzl N, Sweeney C, Takahashi T, Tilbrook B, Wanninkhof R (2015) The reinvigoration of the Southern Ocean carbon sink. Science **349**:1221-1224. doi:10.1126/science.aab2620

Langer G, Geisen M, Baumann K-H, Kläs J, Riebesell U, Thoms S, Young JR (2006) Species-specific responses of calcifying algae to changing seawater carbonate chemistry. Geochemistry, Geophysics, Geosystems 7. doi:10.1029/2005GC001227

Laurenceau-Cornec E, Trull T, Davies D, Bray S, Doran J, Planchon F, Carlotti F, Jouandet M-P, Cavagna A-J, Waite A (2015) The relative importance of phytoplankton aggregates and zooplankton fecal pellets to carbon export: insights from free-drifting sediment trap deployments in naturally iron-fertilised waters near the Kerguelen plateau. Biogeosciences Discussions **11**:13623-13673.

Law CS, Bell JJ, Bostock HC, Cornwall CE, Cummings VJ, Currie K, Davy SK, Gammon M, Hepburn CD, Hurd CL, Lamare M, Mikaloff-Fletcher SE, Nelson WA, Parsons DM, Ragg NLC, Sewell MA, Smith AM, Tracey DM (2017) Ocean acidification in New Zealand waters: trends and impacts. New Zealand Journal of Marine and Freshwater Research **52**:155-195. doi:10.1080/00288330.2017.1374983

Leblanc K, Quéguiner B, Diaz F, Cornet V, Michel-Rodriguez M, de Madron XD, Bowler C, Malviya S, Thyssen M, Grégori G (2018) Nanoplanktonic diatoms are globally overlooked but play a role in spring blooms and carbon export. Nature Communications **9**:953.

Lenton A, Tilbrook B, Law R, Bakker DC, Doney SC, Gruber N, Hoppema M, Ishii M, Lovenduski NS, Matear RJ (2013) Sea-air CO 2 fluxes in the Southern Ocean for the period 1990-2009. Biogeosciences Discussions **10**:285-333.

Little HJ, Vichi M, Thomalla SJ, Swart S (2018) Spatial and temporal scales of chlorophyll variability using high-resolution glider data. Journal of Marine Systems **187**:1-12. doi:https://doi.org/10.1016/j.jmarsys.2018.06.011

Locarnini R, Mishonov A, Antonov J, Boyer T, Garcia H, Baranova O, Zweng M, Johnson D (2010) World Ocean Atlas 2009, Volume 1: Temperature US Government Printing Office, Washington, DC.

Maiti K, Charette MA, Buesseler KO, Kahru M (2013) An inverse relationship between production and export efficiency in the Southern Ocean. Geophysical Research Letters **40**:1557-1561. doi:10.1002/grl.50219

Malinverno E, Maffioli P, Corselli C, De Lange GJ (2014) Present-day fluxes of coccolithophores and diatoms in the pelagic Ionian Sea. Journal of Marine Systems **132**:13-27. doi:https://doi.org/10.1016/j.jmarsys.2013.12.009

Malinverno E, Triantaphyllou MV, Dimiza MD (2015) Coccolithophore assemblage distribution along a temperate to polar gradient in the West Pacific sector of the Southern Ocean (January 2005). Micropaleontology **61**:489-506.

Martin JH (1990) Glacial‐interglacial CO2 change: The iron hypothesis. Paleoceanography **5**:1-13.

Moore JK, Doney SC, Glover DM, Fung IY (2001) Iron cycling and nutrient-limitation patterns in surface waters of the World Ocean. Deep Sea Research Part II: Topical Studies in Oceanography **49**:463-507. doi:http://dx.doi.org/10.1016/S0967-0645(01)00109-6

Mouw CB, Barnett A, McKinley GA, Gloege L, Pilcher D (2016) Phytoplankton size impact on export flux in the global ocean. Global Biogeochemical Cycles **30**:1542-1562.

Nelson DM, Tréguer P, Brzezinski MA, Leynaert A, Quéguiner B (1995) Production and dissolution of biogenic silica in the ocean: revised global estimates, comparison with regional data and relationship to biogenic sedimentation. Global Biogeochemical Cycles **9**:359-372.

Orsi AH, Whitworth T, Nowlin WD (1995) On the meridional extent and fronts of the Antarctic Circumpolar Current. Deep Sea Research Part I: Oceanographic Research Papers **42**:641-673.

Pearson PN, Palmer MR (2000) Atmospheric carbon dioxide concentrations over the past 60 million years. Nature **406**:695. doi:10.1038/35021000

Petit JR, Jouzel J, Raynaud D, Barkov NI, Barnola JM, Basile I, Bender M, Chappellaz J, Davis M, Delaygue G, Delmotte M, Kotlyakov VM, Legrand M, Lipenkov VY, Lorius C, PÉpin L, Ritz C, Saltzman E, Stievenard M (1999) Climate and atmospheric history of the past 420,000 years from the Vostok ice core, Antarctica. Nature **399**:429. doi:10.1038/20859

R Core Team (2018) R: A language and environment for statistical computing. R Foundation for Statistical Computing, Vienna, Austria, https://www.R-project.org/

Richardson T (2018) Contributions of Small Particles to Particle Flux and Attenuation. Annual Review of Marine Science **10.**

Riebesell U, Körtzinger A, Oschlies A (2009) Sensitivities of marine carbon fluxes to ocean change. Proceedings of the National Academy of Sciences **106**:20602-20609. doi:10.1073/pnas.0813291106

Rigual-Hernández AS, Bárcena MA, Jordan RW, Sierro FJ, Flores JA, Meier KJS, Beaufort L, Heussner S (2013) Diatom fluxes in the NW Mediterranean: evidence from a 12-year sediment trap record and surficial sediments. Journal of Plankton Research **35**:1109-1125. doi:10.1093/plankt/fbt055

Rintoul SR, Trull TW (2001) Seasonal evolution of the mixed layer in the Subantarctic Zone south of Australia. Journal of Geophysical Research: Oceans **106**:31447-31462.

Romero O, Boeckel B, Donner B, Lavik G, Fischer G, Wefer G (2002) Seasonal productivity dynamics in the pelagic central Benguela System inferred from the flux of carbonate and silicate organisms. Journal of Marine Systems **37**:259-278.

Ronge T, Geibert W, Lippold J, Lamy F, Schnetger B, Prange M, Tiedemann R (2018) Climate, CO2 and Ice Sheets-A Southern Ocean Perspective. 27th International Polar Conference, Rostock, 25 March 2018 - 29 March 2018.

Rosenthal Y, Dahan M, Shemesh A (2000) Southern Ocean contributions to glacial‐interglacial changes of atmospheric pCO2: An assessment of carbon isotope records in diatoms. Paleoceanography and Paleoclimatology **15**:65-75.

Samtleben C, Schäfer P, Andruleit H, Baumann A, Baumann K-H, Kohly A, Matthiessen J, Schröder-Ritzrau A (1995) Plankton in the Norwegian-Greenland Sea: from living communities to sediment assemblages —an actualistic approach. Geologische Rundschau **84**:108-136. doi:10.1007/bf00192245

Sancetta C, Calvert SE (1988) The annual cycle of sedimentation in Saanich Inlet, British Columbia: implications for the interpretation of diatom fossil assemblages. Deep Sea Research Part A. Oceanographic Research Papers **35**:71-90

Schlitzer R (2000) Applying the adjoint method for biogeochemical modeling: export of participate organic matter in the world ocean. Inverse methods in global biogeochemical cycles **114**:107-124.

Sigman DM, Boyle EA (2000) Glacial/interglacial variations in atmospheric carbon dioxide. Nature **407**:859. doi:10.1038/35038000

Sigman D, Haug G (2003) The biological pump in the past. Treatise on geochemistry **6**:625.

Smith S, Key G (1975) Carbon dioxide and metabolism in marine environments 1. Limnology and Oceanography **20**:493-495.

Smith WO, Nelson DM (1986) Importance of ice edge phytoplankton production in the Southern Ocean. BioScience **36**:251-257.

Stephens BB, Keeling RF (2000) The influence of Antarctic sea ice on glacial–interglacial CO 2 variations. Nature **404**:171. doi:10.1038/35004556

Sutton P (2001) Detailed structure of the subtropical front over Chatham Rise, east of New Zealand. Journal of Geophysical Research: Oceans **106**:31045-31056.

Taffs KH, Saunders KM, Logan B (2017) Diatoms as Indicators of Environmental Change in Estuaries. In: Weckström K, Saunders KM, Gell PA, Skilbeck CG (eds) Applications of Paleoenvironmental Techniques in Estuarine Studies. Springer Netherlands, Dordrecht, pp 277-294.

Takahashi K (1994) From modern flux to paleoflux: assessment from sinking assemblages to thanatocoenosis. In: Carbon Cycling in the Glacial Ocean: Constraints on the Ocean's Role in Global Change. Springer, pp. 413-424.

Takahashi K, Fujitani N, Yanada M (2002) Long term monitoring of particle fluxes in the Bering Sea and the central subarctic Pacific Ocean, 1990–2000. Progress in Oceanography **55**:95-112. doi:http://dx.doi.org/10.1016/S0079-6611(02)00072-1

Toggweiler JR, Russell JL, Carson SR (2006) Midlatitude westerlies, atmospheric CO2, and climate change during the ice ages. Paleoceanography **21**:PA2005.

Tréguer P, Bowler C, Moriceau B, Dutkiewicz S, Gehlen M, Aumont O, Bittner L, Dugdale R, Finkel Z, Iudicone D, Jahn O, Guidi L, Lasbleiz M, Leblanc K, Levy M, Pondaven P (2018) Influence of diatom diversity on the ocean biological carbon pump. Nature Geoscience **11**:27-37. doi:10.1038/s41561-017-0028-x

Trull T, Bray S, Manganini S, Honjo S, Francois R (2001a) Moored sediment trap measurements of carbon export in the Subantarctic and Polar Frontal Zones of the Southern Ocean, south of Australia. Journal of Geophysical Research: Oceans (1978–2012) **106**:31489-31509

Trull T, Sedwick P, Griffiths F, Rintoul S (2001b) Introduction to special section: SAZ Project. Journal of Geophysical Research: Oceans (1978–2012) **106**:31425-31429

Volk T, Hoffert MI (1985) Ocean carbon pumps: Analysis of relative strengths and efficiencies in ocean‐driven atmospheric CO2 changes. Geophysical Monograph Series **32**:99-110.

Weber LH, El-Sayed SZ (1987) Contributions of the net, nano- and picoplankton to the phytoplankton standing crop and primary productivity in the Southern Ocean. Journal of Plankton Research **9**:973-994. doi:10.1093/plankt/9.5.973

Weber T, Cram JA, Leung SW, DeVries T, Deutsch C (2016) Deep ocean nutrients imply large latitudinal variation in particle transfer efficiency. Proceedings of the National Academy of Sciences **113**:8606-8611. doi:10.1073/pnas.1604414113

Winter A, Henderiks J, Beaufort L, Rickaby RE, Brown CW (2014) Poleward expansion of the coccolithophore Emiliania huxleyi. Journal of Plankton Research **36**:316-325.

World Ocean Atlas (WOA) (2009). Available at https://www.nodc.noaa.gov/OC5/WOA09/pr_woa09.html

Young JR, Geisen M, Cros L, Kleijne A, Sprengel C, Probert I, Østergaard J (2003) A guide to extant coccolithophore taxonomy. Journal of Nannoplankton Research Special Issue 1.

Young J, Bown P, Lees J (2014) Nannotax3 website. International Nannoplankton Association. ⟨http://ina.tmsoc.org/Nannotax3⟩. (accessed 21.04.14)

Ziveri P, de Bernardi B, Baumann K-H, Stoll HM, Mortyn PG (2007) Sinking of coccolith carbonate and potential contribution to organic carbon ballasting in the deep ocean. Deep Sea Research Part II: Topical Studies in Oceanography **54**:659-675.

Ziveri P, Rutten A, De Lange G, Thomson J, Corselli C (2000) Present-day coccolith fluxes recorded in central eastern Mediterranean sediment traps and surface sediments. Palaeogeography, Palaeoclimatology, Palaeoecology **158**:175-195.

Chapter Two
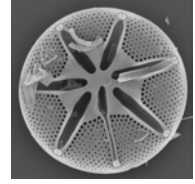
Biogeochemical flux and phytoplankton succession: A year-long sediment trap record in the Australian sector of the Subantarctic Zone

The following chapter is presented in the format in which it was published.

Biogeochemical flux and phytoplankton succession: A year-long sediment trap record in the Australian sector of the Subantarctic Zone

Jessica V. Wilks[a,*], Andrés S. Rigual-Hernández[a,b], Thomas W. Trull[c,d], Stephen G. Bray[c], José-Abel Flores[b], Leanne K. Armand[a]

[a] MQ Marine Research Centre and Department of Biological Sciences, Macquarie University, North Ryde, NSW 2109, Australia
[b] Department of Geology. Universidad de Salamanca, Salamanca 37008, Spain
[c] Antarctic Climate and Ecosystems Cooperative Research Centre, University of Tasmania, Hobart, Tasmania 7001, Australia
[d] CSIRO Oceans and Atmosphere Flagship, Hobart, Tasmania 7001, Australia

ARTICLE INFO

ABSTRACT

The Subantarctic Zone (SAZ) plays a crucial role in global carbon cycling as a significant sink for atmospheric CO_2. In the Australian sector, the SAZ exports large quantities of organic carbon from the surface ocean, despite lower algal biomass accumulation in surface waters than other Southern Ocean sectors. We present the first analysis of diatom and coccolithophore assemblages and seasonality, as well as the first annual quantification of bulk organic components of captured material at the base of the mixed layer (500 m depth) in the SAZ. Sediment traps were moored in the SAZ southwest of Tasmania as part of the long-term SAZ Project for one year (September 2003 to September 2004). Annual mass flux at 500 m and 2000 m was composed mainly of calcium carbonate, while biogenic silica made up on average < 10% of material captured in the traps. Organic carbon flux was estimated at $1.1 \text{ g m}^{-2} \text{ y}^{-1}$ at 500 m, close to the estimated global mean carbon flux. Low diatom fluxes and high fluxes of coccoliths were consistent with low biogenic silica and high calcium carbonate fluxes, respectively. Diatoms and coccoliths were identified to species level. Diatom and coccolithophore sinking assemblages reflected some seasonal ecological succession. A theoretical scheme of diatom succession in live assemblages is compared to successional patterns presented in sediment traps. This study provides a unique, direct measurement of the biogeochemical fluxes and their main biological carbon vectors just below the winter mixed layer depth at which effective sequestration of carbon occurs. Comparison of these results with previous sediment trap deployments at the same site at deeper depths (i.e. 1000, 2000 and 3800 m) documents the changes particle fluxes experience in the lower "twilight zone" where biological processes and remineralisation of carbon reduce the efficiency of carbon sequestration.

1. Introduction

The Subantarctic Zone (SAZ) is the northernmost zone of the Southern Ocean, delineated by the Subtropical Front to the north and the Subantarctic Front to the south. The SAZ is the Southern Ocean's warmest zone, and comprises > 50% of its surface area (Orsi et al., 1995). Yet, the SAZ is a High-Nitrate, Low-Chlorophyll (HNLC) zone due to low phytoplankton biomass production, despite the excess in nitrate and phosphate in surface waters (Bucciarelli et al., 2001). Strong silicate and iron limitation (Blain et al., 2001; Hutchins et al., 2001; Fripiat et al., 2011), as well as light limitation due to deep winter mixing, each contribute to the zone's HNLC status (Bucciarelli et al., 2001; Trull et al., 2001c). Nonetheless, the SAZ is significant as one of the strongest oceanic sinks of atmospheric CO_2 in global climate (Metzl

et al., 1999; Trull et al., 2001c; Shadwick et al., 2015), driven by phytoplankton primary production and subsequent particle export (i.e. the biological pump), and by uptake via dissolution in newly formed waters (i.e. the solubility pump) (Honjo et al., 2000; Trull et al., 2001c).

Sediment traps measure biological and particulate matter exported from the photic zone to the ocean interior, providing insights into oceanic particle flux and phytoplankton ecology (e.g. Honjo et al., 2008; Romero and Armand, 2010). The multidisciplinary SAZ Project was initiated in 1997 by the Antarctic Cooperative Research Centre (ACE CRC) in Tasmania to remedy the lack of oceanographic data within the SAZ and the Polar Frontal Zone (PFZ) (Trull et al., 2001c). The SAZ Project deployed bottom-tethered sediment traps to quantify and characterise the particle fluxes from the Subantarctic to the Antarctic along 140°E, enabling comparisons between zones (Trull
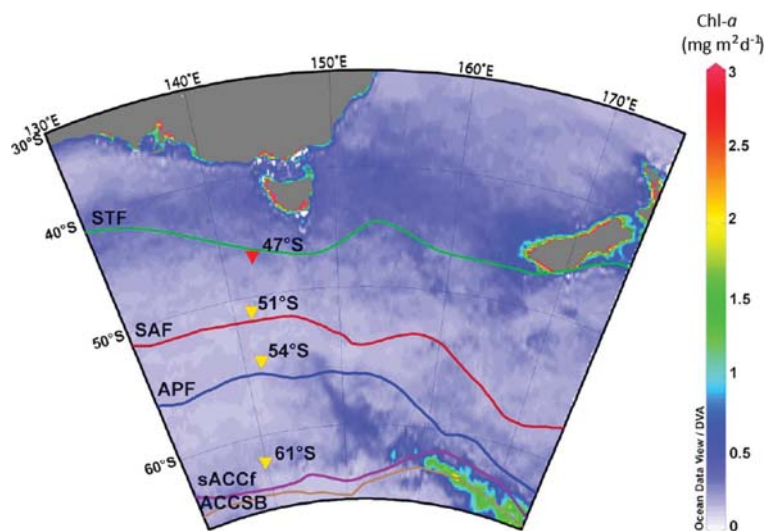
Fig. 1. Regional context of sediment trap deployment (SAZ Project) 2003–2004 showing fronts and zones (adapted from Orsi et al., 1995). Triangles indicate SAZ Project sediment trap deployment locations; red triangle shows current site at 47ºS. Lines indicate front locations, from top to bottom: Subtropical Front (STF) green line; Subantarctic Front (SAF) red line; Antarctic Polar Front (APF) blue line; south Antarctic Circumpolar Current front (sACCf) purple line; Antarctic Circumpolar Current Southern Boundary (ACCSB) brown line. Coloured bar denotes Chlorophyll-a concentrations (mg m^2 d^{-1}), August 2003 to August 2004. Map created with Ocean Data View, available at http://odv.awi.de (Schlitzer, 2016).

et al., 2001c, 2001a; Rigual-Hernández et al., 2015a, 2016b). The SAZ Project also allowed comparison to other particle flux studies in nearby regions, such as the Antarctic Environment and Southern Ocean Process Study (AESOPS), which deployed sediment traps in the SAZ, PFZ, AZ, and Ross Sea along 170ºW (Smith et al., 2000; Honjo et al., 2000; Anderson and Smith, 2001), the Subantarctic National Institute of Water and Atmospheric Research (NIWA) studies (Nodder and Northcote, 2001); and trapping studies in the Atlantic sector (Wefer and Fischer 1991; Fischer et al., 2002). Early results of the SAZ Project time-series traps focused on the bulk particulate components, reporting lower algal biomass accumulation in the Australian sector than in the Atlantic or New Zealand sectors of the SAZ (Rintoul and Trull, 2001; Trull et al., 2001a), although total particulate organic carbon flux was similar to the global ocean median (Lampitt and Antia, 1997).

A series of papers succeeding the SAZ Project have contributed to our understanding of production and carbon fluxes in the Australian sector across oceanographic zones, and the influence of phytoplankton assemblages on Southern Ocean biogeochemistry (Ebersbach et al., 2011; De Salas et al., 2011; Rigual-Hernández et al., 2015a, 2015b). Work remains to be undertaken to quantify the carbon exporting capacity of the range of phytoplankton species in this region.

Diatoms are a diverse group of unicellular phytoplankton that occur in high abundances in the Southern Ocean (Alvain et al., 2008), and are the most significant contributors of biogenic silica to the Southern Ocean's sediments, particularly south of the Polar Front (Ragueneau et al., 2000; Rigual-Hernández et al., 2016). Both live and sediment-trap records of diatom assemblages have been studied in the Australian sector (De Salas et al., 2011; Kopczyńska et al., 2007; Rigual-Hernández et al., 2015a; Rigual-Hernández et al., 2015b). Analyses of live coccolithophore assemblages (Nishida, 1986; Findlay and Giraudeau, 2000), and past and present calcification (Cubillos et al., 2007, 2012), have also been conducted in the Australian sector whilst seafloor sediment core-top analyses have recently revealed that coccoliths comprise a significant percentage of sediment in the Pacific sector of the SAZ (Saavedra-Pellitero et al., 2014). Sediment traps deployed near the Crozet Plateau (PFZ) revealed that coccoliths were responsible for roughly a third of particulate inorganic carbon (PIC) export (Salter et al., 2014), while coccoliths made up > 85% PIC exported over the Kerguelen Plateau (AZ) (Rembauville et al., 2016). Yet despite their

significance to PIC production and export, coccolithophore fluxes have not been quantified within the pelagic waters of the SAZ.

To address the need for a comprehensive understanding of the major biological export flux taxa and their seasonal contribution to particle export in the Australian sector of the SAZ, this study returns to the SAZ Project trap programme's 47ºS trap sample splits (Sept. 2003– Oct. 2004, 47ºS, 140°E; 500 m and 2000 m depth). This new investigation on the preserved material enables:

1) A description of temporal seasonality and composition of particle fluxes at the base of the mixed layer in the SAZ, and
2) The documentation of assemblage composition of two of the main groups of phytoplankton in the region: diatoms and coccolithophores.

Aim 1 delivers the first annual quantification of biogenic silica, calcium carbonate and POC export for the Australian sector of the SAZ at the base of the winter mixed layer. The second aim provides the first report of seasonal variability of diatom and coccolithophore assemblages for the pelagic waters of the SAZ in the Southern Ocean. Additionally, we present a comparison of how theoretical live diatom ecological succession is reflected in sediment trap records.

1.1. Oceanographic setting

The Southern Ocean is banded by approximately concentric zones of water masses (Orsi et al., 1995), possessing distinct and relatively uniform hydrological properties that influence the phytoplankton species found (Boyd et al., 2000; Sokolov and Rintoul, 2002; Pollard et al., 2002) (Fig. 1). These water masses make up the Antarctic Circumpolar Current (ACC), which includes, from north to south, the Subantarctic Zone (SAZ), Polar Frontal Zone (PFZ), and the Antarctic Zone (AZ). Zones are defined by the fronts at which they meet, where the characteristics of the water masses (particularly temperature and salinity) sharply change. The SAZ stretches from the Subtropical Front (STF), the boundary between subtropical and subantarctic waters to the north (44.5–45.6ºS in the Australian region), to the Subantarctic Front (SAF), the strongest front within the ACC (50–53ºS) (Sokolov and Rintoul, 2002). The water masses of the SAZ are stratified in

144

austral summer, with stratification controlled mainly by temperature, and weakening stratification in winter (Rintoul and Trull, 2001; Pollard et al., 2002). In this study, we use the front definitions of Orsi et al. (1995).

The trap deployment site (46°48′S, 142°6′E) is biogeochemically typical of the SAZ, being low in silica and iron year-round but replete in nitrate (Rintoul and Trull, 2001; Sedwick et al., 1999, 2008). The site is representative of the SAZ between 90° and 145°E (Trull et al., 2001a). The SAZ has a deep mixed layer in winter (up to 600 m during more extreme years) that shallows to 75–100 m in summer (Rintoul and Trull, 2001; Trull et al., 2001c). In general, the mixed layer is deeper than the euphotic zone in this region throughout the year. The euphotic zone (the depth at which PAR is 1% of the surface incident PAR) ranges from ~115 m in winter, when phytoplankton abundance is lowest, to ~45 m in summer when algal biomass reaches maximal values (Westwood et al., 2011). During sunny, calm weather in summer, the mixed layer can be shallower (to ~25 m) than the euphotic zone, and production below the mixed layer may reach 10% of the total water column production (Westwood et al., 2011). These conditions are short-lived and chlorophyll fluorescence profiles show that phytoplankton biomass is distributed uniformly within the mixed layer without subsurface maxima (Rintoul and Griffiths, 2001; Bowie et al., 2011). Regionally, the SAZ has slightly higher silicate and slightly deeper mixed layer depths to the south due to the input of cooler, fresher water moving northwards across the SAF. Such differences in hydrological properties between the north and south of the SAZ are more pronounced during summer than winter (Lourey and Trull, 2001; Rintoul and Trull, 2001).

2. Materials and methods

2.1. Field Experiment

McLane PARFLUX sediment traps ($0.5 \, \mathrm{m}^2$ capture area) were deployed for one year (2003–2004) in the Australian sector of the Subantarctic Zone (46°46′ S, 142°4′ E) via the SAZ Project (Trull et al., 2001c) (Fig. 1). Traps were deployed on one mooring line at 500 m, 1000 m and 2000 m, however, the 1000 m trap captured little material and was not analysed.

The 500 m trap was equipped with a tilt meter, and an Aanderaa RCM8 current meter placed 50 m below it on the mooring line. Current speeds for the duration of the deployment averaged $10.9 \, \mathrm{cm \, s^{-1}}$ (Supplementary Table 1); slightly below speeds at which trapping efficiency is considered to decrease (~$12 \, \mathrm{cm \, s^{-1}}$; Baker et al., 1988). There were occasional short excursions to higher velocities during the autumn and winter months, however, 95% of the time current speeds were below $23 \, \mathrm{cm \, s^{-1}}$.

Each trap consisted of 21×500 mL collection cups rotated on a 14 d (summer and spring) or a 35 d (autumn and winter) pre-programmed schedule. All traps successfully completed collection for the entire sampling period, though some cups contained too little material to analyse. At 500 m, cup 12 was omitted from analyses, while for the 2000 m trap, only cups 1 – 11 (spring to summer) and 17 (autumn) were exploitable for this study as the remaining cups captured too little material to analyse (Supplementary Table 1). Sampling dates and lengths are given in Table 1.

After retrieval, samples were sieved with a 1 mm sieve to remove large swimmers. Samples were split into ten fractions using a McLane rotary splitter, and were stored at 4 °C in the dark in 50 mL tubes (Bray et al., 2000; Trull et al., 2001b).

2.2. Biogeochemical flux determination

Detailed explanation of Total Mass Flux (TMF), Particulate Organic Carbon (POC), calcium carbonate ($CaCO_3$), and Biogenic Silica (BSi) calculations are given in Bray et al. (2000) and Trull et al. (2001a).

POC, $CaCO_3$ and BSi were not calculated for cups 13–21 at 2000 m, as too little material was captured. Annual TMF was calculated for the 500 m trap only, as the 2000 m trap did not contain an entire year's useable samples. Three 1/10 splits of the < 1 mm fraction were stored for later microscopic analyses. The remainder was filtered, dried, weighed, and ground. Samples were filtered using 0.4 μm Millipore polycarbonate membranes. Samples were dried at 60 °C in a forced convection oven. Particulate inorganic carbonate (PIC) was measured by adding phosphoric acid to the dry sample, and measuring CO_2 produced using a colourimeter. Total particulate carbon (PC) and nitrogen (PN) were determined using a Perkin Elmer CHN Analyser, and POC was estimated by difference, i.e. POC=PC–PIC. BSi was estimated using hot alkaline digestion and visible spectrometry following Quéguiner (2001).

2.3. Siliceous microplankton preparation and identification

One 1/10 split of the sieved fraction was used for the biological flux analyses. This split was topped up to 40 mL using distilled water, and a 10 mL subsample was taken for coccolith analyses. The remaining split was cleaned of organic material using potassium permanganate, hydrochloric acid, and hydrogen peroxide as per Romero et al. (1999). After organic material removal, samples were centrifuged, the supernatant removed, and topped up with distilled water.

Slides were prepared using a modified form of the random settling method (Flores and Sierro, 1997), to ensure even diatom distribution within the suspension to avoid frustule overlap or clumping on slides. A known fraction (4 mL standard, up to 25 mL for very sparse samples) of the diatom suspension was used to make three microscope slides/sample.

The slides were analysed using an Olympus BH-2 compound light microscope at 1000x magnification. Counts were undertaken along non-overlapping transects on each slide, evenly spaced and avoiding coverslip edges. All diatoms within the field of view along each transect were visually identified to species or genus level and 400 individual diatoms were counted per sample (Armand and Leventer, 2010). Winter cup sample splits contained sparse material, so for these samples, the enumeration protocol was lowered to 100 individuals (Fatela and Taborda, 2002). Samples containing fewer than 100 diatoms are indicated with asterisks in Supplementary Tables 2a and 2b.

Taxonomic identification followed modern taxonomy as per Hasle and Syvertsen (1997). Diatoms that could not be identified to genus level were placed into additional categories: unknown pennate, unknown centric, and unknown centric < 20 μm. One group of diatoms could not be identified past genus level and was named "*Thalassiosira* sp. 1" (Rigual-Hernández et al., 2015b). This grouping contained centric diatoms larger than 20 μm with radial-style areolation, appearing to be poorly-preserved valves of the genus *Thalassiosira*. The resting spores of *Chaetoceros* species were grouped simply as *Chaetoceros* resting spores.

2.4. Calcareous microplankton sample preparation and identification

A 10 mL subsample of each split was removed prior to acid digestion to allow an analysis of the coccolithophore community assemblage and flux. The entire 10 mL subsample was used to prepare slides for light microscopy. As flux captured in the traps was low, due to limited material SEM analysis of coccoliths was not undertaken. Slides were prepared as per diatoms. Coccoliths were counted under 1000× magnification using a LEICA DMRXE polarised light microscope, and 300 coccoliths were identified per sample.

Identification of coccolithophore taxa followed Young et al. (2003) and Young et al. (2014). In total eleven coccolithophore taxa were identified from coccoliths. Only few coccospheres were detected in the samples, most likely due to the fact that the majority of the material

145

Table 1

Daily and annual fluxes of total mass flux, biogenic silica (BSiO2), calcium carbonate (CaCO3), particulate organic carbon (POC), diatom and coccolith flux, and Shannon's Equitability Index (Eh), for every cup at both trap depths (500 m and 2000 m). * indicates "annualised values." Mean annual bulk component fluxes were not calculated for the 2000 m trap due to lack of cups retrieved. Mean flux spring/summer[†] refers to the overlapping sampling period (spring and summer; cups 1−11) in which enough material was captured for analysis at both 500 m and 2000 m traps.

Cup #	Sampling midpoint	Sampling length	Total Mass Flux	BSiO$_2$		CaCO$_3$		POC		Diatom flux	Coccolith flux	Shannon's Equitability
		(days)	(mg m^{-2} d^{-1})	(mg m^{-2} d^{-1})	(%)	(mg m^{-2} d^{-1})	(%)	(mg m^{-2} d^{-1})	(%)	(x10^3 valves m^{-2} d^{-1})	(x10^6 coccoliths m^{-2} d^{-1})	Eh
500 m												
1	28/09/2003	14	26.2	1.88	7.2	16.5	63	2.7	10.2	28.3	310	0.70
2	12/10/2003	14	106.8	7.66	7.2	80.1	75	6.8	6.4	721.3	720	0.75
3	26/10/2003	14	59.3	3.06	5.2	44.4	75	4.4	7.4	229.7	825	0.72
4	9/11/2003	14	123.3	7.86	6.4	100.8	82	6.5	5.3	1248.6	1539	0.76
5	23/11/2003	14	139.1	8.79	6.3	105.1	76	8.9	6.4	810.2	2543	0.70
6	7/12/2003	14	174.6	13.59	7.8	132.0	76	11.1	6.3	7384.3	5203	0.69
7	21/12/2003	14	16.6	0.83	5.0	11.4	69	1.7	9.9	13.6	482	0.67
8	4/01/2004	14	9.0	0.37	4.1	6.5	72	0.8	9.1	12.7	205	0.67
9	18/01/2004	14	3.5	0.14	4.1	2.4	69	0.4	10.8	0.8	79	0.82
10	1/02/2004	14	6.1	0.25	4.1	4.2	69	0.7	10.8	1.5	81	0.70
11	15/02/2004	14	0.7	0.03	4.1	0.5	69	0.1	10.8	0.2	13	0.95
13	14/03/2004	14	16.9	0.54	3.2	11.1	65	2.1	12.5	64.6	221	0.63
14	28/03/2004	14	1.6	0.06	3.8	1.2	71	0.2	9.4	0.2	27	0.93
15	11/04/2004	14	2.8	0.11	3.8	2.0	71	0.3	9.4	0.4	58	0.58
16	25/04/2004	14	1.3	0.05	3.8	0.9	71	0.1	9.4	0.4	31	0.34
17	19/05/2004	35	0.2	0.01	3.8	0.1	71	0.0	9.4	0.03	5	0.77
18	23/06/2004	35	0.8	0.03	3.8	0.6	71	0.1	9.4	0.2	29	0.65
19	28/07/2004	35	0.3	0.01	3.8	0.2	71	0.0	9.4	0.09	4	0.19
20	1/09/2004	35	1.3	0.05	3.8	0.9	71	0.1	9.4	0.2	48	0.80
21	26/09/2004	14	533.1	23.41	4.4	411.1	77	33.8	6.3	5750.1	23221	0.59
Mean daily flux			**47.2**	**2.6**	**4.78**	**35.9**	**71.73**	**3.1**	**8.91**	**813.38**	**1782.22**	
Mean flux spring/summer[†]			**60.5**	**4.0**	**6.6**	**45.8**	**75.7**	**4.0**	**6.6**	**950.1**	**1091.0**	
Annual flux (g m^{-2} y^{-1})			**17***	**0.9**		**13.1**		**1.1**		**2.3 × 10^8 m^{-2} y^{-1}**	**6.5 × 10^{11} m^{-2} y^{-1}**	
Mean Eh												**0.68**
2000 m												
1	28/09/2003	14	23.1	1.9	8.3	18	76	1.38	6.0	36	78	0.78
2	12/10/2003	14	60.9	5.0	8.2	47	77	2.84	4.7	103	340	0.74
3	26/10/2003	14	52.2	4.1	7.8	39	76	2.48	4.8	169	458	0.76
4	9/11/2003	14	52.8	3.4	6.5	42	80	2.24	4.2	95	551	0.73
5	23/11/2003	14	125.0	8.7	6.9	98	78	6.11	4.9	892	1911	0.78
6	7/12/2003	14	152.2	12.3	8.1	119	78	7.36	4.8	1699	2304	0.71
7	21/12/2003	14	138.7	12.9	9.3	110	79	5.29	3.8	1081	3356	0.71
8	4/01/2004	14	74.5	6.4	8.6	58	78	3.00	4.0	326	1454	0.70
9	18/01/2004	14	118.4	14.7	12.4	86	73	5.34	4.5	1258	1316	0.70
10	1/02/2004	14	171.7	16.9	9.9	129	75	8.47	4.9	2724	1201	0.68
11	15/02/2004	14	161.1	21.3	13.2	106	66	10.86	6.7	3650	891	0.68
17	19/05/2004	35								0.39	5.01	0.80
Mean flux spring/summer[†]			**102.76**	**9.79**	**9.03**	**77.53**	**76.10**	**5.03**	**4.85**	**1093.82**	**1260.09**	
Annual flux (g m^{-2} y^{-1})			**38***	–	–	–	–	–	–	–	–	
Mean Eh												**0.73**

sinking out of the mixed layer in this region has been heavily processed by phytoplankton (Ebersbach, 2011). In addition, it is possible that some disaggregation of coccoliths from coccospheres may have occurred during sample storage, splitting and sample processing. It is worth noting that the 47°S sediment trap site location is considered representative of a large portion of the zonal SAZ (i.e. between 90 and 145°E; Trull et al., 2001c). Therefore, even if some coccoliths would have been laterally transported from a relatively distant area, it is likely that the sinking coccolith assemblages captured by the traps are still representative of the homogenous environmental conditions this sector of the SAZ. While *Gephyrocapsa muellerae* and *G. oceanica* were counted separately, coccoliths that were clearly of the genus *Gephyrocapsa*, but < 3 μm in diameter, were placed in their own grouping (*Gephyrocapsa* < 3 μm) (Flores et al., 2000). The grouping *Gephyrocapsa* < 3 μm contained *G. ericsonii* and *G. ampliaperta*, both

of which are difficult to discern under light microscopy. Most of the specimens of *Calcidiscus leptoporus* were subspecies *leptoporus*, however some of the small *C. leptoporus* complex were occasionally encountered. Coccoliths attributed to the genera *Syracosphaera, Pontosphaera, Oolithothus* and *Umbilicosphaera* were not identified past genus level.

2.5. Flux calculations and statistics

Raw counts per sample were transformed into daily fluxes using the following equation (Sancetta and Calvert 1988):

$$\text{Valve or coccolith flux } m^{-2}d^{-1} = \left(\frac{N \cdot \left(\frac{A}{a}\right) \cdot \left(\frac{V}{v}\right)}{D \cdot T} \right)$$

146

where N is the number of specimens counted, A is the area of the petri dish upon which the slide was made, a is the area of the slide counted, V is the volume of the diluted total sample, v is the volume of the split of each cup, D is the number of days of trap deployment, and T is the area of the sediment trap opening in m^2. For the diatom flux calculations, a modifier was applied after flux was calculated to compensate for the 10 mL subsample for the calcareous phytoplankton. For graphing, fluxes were transformed into relative abundances.

The Shannon-Weaver Equitability index (E_h) was used to estimate the diversity and evenness of species assemblages (Shannon and Weaver, 1949). E_h values range between zero and one, with values close to zero indicating poor diversity and evenness, and values close to one indicating high diversity and evenness.

A table of correlation matrices was constructed in order to identify relationships present between diatom and coccolith flux, and annual biogeochemical fluxes.

2.6. Meteorological and environmental data

Photosynthetically Active Radiation (PAR), chlorophyll-*a* concentration (Chl-*a*) and Sea Surface Temperature (SST) data for the trap deployment period (Aug. 2003–Oct. 2004) were obtained from the Goddard Earth Sciences Data and Information Services Centre (GES DISC) for the area 48° 30′ 0″ S–46° 30′ 0″ S×130° 0′ 0″ E–150° 0′ 0″ E (Fig. 2a; Supplementary Table 3).

2.7. Canonical correspondence analysis

Canonical Correspondence Analysis (CCA) was conducted using the free software PAST (Hammer et al., 2001). Fluxes were normalised with a log10 transformation, and CCA was applied to 19 diatom species of greater than 0.5% relative abundance present at 500 m, and to the eight coccolithophore taxa observed in two or more cups at 500 m. The environmental constraints applied were SST and PAR for both groups (Supplementary Table 3). Diatom and coccolithophore taxa groupings that emerged from the CCA were combined by relative abundance, and plotted separately over time.

3. Results

3.1. Satellite-derived environmental parameters

Photosynthetically Active Radiation (PAR) increased gradually from 21 Einstein m^{-2} d^{-1} at the beginning of the time series, and peaked in December at 45.1 Einstein m^{-2} d^{-1} (Fig. 2a; Supplementary Table 3). Then PAR values steadily decreased over autumn, reaching the annual minimum by June. Sea Surface Temperature (SST) increased slowly during spring, beginning to rise nearly 2 months after the winter-to-spring PAR increase, and eventually peaked in late December at 11 °C (Fig. 2a; Supplementary Table 3). Minimum SST was observed in June (8.3 °C). Chlorophyll-*a* concentrations in surface waters ranged from the summer maximum of 0.317 mg m^{-3}, occurring
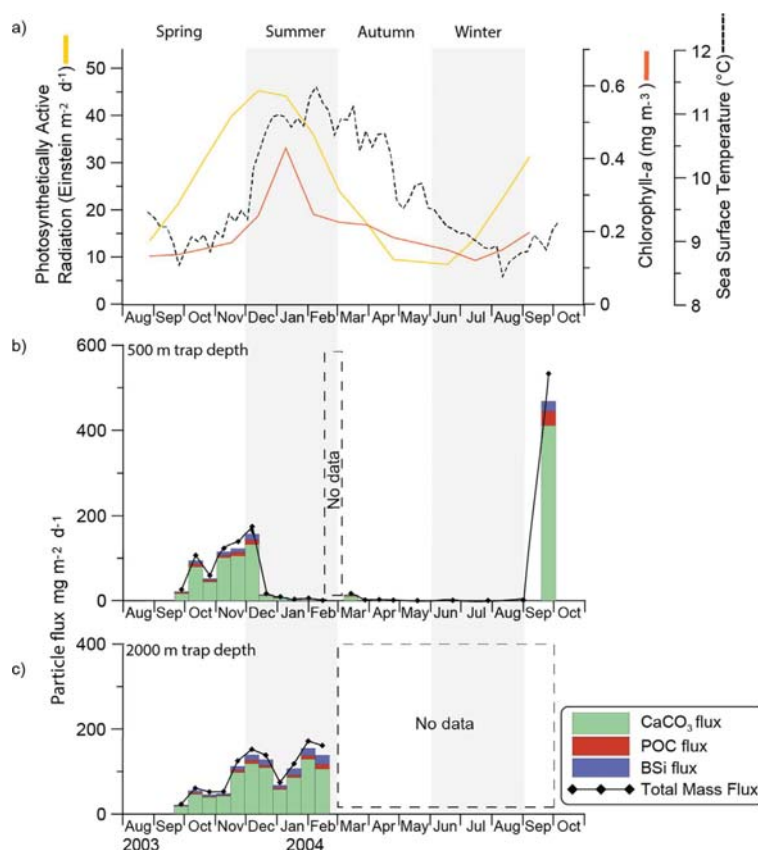
Fig. 2. Surface environmental parameters, and particle flux measurements at 500 m and 2000 m traps across the 2003–2004 study period. (a) Photosynthetically Active Radiation (PAR) (yellow line), Chlorophyll-a concentration (orange line) and Sea-Surface Temperature (SST) (black dotted line), across sampling year; (b) Carbonate (CaCO₃) (green bar), Particulate Organic Carbon (POC) (red bar), Biogenic Silica (BSi) (blue bar), and total mass flux (black line) at 500 m trap across sampling year; (c) CaCO₃, POC, BSi, and total mass flux at 2000 m trap across sampling year.

147

in late December, to winter lows of 0.12 mg m^{-3} in July (Fig. 2a; Supplementary Table 3).

3.2. Mean total mass flux and seasonality

Total Mass Flux (TMF) was calculated for the entire sampling period for 500 m (Fig. 2b; Table 1), but was only calculated for spring and summer (September-February) at 2000 m as capture was too low for the rest of the sampling year (see Section 2.1) (Fig. 2c; Table 1). TMF at 500 m ranged from a peak of 175 mg m^{-2} d^{-1} during the summer maximum in December, and dropped to below 3 mg m^{-2} d^{-1} for 6 months of the year (Table 1), and approximately 50% of the TMF accumulated between October and early December (Fig. 2b). An exceptionally high TMF value of 533 mg m^{-2} d^{-1} was recorded in a peak-flux event in September 2004 at 500 m (Fig. 2b; Table 1).

A first peak in TMF at 2000 m (152 mg m^{-2} d^{-1}) was captured in December, coinciding with the TMF peak at 500 m (Fig. 2c; Table 1). A second TMF peak, and the maximum observed at 2000 m at 172 mg m^{-2} d^{-1}, occurred in February (Fig. 2c; Table 1). Mean annual TMF was calculated at 17 g m^{-2} d^{-1} at 500 m, but was not estimated at 2000 m as capture was too low after the spring/summer months (Table 1).

The mean annual contributions of the three major components of biogeochemical flux, CaCO$_3$ POC and BSi, were calculated for the 500 m trap (Table 1). Annual values could not be determined for the 2000 m trap (see above), however mean spring/summer fluxes were calculated. CaCO$_3$ represented the bulk of TMF during the spring/summer period, averaging 76% of TMF at both trap depths (Figs. 2b and 2c; Table 1). CaCO$_3$ flux peaked in early December at 500 m, however, maximum CaCO$_3$ flux occurred during the September 2004 peak-flux event (Fig. 2b; Table 1). At 2000 m, CaCO$_3$ flux peaked in December, and reached a maximum in February (129 mg m^{-2} d^{-1}) (Fig. 2b; Table 1). POC flux during the spring/summer period averaged 7% and 5% of annual TMF at 500 m and 2000 m, respectively (Table 1). POC flux followed a similar trend at both depths, with small flux peaks in December, followed by maxima occurring simultaneously in February (Table 1). BSi fluxes were the most variable of the bulk components at 500 m. BSi made up on average 7% and 9% of TMF at 500 m and 2000 m over the spring/summer period, respectively (Table 1). BSi fluxes, as per the other bulk components, peaked in December, however maximum BSi flux was registered in the September 2004 peak-flux event (Table 1).

3.3. Diatom and coccolith total fluxes

Mean annual diatom and coccolith fluxes at 500 m were 2.3×10^8 valves m^{-2} y^{-1}, and 6.5×10^{11} coccoliths m^{-2} yr^{-1}, respectively (Table 1). Mean annual flux values of diatoms and coccoliths were not determined for the 2000 m trap, as too little material was captured after February (see Section 2.1).

At 500 m, diatom flux increased gradually from September to November, and peaked sharply to reach a maximum of 7.4×10^6 valves m^{-2} d^{-1} in December (Fig. 3a; Table 1). A second maximal peak occurred in the September 2004 peak-flux event (Fig. 3a; Table 1). From mid-summer through winter (January to September) diatom flux was low (a few hundred valves m^{-2} d^{-1}), with the exception of a small peak event in March (Fig. 3a; Table 1).

At the 2000 m trap, diatom flux increased from the beginning of the sample period to peak first in December, and again in February at which time peak fluxes occurred (3.7×10^6) (Fig. 3b; Table 1). Only one cup exists for the period after February at 2000 m (May), in which diatom fluxes were low (3.9×10^2 valves m^{-2} d^{-1}) (Fig. 3b; Table 1).

At 500 m, coccolith fluxes increased gradually between the start of sampling and spring/summer peak fluxes of 5.2×10^9 coccoliths m^{-2} d^{-1} in December (Fig. 3a; Table 1). Coccolith fluxes declined sharply in late December following the peak, and remained low until the
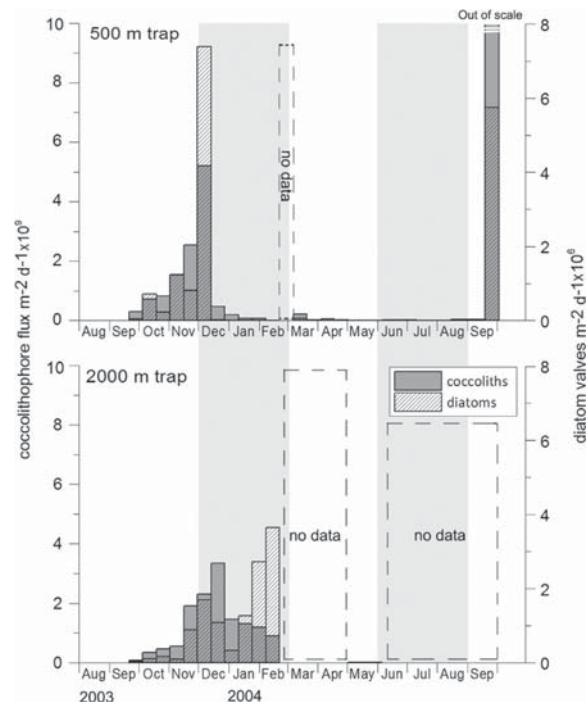
Fig. 3. Coccolith flux (coccoliths m^{-2} d^{-1}, solid grey bars), and diatom flux (valves m^{-2} d^{-1}, hashed bars) at (A) 500 m trap depth, and (B) 2000 m trap depth across the sampling year. Boxes delineated by dotted line indicate no data retrieved by sediment traps. Grey vertical bars differentiate the summer and winter months.

September 2004 peak-flux event (Fig. 3a; Table 1).

Coccolith flux at 2000 m also increased gradually before a spring/summer maximum in late December of 3.4×10^9 coccoliths m^{-2} d^{-1}, one cup later than at 500 m (Fig. 3b; Table 1). Coccolith flux declined sharply in January, after which a more gradual decline can be inferred before reaching winter lows of 5.01×10^6 coccoliths m^{-2} d^{-1} in May (Fig. 3b; Table 1).

The correlation matrices revealed correlation, to a greater or lesser extent, between all pairs of biogeochemical flux components, and diatom and coccolith flux, at both depths (p > 0.05; Table 2). Coccolith fluxes most strongly correlated with CaCO$_3$ fluxes, while diatom fluxes most strongly correlated with BSi fluxes, at both depths. Diatom flux and coccolith flux were weakly correlated with each other at both depths, but particularly at 2000 m (Table 2).

3.4. Diatom flux and seasonality

In total, 64 species or groupings of diatoms were identified between the two trap depths, with 57 diatom taxa at 500 m, and 51 taxa at 2000 m (excluding unidentified pennates and centrics) (Supplementary Tables 2a and 2b). The Shannon-Weaver Equitability index (E$_h$) for diversity and evenness was calculated for diatom assemblages at all sampling intervals, at both depths (Table 1). At 500 m, mean E$_h$ was 0.74, with greatest diversity in February, and lowest in July (Table 1). Mean E$_h$ for the spring/summer period at 2000 m was 0.73, and greatest species diversity was seen in May (Table 1).

Canonical Correspondence Analysis (CCA) was applied to log-transformed fluxes of 19 diatom species, each over 0.5% mean relative abundance at 500 m (Table 3), constrained by two environmental variables (PAR and SST) (Fig. 4a). Axis one accounted for 99.9% of the variation observed, while axis two explained the remainder. Three rough groupings of diatoms were identified, with two species,

Table 2
Correlation matrices between biogeochemical fluxes and diatom /coccolith flux. Values above 0.05 indicate significance.

500 m trap	Mass Flux	BSi flux	CaCO₃ flux	POC flux	Diatom flux	Coccolith flux
Mass Flux	–					
BSi flux	0.97	–				
CaCO3 flux	1.0	0.97	–			
POC flux	1.0	0.96	1.0	–		
Diatom flux	0.79	0.87	0.78	0.78	–	
Coccolith flux	0.97	0.89	0.97	0.97	0.74	–
2000 m trap	Mass Flux	BSi flux	CaCO₃ flux	POC flux	Diatom flux	Coccolith flux
Mass Flux	–					
BSi flux	0.92	–				
CaCO3 flux	0.99	0.86	–			
POC flux	0.94	0.94	0.88	–		
Diatom flux	0.87	0.95	0.80	0.97	–	
Coccolith flux	0.64	0.43	0.71	0.39	0.25	–

Table 3
Annual percentage contribution (Relative Abundance, RA) of diatom and coccolithophore species to total annual flux. (Note: only diatom species > 0.5% annual RA are included, and only coccolithophore taxa seen in two or more cups are included). See Supplementary Tables 2a, 2b, 4a, 4b for complete species listing.

Species	500 m		2000 m
	% flux annual	% flux spring/ summer	% flux spring/ summer
Fragilariopsis kerguelensis	24.8	21.1	15.3
Azpeitia tabularis	10.8	12.9	5.0
Chaetoceros resting spore	7.2	3.2	5.9
Thalassiosira sp. 1	7.0	10.1	3.4
Thalassiosira lineata	6.0	7.3	2.9
Roperia tesselata	2.9	3.7	1.6
Stellarima microtrias	2.5	3.2	1.3
Nitzschia bicapitata	2.3	3.2	5.9
Thalssiothrix spp.	1.7	1.1	2.4
Rhizosolenia bergonii	1.7	2.0	0.9
Hemidiscus cuneiformis	1.6	2.0	1.1
Shionodiscus oestrupii	1.6	1.6	1.4
Nitzschia sicula var. bicuneata	1.5	2.1	2.2
Shionodiscus frenguellii group	1.3	2.1	0.5
Fragilariopsis doliolus	1.2	1.5	1.0
Thalassiosira lentiginosa	0.8	1.0	0.5
Nitzschia kolaczekii	0.8	1.1	0.7
Chaetoceros vegetative cell	0.7	1.0	8.3
Thalassiosira ferelineata	0.7	0.5	0.8
Emiliania huxleyi	59.3	52.3	78.5
Gephyrocapsa spp. < 3 μm	37.9	43.3	13.0
Calcidiscus leptoporus	1.3	1.9	4.6
Helicosphaera carteri	0.8	1.0	1.7
Syracosphaera spp.	0.2	0.4	0.5
Coccolithus pelagicus	0.2	0.5	0.8
Gephyrocapsa mullerae	0.2	0.3	0.5
Gephyrocapsa oceanica	0.1	0.3	0.4

Fig. 4. Canonical Correspondence Analysis (CCA) of (A) 19 diatom; and (B) 8 coccolithophore taxa from 500 m, constrained by PAR and SST (black lines). Numbers represent sample cups. Dots represent individual species/taxa. Solid lines=ecological groupings; dashed lines=tentative groupings. (A) Diatom taxa. PAR gp.=first grouping, or PAR group; Trans gp.=second grouping, Transition group; Pres gp.=third grouping, Preservation group, as defined in text. Key: A. tab=*Azpeitia tabularis*; CRS=*Chaetoceros* resting spores; CVC=*Chaetoceros* vegetative cells; F. dol=*Fragilariopsis doliolus*; F. kerg=F. *kerguelensis*; H. cun=*Hemidiscus cuneiformis*; N. bic=*Nitzschia bicapitata*; N. kola=*N. kolaczekii*; N. sic=*Nitzschia sicula* var. *bicuneata*; R. berg=*Rhizosolenia bergonii*; R. tess=*Roperia tesselata*; S. freng. gp.=*Shionodoscus frenguellii* group; S. micro=*Stellarima microtrias*; S. oest=*Shionodiscus oestrupii* ; T. lent=*Thalassiosira lentiginosa*; T. lin=*T. lineata*; T. sp 1=*Thalassiosira* species 1; Thal'thrix=*Thalassiothrix* spp. (B) Coccolithophore taxa.

Thalassiosira ferelineata and *Nitzschia sicula* var. *bicuneata* falling outside of these groupings (Fig. 4a). The first grouping identified correlated most strongly with PAR. Group one contained *Thalassiothrix* spp., *Thalassiosira* sp. 1, *Rhizosolenia bergonii, Nitzschia kolaczekii,* and *Fragilariopsis doliolus*, with the *Shionodiscus frenguellii* group tentatively included (Fig. 4a). Combined group one reached maximum abundance peaks during spring and early summer, between September and November, and up to December (Fig. 5). *Shionodiscus frenguellii* group was included as it also displays the early growth pattern of the other group one species. The second grouping identified contained species that reached maximum abundances in late summer and autumn (end of February onwards), but were also present earlier in the season. This grouping was more closely related to SST, and included *Chaetoceros* resting spores, *Stellarima microtrias*, and *Roperia tesselata,* with the speculative inclusion of *Nitzschia bicapitata,* which also displayed high relative abundances in late summer, and in winter (Fig. 4a; Fig. 5). The third grouping identified contained the heavily silicified species *Fragilariopsis kerguelensis, Azpeitia tabularis, Thalassiosira lentiginosa, Chaetoceros* vegetative cells, *T. lineata,* and *Hemidiscus cuneiformis* (Fig. 4a). The group three species tended to occur at maximum abundances at higher SSTs (usually > 10 °C) and later in the sample
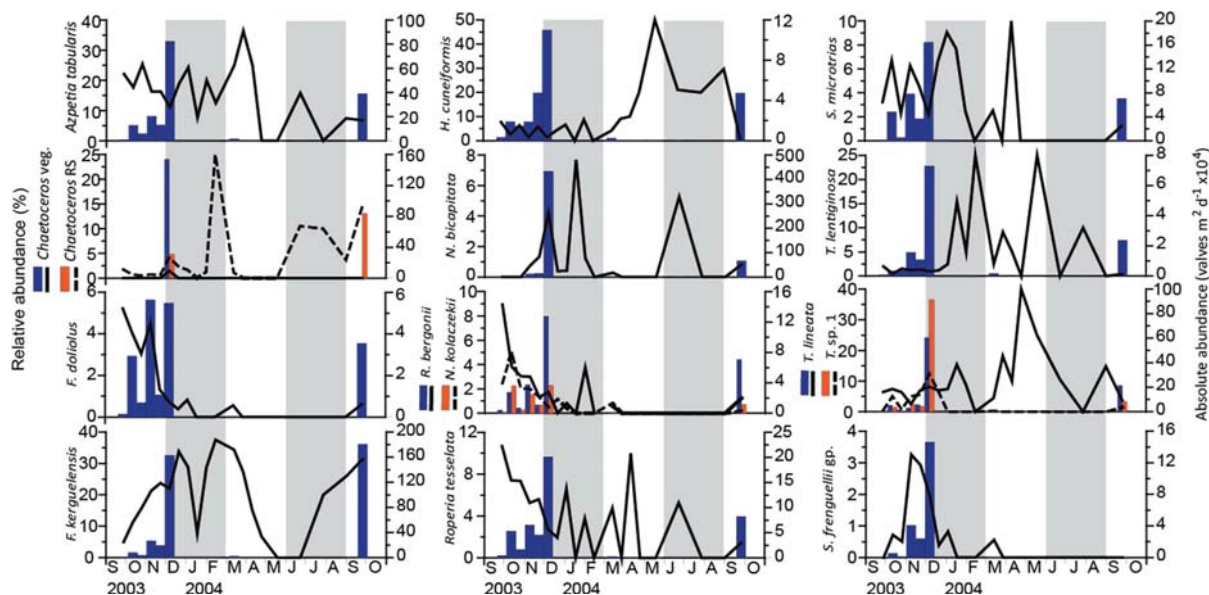
Fig. 5. Relative abundance (%; lines) and absolute abundance (valves m^2 d^{-1} × 10^4; bars) at 500 m of 15 diatom taxa of over 1% spring/summer relative abundance. Grey vertical bars differentiate the summer and winter months.

period, but were generally present year-round.

Figs. 5 and 6 show the relative and absolute abundances of the most abundant diatom species, at both depths. Species present throughout, or for most of the year, were *Azpeitia tabularis, Fragilariopsis kerguelensis* and *Roperia tesselata. Fragilariopsis kerguelensis* was the most abundant diatom in almost every month at 500 m, comprising 25% of mean annual abundance (Table 3). During the spring/summer period, *F. kerguelensis* was 21% and 15% of total diatoms captured at 500 m and 2000 m, respectively (Table 3). Seasonally, *F. kerguelensis* made up a greater portion of the diatoms captured during the mid/late summer period (–December to February), although this trend was more pro-

nounced at 500 m than at 2000 m (Figs. 5 and 6). *Azpeitia tabularis* also constituted a significant fraction of diatoms observed year-round at both depths. At 500 m, *A. tabularis* averaged 13% mean relative abundance during the spring/summer period, and reached 39% abundance at its peak in March (Fig. 5). *Azpeitia tabularis* averaged 5% across the spring/summer period at 2000 m (Fig. 6). Maximum relative abundances of *Roperia tesselata* at both 500 m and 2000 m were seen at the beginning of the sampling period in September (11% and 12%, respectively) (Figs. 5 and 6). *Roperia tesselata* relative abundances declined after September at both depths, with fluctuating abundances for the remainder of sampling (Figs. 5 and 6).
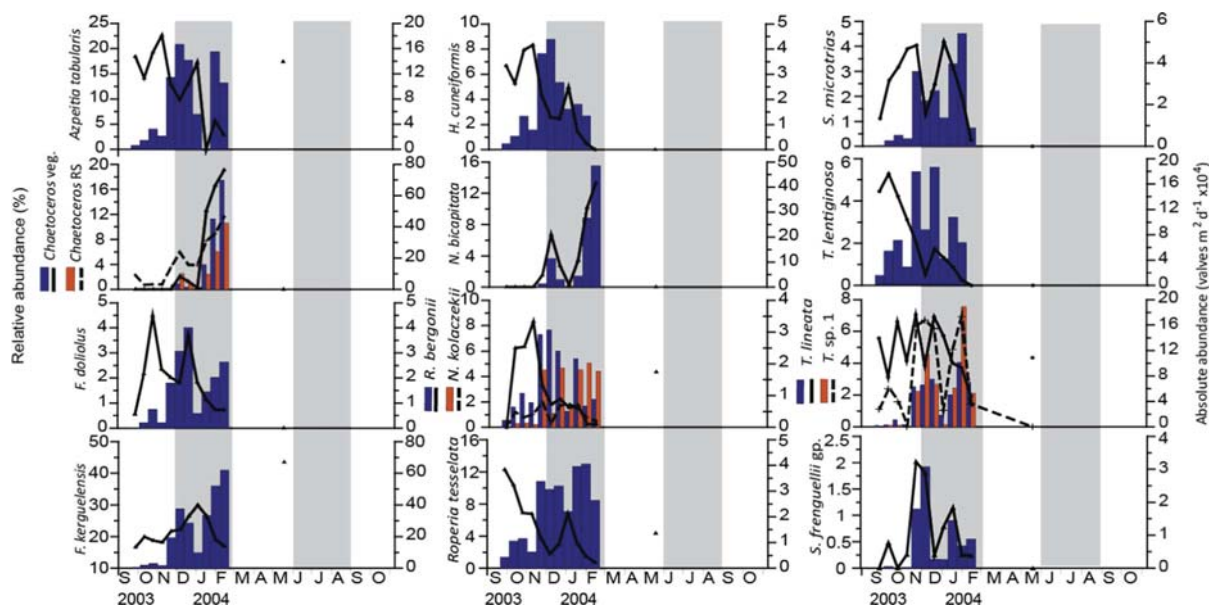
Fig. 6. Relative abundance (%; lines) and absolute abundance (valves m^2 d^{-1} ×10^4; bars) at 2000 m of 15 diatom taxa of over 1% spring/summer relative abundance. Grey vertical bars differentiate the summer and winter months.

The species present during the spring/summer period, but absent or exhibiting low abundances during the autumn and winter months were *Fragilariopsis doliolus, Nitzschia kolaczekii, Rhizosolenia bergonii, Thalassiosira* species 1, and *Shionodiscus frenguellii* group (Fig. 5). *Chaetoceros* vegetative cells were present only in one cup in early December at 500 m, but appeared slightly later at 2000 m, although they constituted a substantial 20% of relative abundances in February at 2000 m.

Several diatom species appeared at low abundances or were absent early in the year, but were present during the autumn/winter months. *Hemidiscus cuneiformis* was present throughout the spring/summer period at ~5% relative abundance, but was significant in winter assemblages, peaking to 50% relative abundance in May at 500 m (Fig. 5). At 2000 m, highest *H. cuneiformis* abundances of approximately 8% were seen in November (Fig. 6). *Thalassiosira lineata* was present throughout the sampling period at 500 m, although highest abundances occurred in late April (Fig. 5). To a lesser extent, at 2000 m *T. lineata* averaged only 3% relative abundance in the spring/ summer period, but was almost 5% of diatoms present in winter (Fig. 6).

Chaetoceros resting spores contributed little to total flux between September and early December at 500 m (~1%), but peaked in cup 11 at 25% of diatom relative abundance. Annually, *Chaetoceros* resting spores averaged 7.2% of diatom assemblages (Table 3). *Chaetoceros* resting spores were also present in winter, and towards the end of the sampling period (June to September) (Fig. 5). *Thalassiosira lentiginosa* followed a similar late-blooming trend at 500 m, with a peak abundance of 25% in February (Fig. 5). At 2000 m, *Chaetoceros* resting spores and *T. lentiginosa* comprised a relatively small component of the diatom fluxes in the spring/summer period (6% and 0.5% of relative abundance, respectively).

3.5. Coccolithophore flux and seasonality

In total, eleven coccolithophore species or groups were found in the sediment traps. *Emiliania huxleyi* dominated coccolithophore assemblages at both depths, representing 59% of total annual coccolithophore flux (Table 1).

A CCA was applied to the eight most abundant coccolithophore taxa observed in this study, constrained by PAR and SST (Fig. 4b). Axis one revealed 93% of variation in the dataset. The CCA indicated two major groupings of coccolithophore taxa (Fig. 4b). The first grouping contained three taxa: *Coccolithus pelagicus, Syracosphaera* spp.*, and *Gephyrocapsa muellerae*. The species in this grouping exhibited peak abundances in spring and summer, with lower abundances later in the sampling period, with the exception of the more complex pattern shown by *G. muellerae* (Fig. 7). The second grouping of coccolithophore taxa revealed by the CCA was composed of *Emiliania huxleyi, Gephyrocapsa* spp. < 3 μm, and *Calcidiscus leptoporus*. The species in the second grouping either exhibited peak abundances in spring/ summer and remained abundant throughout the sampling year, or were most abundant during the autumn/winter period (*E. huxleyi, C. leptoporus,* and *Gephyrocapsa* spp.; Fig. 7). Two species, *Helicosphaera carteri* and *Gephyrocapsa oceanica,* did not appear to fit with either grouping.

The relative abundance of *Emiliania huxleyi* was stable throughout the sampling period. *Emiliania huxleyi* represented 52%, and nearly 80% of spring/summer coccolith flux at 500 m and 2000 m, respectively (Table 3). Maximum *E. huxleyi* abundances occurred in April at 500 m, at which point it dominated coccolith flux at 94% of total coccolith abundance (Fig. 7). At 2000 m, the maximum peak of *E. huxleyi* occurred in December, representing 90% of coccolith abundance (Fig. 8).

Gephyrocapsa spp. < 3 μm averaged 43% of spring/summer coccolith fluxes at 500 m, but were less abundant at 2000 m, at only 13% of coccolith fluxes (Table 3). Peak abundances occurred in November at 500 m, where *Gephyrocapsa* spp. < 3 μm comprised 57% of the coccolithophore assemblage. Abundances of this group were lower in the autumn/winter period, but remained a significant fraction of the fluxes (Fig. 7). Peak *Gephyrocapsa* spp. < 3 μm abundances of about 50% of all coccoliths at 2000 m were seen in May (Fig. 8). *Calcidiscus leptoporus* and *Gephyrocapsa oceanica* showed similar trends in abudance as *Gephyrocapsa* spp., whereby both species appeared most abundant in the 500 m sediment trap in late summer/early autumn (Figs. 7 and 8) at both depths. *Calcidiscus leptoporus* reached a maximum 13% of the coccolithophore assemblage in February, but was a small contributor (av. < 4%) to coccolith fluxes for the rest of the sampling period (Fig. 7).

Syracosphaera spp. and *Coccolithus pelagicus* exhibited highest relative abundances in spring, with peaks in September and October, respectively (Fig. 7), and lower or fluctuating abundances for the rest of the sampling year. *Gephyrocapsa muellerae* was found at highest relative abundances in winter, but peaked in absolute abundance in late spring/early summer at 500 m (Fig. 7).

4. Discussion

4.1. Magnitude and composition of the particle fluxes

The annual TMF in the 500 m trap (17 g m^{-2} y^{-1}) was within the range of previous flux measurements at 1000 m at the 47°S site (15 ± 3 g m^{-2} y^{-1} at 1000 m; Rigual-Hernández et al., 2015b; Trull et al., 2001c). Moreover, annual TMF at 500 m was of the same order of magnitude as, though slightly higher than, fluxes measured in the western Pacific and New Zealand sectors of the SAZ (11.5 g m^{-2} y^{-1} at 1000 m (Honjo et al., 2000) and 14.9 g m^{-2} y^{-1} at 1500 m (Nodder et al., 2016), respectively). The similarity between fluxes recorded at 500 m (present study) and the fluxes recorded at 1000 m (Honjo et al., 2000; Nodder and Northcote, 2001) indicate that the particle fluxes experienced little change between the base of the mixed layer and the mesopelagic zone (~1000 m) (i.e. the deep twilight). Annual TMF was not calculated for the 2000 m trap, as only cups 1–11 and 17 contained enough material for analysis. When only these first 11 sampling cups representing the spring/summer period were taken into account, TMF at the 2000 m trap was higher than at the 500 m trap (103 vs. 60.5 mg m^{-2} d^{-1}, respectively) (Table 1). Trapping efficiency is often greater at depth due to lower current speeds and greater consolidation of aggregates (Scholten et al., 2001; Yu et al., 2001), potentially explaining the higher fluxes at the 2000 m trap. Input of resuspended sediment into deep sediment traps has been reported in pelagic systems (e.g. Treppke et al., 1996). The potential lithogenic transport and input from the Tasmanian coast via the Tasman Outflow (EAC derived; Herraiz-Borreguero and Rintoul, 2011) has been considered previously (Findlay, 1998; Findlay and Giraudeau, 2000; Rigual-Hernández et al., 2016b). Yet, evidence from lithogenic fluxes calculated from the initial SAZ project sediment trap deployment at 47°S (1997–1998) were very low: 0.66 g m^{-2} y^{-1} at 2000 m (Trull et al., 2001a), suggesting that the influence of resuspended sediments can be considered negligible in this study.

Biogeochemical fluxes at 47°S were carbonate-rich (> 70% annual TMF; Table 1) and silicate-poor, confirming previous regional microplankton investigations where live assemblages were dominated by non-siliceous taxa (de Salas et al., 2011; Kopczyńska et al., 2001). Coccolith flux to both depths was over three orders of magnitude greater than diatom flux. Although this study did not calculate the specific contribution of coccoliths to the carbonate component of fluxes captured in the traps, the very high correlation between coccolith and CaCO$_3$ fluxes (Table 2) suggest that coccoliths were likely an important contributor to the carbonate fraction. Likewise, diatom flux was strongly correlated with BSi flux, again suggesting that diatoms were an important component of BSi fluxes at both depths (Table 1).

151
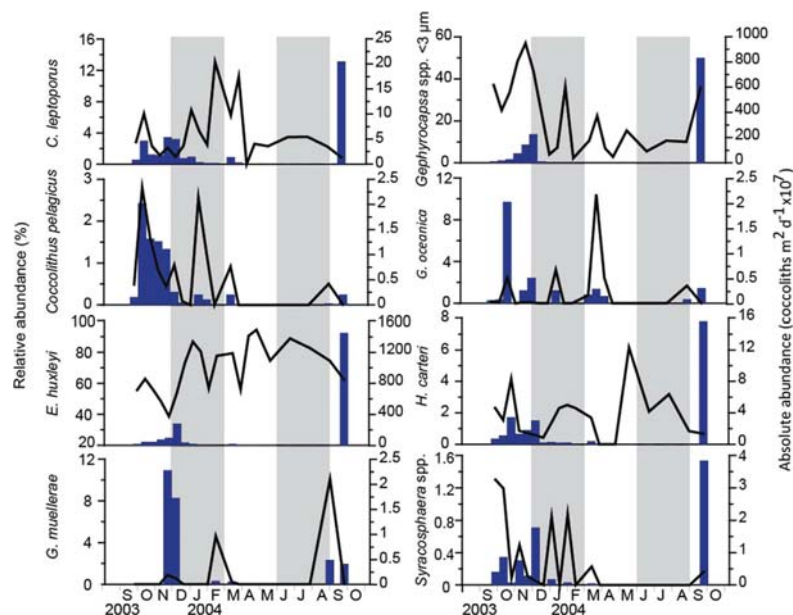
Fig. 7. Relative flux contributions (%; lines) and absolute abundance (coccoliths m^{-2} d^{-1} ×10^7; bars) of eight major coccolithophore taxa across the sampling year at 500 m. Grey vertical bars differentiate the four seasons. Missing cup 12 not indicated.

Foraminifera and pteropods are also known to be important contributors to Southern Ocean CaCO$_3$ export (Schiebel, 2002; King and Howard, 2005; Howard et al., 2011; Roberts et al., 2011), but were not considered in this study. However, both pteropod and foraminifera fluxes have been previously documented in sediment traps from the region (Howard et al., 2011 and King and Howard, 2003, respectively).

The BSi: PIC molar ratio at this site was «1 (Table 1), placing it within the "carbonate ocean" defined by Honjo et al. (2008), as

opposed to zonal systems further south where particle fluxes are diatom-dominated (i.e. "silica ocean"). The annual POC flux measured at 500 m at 47°S (1.1 g m^{-2} yr^{-1}) was similar to those reported in previous 1000 m depth deployments at the same site (0.9–1.4 g m^{-2} yr^{-1}; Rigual-Hernández et al., 2015b; Trull et al., 2001c), and in the SAZ of the western Pacific sector (1.0 g m^{-2} yr^{-1}; Honjo et al., 2000). The annual POC flux values at 500 m were similar to the global average of 1.4 g C m^{-2} d^{-1} (normalised to 2000 m; Lampitt and Antia (1997)),
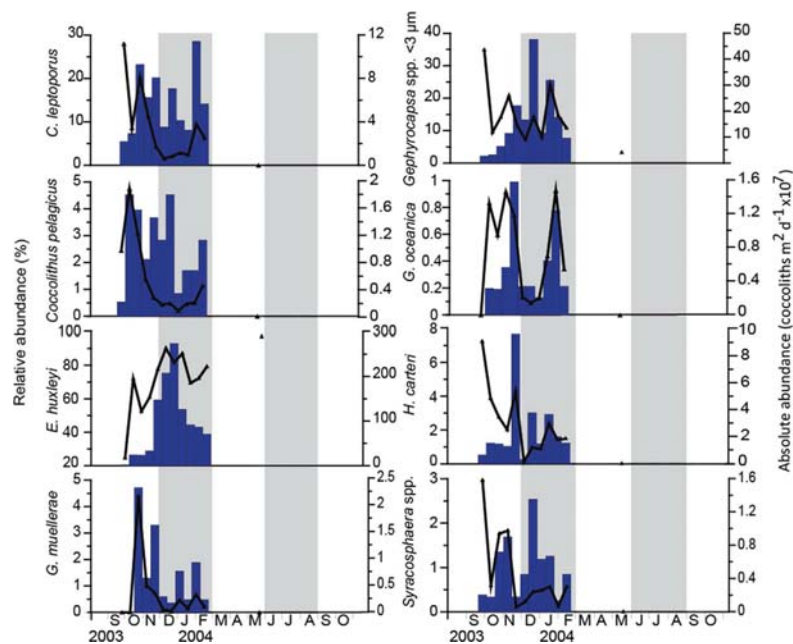
Fig. 8. Relative flux contributions (%; lines) and absolute abundance (coccoliths m^{-2} d^{-1} ×10^7; bars) of eight major coccolithophore taxa across the sampling year at 2000 m. Grey vertical bars differentiate the four seasons. No data available in March and April, and from June to October. Data from cup 17 (May) is shown as a data point on each plot.

152

45

which highlights the importance of this region for carbon sequestration despite its relatively low algal biomass accumulation (Bowie et al., 2011). In this study POC flux was not normalised due to the lack of a full annual data series from this study, and would be slightly lower if normalised to 2000 m.

4.2. Temporal dynamics of particle fluxes

Total Mass Flux (TMF) peaked in December in both the 500 and 2000 m traps, and again in February at the 2000 m trap only (Fig. 2a and b). Maximum TMF occurred one month prior to peak chlorophyll-*a* concentrations, and one sampling interval later than maximum PAR (Fig. 2a). Peak Chl-*a* represents the time at which plankton abundances are greatest, and yet TMF in the sediment trap peaked and began to decline before the Chl-*a* maximum. Although speculative, if the sediment traps were capturing material from an earlier-blooming patch of ocean due to lateral transport, then maximum trap abundances could appear to occur before peak Chl-*a* was measured. The second TMF peak at 2000 m occurred one cup later than maximum Chl-*a*, but was not observed in the 500 m trap, again suggesting the capture of a bloom upstream of the mooring site at 2000 m.

Both diatom and coccolith fluxes peaked simultaneously in December (Fig. 3), and subsided before peak Chl-*a* concentration in surface waters (Fig. 2). This observation is surprising, as diatoms typically bloom before coccolithophores in temperate (e.g. Margalef, 1978; Rigual-Hernández et al., 2013; Thunell et al., 1996) and polar regions (Alvain et al., 2008). The simultaneous peaks in biogeochemical flux components and both diatoms and coccoliths could be due to the co-sedimentation of material into the sediment traps, caused by aggregation of material (Rigual-Hernández et al., 2015b), with this speculation consistent with the correlation matrix outcomes.

The bulk of oceanic POC export in many pelagic ecosystems often occurs in the form of aggregates, which can be clusters of cells and particles ballasted by lithogenic material and phytoplankton remains and/or zooplankton faecal pellets (Honjo et al., 2008). Coccolith-ballasted aggregates are denser and tend to fall faster through the water column than diatom-ballasted aggregates (Klaas and Archer, 2002; Iversen and Ploug, 2010). Coccoliths can be "scavenged" by aggregates (De La Rocha and Passow, 2007; Iversen et al., 2010), enhancing transport speed (Iversen and Ploug, 2010). During times of high productivity (e.g. September to December at 500 m), rapid aggregate or faecal pellet formation and scavenging of smaller particles could lead to the simultaneous peaking of coccoliths and diatoms in sediment traps, as previously suggested by Rigual-Hernández et al. (2015b). The correlation between all biogeochemical components, and both phytoplankton groups shown in the correlation matrix (Table 2) lends further support to the suggestion of co-sedimentation of material, and explains why the two groups appear to flourish at the same time in sediment traps.

Particle sinking speed was not estimated in this study, however, the peaks in TMF at both 500 m and 2000 m depth that occurred in December were presumed to represent the capture of the same bloom material. For this to be the case, sinking speeds of ~107 m d^{-1} are sufficient for the 14 d capture interval in the spring/summer period. A sediment trap study in the Australian sector of the PFZ found POC sinking rates of up to 850 m d^{-1} (Ebersbach et al., 2011), hence the estimated ~107 m d^{-1} is plausible. At 47°S, however, Rigual-Hernández et al. (2016b) calculated particle settling speeds of only 20 m d^{-1} between 1000 m and 2000 m depth. These latter settling speed estimates at the deeper depths did not investigate the type or form of exported particles. Particles packaged within faecal pellets, for example, will fall much faster than amorphous aggregates (Ebersbach et al., 2011). In order for particles to travel the estimated ~107 m d^{-1} required in the present study, aggregated faecal pellets would have been the likely export particle form. The state of particles captured in this study's sediment traps was not noted due to post-collection

modification of material, however, it is possible that faecal pellets were also the main form of particle packaging and settling in this study.

Fluxes between autumn and winter (March–August, 500 m) were uncharacteristically low in comparison to a multi-year trapping study at 800 m at the same site (Rigual-Hernández et al., 2015b), while fluxes registered in September 2004 during the peak-flux event were atypically high. A potential explanation is that the trap opening clogged in mid-February, resulting in low capture for the remainder of the year, until the built-up material presumably fell, all at once, into the final cup. If this was the case, then estimates of annual TMF are still valid, as the material captured in the peak-flux event represents that of the entire late summer to winter period. However, it may not be meaningful to analyse winter flux seasonality, thus discussion hereafter focuses on the spring/summer capture period.

4.3. Coccolith and diatom fluxes

The coccolith flux values in this study are some of the highest recorded in sediment traps deployed in the Southern Ocean. By way of comparison, a study by Ternois et al. (1998) in the Indian sector of the Southern Ocean (50°S, 68°E), within the PFZ, documented coccolith fluxes four orders of magnitude lower (4.7×10^7 m^{-2} yr^{-1}), despite trapping at a similar latitude. Contrarily, studies on living coccolithophore assemblages in the New Zealand sector indicated the highest concentrations of coccolithophores within the PFZ, and lowest within the SAZ (Malinverno et al., 2015, 2016). Coccolith concentrations are seasonally so high in the Southern Ocean, particularly near the Subantarctic Front, that the region has been termed the "Great Calcite Belt" (Balch et al., 2011, 2016).

Coccolith fluxes in this study were similar to findings at more temperate sites. Broerse et al. (2000) calculated 4.4×10^{11}, and 1.4×10^{11} coccoliths m^{-2} yr^{-1} in sediment traps deployed in the subtropical (34°N) and temperate (48°N) northeast Atlantic, respectively. Ziveri et al. (2000) captured coccolith fluxes from traps placed in the northeast Atlantic (48°S) of 1×10^{10} coccoliths m^{-2} y^{-1}. In the tropical Panama Basin (2°S–8°N), traps deployed by Steinmetz (1994) recorded coccolith fluxes of 1.2×10^{11} m^{-2} yr^{-1}, and 3.3×10^{11} m^{-2} yr^{-1}. The coccolith fluxes found in the SAZ, south of Australia, appear to represent abundances transitional between those seen in polar or warmer temperate regions.

Annual diatom valve fluxes at 500 m in the present study (2.3×10^8 valves m^{-2} yr^{-1}) are in agreement with the diatom flux estimate of 0.3×10^8 valves m^{-2} yr^{-1} at 1000 m at the same site (Rigual-Hernández et al., 2015b). The latter authors' findings suggest little silica dissolution below the mixed layer, and that annual diatom export at 47°S in the SAZ, south of Australia, is relatively constant.

The temporal flux observations from the 47°S traps are in line with previous studies globally and regionally. Low diatom fluxes are typical of low-productivity areas of the carbonate ocean, such as much of the SAZ, including the present study region (Trull et al., 2001b; Honjo et al., 2008). Diatom growth in the SAZ is thought to be limited by low iron and silicic acid availability (Hutchins et al., 2001; Leblanc et al., 2005), as well as light limitation due to the deep mixed layer (Rintoul and Trull, 2001). Coccolithophores are not Si-dependent, and can tolerate low nutrient concentrations (Balch, 2004). The southernmost extent for coccolithophore growth appears to be at around 2 °C (Gravalosa et al., 2008). In the Australian sector, with the exception of *Emiliania huxleyi,* coccolithophore abundances decrease south of the SAZ, and are not found below the Polar Front (Findlay and Giraudeau, 2000). The distribution of *E. huxleyi* is more complex, forming a monospecific assemblage south of the Polar Front, before abundances halt polewards of ~60°S (Nishida, 1986; Findlay and Giraudeau, 2000). In the Indian sector of the STZ and PFZ, the high abundances of the ubiquitous *E. huxleyi* have been attributed to the inability of diatoms to take advantage of the available nutrients (Patil et al., 2014). It is likely that a similar situation occurs in the Australian

153

sector of the SAZ, whereby coccolithophores and other phytoflagellates are able to capitalise on available nutrients, hence the low diatom abundances reported in both live (Kopczyńska et al., 2007) and sediment trap samples (this study; Rigual-Hernández et al., 2015b).

4.4. Diatom assemblage composition and seasonality

The diatom assemblage at 47ºS was consistent with Subantarctic assemblages influenced by Subtropical waters, as previously reported from studies focused on both live assemblages (e.g. Kopczyńska et al., 2001; Kopczyńska et al., 2007; De Salas et al., 2011; Olguín et al., 2011; Assmy et al., 2013) and more regionalised seafloor sediment distributions (e.g. Armand et al., 2005; Crosta et al., 2005; Romero et al., 2005a, 2005b; Rigual-Hernández et al., 2016b). The influence of warmer waters relative to the trap location was demonstrated via moderate to rare occurrences of diatom taxa such as *Thalassiosira lineata, Fragilariopsis doliolus, Nitzschia* spp.*, Hemidiscus cuneiformis*, and isolated occurrences of *Cocconeis* spp. and *Diploneis* spp. (Table 3). The Zeehan Current, which flows from coastal South Australia, and southwards along western Tasmania, is a possible source of warm water species input, in conjunction with the East Australia Current (EAC)-derived Tasman Outflow (Herraiz-Borreguero and Rintoul, 2011). Thus, the possibility of diatom species input from the Tasmanian shelf is not unlikely, and previous studies have speculated on the influence of Tasmanian waters on sediment trap assemblages at the same site (Rigual-Hernández et al., 2016b). Seafloor sediment assemblages reported elsewhere resembled the species compositions observed in the traps more closely than in surface water studies, with high sediment abundances of *Azpeitia tabularis* (Romero et al., 2005a, 2005b) and *Fragilariopsis kerguelensis* (Crosta et al., 2005). Some subtropical species occurred at 47ºS, including *Fragilariopsis doliolus, Roperia tesselata, Thalassiosira symmetrica, Hemidiscus cuneiformis* and *Shionodiscus oestrupii* (formerly *Thalassiosira oestrupii*) (Crosta et al., 2005; Romero et al., 2005a, 2005b). Lower diatom assemblage diversity in winter cups was likely a product of the low sample sizes (Table 1; Supplementary Tables 2a and 2b).

The results of the CCA performed on the diatom fluxes revealed three rough ecological groupings found within sediment traps: the PAR (first group), Transition (second group), and Preservation (third group) species, which were collectively plotted by way of comparison with the current understanding of live diatom succession (Fig. 9b). These ecological groupings are consistent with the theories of diatom succession proposed by both Guillard and Kilham (1977) for the Southern Ocean, and Quéguiner (2013) for the Permanently Open Ocean Zone (POOZ) and the PFZ, summarised in Fig. 9a. Diatom succession schemes for the Southern Ocean identify two different "groups" of diatoms, forming three different assemblage stages. Early diatom assemblage succession in the POOZ and PFZ is generally dominated by fast-growing, lightly silicified species (i.e. opportunistic or r-strategists) that take quick advantage of the increased light in spring- the "group 1" species (Quéguiner 2013), forming the stage 1 assemblage (Guillard and Kilham, 1977) (Fig. 9a). As "group 1" species decline, they are overtaken by "group 2" species, which are slower-growing, large, and more heavily silicified, with a more persistent growth strategy. High abundances of "group 2" species represent stage 3 of diatom succession. Stage 2 occurs at the point junction between "group 1" and "group 2" species, and represents the most diverse stage of diatom succession (Guillard and Kilham, 1977).

Diatoms, as well as other plankton groups, preserved within sediment traps, reflect live assemblage succession after the filter of transformational processes, which occur during particle sinking, have taken place. These transformational processes include lateral transport, particle repackaging and dissolution, and as such, sediment traps are likely to provide an altered chronology of species succession and relative abundances to live assemblage studies. Fig. 9b highlights the apparent succession of the three ecological groupings identified by the
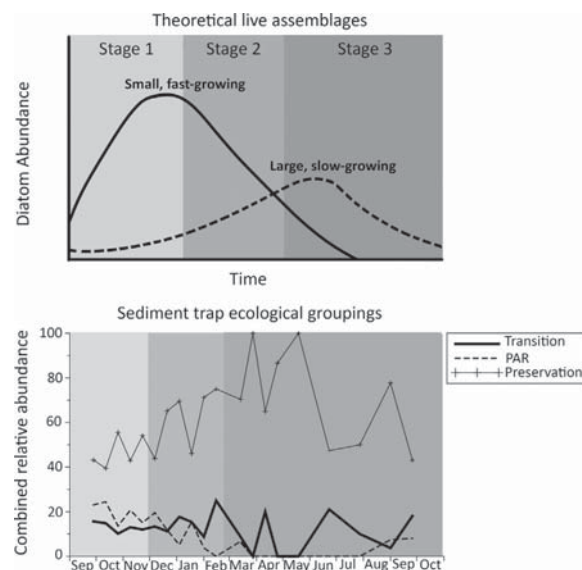
Fig. 9. Schematic illustrating theoretical diatom succession in live assemblages and sediment traps across a year in the SAZ (adapted from Guillard and Kilham (1977) and Quéguiner (2013)). (A) Theoretical live assemblage succession of diatom groups: Stage 1 (light grey)=assemblage type dominated by small, fast-growing diatoms; Stage 2 (mid grey)=transitional assemblage type with high-diversity diatom assemblage; Stage 3 (dark grey)=assemblage dominated by large, slow-growing diatoms. (B) Combined relative abundances of diatoms grouped into PAR, Transition and Preservation groups in this study, across sampling year, as per groups indicated on Fig. 4.

CCA. In 9b, the Preservation ecological grouping appears abundant year-round, and particularly in winter. Of the other two groupings, the PAR group reaches maximum abundances in early spring (during the theoretical stage 1), and is overtaken by the Transition grouping in summer (theoretical stage 2). During this theoretical stage 2 within the sediment trap assemblages, diversity indices were highest (Table 1), as per Guillard and Kilham (1977). In sediment trap stage 3, the heavily silicified Preservation grouping dominated diatom assemblages, with a sporadic presence of Transition species.

The PAR group identified from sediment trap assemblages was analogous to the stage 1 of diatom succession identified by Guillard and Kilham (1977) (Fig. 9a). This is supported by the correlation between PAR and the PAR group species in the CCA (Fig. 4a). *Chaetoceros* vegetative cells are commonly cited as the quintessential early-blooming species characteristic of this growth pattern (Smetacek et al., 2004; Assmy et al., 2013; Boyd, 2013). While the vegetative cells of *Chaetoceros* were almost absent at 500 m, they made up on average 8% of assemblages at 2000 m, appearing in late summer (December to February). *Chaetoceros* spp. are opportunistic and form localised blooms (Assmy et al., 2013), which could explain the appearance of *Chaetoceros* vegetative cells in the deeper trap alone if the 500 m and 2000 m traps were sampling from different surface ocean patches.

Of the PAR group species, *Fragilariopsis doliolus, Rhizosolenia bergonii* and *Nitzschia kolaczekii* typically inhabit more temperate waters (Hasle and Syvertsen, 1997). *Fragilariopsis doliolus* and *R. bergonii* exhibit persistent, but low, abundances within the northern SAZ (Zielinski and Gersonde, 1997). The light silicification of "group 1" species means that they are likely to be dissolved or fractured via predation in the water column, leaving a much smaller record in sediments than reflects their live abundances (Romero et al., 2000; Romero et al., 2005a, 2005b). As a result, the "group 1" diatom signal may be reduced or possibly invisible in sediment trap and seafloor sediment studies compared to live observations. In addition to this, sediment trap and seafloor sediment studies are likely to find that

154

"group 1" species appear later in the season than expected, simply due to the time elapsed between photic zone production and trap capture or sedimentation (Fig. 9a; b).

The second successional grouping, the Transition group, was characterised by the appearance of *Chaetoceros* resting spores (CRS) within the sediment traps at 500 m and 2000 m. CRS were present in spring, but appeared in significant numbers in late summer as the bloom subsided (February and January; 500 m and 2000 m respectively) (Figs. 5 and 6). CRS formation is triggered by declining environmental conditions, particularly nitrogen limitation, but also iron, silica and light limitation, such as occurs later in a bloom (e.g. Leventer, 1991; Assmy et al., 2013). Resting spore formation represents the transition from the fast-growing PAR group towards an assemblage characterised by slower-growing, heavily silicified species (Quéguiner, 2013; Boyd et al., 2013; Guillard and Kilham, 1977) (Fig. 9). Two centric species, *Stellarima microtrias* and *Roperia tesselata*, appeared within the Transition group. Both of these species were present throughout the spring sampling period, but reached maximum abundances in April before declining to almost zero abundances during the rest of the sample interval (Fig. 5). While *R. tesselata* is commonly reported from the Subantarctic, *S. microtrias* is endemic to the colder waters of the Southern Ocean (Hasle and Syvertsen, 1997). This is potentially due to the transport of cooler water northwards crossing the SAF (Rintoul and Trull, 2001), carrying this species into the study area. *Nitzschia bicapitata* was also tentatively placed within the Transition grouping, as it showed peak abundances within spring and summer, but was also present in one winter month (Fig. 5).

The third diatom grouping observed was named the Preservation group, containing almost exclusively large, well-silicified diatoms, with persistent year-round abundances, particularly abundant in the autumn and winter months from March onwards. The Preservation group archetype was *Fragilariopsis kerguelensis*, the most abundant and widespread diatom in the surface sediments of the Southern Ocean (Crosta et al., 2005). It was the most abundant diatom found in sediment traps at both depths, and present year-round, (Figs. 5 and 6; Table 3). *Fragilariopsis kerguelensis* exhibits a persistent strategy (slow growing but present season-round), and is considered to sink silica rather than carbon due to its thick, grazing and dissolution-resistant frustule (Assmy et al., 2013). Despite being abundant in traps, *F. kerguelensis* was rare in live assemblages at latitudes north of 53.7°S (Kopczyńska et al., 2007). The relative rarity of this species in surface waters compared to sediment traps points to selective enhancement of abundances due to the dissolution of lighter species, as appears the case with all of the Preservation group species.

Other preservation group diatoms included *Azpeitia tabularis*, *Thalassiosira lentiginosa*, *T. lineata*, and *Hemidiscus cuneiformis*; each considered heavily silicified and dissolution resistant species that were well preserved in the 47°S sediment traps. *Azpeitia tabularis* and *H. cuneiformis* are most abundant in subtropical waters, however *A. tabularis* is considered cold tolerant and is abundant within sediments in the SAZ (Romero et al., 2005a, 2005b). The strong presence of *H. cuneiformis* is additional evidence for potential warm, coastal water input from the north to the 47°S site, as this species tends to be associated with more saline, oligotrophic water masses (Romero et al., 2005a, 2005b). *Thalassiosira lentiginosa* is a widespread, open ocean species endemic to the Southern Ocean (Zielinski and Gersonde, 1997), and the large valves of this species were often found intact even in poorly preserved samples. The preservation group in this study can be considered akin to the "group 2" assemblage proposed by Quéguiner (2013), heralding stage 3 of diatom bloom evolution (Guillard and Kilham, 1977).

The diatoms that did not appear to sit within any grouping were *Thalassiosira ferelineata,* and the *Shionodiscus frenguellii* group. It is possible that the chosen environmental variables, SST and PAR, cannot adequately explain the abundance patterns of any of these species, and

that other variables are in play, such as nutrient availability and/or zooplankton grazing.

4.5. Coccolithophore assemblage composition and seasonality

The coccolithophores recovered from sediment traps at 47°S were similar to the *Emiliania huxleyi*-dominated assemblage observed by Findlay and Giraudeau (2000) taken from live samples at the same site.

The CCA performed on the coccoliths found in this study revealed two major ecological groupings. The first grouping contained the taxa *Coccolithus pelagicus, Syracosphaera* spp., and *Gephyrocapsa muellerae*, and appeared more strongly correlated with PAR than the second grouping (Fig. 4b). Both *C. pelagicus* and *Syracosphaera* spp. comprised more of the coccolithophore assemblage within the spring/summer period, and were largely absent during the autumn and winter months. This pattern was less distinct with *G. muellerae*, which displayed sporadic peaks in abundance between periods of absence within the traps (Fig. 7). Despite the incomplete record, the early-peaking trend of the first grouping species was more pronounced at 2000 m, with all three taxa exhibiting highest abundances in September or October, before declining to low winter abundances. Contrary to the apparent seasonal succession recorded in the traps, *Syracosphaera* spp. tend to be K-selected in other settings of the world's oceans, often reaching maximum abundances later in the productive season than more opportunistic coccolithophores (Broerse et al., 2000; Dimiza et al., 2008). In the Australian sector, *Syracosphaera* spp. were described as preferring warmer waters, and were not found live south of 49°S (Findlay and Giraudeau, 2000). Though speculative, the intrusion of warmer water filaments from the north from earlier-blooming coccolithophore populations could have resulted in the early-blooming appearance of *Syracosphaera* spp. captured by these sediment traps. In contrast to the latter species, both *C. pelagicus* and *G. muellerae* exist preferentially in cooler waters (Findlay and Giraudeau, 2000).

The second grouping revealed by the CCA included the three most abundant taxa found in sediment traps, with a preference for cooler waters: *E. huxleyi, Gephyrocapsa* spp. < 3 μm, and *C. leptoporus*, with the tentative inclusion of *G. oceanica* (Fig. 4b). The sharp rise in small *Gephyrocapsa* spp. in late spring was followed by the rise in *C. leptoporus* and *E. huxleyi* between summer and early autumn, and the subsequent assemblage dominance of *E. huxleyi* for the remainder of the year. The ubiquitous cosmopolitan *E. huxleyi* is considered the most abundant coccolithophore species at high latitudes in both hemispheres (e.g. Gravalosa et al., 2008; Saavedra-Pellitero et al., 2014; Winter et al., 2014).

Emiliania huxleyi can be broadly defined as a R-selected, opportunistic species that exhibits a high growth rate compared to other coccolithophore species (Tyrrell and Merico, 2004). High *E. huxleyi* concentrations are a common feature in the Subtropical, Subantarctic, and Polar Fronts (Balch et al., 2011). Although the factors selecting for *E. huxleyi* blooms are still unclear, the development of this species seems to be favoured by water column stability, high incident irradiance, and relatively low nutrient concentrations (Iglesias-Rodríguez et al., 2002). Indeed, *E. huxleyi* blooms in high latitude systems are often associated with moderate stratification of the water column and take place within a few weeks of the summer solstice in high latitude systems of both hemispheres (Balch, 2004). Our results agree well with this pattern as maximum of *E. huxleyi* were registered in December coinciding with both the austral summer solstice and a relatively stratified water column. Several morphotypes of this species exist, though they were not discriminated in this study, as limited material was available for coccolith analysis, and thus only light microscopy was undertaken (see Section 2.4). However, a study by Cubillos et al. (2007) identified *E. huxleyi* morphotypes in the Australian sector of the Southern Ocean, finding the overcalcified "type A" dominant within the SAZ, and replaced by lesser-calcified morpho-

155

48

types south of the SAF. Type A *E. huxleyi* coccoliths were likely the main morphotype captured in the present study.

Gephyrocapsa spp. < 3 μm were the next most abundant coccolith grouping following *E. huxleyi*, making up 37.9% mean relative abundance at 500 m, while the remaining species observed each accounted for less than 2% of total coccoliths (Table 3). *Gephyrocapsa* spp. < 3 μm are indicative of high productivity regions such as areas of upwelling (Andruleit et al., 2003). *Gephyrocapsa* spp. < 3 μm respond quickly to nutrient input, and are considered R-selected in strategy (Dimiza et al., 2008), which could explain the greater abundances of *Gephyrocapsa* spp. < 3 μm observed in the late spring/early summer period. *G. oceanica,* like the small *Gephyrocapsa* spp., are also considered R-selected (Dimiza et al., 2008), which lead to the expectation that it would peak earlier in sediment trap assemblages. While it appeared in the summer period, maximum abundances of *G. oceanica* occurred in autumn, hence its inclusion within the second coccolithophore grouping.

Calcidiscus leptoporus represented a small (usually < 10% mean relative abundance) but omnipresent component of coccoliths fluxes throughout the sampling period, at both depths (Fig. 6). This species tends to inhabit cool, nutrient rich waters (Boeckel et al., 2006). Like *E. huxleyi*, several morphotypes of this species exist, however, they were not identified in this study. Future work on sediment trap records in the Australian sector will help to clarify the morphologies of *C. leptoporus* in the SAZ. The abundance of *C. leptoporus* at 2000 m was greater than twice that at 500 m during the spring/summer period (Table 3), again possibly the result of some lateral transport of coccoliths.

Helicosphaera carteri exhibited patchy abundances throughout the year, peaking in both spring and autumn/winter (Fig. 7), which likely resulted in it appearing distinct from both groups in the CCA (Fig. 4b). The placement of *H. carteri* closer to the second coccolithophore grouping could reflect its preference for cooler waters, like the majority of the second grouping species.

4.6. Ecology and seasonal succession of diatoms and coccolithophores

This study found evidence largely consistent with the previously diatom succession schemes. All three stages of diatom succession were visible in the 47°S sediment trap assemblages, and corresponded to the stages/groups outlined by previous workers on diatom succession. We presumed that the second stage in diatom succession (i.e. Transitional assemblage group; Fig. 9) was likely to be of shorter duration at depth than in live assemblages. This is believed to be because the signal of early-blooming taxa is small within traps due to dissolution, thus assemblages are soon dominated by Preservation species, which represent the greater fraction of diatoms captured in sediment traps. Of the Transition group, only the presence of *Chaetoceros* resting spores was an undeniable indicator. The Preservation group on the other hand was unmistakeable in sediment traps, being more likely to survive export intact than the other two groups. Selective preservation of heavily silicified diatom species is most likely the main factor determining the strongest evidence for stage 3 diatom succession in the sediment traps (Fig. 9). The links between photic zone production and sediment preservation are complex and unclear, with implications for studies aiming to reconstruct past oceanic conditions using seafloor sediment. Thus, further investigations in both surface layer and sediment traps as well as in other sectors of the circumpolar SAZ are required to better understand the diatom seasonal succession and links between production and export in this region of the world's ocean.

Moreover, the data presented here represents the first seasonal record of coccolithophore species succession in the SAZ. Coccolithophore assemblage composition, registered by the sediment traps, were consistent with previously reported live coccolithophore assemblages in the surface waters of the region. Coccolithophore assemblages were dominated by the ubiquitous species *E. huxleyi*

which represented 59% of the annual assemblage. Two ecological groupings were observed relating to the seasonal succession of coccolithophores captured in traps. The first grouping contained three taxa (*Coccolithus pelagicus*, *Syracosphaera* spp., and *Gephyrocapsa muellerae*) with seasonality associated with PAR. These species tended to peak within the spring/summer period, and were absent or low in autumn and winter. The second ecological grouping contained taxa either displaying greater abundances outside of the spring/summer period (e.g. *C. leptoporus*), or that were present persistently year-round (such as *E. huxleyi*). The appearance of coccolithophore succession from these sediment trap records was complex, and it is speculated that oceanographic influences, such as warm water intrusion from the north, influenced assemblages captured by the sediment traps. A seasonal evolution scheme of coccolithophore communities, like that of diatoms, remains to be constructed. Further sediment trap studies of seasonal coccolithophore assemblages will allow for a deeper understanding of coccolithophore ecology. Live assemblage sampling in the SAZ, and analyses of coccolithophore assemblages within, will be necessary to begin to identify a generalised successional scheme for this group.

5. Conclusions

This study reports on the biochemical, siliceous and calcareous phytoplankton fluxes registered by a time-series sediment trap deployed during a year in the Australian sector of the SAZ at 500 m and 2000 m depths. The BSi: PIC reflects the high abundance of coccolithophores and other calcareous microplankton in comparison with diatoms (three orders of magnitude lower). The specific contribution of the two phytoplankton groups to POC export could not be quantified, however, it is suggested that coccoliths provide a major source of ballast for settling particles in this sector of the SAZ. Total mass fluxes were seasonal, with the overwhelming majority of material captured between spring and early summer. The maximum particle flux was registered at the same time at both depths, despite a 1500 m vertical disparity between the traps, leading to the inference that particle settling speed was high, at ~100 m d^{-1}.

Diatom assemblages in this study displayed some expected successional trends in keeping with ecological succession theory, with some differences thought to have resulted from the transformation of particles anticipated to have occurred at depth and with particle export. Diatom assemblages were roughly categorised into three ecological groupings: the "PAR group" of fast-proliferating, early blooming species, the "Transition group", and the "Preservation group" of heavily silicified large diatoms. A scheme is presented illustrating the effects of transport through the water column on the appearance of diatom succession from sediment trap records in the SAZ. Further comparison of diatom successional patterns between live and sediment assemblages is warranted to better understand the transformational processes at play in this region. Palaeoreconstructions using preserved diatoms, and particularly those that use diatoms as seasonal signals, rely upon accurately linking surface processes to the sediment. Future clarification of how live diatom assemblage seasonality is reflected in the sediment or in sediment traps will lend greater accuracy to palaeoreconstructive work.

Coccolith assemblages also displayed some successional trends, with two ecological groupings of taxa identified within sediment traps. The precise interaction between these ecological groupings and environmental variables is yet to be determined, and will require further sediment trap analysis. Work on differentiating the morphological variations among coccoliths captured by sediment traps in the Australian sector will be conducted in future studies.

A deeper understanding of the biological and physical processes that control the carbon export in the SAZ is of critical importance to determine of the role of the Southern Ocean in the global cycling of nutrients and climate. The results of the present and previous studies

156

on the 47ºS site show that the carbon export in the Australian sector of the SAZ is similar to those reported in other zonal systems further south (PFZ and AZ). Coccolithophore-related carbon export has been found to be significant in the SAZ, however, the specific contribution of different species to export, and the expression of coccolithophore seasonality in sediment traps, will be the focus of future trapping studies.

Acknowledgements

Appendix A. Supplementary material

Supplementary data associated with this article can be found in the online version at doi:10.1016/j.dsr.2017.01.001.

References

Alvain, S., Moulin, C., Dandonneau, Y., Loisel, H., 2008. Seasonal distribution and succession of dominant phytoplankton groups in the global ocean: a satellite view. Glob. Biogeochem. Cycles 22.

Anderson, R.F., Smith, W.O., Jr, 2001. The US Southern Ocean joint Global Ocean flux study: volume two. Deep-Sea Res. Part II: Top. Stud. Oceanogr. 48, 3883–3889. http://dx.doi.org/10.1016/S0967-0645(01)00072-8.

Andruleit, H., Stäger, S., Rogalla, U., Čepek, P., 2003. Living coccolithophores in the northern Arabian Sea: ecological tolerances and environmental control. Mar. Micropaleontol. 49, 157–181.

Armand, L.K., Crosta, X., Romero, O., Pichon, J.-J., 2005. The biogeography of major diatom taxa in Southern Ocean sediments: 1. Sea ice related species. Palaeogeography, Palaeoecology. Palaeoecology 223, 93–126.

Armand, L.K., Leventer, A., 2010. Palaeo sea ice distribution and reconstruction derived from the geological records. Sea ice, 469–530.

Assmy, P., Smetacek, V., Montresor, M., Klaas, C., Henjes, J., Strass, V.H., Arrieta, J.M., Bathmann, U., Berg, G.M., Breitbarth, E., 2013. Thick-shelled, grazer-protected diatoms decouple ocean carbon and silicon cycles in the iron-limited Antarctic circumpolar current. Proc. Natl. Acad. Sci. 110, 20633–20638.

Balch, W.M., 2004. Re-evaluation of the physiological ecology of coccolithophores. In: Thierstein, H.R., Young, J.R. (Eds.), Coccolithophores: from molecular processes to global impact. Springer Science & Business Media, 156–190.

Balch, W.M., Drapeau, D.T., Bowler, B.C., Lyczskowski, E., Booth, E.S., Alley, D., 2011. The contribution of coccolithophores to the optical and inorganic carbon budgets during the Southern Ocean gas exchange experiment: new evidence in support of the "Great calcite Belt" hypothesis. J. Geophys. Res.: Oceans 1978–2012, 116. http://dx.doi.org/10.1029/2011JC006941.

Balch, W.M., Bates, N.R., Lam, P.J., Twining, B.S., Rosengard, S.Z., Bowler, B.C., Drapeau, D.T., Garley, R., Lubelczyk, L.C., Mitchell, C., Rauschenberg, S., 2016. Factors regulating the Great Calcite Belt in the Southern Ocean and its biogeochemical significance. Glob. Biogeochem. Cycles 30, 1124–1144. http://dx.doi.org/10.1002/2016GB005414.

Baker, E.T., Milburn, H.B., Tennant, D.A., 1988. Field assessment of sediment trap efficiency under varying flow conditions. J. Mar. Res. 46, 573–592.

Blain, S., Tréguer, P., Belviso, S., Bucciarelli, E., Denis, M., Desabre, S., Fiala, M., Jézéquel, V.M., Le Fèvre, J., Mayzaud, P., 2001. A biogeochemical study of the island mass effect in the context of the iron hypothesis: Kerguelen Islands, Southern Ocean. Deep-Sea Res. Part I:Oceanogr. Res.Pap. 48, 163–187.

Boeckel, B., Baumann, K.-H., Henrich, H., Kinkel, H., 2006. Coccolith distribution patterns in South Atlantic and Southern Ocean surface sediments in relation to environmental gradients. Deep-Sea Res. Part I: Oceanogr. Res. Pap. 53, 1073–1099.

Bowie, A.R., Brian Griffiths, F., Dehairs, F., Trull, T.W., 2011. Oceanography of the subantarctic and Polar Frontal Zones south of Australia during summer: Setting for the SAZ-Sense study. Deep-Sea Res. Part II: Top. Stud. Oceanogr. 58, 2059–2070. http://dx.doi.org/10.1016/j.dsr2.2011.05.033.

Boyd, P.W., Watson, A.J., Law, C.S., Abraham, E.R., Trull, T., Murdoch, R., Bakker, D.C.E., Bowie, A.R., Buesseler, K.O., Chang, H., Charette, M., Croot, P., Downing, K., Frew, R., Gall, M., Hadfield, M., Hall, J., Harvey, M., Jameson, G., LaRoche, J., Liddicoat, M., Ling, R., Maldonado, M.T., McKay, R.M., Nodder, S., Pickmere, S., Pridmore, R., Rintoul, S., Safi, K., Sutton, P., Strzepek, R., Tanneberger, K., Turner, S., Waite, A., Zeldis, J., 2000. A mesoscale phytoplankton bloom in the polar Southern Ocean stimulated by iron fertilization. Nature 407, 695–702.

Boyd, P.W., 2013. Diatom traits regulate Southern Ocean silica leakage. Proc. Natl. Acad. Sci. 110, 20358–20359.

Bray, S., Trull, T., Manganini, S., 2000. SAZ project moored sediment traps: results of the 1997–1998 deployments. Antarctic CRC.

Broerse, A.T., Ziveri, P., van Hinte, J.E., Honjo, S., 2000. Coccolithophore export production, species composition, and coccolith-CaCO 3 fluxes in the NE Atlantic (34ºN21ºW and 48ºN21ºW). Deep-Sea Res. Part II: Top. Stud. Oceanogr. 47, 1877–1905.

Bucciarelli, E., Blain, S., Tréguer, P., 2001. ron and manganese in the wake of the Kerguelen Islands (Southern Ocean). Mar. Chem. 73, 21–36.

Crosta, X., Romero, O., Armand, L.K., Pichon, J.-J., 2005. The biogeography of major diatom taxa in Southern Ocean sediments: 2. open ocean related species. Palaeogeogr., Palaeoclimatol., Palaeoecol. 223, 66–92.

Cubillos, J., Wright, S., Nash, G., De Salas, M., Griffiths, B., Tilbrook, B., Poisson, A., Hallegraeff, G., 2007. Calcification morphotypes of the coccolithophorid *Emiliania huxleyi* in the Southern Ocean: changes in 2001 to 2006 compared to historical data. Mar. Ecol. Prog. Ser. 348, 47–54.

Cubillos, J.C., Henderiks, J., Beaufort, L., Howard, W.R., Hallegraeff, G.M., 2012. Reconstructing calcification in ancient coccolithophores: individual coccolith weight and morphology of *Coccolithus pelagicus* (sensu lato). Mar. Micropaleontol. 92–93, 29–39. http://dx.doi.org/10.1016/j.marmicro.2012.04.005.

De La Rocha, C.L., Passow, U., 2007. Factors influencing the sinking of POC and the efficiency of the biological carbon pump. Deep-Sea Res. Part II: Top. Stud. Oceanogr. 54, 639–658.

De Salas, M.F., Eriksen, R., Davidson, A.T., Wright, S.W., 2011. Protistan communities in the Australian sector of the Sub-Antarctic Zone during SAZ-Sense. Deep-Sea Res. Part II: Top. Stud. Oceanogr. 58, 2135–2149. http://dx.doi.org/10.1016/j.dsr2.2011.05.032.

Dimiza, M.D., Triantaphyllou, M.V., Dermitzakis, M.D., 2008. Seasonality and ecology of living coccolithophores in eastern Mediterranean coastal environment (Andros Island, middle Aegean Sea). Micropaleontology 54, 159–175. http://dx.doi.org/10.2307/30130910.

Ebersbach, F., Trull, T.W., Davies, D.M., Bray, S.G., 2011. Controls on mesopelagic particle fluxes in the Sub-Antarctic and Polar Frontal Zones in the Southern Ocean south of Australia in summer—Perspectives from free-drifting sediment traps. Deep-Sea Res. Part II: Top. Stud. Oceanogr. 58, 2260–2276.

Fatela, F., Taborda, R., 2002. Confidence limits of species proportions in microfossil assemblages. Mar. Micropaleontol. 45, 169–174.

Findlay, C.S., 1998. Living and fossil calcareous nannoplankton from the Australian sector of the Southern Ocean: implications for paleoceanography (PhD dissertation). University of Tasmania.

Findlay, C.S., Giraudeau, J., 2000. Extant calcareous nannoplankton in the Australian Sector of the Southern Ocean (austral summers 1994 and 1995). Mar. Micropaleontol. 40, 417–439. http://dx.doi.org/10.1016/S0377-8398(00)00046-3.

Fischer, G., Gersonde, R., Wefer, G., 2002. Organic carbon, biogenic silica and diatom fluxes in the marginal winter sea-ice zone and in the Polar Front Region: interannual variations and differences in composition. Deep.-Sea Res. Part II:Top. Stud.Oceanogr. 49, 1721–1745.

Flores, J.-A., Gersonde, R., Sierro, F., Niebler, H.-S., 2000. Southern Ocean Pleistocene calcareous nannofossil events: calibration with isotope and geomagnetic stratigraphies. Mar. Micropaleontol. 40, 377–402.

Flores, J., Sierro, F., 1997. Revised technique for calculation of calcareous nannofossil accumulation rates. Micropaleontology, 321–324.

Fripat, F., Leblanc, K., Elskens, M., Cavagna, A.-J., Armand, L., André, L., Dehairs, F., Cardinal, D., 2011. Efficient silicon recycling in summer in both the Polar Frontal and Subantarctic Zones of the Southern Ocean. Mar. Ecol. Prog. Ser. 435, 47–61.

Goddard Earth Sciences Data and Information Services Centre (2012, last updated 2013) 〈http://disc.sci.gsfc.nasa.gov/giovanni#maincontent〉, accessed 14/07/2014

Gravalosa, J.M., Flores, J.-A., Sierro, F.J., Gersonde, R., 2008. Sea surface distribution of coccolithophores in the eastern Pacific sector of the Southern Ocean (Bellingshausen and Amundsen Seas) during the late austral summer of 2001. Mar. Micropaleontol. 69, 16–25.

Guillard, R.R.L., Kilham, P., 1977. The ecology of marine planktonic diatoms. In: Werner, D. (Ed.), The Biology of Diatoms. Blackwell Oxford, 372–469.

Hammer, Ø., Harper, D.A.T., Ryan, P.D., 2001. PAST: Paleontological statistics software package for education and data analysis. Palaeontol. Electron. 4, 9.

Hasle, G., Syvertsen, E., 1997. Identifying Marine Phytoplankton. Academic Press, San Diego, CA.

Herraiz-Borreguero, L., Rintoul, S.R., 2011. Regional circulation and its impact on upper ocean variability south of Tasmania. Deep-Sea Res. Part II: Top. Stud. Oceanogr. 58, 2071–2081. http://dx.doi.org/10.1016/j.dsr2.2011.05.022.

Honjo, S., Francois, R., Manganini, S., Dymond, J., Collier, R., 2000. Particle fluxes to the interior of the Southern Ocean in the Western Pacific sector along 170°W. Deep-Sea Res. Part II: Top. Stud. Oceanogr. 47, 3521–3548. http://dx.doi.org/10.1016/S0967-0645(00)00077-1.

Honjo, S., Manganini, S.J., Krishfield, R.A., Francois, R., 2008. Particulate organic carbon fluxes to the ocean interior and factors controlling the biological pump: a synthesis of global sediment trap programs since 1983. Prog. Oceanogr. 76, 217–285.

157

Howard, W.R., Roberts, D., Moy, A.D., Lindsay, M.C.M., Hopcroft, R.R., Trull, T.W., Bray, S.G., 2011. Distribution, abundance and seasonal flux of pteropods in the Sub-Antarctic Zone. Deep-Sea Res. Part II: Top. Stud. Oceanogr. 58, 2293–2300. http://dx.doi.org/10.1016/j.dsr2.2011.05.031.

Hutchins, D.A., Sedwick, P.N., DiTullio, G.R., Boyd, P.W., Quéguiner, B., Griffiths, F.B., Crossley, C., 2001. Control of phytoplankton growth by iron and silicic acid availability in the subantarctic Southern Ocean: experimental results from the SAZ Project. J. Geophys. Res.: Oceans 106, 31559–31572. http://dx.doi.org/10.1029/2000JC000333.

Iversen, M.H., Nowald, N., Ploug, H., Jackson, G.A., Fischer, G., 2010. High resolution profiles of vertical particulate organic matter export off Cape blanc, Mauritania: degradation processes and ballasting effects. Deep-Sea Res. Part I: Oceanogr. Res. Pap. 57, 771–784.

Iversen, M., Ploug, H., 2010. Ballast minerals and the sinking carbon flux in the ocean: carbon-specific respiration rates and sinking velocity of marine snow aggregates. Biogeosciences 7, 2613–2624.

King, A.L., Howard, W.R., 2003. Planktonic foraminiferal flux seasonality in Subantarctic sediment traps: a test for paleoclimate reconstructions. Paleoceanography 18.

King, A.L., Howard, W.R., 2005. δ18O seasonality of planktonic foraminifera from Southern Ocean sediment traps: latitudinal gradients and implications for paleoclimate reconstructions. Mar. Micropaleontol. 56, 1–24. http://dx.doi.org/10.1016/j.marmicro.2005.02.008.

Klaas, C., Archer, D.E., 2002. Association of sinking organic matter with various types of mineral ballast in the deep-sea: implications for the rain ratio. Glob. Biogeochem. Cycles 16, 63–61-63-14.

Kopczyńska, E.E., Dehairs, F., Elskens, M., Wright, S., 2001. Phytoplankton and microzooplankton variability between the Subtropical and Polar Fronts south of Australia: thriving under regenerative and new production in late summer. J. Geophys. Res.: Oceans (1978–2012) 106, 31597–31609.

Kopczyńska, E.E., Savoye, N., Dehairs, F., Cardinal, D., Elskens, M., 2007. spring phytoplankton assemblages in the Southern Ocean between Australia and Antarctica. Polar Biol. 31, 77–88.

Lampitt, R., Antia, A., 1997. Particle flux in deep seas: regional characteristics and temporal variability. Deep-Sea Res. Part I: Oceanogr.Res. Pap. 44, 1377–1403.

Leblanc, K., Hare, C.E., Boyd, P.W., Bruland, K.W., Sohst, B., Pickmere, S., Lohan, M.C., Buck, K., Ellwood, M., Hutchins, D.A., 2005. Fe and Zn effects on the Si cycle and diatom community structure in two contrasting high and low-silicate HNLC areas. Deep-Sea Res. Part I: Oceanogr. Res. Pap. 52, 1842–1864. http://dx.doi.org/10.1016/j.dsr.2005.06.005.

Leventer, A., 1991. Sediment trap diatom assemblages from the northern Antarctic Peninsula region. Deep-Sea Res. Part A. Oceanogr. Res. Pap. 38, 1127–1143. http://dx.doi.org/10.1016/0198-0149(91)90099-2.

Lourey, M.J., Trull, T.W., 2001. Seasonal nutrient depletion and carbon export in the Subantarctic and Polar Frontal Zones of the Southern Ocean south of Australia. J. Geophys. Res.: Oceans 106, 31463–31487.

Malinverno, E., Triantaphyllou, M.V., Dimiza, M.D., 2015. Coccolithophore assemblage distribution along a temperate to polar gradient in the West Pacific sector of the Southern Ocean (January 2005). Micropaleontology 61, 489–506.

Malinverno, E., Maffioli, P., Gariboldi, K., 2016. Latitudinal distribution of extant fossilizable phytoplankton in the Southern Ocean: planktonic provinces, hydrographic fronts and palaeoecological perspectives. Mar. Micropaleontol. 123, 41–58.

Margalef, R., 1978. Life-forms of phytoplankton as survival alternatives in an unstable environment. Oceanol. Acta 1, 493–509.

Metzl, N., Tilbrook, B., Poisson, A., 1999. The annual fCO2 cycle and the air–sea CO2 flux in the sub-Antarctic Ocean. Tellus B 51, 849–861.

Nishida, S., 1986. Nannoplankton flora in the Southern Ocean, with special reference to siliceous varieties. Mem. Natl. Inst. Polar Res. 40, 56–68.

Nodder, S.D., Northcote, L.C., 2001. Episodic particulate fluxes at southern temperate mid-latitudes (42–45 S) in the Subtropical Front region, east of New Zealand. Deep-Sea Res. Part I: Oceanogr. Res. Pap. 48, 833–864.

Nodder, S.D., Chiswell, S.M., Northcote, L.C., 2016. Annual cycles of deep-ocean biogeochemical export fluxes in subtropical and subantarctic waters, southwest Pacific ocean. J. Geophys. Res.: Oceans 121, 2405–2424. http://dx.doi.org/10.1002/2015JC011243.

Olguín, H.F., Alder, V.A., 2011. Species composition and biogeography of diatoms in antarctic and subantarctic (Argentine shelf) waters (37–76 S). Deep Sea Res. Part II: Top. Stud. Oceanogr. 58, 139–152.

Orsi, A.H., Whitworth, T., Nowlin, W.D., 1995. On the meridional extent and fronts of the Antarctic circumpolar Current. Deep-Sea Res. Part I: Oceanogr. Res. Pap. 42, 641–673.

Patil, S.M., Mohan, R., Shetye, S., Gazi, S., Jafar, S., 2014. Morphological variability of *Emiliania huxleyi* in the Indian sector of the Southern Ocean during the austral summer of 2010. Mar. Micropaleontol. 107, 44–58.

Pollard, R., Lucas, M., Read, J., 2002. Physical controls on biogeochemical zonation in the Southern Ocean. Deep-Sea Res. Part II: Top. Stud. Oceanogr. 49, 3289–3305.

Quéguiner, B., 2001. Biogenic silica production in the Australian sector of the Subantarctic zone of the Southern Ocean. J. Geophys. Res. 106, 31627–631,636.

Quéguiner, B., 2013. Iron fertilization and the structure of planktonic communities in high nutrient regions of the Southern Ocean. Deep-Sea Res. Part II: Top. Stud. Oceanogr. 90, 43–54. http://dx.doi.org/10.1016/j.dsr2.2012.07.024.

Ragueneau, O., Tréguer, P., Leynaert, A., Anderson, R.F., Brzezinski, M.A., DeMaster, D.J., Dugdale, R.C., Dymond, J., Fischer, G., François, R., Heinze, C., Maier-Reimer, E., Martin-Jézéquel, V., Nelson, D.M., Quéguiner, B., 2000. A review of the Si cycle in the modern ocean: recent progress and missing gaps in the application of biogenic opal as a paleoproductivity proxy. Glob. Planet. Change 26, 317–365. http://

dx.doi.org/10.1016/S0921-8181(00)00052-7.

Rembauville, M., Meilland, J., Ziveri, P., Schiebel, R., Blain, S., Salter, I., 2016. Planktic foraminifer and coccolith contribution to carbonate export fluxes over the central Kerguelen Plateau. Deep-Sea Res. Part I: Oceanogr. Res. Pap. 111, 91–101. http://dx.doi.org/10.1016/j.dsr.2016.02.017.

Rigual-Hernández, A.S., Bárcena, M.A., Jordan, R.W., Sierro, F.J., Flores, J.A., Meier, K.S., Beaufort, L., Heussner, S., 2013. Diatom fluxes in the NW Mediterranean: evidence from a 12-year sediment trap record and surficial sediments. J. Plankton Res. 35, 1109–1125.

Rigual-Hernández, A.S., Trull, T.W., Bray, S.G., Closset, I., Armand, L.K., 2015a. Seasonal dynamics in diatom and particulate export fluxes to the deep-sea in the Australian sector of the southern Antarctic Zone. J. Mar. Syst. 142, 62–74. http://dx.doi.org/10.1016/j.jmarsys.2014.10.002.

Rigual-Hernández, A, Trull, T., Bray, S., Cortina, A., Armand, L., 2015b. Latitudinal and temporal distributions of diatom populations in the pelagic waters of the Subantarctic and Polar Frontal Zones of the Southern Ocean and their role in the biological pump. Biogeosciences 12, 5309–5337.

Rigual-Hernández, A.S., Trull, T.W., Bray, S.G., Armand, L.K., 2016b. The fate of diatom valves in the Subantarctic and polar frontal zones of the Southern Ocean: sediment trap versus surface sediment assemblages. Palaeogeogr., Palaeoclimatol., Palaeoecol. 457, 129–143. http://dx.doi.org/10.1016/j.palaeo.2016.06.004.

Rintoul, S.R., Griffiths, F.B., 2001. A persistent subsurface chlorophyll maximum in the. J. Geophys. Res. 106, 31,543–531,557.

Rintoul, S.R., Trull, T.W., 2001. Seasonal evolution of the mixed layer in the Subantarctic zone south of Australia. J. Geophys. Res.: Oceans 106, 31447–31462.

Roberts, D., Howard, W.R., Moy, A.D., Roberts, J.L., Trull, T.W., Bray, S.G., Hopcroft, R.R., 2011. Interannual variability in sediment traps deployed above and below the aragonite saturation horizon in the Sub-Antarctic Southern Ocean. Polar Biol. 34, 1739–1750.

Romero, O., Armand, L., Crosta, X., Pichon, J.-J., 2005a. The biogeography of major diatom taxa in Southern Ocean surface sediments: 3. tropical/subtropical species. Palaeogeogr., Palaeoclimatol., Palaeoecol. 223, 49–65.

Romero, O., Lange, C., Fischer, G., Treppke, U., Wefer, G., 1999. Variability in export production documented by downward fluxes and species composition of marine planktic diatoms: observations from the tropical and equatorial Atlantic. In: Use of Proxies in Paleoceanography. Springer, 365–392.

Romero, O., Fischer, G., Lange, C., Wefer, G., 2000. Siliceous phytoplankton of the western equatorial Atlantic: sediment traps and surface sediments. Deep-Sea Res. Part II: Top. Stud. Oceanogr. 47, 1939–1959.

Romero, O., Armand, L., Crosta, X., Pichon, J.-J., 2005b. The biogeography of major diatom taxa in Southern Ocean surface sediments: 3. tropical/subtropical species. Palaeogeogr., Palaeoclimatol., Palaeoecol. 223, 49–65.

Romero O., Armand L., 2010. Marine diatoms as indicators of modern changes in oceanographic conditions. In: Smol, J., Stoermer, E., (Eds.). The diatoms: applications for the environmental and earth sciences, pp. 373–400.

Saavedra-Pellitero, M., Baumann, K.-H., Flores, J.-A., Gersonde, R., 2014. Biogeographic distribution of living coccolithophores in the Pacific sector of the Southern Ocean. Mar. Micropaleontol. 109, 1–20.

Sancetta, C., Calvert, S.E., 1988. The annual cycle of sedimentation in Saanich Inlet, British Columbia: implications for the interpretation of diatom fossil assemblages. Deep-Sea Res. Part A. Oceanogr.Res. Pap. 35, 71–90.

Salter, I., Schiebel, R., Ziveri, P., Movellan, A., Lampitt, R., Wolff, G.A., 2014. Carbonate counter pump stimulated by natural iron fertilization in the Polar Frontal Zone. Nat. Geosci. 7, 885–889.

Schiebel, R., 2002. Planktic foraminiferal sedimentation and the marine calcite budget. Glob. Biogeochem. Cycles 16.

Schlitzer R., 2016. Ocean Data View Software, ⟨http://odv.awi.de⟩.

Scholten, J.C., Fietzke, J., Vogler, S., Rutgers van der Loeff, M.M., Mangini, A., Koeve, W., Waniek, J., Stoffers, P., Antia, A., Kuss, J., 2001. Trapping efficiencies of sediment traps from the deep eastern North Atlantic: the 230Th calibration. Deep-Sea Res. Part II: Top. Stud. Oceanogr. 48, 2383–2408. http://dx.doi.org/10.1016/S0967-0645(00)00176-4.

Sedwick, P.N., DiTullio, G.R., Hutchins, D.A., Boyd, P.W., Griffiths, F.B., Crossley, A.C., Trull, T.W., Quéguiner, B., 1999. Limitation of algal growth by iron deficiency in the Australian Subantarctic Region. Geophys. Res. Lett. 26, 2865–2868.

Sedwick, P., Bowie, A., Trull, T., 2008. Dissolved iron in the Australian sector of the Southern Ocean (CLIVAR SR3 section): Meridional and seasonal trends. Deep-Sea Res. Part I: Oceanogr. Res. Pap. 55, 911–925.

Shadwick, E., Trull, T., Tilbrook, B., Sutton, A., Schulz, E., Sabine, C., 2015. Seasonality of biological and physical controls on surface ocean CO2 from hourly observations at the Southern Ocean time series site south of Australia. Glob. Biogeochem. Cycles 29, 223–238.

Shannon, C.E., Weaver, W., 1949. The mathematical theory of communication (Dissertation). University of Illinois.

Smetacek, V., Assmy, P., Henjes, J., 2004. The role of grazing in structuring Southern Ocean pelagic ecosystems and biogeochemical cycles. Antarct. Sci. 16, 541–558.

Smith, W.O., Anderson, R.F., Moore, J.K., Codispoti, L.A., Morrison, J.M., 2000. The US southern ocean joint global ocean flux study: an introduction to AESOPS. Deep-Sea Res. Part II: Top. Stud. Oceanogr. 47, 3073–3093.

Sokolov, S., Rintoul, S.R., 2002. Structure of Southern Ocean fronts at 140 E. J. Mar. Syst. 37, 151–184.

Steinmetz, J.C., 1994. Sedimentation of coccolithophores. Coccolithophores, 179–198.

Ternois, Y., Sicre, M.-A., Boireau, A., Beaufort, L., Miquel, J.-C., Jeandel, C., 1998. Hydrocarbons, sterols and alkenones in sinking particles in the Indian Ocean sector of the Southern Ocean. Org. Geochem. 28, 489–501.

Thunell, R., Pride, C., Ziveri, P., Muller-Karger, F., Sancetta, C., Murray, D., 1996.

158

Plankton response to physical forcing in the Gulf of California. J. Plankton Res. 18, 2017–2026.

Treppke, U.F., Lange, C.B., Wefer, G., 1996. Vertical fluxes of diatoms and silicoflagellates in the eastern equatorial Atlantic, and their contribution to the sedimentary record. Mar. Micropaleontol. 28, 73–96.

Trull, T., Bray, S., Manganini, S., Honjo, S., Francois, R., 2001a. Moored sediment trap measurements of carbon export in the Subantarctic and Polar Frontal zones of the Southern Ocean, south of Australia. J. Geophys. Res.: Oceans (1978–2012) 106, 31489–31509.

Trull, T., Rintoul, S.R., Hadfield, M., Abraham, E.R., 2001b. Circulation and seasonal evolution of polar waters south of Australia: implications for iron fertilization of the Southern Ocean. Deep-Sea Res. Part II: Top. Stud. Oceanogr. 48, 2439–2466.

Trull, T., Sedwick, P., Griffiths, F., Rintoul, S., 2001c. Introduction to special section: SAZ Project. J. Geophys. Res.: Oceans (1978–2012) 106, 31425–31429.

Tyrrell, T., Merico, A., 2004. Emiliania huxleyi: bloom observations and the conditions that induce them. In: Coccolithophores. Springer, pp. 75–97.

Wefer, G., Fischer, G., 1991. Annual primary production and export flux in the Southern Ocean from sediment trap data. Mar. Chem. 35, 597–613.

Westwood, K.J., Griffiths, F.B., Webb, J.P., Wright, S.W., 2011. Primary production in the Sub-Antarctic and Polar Frontal zones south of Tasmania, Australia; SAZ-Sense survey, 2007. Deep Sea Res. Part II: Top. Stud. Oceanogr. 58, 2162–2178.

Winter, A., Henderiks, J., Beaufort, L., Rickaby, R.E., Brown, C.W., 2014. Poleward expansion of the coccolithophore *Emiliania huxleyi*. J. Plankton Res. 36, 316–325.

Young, J., Geisen, M., Cros, L., Kleijne, A., Sprengel, C., Probert, I., Østergaard, J., 2003. A guide to extant coccolithophore taxonomy. J. Nannoplankton Res. Spec. 1, 1–124.

Young J., Bown P., Lees J., 2014. Nannotax3 website. International Nannoplankton Association. ⟨http://ina.tmsoc.org/Nannotax3⟩.(accessed 21.04.14)

Yu, E.F., Francois, R., Bacon, M.P., Honjo, S., Fleer, A.P., Manganini, S.J., Rutgers van der Loeff, M.M., Ittekot, V., 2001. Trapping efficiency of bottom-tethered sediment traps estimated from the intercepted fluxes of 230Th and 231Pa. Deep-Sea Res. Part I: Oceanogr. Res. Pap. 48, 865–889. http://dx.doi.org/10.1016/S0967-0637(00)00067-4.

Zielinski, U., Gersonde, R., 1997. Diatom distribution in Southern Ocean surface sediments (Atlantic sector): implications for paleoenvironmental reconstructions. Palaeogeogr. Palaeocl. 129, 213–250. http://dx.doi.org/10.1016/S003-0182(96)00130-73.

Ziveri, P., Rutten, A., De Lange, G., Thomson, J., Corselli, C., 2000. Present-day coccolith fluxes recorded in central eastern Mediterranean sediment traps and surface sediments. Palaeogeogr., Palaeoclimatol., Palaeoecol. 158, 175–195.
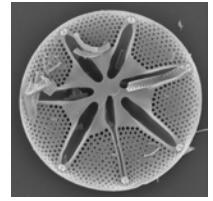
159

Chapter Three

Diatom and coccolithophore flux assemblages
from the Subtropical Frontal region, east of New Zealand

1 **Diatom and coccolithophore flux assemblages from the Subtropical Frontal region, east of New**
2 **Zealand.**

3 Jessica V. Wilks[1*], Scott D. Nodder[2], Andrés Rigual-Hernández[3], Glenn A. Brock[1] and Leanne K.
4 Armand[4].

5 [1]Department of Biological Sciences, Macquarie University, North Ryde, NSW 2109, Australia.

6 [2]National Institute of Water and Atmospheric Research, Hataitai, Wellington 6021, New Zealand.

7 [3]Department of Geology. Universidad de Salamanca, Salamanca 37008, Spain.

8 [4]Research School of Earth Sciences, The Australian National University, Canberra, ACT 2601,
9 Australia.

10 *Correspondence: (jessicavwilks@gmail.com, Tel: +61 468 585 443)

11 **Abstract**

12 The Chatham Rise supports some of New Zealand's most economically and environmentally valuable
13 fish species, fuelled by the productive waters of the Subtropical Frontal Zone. Climate change-related
14 shifts in phytoplankton community structures are predicted and may affect Chatham Rise
15 productivity. However, little is known about how two major groups, the diatoms and
16 coccolithophores, will respond, as knowledge of their export and seasonality is not known in the SW
17 Pacific sector. This study is the first to report on phytoplankton seasonality in this region, using a 12-
18 month sediment trap record (1996-1997), both north (subtropical) and south of the Chatham Rise
19 (subantarctic). Diatom and coccolithophore flux assemblages were characterised at 300 and 1000 m
20 trap depths. Northern phytoplankton assemblages were typical of the subtropics, with most
21 particulate organic carbon and biogenic silica export associated with diatoms. A significant
22 contribution of coastal and benthic diatom species in the northern traps suggests advection from a
23 coastal regime, driven by the Wairarapa Eddy, but particle input via seafloor resuspension into the
24 deep trap is also inferred. In the south, a combination of subantarctic and frontal zone communities
25 were observed. Southern phytoplankton fluxes were on average an order of magnitude higher than
26 the northern site, possibly due to the traps' proximity to the productive Subtropical Frontal Zone.
27 The bulk of diatom flux in the southern trap occurred during a 16-day spring *Pseudo-nitzschia* "pulse"
28 event associated with high biogenic silica flux. High coccolith flux in the south was typical of
29 subantarctic export regimes. This paper provides a baseline of phytoplankton assemblages across
30 Chatham Rise, against which current and projected changes in environmental parameters may be
31 assessed.

32 **Keywords**
33 Sediment trap; phytoplankton; diatom; coccolithophore; SW Pacific; export flux.

34 **1. Introduction**

35 Phytoplankton are responsible for ~50% of global carbon fixation (Field et al. 1998), and form the
36 basis of marine food webs. The carbon fixed by phytoplankton may be exported to the deep ocean
37 as cells sink, either individually, in aggregates, or as faecal pellets, in a process known as the biological
38 pump (Honjo et al. 2014). The volume of carbon exported varies globally, as does the role of different
39 phytoplankton groups in this process (De La Rocha and Passow 2007). Phytoplankton assemblage
40 dynamics are predicted to shift under future climate change scenarios (Law et al. 2017), with
41 implications for the strength and efficiency of the biological pump (Boyd 2015; Deppeler and
42 Davidson 2017).

43 Siliceous and calcareous phytoplankton fluxes are reported in this study for the first time in this
44 region, allowing new insights into particle export and community assemblages. The focus is on
45 diatoms and coccolithophores. Diatoms are diverse, widespread aquatic phytoplankton that exist in
46 both fresh and marine environments, as well as terrestrial environments and ice. They are major
47 contributors to carbon export due to their robust, siliceous frustules (Honjo 1997). Coccolithophores
48 are unicellular marine phytoplankton that possess calcareous scales (coccoliths). They contribute
49 significantly to the global carbon cycle as both organic carbon and carbonate-producers (Broecker
50 and Clark 2009), because the coccoliths provide ballast, which may boost sinking rates of organic
51 matter (Klaas and Archer 2002). The productivity and assemblage composition of both diatoms and
52 coccolithophores are predicted to be affected by increasing ocean acidification, as well as climate-

53 change-related changes in light, temperature and nutrient availability in the future (Lefebvre et al.
54 2012; Kottmeier et al. 2016; Trimborn et al. 2017).

55 The Chatham Rise is an undersea ridge extending due east from the north-eastern coast of the South
56 Island of New Zealand (Nodder et al. 2012). The rise constrains the passage of the Subtropical Frontal
57 Zone (STFZ), representing the convergence of subtropical and subantarctic waters (Sutton 2001;
58 Chiswell et al. 2015a). The zone is a significant, seasonal sink for atmospheric carbon due to elevated
59 phytoplankton productivity (Currie and Hunter 1998), and supports important deep-water fish stocks
60 (Bull and Livingston 2001; Clark 2001). Phytoplankton composition has been analysed from water
61 samples across and on the Chatham Rise (Bradford-Grieve et al. 1997; Chang and Gall 1998; Boyd et
62 al. 1999; Chang and Northcote 2016). Remotely-sensed ocean colour data has been used effectively
63 to estimate phytoplankton abundance and composition on seasonal timescales (Murphy et al. 2001),
64 and diatom microfossil assemblage distributions either side of the Rise have been mapped using
65 sediment core-tops (Fenner et al. 1992; Cochran and Neil 2009). Recent studies of coccolithophore
66 biogeography have been conducted in the New Zealand region on surface water samples (Saavedra-
67 Pellitero et al. 2014; Chang and Northcote 2016), reporting high coccolithophore diversity in New
68 Zealand waters.

69 Sediment traps are used to sample the composition and seasonality of export fluxes and link surface
70 processes with the sedimentary record (Buesseler et al. 2007). In the New Zealand region, short-
71 term floating traps (1-3 days deployment) have been used to measure total mass flux, and analyses
72 of phytoplankton groups present in the subtropical, subantarctic, and frontal zones (Nodder 1997a;
73 Nodder and Gall 1998; Nodder and Alexander 1998), while longer term moored sediment trap
74 records have been obtained from the flanks of the Chatham Rise and in the subtropics and
75 subantarctic (Nodder and Northcote 2001; Nodder et al. 2005; Northcote and Neil 2005; Sikes et al.
76 2005; Nodder et al. 2016). However, no study has specifically quantified diatom or coccolithophore
77 assemblage composition nor seasonality from sediment trap records across this region.

78 This study reports on diatom and coccolithophore fluxes and assemblage seasonality from a pair of
79 sediment trap deployments moored on the northern and southern flanks of the Chatham Rise
80 between June 1996 and May 1997, to test if differences would be observed in production and
81 sedimentation between the two distinct oceanographic zones (Nodder and Northcote 2001). These
82 20-year-old historical samples are an important archival record of diatom and coccolithophore mass
83 flux and assemblage seasonality from the SW Pacific Ocean. By analysing these trap archives, this
84 study adds to existing knowledge on fluxes over the rise since Nodder and Northcote (2001). This
85 record may be used as a point of comparison for future studies.

86 *1.1 Oceanographic setting*

87 The Chatham Rise is a ~1500 km long submarine rise, spanning 42° 12'-45° S, and from the eastern
88 coast of New Zealand (172° 48' E) to roughly 168° 6' W. The convergence of subtropical water (north)
89 and subantarctic water (south) over the Chatham Rise occurs at the Subtropical Frontal Zone (STFZ).
90 The zone is ~150 km wide (Sutton 2001), and is characterised by strong temperature and salinity
91 gradients (Chiswell 2001; Sutton 2001; Chiswell 2002). It is bounded by two fronts, the north
92 Subtropical Front (NSTF) and the stronger south Subtropical Front (SSTF) (Belkin 1988, Stanton and

93   Ridgway 1988, Belkin and Gordon 1996, Sutton 2001; Fig. 1). The STFZ is considered "bathymetrically

94   locked" to the Chatham Rise (Heath 1985; Chiswell 2001; Sutton 2001; Chiswell et al. 2015a; Fig. 1),

95   thus occupying a relatively constant position in this region. The NSTF meanders north and south

96   (Stanton and Ridgway 1988) and is impacted by the large Wairarapa Eddy to the north of the rise

97   (Roemmich and Sutton, 1998; Chiswell 2005).
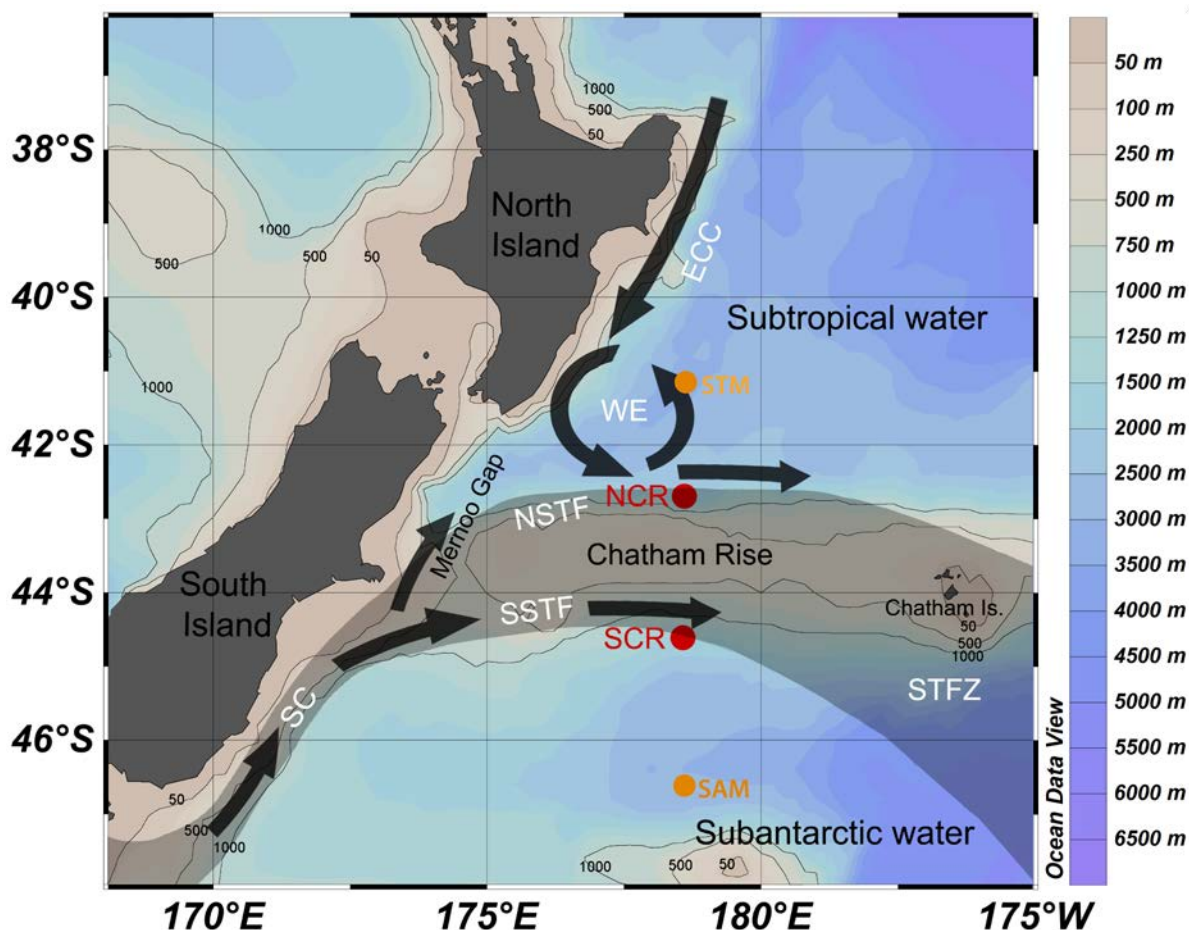
98

99   *Figure 1. Schematic of New Zealand region showing generalized oceanographic features influencing the mooring sites, and*
100   *front positions (after Sutton 2001, Fig. 1). Abbreviations: East Cape Current, ECC; Wairarapa Eddy, WE; Southland Current,*
101   *SC; North Subtropical Front, NSTF; South Subtropical Front, SSTF; Subtropical Frontal Zone, STFZ (gray region); North*
102   *Chatham Rise, NCR; South Chatham Rise, SCR. Nearby trap deployments STM and SAM (indicated as orange dots; Nodder*
103   *et al. 2016). Plotted using Ocean Data View 4, available at http://odv.awi.de (Schlitzer 2016).*

104   The two mooring location sites, North Chatham Rise (NCR) and South Chatham Rise (SCR), are ~200

105   km apart, and subject to distinct hydrological and oceanographic conditions, but experience similar

106   climatic conditions (Sikes et al. 2005). The mooring sites were chosen to represent the Subtropical

107   Zone (STZ) and Subantarctic Zone (SAZ); however, it has more recently been established that the

108   NCR and SCR mooring sites are both within the outer fringes of the STFZ (Sutton 2001). Also pictured

109   in Fig. 1 are two nearby sediment trap deployments, the Subtropical Mooring (STM, north) and the

110   Subantarctic Mooring (SBM, south) (Nodder et al. 2016).

111   Despite their proximity to the STFZ, NCR and SCR are also influenced by subtropical and subantarctic

112   waters, respectively. Water masses over NCR originate from the East Cape Current (ECC), which

113   travels south-west along the east coast of the North Island, carrying warm, saline waters to the trap

114 site. These waters may become entrained into the Wairarapa Eddy (WE), a semi-permanent, 2000 m
115 deep anticyclonic eddy system situated off the eastern coast of the North Island (Chiswell 2005) (Fig.
116 1). The eddy circulates warmer subtropical water to the coast, periodically casting off smaller eddies
117 (Chiswell 2005). The ECC is deflected east upon reaching the Chatham Rise (Heath 1985; Chiswell et
118 al. 2015a), and continues eastwards along its northern flank. Subantarctic water may be advected
119 northward at the western end of the rise through the Mernoo Gap, and become entrained into
120 subtropical waters (Boyd et al. 1999; Chiswell 2001).

121 The bulk of STFZ flow is thought to occur on the southern flank of the Chatham Rise (Chiswell 2001),
122 associated with the southern front, explaining higher, but less variable current speeds measured at
123 SCR than NCR (Chiswell 2001; Nodder and Northcote 2001). The southern boundary of the STFZ is
124 derived from the Southland Current, which travels northwards along the east coast of the South
125 Island, carrying subantarctic waters to the STFZ (Hopkins et al. 2010; Smith et al. 2013). The
126 Southland Current varies seasonally and inter-annually, influencing the strength of the SSTF over the
127 rise (Chiswell 2001; Sutton 2003; Hopkins et al. 2010). The SCR mooring was deployed on the
128 southern flank of the Chatham Rise, which is influenced by typical cooler, less saline subantarctic
129 waters. CTD data for the trap sites were obtained between 1991 and 1999, but not published (S.
130 Nodder, NIWA unpublished data). However, data from the CSIRO Atlas of Regional Seas (Ridgway et
131 al. 2002) indicates higher year-round silicate concentrations (µmol/L) at NCR than SCR, and higher
132 concentrations of the nutrients nitrate and phosphate at SCR than NCR (Sikes et al. 2005). This is
133 consistent with the general High-Nitrate, Low-Chlorophyll, Low-Silicate status of subantarctic waters
134 (Dugdale et al. 1995). Oxygen concentration (µmol/L) is not, on average, vastly different between
135 the two sites (World Ocean Atlas 2009, Locarini et al. 2010).

136 Mixed layer depths determined using the potential density difference from Argo floats deployed
137 between 2001 and 2006 indicate generally deeper and more seasonally variable mixed layers at NCR
138 than SCR (Supplementary Figure 1) (data from Dong et al. 2008). NCR mixed layers published in Dong
139 et al. (2008) range between 220 m (August) and ~30 m (December/January), consistent with
140 maximum depth determined by Sutton (2001) of roughly 200 m in winter. At SCR, maximum winter
141 mixed layer depth was 117 m, while the minimum was 20 m (Supplementary Figure 1).

142 **2. Methodology**

143 *2.1 Trap deployments*

145 A detailed description of the field experiment and equipment used is given in Nodder and Northcote
146 (2001). Briefly, two mooring lines were deployed at the NCR and SCR sites, each equipped with two
147 McLane^{TM} PARFLUX Mk 7G-21 sediment traps placed at 300 m and 1000 m depth, in water depth of
148 1500 m. The NCR trap bottles were poisoned with borax-buffered HgCl$_2$ (0.3%) to allow the
149 deployments to be compared to pre-existing data sets, and to permit organic biomarker analyses
150 planned for NCR samples (see Nodder and Northcote 2001). The SCR bottles were poisoned with
151 borax-buffered formalin (6%). HgCl$_2$ and formalin have similar effectiveness in reducing zooplankton
152 swimmer activity and microbial activity (Hedges et al. 1993).

152 The NCR traps were deployed at 42°42'S 178°38'E in early September 1996 while the SCR traps were
153 deployed at 44°37'S 178°37'E in late May 1996. Both NCR and SCR moorings were recovered in May
154 1997, sampling for 243, and 340 days, respectively. From mid-September 1996 until mid-December
155 1996 the sampling interval at NCR was 7-8 days, with twice as many sampling intervals in this period
156 at NCR than SCR. Sampling intervals for the SCR deployment were 16 days during the entire sampling
157 period. From mid-December 1996 until the recovery of the traps, sampling intervals were
158 synchronised between the two sites (Table 1). At NCR 300 m, five sample cups were inexplicably
159 broken possibly at the time of retrieval between November 1996 and January 1997, as well as
160 another single cup in April, leaving 178 sampling days.

		NCR 300 m		SCR 300 m	
Cup	Cup opening/ closing	Diatom Flux (x10³ m⁻² d⁻¹)	Coccolith Flux (x10³ m⁻² d⁻¹)	Diatom Flux (x10³ m⁻² d⁻¹)	Coccolith Flux (x10³ m⁻² d⁻¹)
1	6/9-6/25/96	†	†	0.1	37.2
2	6/25-7/11/96	†	†	0.2	116.9
3	7/11-7/28/96	†	†	0.3	60.3
4	7/28-8/13/96	†	†	0.02*	16.3
5	8/13-8/29/96	†	†	1.0	351.2
6	8/29-9/14/96	†	†	4.5	33.2
7a	9/14-9/22/96	4.2	330.3	25.7	3531.8
7b	9/22-9/30/96	6.5	333.6	-	-
8a	9/30-10/8/96	32.0	0.5	23.4	1690.9
8b	10/8-10/17/96	294.0	7.3	-	-
9a	10/17-10/25/96	0.08*	5.3	1577.8	600.9
9b	10/25-11/2/96	0.03*	2.7	-	-
10a	11/2-11/10/96	0.03*	6.0	3432.7	1282.4
10b	11/10-11/18/96	0.03*	0.3	-	-
11a	11/18-11/26/96	Sample missing		30.3	272.0
11b	11/26-12/4/96	"	"	-	-
12a	12/4-12/12/96	"	"	0.9	496.4
12b	12/12-12/20/96	"	"	-	-
13	12/20-1/5/97	"	"	0.04*	5.4
14	1/5-1/21/97	4.4	54.0	0.05*	17.8
15	1/21-2/7/97	0.05*	135.4	0.08*	57.4
16	2/7-2/23/97	1.2	2.4	0.2	117.9
17	2/23-3/11/97	2.3	130.0	0.03*	47.9
18	3/11-3/27/97	2.4	9.2	0.07*	8.0
19	3/27-4/13/97	Sample missing		Sample missing	Sample missing
20	4/13-4/29/97	0.5	139.2	0.1	43.1
21	4/29-5/15/97	0.02*	14.0	0.1*	8.0
Annualized flux		-	-	8.2 x10⁷ m⁻² y⁻¹	1.4 x10⁸ m⁻² y⁻¹
Mean spring flux		4.2 x 10⁴ m⁻² d⁻¹	8.5 x 10³ m⁻² d⁻¹	5.1 x 10⁶ m⁻² d⁻¹	7.6 x 10⁴ m⁻² d⁻¹
		NCR 1000 m		SCR 1000 m	
1	6/9-6/25/96	†	†	3.1	Not calculated
2	6/25-7/11/96	†	†	5.7	"
3	7/11-7/28/96	†	†	3.6	"
4	7/28-8/13/96	†	†	7.7	"
5	8/13-8/29/96	†	†	9.2	"
6	8/29-9/14/96	†	†	37.5	"
7a	9/14-9/22/96	1.6	Not calculated	45.3	"
7b	9/22-9/30/96	11.6	"	-	"
8a	9/30-10/8/96	6.6	"	29.1	"
8b	10/8-10/17/96	39.9	"	-	"
9a	10/17-10/25/96	37.5	"	1856.2	"
9b	10/25-11/2/96	17.9	"	-	"
10a	11/2-11/10/96	18.2	"	5378.7	"
10b	11/10-11/18/96	9.8	"	-	"
11a	11/18-11/26/96	14.7	"	1024.9	"
11b	11/26-12/4/96	9.5	"	-	"
12a	12/4-12/12/96	26.8	"	8.5	"
12b	12/12-12/20/96	7.4	"	-	"
13	12/20-1/5/97	22.7	"	0.9	"
14	1/5-1/21/97	24.5	"	1.1	"
15	1/21-2/7/97	11.3	"	11.6	"
16	2/7-2/23/97	23.0	"	19.1	"
17	2/23-3/11/97	16.1	"	4.8	"
18	3/11-3/27/97	8.2	"	0.8	"
19	3/27-4/13/97	11.8	"	0.4	"
20	4/13-4/29/97	13.7	"	0.4	"
21	4/29-5/15/97	9.8	"	0.3	"
Annualized flux		1.5 x 10⁶ m⁻² y⁻¹	-	1.4 x 10⁸ m⁻² y⁻¹	-
Mean spring flux		1.8 x 10⁴ m⁻² d⁻¹	-	8.3 x 10⁶ m⁻² d⁻¹	-

Table 1. North Chatham Rise (NCR) and South Chatham Rise (SCR) mooring cup numbers and sampling intervals, Diatom Flux and Coccolith Flux. * indicates cups in which fewer than 100 diatom valves were enumerated. † indicates cups for which sampling was yet to commence.

165   Aanderaa current meters were included in the trap deployment, indicating speeds on average higher
166   at the SCR deployment site (maximum 50 cm s^{-1}), but were occasionally high at NCR too (maximum
167   48 cm s^{-1}). The threshold current speed over which trapping efficiency beings to decrease is 12 cm s^{-1}
168   ^{1} (Baker et al. 1988). Current speeds during this deployment were mainly below this threshold, and
169   Nodder and Northcote (2001) did not find a strong relationship between current speed and mass
170   flux capture efficiency, at either site or trap depths. They concluded that hydrodynamic bias of
171   particle capture by the sediment traps is not a significant issue in the present study.

172   *2.2 Trap recovery and sample processing*
173   The trap sample processing protocol is provided by Nodder and Northcote (2001). After retrieval,
174   subsamples were taken from each 250 mL sample bottle for nutrient analyses. The remaining
175   material was sieved through a 1 mm mesh to remove swimmers, and split using a McLane^{TM} wet-
176   splitter. Several fractions were used in determining biogeochemical fluxes, discussed in Nodder and
177   Northcote (2001). This study uses one 1/16th split from each trap depth at each site. Of the 1/16th
178   split, 10 mL was set aside for coccolith analysis (1/80th of original sample). Although this is a small
179   split, in most cases the minimum number of coccoliths counted to obtain a reasonable capture of
180   species diversity was met. The remaining portion was cleaned for diatom counting.

181   Sample cleaning for diatom analysis followed Romero et al. (1999), involving a treatment of
182   saturated potassium permanganate, 3M hydrochloric acid and 30% hydrogen peroxide to remove
183   organic material. The remaining siliceous material was transferred to a centrifuge tube and topped
184   up with MilliQ water. The samples were then serially spun at low speeds (800 rpm) to avoid frustule
185   breakage, the supernatant removed, the water topped up, and spun again until the pH of the samples
186   was neutral for storage.

187   *2.3 Slide preparation and phytoplankton identification*

188   Diatom slides were prepared using a modified random settling method of Flores and Sierro (1997),
189   with a known quantity of the suspension (200 µL to 25 mL, depending on sample density). Four slides
190   were made per sample.

191   Slides were viewed using an Olympus BH-2 compound light microscope at 1000x magnification.
192   Diatom frustules were counted and identified to species level along 10 non-overlapping transects
193   until 300 frustules per sample had been counted. 300 cells is the minimum threshold at which error
194   stabilizes between replicate counts of the same sample, and a good balance is achieved between
195   time taken and breadth of coverage of rare species (Bodén 1991). Diatom identification followed
196   modern taxonomy as per Tomas (1997). Silicoflagellates and radiolarians encountered on these
197   transects were also counted, but not identified. Diatoms that were poorly preserved, too small, or
198   missing key taxonomic features were grouped into additional categories: unknown pennate,
199   unknown centric, and unknown centric <15 µm. *Chaetoceros* vegetative cells were identified as
200   subgenus *Hyalochaete* or *Phaeoceros*, and all resting spores of *Chaetoceros* were counted together.
201   *Pseudo-nitzschia* spp. were not identified past genus level at SCR as accurate identification of this
202   group requires scanning electron microscopy (Ajani et al. 2013), and the samples were too dense.
203   Determination of NCR diatom taxa as coastal, benthic, coastal and cosmopolitan, or open-ocean was
204   as per ecological descriptions in Hallegraeff et al. (2010), Chang (1983) and Tomas (1997).

205   Slides for coccolith identification were prepared as per Flores and Sierro (1997), using the entire 10
206   mL subsample. Only 300 m traps were used for coccolith analysis due to time constraints. 300
207   coccoliths per sample were counted and identified to species level where possible under 1000x
208   magnification using a LEICA DMRXE polarized light microscope, following the procedure of diatoms.
209   Identification of coccolithophore taxa followed Young et al. (2003). Additional groupings were used
210   to count unknown *Gephyrocapsa* spp., and *Gephyrocapsa* spp. <3 μm. *Oolithotus* spp., *Pontosphaera*
211   spp., and *Syracosphaera* spp. were not identified past genus level.

212   A list of all diatom and coccolithophore species encountered is given in Supplementary Tables 1a-2b.

213   *2.4 Flux calculations*

214   Diatom and silicoflagellate flux were calculated per m^2 per day at each sampling interval using the
215   equation of Sancetta and Calvert (1988), and modified to compensate for the 10 mL subsample set
216   aside for the coccolith identification and flux calculation. For graphing, fluxes were transformed into
217   relative abundances. Annual fluxes were calculated using the extrapolation method, whereby fluxes
218   in missing samples were estimated based on the general flux trend (e.g. low fluxes in winter, high
219   fluxes in spring). The SCR traps sampled for nearly a full annual cycle (340 days). Annualized fluxes
220   at NCR 1000 m were based on 242 days and may be less accurate. Fluxes were not annualized at NCR
221   300 m because only 178 days' material was recovered.

222   *2.5 Environmental data from satellite remote-sensing*

223   Since the field experiment was conducted before the commencement of the Sea WIFS chlorophyll-*a*
224   data record in September 1997, no chlorophyll-*a* data was available for the collection intervals of
225   our sediment traps. Nonetheless, in order to have a general view of the timing of biomass
226   accumulation, an inter-annual average of SeaWiFS ocean colour estimate of chlorophyll-*a* was
227   obtained (Fig. 2A). Ten-year monthly average NASA Ocean Biogeochemical Model (NOBM)
228   Photosynthetically Active Radiation (PAR; 2000 to 2010, 9 km resolution) and Chlorophyll-*a*
229   concentration (Chl-*a*; 2002 to 2012, 4 km resolution) was obtained from the Goddard Earth Sciences
230   Data and Information Services Centre (GES DISC) for 0.5 decimal degrees around each study site at
231   NCR and SCR. Advanced Very High Resolution Radiometer (AVHRR) Sea Surface Temperature (SST; 9
232   km resolution) data are reported in King and Howard (2001).

233   *2.6 Statistical Analyses*

234   Canonical Correspondence Analysis (CCA) was performed on the most abundant diatoms (>1%
235   annual weighted abundance, and >5% relative abundance in any cup) and coccolithophore taxa
236   (present in >1 cup) for both 300 m traps. Advanced Very High Resolution Radiometer (ADHRR) SST,
237   10-year monthly average Photosynthetically Active Radiation (PAR), and 10-year monthly average
238   Chlorophyll-*a* (Chl-*a*) concentration data were used as environmental parameters. Due to the
239   apparent input of bottom-resuspended material within the 1000 m traps (Nodder and Northcote
240   2001), CCA was only performed on the 300 m traps.

241   Correlation matrices were constructed to compare seasonality of total diatom flux, total coccolith
242   flux and silicoflagellate flux at both sites and depths, with the particle fluxes published in Nodder and
243   Northcote (2001) (i.e. total mass flux (TMF), Particulate Organic Carbon (POC), Biogenic Silica (BSi),
244   and Lithogenic Silica (LSi)). *Chaetoceros* resting spores and *Pseudo-nitzschia* spp. fluxes were

245   included in the matrices at NCR and SCR, respectively, as they comprised the bulk of diatom fluxes

246   at their respective mooring sites.

247   Assemblage diversity and evenness was calculated for diatoms and coccolithophores using the

248   Shannon-Weaver Equitability index (Eh) (Shannon and Weaver 1949).

249   **3. Results**

250   *3.1 Satellite-derived environmental parameters*

251   Chl-*a* was higher at NCR than SCR, and showed two peaks in production in an average year (Fig. 2A).

252   Peak Chl-*a* occurred in November at 1 mg m^{-3} at NCR, with another small peak tending to occur in

253   April at ~60% of the main spring peak (Fig. 2A). At SCR, maximum Chl-*a* tended to occur in February

254   (0.72 mg m^{-3}; Fig. 2A). PAR levels throughout an average year were similar at both NCR and SCR,

255   increasing from austral winter lows in June, and peaking in mid-summer between December and

256   January at 51 - 53 Einstein m^{-2} d^{-1} (Fig. 2B). Peak SST occurred at both sites in February at ~18°C and

257   15°C, NCR and SCR, respectively (Fig. 2C).
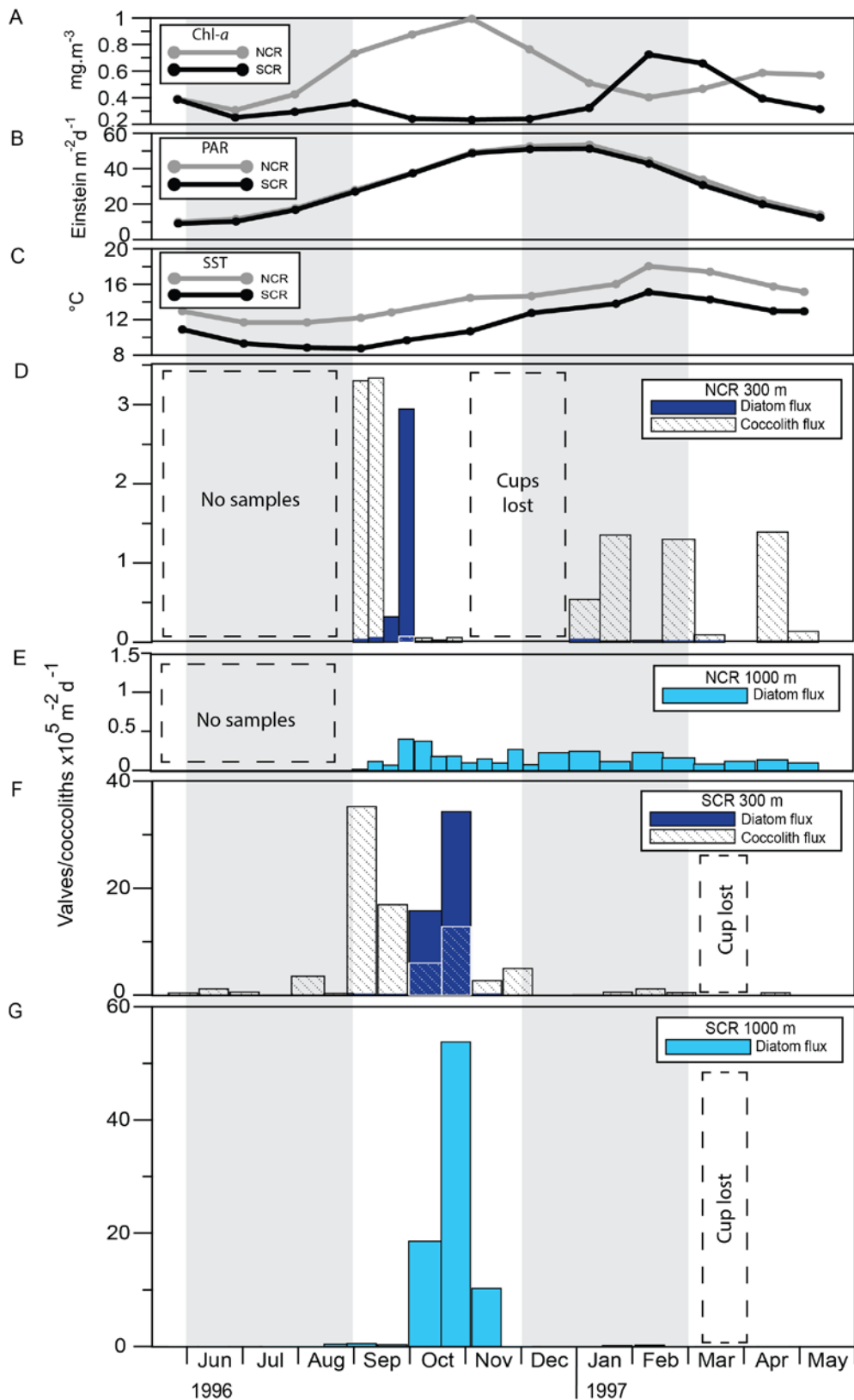
Figure 2. Fluxes and environmental parameters across sampling period at NCR and SCR. A, NOBM-derived, 10 year monthly average Chlorophyll-*a* concentration (Chl-*a*; mg m^{-3}); B, NOBM-derived 10 year monthly average Photosynthetically Active Radiation (PAR; Einstein m^{-2} d^{-1}); C, AVHRR Sea Surface Temperature (SST; °C); D, total diatom and coccolith flux (valves and coccoliths m^{-2} d^{-1}) at North Chatham Rise 300 m; E, total diatom flux at NCR 1000 m; F, total diatom and coccolith flux (valves and coccoliths m^{-2} d^{-1}) at South Chatham Rise 300 m; G, total diatom flux at SCR 1000 m. SST data from King and Howard (2001). Gray bars delineate winter and summer months.

265   *3.2 Phytoplankton flux seasonality*

266   Total diatom flux was higher at SCR than NCR (Table 1). At NCR, maximum flux occurred in mid-
267   October at 300 and 1000 m (29.4 x 10^4 and 4.0 x 10^4 valves m^{-2} d^{-1}, respectively), though this
268   maximum was less pronounced at 1000 m (Table 1; Figs. 2D-E). The bulk of diatom flux at NCR 300
269   m was captured during an 8-day sampling interval in October (Fig. 2D). The 1000 m trap at NCR
270   captured lower, but more consistent flux for the duration of sampling, though with slightly lower
271   values over winter (Fig. 2D). Due to missing samples at NCR, the magnitude of summer fluxes at 300
272   m are unknown. Diatom and coccolith flux was calculated for the 65-day spring bloom at both depths.
273   Mean spring flux at NCR 300 m and 1000 m was 4.2 x 10^4 valves m^{-2} d^{-1} (or 3.4 x 10^5 m^{-2} for the
274   season), and 1.8 x 10^4 diatom valves m^{-2} d^{-1} (1.4 x 10^5 m^{-2} per season), respectively. Annualized diatom
275   flux at NCR 1000 m was 1.5 x 10^6 m^{-2}y^{-1} (Table 1).

276   Diatom flux peaked later in the season at SCR, and was captured during the late October-early
277   November sampling interval at both trap depths (Fig. 2F-G). Total diatom flux for the SCR spring peak
278   was 5.1 x 10^6 (300 m) and 8.3 x 10^6 (1000 m) diatom valves m^{-2} d^{-1}. In contrast to NCR, peak diatom
279   flux at SCR was greater at 1000 m than at 300 m (5.4 x 10^6, and 3.4 x 10^6 valves m^{-2} d^{-1}, respectively;
280   Table 1, Figs. 2F-G). Annual diatom flux was estimated at 8.2 x 10^7 and 1.4 x 10^8 valves m^{-2} y^{-1} at SCR
281   300 m and 1000 m, respectively (Table 1).

282   Silicoflagellates and radiolarians exhibited fluxes at times almost as high as diatom flux, and
283   silicoflagellate and radiolarian fluxes were respectively six and four-times higher at SCR than NCR
284   (Supplementary Tables 1a - 2b). At both sites, radiolarian flux increased with depth, but
285   silicoflagellate flux increased with depth only at SCR (Supplementary Tables 1a - 2b). Peak
286   silicoflagellate flux occurred in September at both NCR depths and at SCR 300 m, and in late-August
287   at SCR 1000 m. Radiolarians, on the other hand, tended to show abundances more evenly spread
288   throughout the sample period at NCR, though highest fluxes occurred in July/August at SCR
289   (Supplementary Tables 1a - 2b).

290   Annual coccolith flux at SCR 300 m was 1.4 x 10^8 coccoliths m^{-2} y^{-1}, and spring coccolith flux was higher
291   at SCR 300 m (7.6 x 10^4 m^{-2} d^{-1} or 7.4 x 10^6 m^{-2} per season) than NCR (8.5 x 10^3 m^{-2} d^{-1} or 6.9 x 10^5 m$^-$
292   ^{2}per season; Table 1). Maximum coccolith flux at NCR 300 m occurred in late-September, at 3.3 x 10^5
293   coccoliths m^{-2} d^{-1}, 16 days before the peak in diatom flux (Table 1, Fig. 2D). Flux was then low from
294   October until after the deployment resumed trapping in mid-January, after which coccolith capture
295   fluctuated with small peaks observed again in January, March and April (Table 1, Fig. 2D). Spring
296   coccolith flux at NCR was 8.5 x 10^3 coccoliths m^{-2} d^{-1} (Table 1). At SCR, coccolith flux reached
297   maximum abundance more than one month before the diatom spring bloom, peaking in late-
298   September at 3.5 x 10^6 coccoliths m^{-2} d^{-1} (Table 1, Fig. 2F). Coccolith flux then exhibited another
299   smaller peak simultaneous with the diatom pulse event at SCR, before decreasing more gradually to
300   summer/autumn lows (Fig. 2F).

301   *3.3 Environmental influences on phytoplankton fluxes*

302   Inter-flux correlations tended to be weaker at SCR than NCR, and weaker at depth (Table 2). At NCR
303   300 m, correlation matrices revealed a strong, positive correlation between diatom flux, and TMF,

304   POC and BSi flux (0.98, 0.99 and 0.97, respectively; Table 2), holding true to a lesser extent at 1000

305   m. Silicoflagellates were strongly correlated (>0.9) with diatom flux, TMF, POC and BSi fluxes at NCR

306   300 m (Table 2). *Chaetoceros* resting spores were associated with TMF, POC and BSi at both depths

307   at NCR.

NCR 300 m	Diatoms	Coccoliths	TMF	POC	BSi	LSi	CRS
Coccoliths	-0.17	-					
TMF	**0.98**	-0.12	-				
POC	**0.99**	-0.17	**0.99**	**-**			
BSi	**0.97**	-0.14	**0.93**	**0.97**	-		
LSi	-0.03	0.37	-0.11	-0.03	0.17	-	
CRS	**0.62**	-0.26	**0.55**	**0.63**	**0.75**	0.33	-
Silicoflagellates	**0.95**	0.11	**0.94**	**0.94**	**0.93**	0.06	**0.54**
NCR 1000 m	Diatoms	Coccoliths	TMF	POC	BSi	LSi	CRS
TMF	**0.68**	n/a	-				
POC	**0.80**		**0.77**	-			
BSi	**0.56**		**0.70**	**0.81**	-		
LSi	-0.03		0.22	0.26	0.24	-	
CRS	**0.98**		**0.64**	**0.79**	**0.52**	-0.03	-
Silicoflagellates	0.45		0.36	**0.55**	**0.71**	0.20	0.35
SCR 300 m	Diatoms	Coccoliths	TMF	POC	BSi	LSi	*Pseudo-nitzschia* spp.
Coccoliths	0.24	-					
TMF	**0.88**	**0.57**	-				
POC	**0.51**	**0.73**	**0.66**	-			
BSi	**0.86**	**0.51**	**0.88**	**0.78**	-		
LSi	0.13	**0.82**	0.49	**0.68**	0.45	-	
Pseudo-nitzschia spp.	**1.00**	-0.10	**0.82**	0.38	**0.92**	-0.33	-
Silicoflagellates	-0.12	**0.86**	0.29	**0.56**	0.23	**0.94**	**-0.53**
SCR 1000 m	Diatoms	Coccoliths	TMF	POC	BSi	LSi	*Pseudo-nitzschia* spp.
TMF	0.17	n/a	-				
POC	**0.76**		**0.56**	-			
BSi	**0.71**		**0.73**	**0.84**	-		
LSi	-0.04		**0.73**	0.27	**0.55**	-	
Pseudo-nitzschia spp.	1.00		-0.01	**0.77**	**0.68**	-0.14	-
Silicoflagellates	0.00		**0.82**	0.35	**0.62**	**0.81**	-0.16

308 ***Table 2.*** *Correlation matrices comparing diatom flux, coccolith flux, silicoflagellate flux and Pseudo-nitzschia spp. flux with Total Mass, POC, BSi and LSi fluxes. Values <-0.5 and >0.5 indicate*
309 *negative and positive correlation, respectively (indicated in bold). Values close to 0 indicate no correlation. Total Mass Flux, TMF; Particulate Organic Carbon, POC; Biogenic Silica, BSi;*
310 *Lithogenic Silica,LSi; Chaetoceros resting spores, CRS.*

311 At SCR 300 m, diatom flux was strongly positively correlated with TMF (0.88) and BSi flux (0.86), but
312 more weakly with POC (0.51) (Table 2). Coccoliths, on the other hand, were more strongly related to
313 POC (0.73). *Pseudo-nitzschia* spp. were correlated with both TMF and BSi, but negatively related to
314 silicoflagellate abundances. Diatom flux remained correlated with POC (0.76) and BSi (0.71) flux at
315 1000 m, but the relationship between diatom and TMF did not hold at SCR 1000 m. LSi and BSi were
316 positively associated, and both were correlated with silicoflagellates at 1000 m (Table 2).

317 *3.4 Phytoplankton diversity*

318 78 diatom and 12 coccolithophore taxa were observed at the NCR site, and 64 diatom and 11
319 coccolithophore taxa at SCR (Supplementary Tables 1a-2b). Diatom diversity was slightly higher at
320 the 300 m traps than at the 1000 m traps (Supplementary Table 3). At NCR, the lowest diversity
321 occurred in late-April at 300 m (E_h = 0.31) and in early-October at 1000 m (0.29). Highest diversity
322 occurred in January at 300 m at 0.81, and in mid-September at 1000 m, 0.91. Coccolithophore
323 diversity was highest in early-October at NCR 300 m (1.0), and lowest in January (0.29), with a mean
324 of 0.6 (Supplementary Table 3).

325 At SCR, the lowest diatom diversity was found in mid-November at both 300 and 1000 m (E_h = 0.11
326 and 0.21, respectively) (Supplementary Table 3). Highest diversity at 300 m was seen in late-
327 December at 0.93, and at 1000 m in the same cup at 0.81. Coccolithophore diversity was lower at
328 SCR than NCR, with a mean of 0.49, and maxima and minima occurring in April and November, at
329 0.71 and 0.24, respectively (Supplementary Table 3).

330 *3.5 NCR phytoplankton assemblages*

331 Coastal and benthic diatoms comprised up to 40% of total diatom flux at NCR 300 m, and ~30% at
332 1000 m early in the sampling period (Fig. 3, Supplementary Tables 1a-1b). At other times, coastal
333 and benthic input consistently represented between 5-10% of assemblages (Fig. 3). The benthic
334 diatom *Delphineis minutissima* was common at both depths, comprising 5% and 5.5% of annual
335 integrated diatom flux, at 300 and 1000 m, respectively (Table 2, Fig. 3). Other common benthic
336 species at NCR included *Navicula directa, Psammodictyon panduriformis, Diploneis bombus* and
337 *Melosira* spp. Several typically coastal diatoms, designated "coastal and cosmopolitan" were also
338 abundant at NCR, including *Chaetoceros* spp. and *Stephanopyxis orbicularis*. The largest contributor
339 to diatom flux over the whole sampling period were *Chaetoceros* resting spores, contributing 45%
340 and 65% of annual integrated fluxes at 300 and 1000 m, respectively (Table 3).
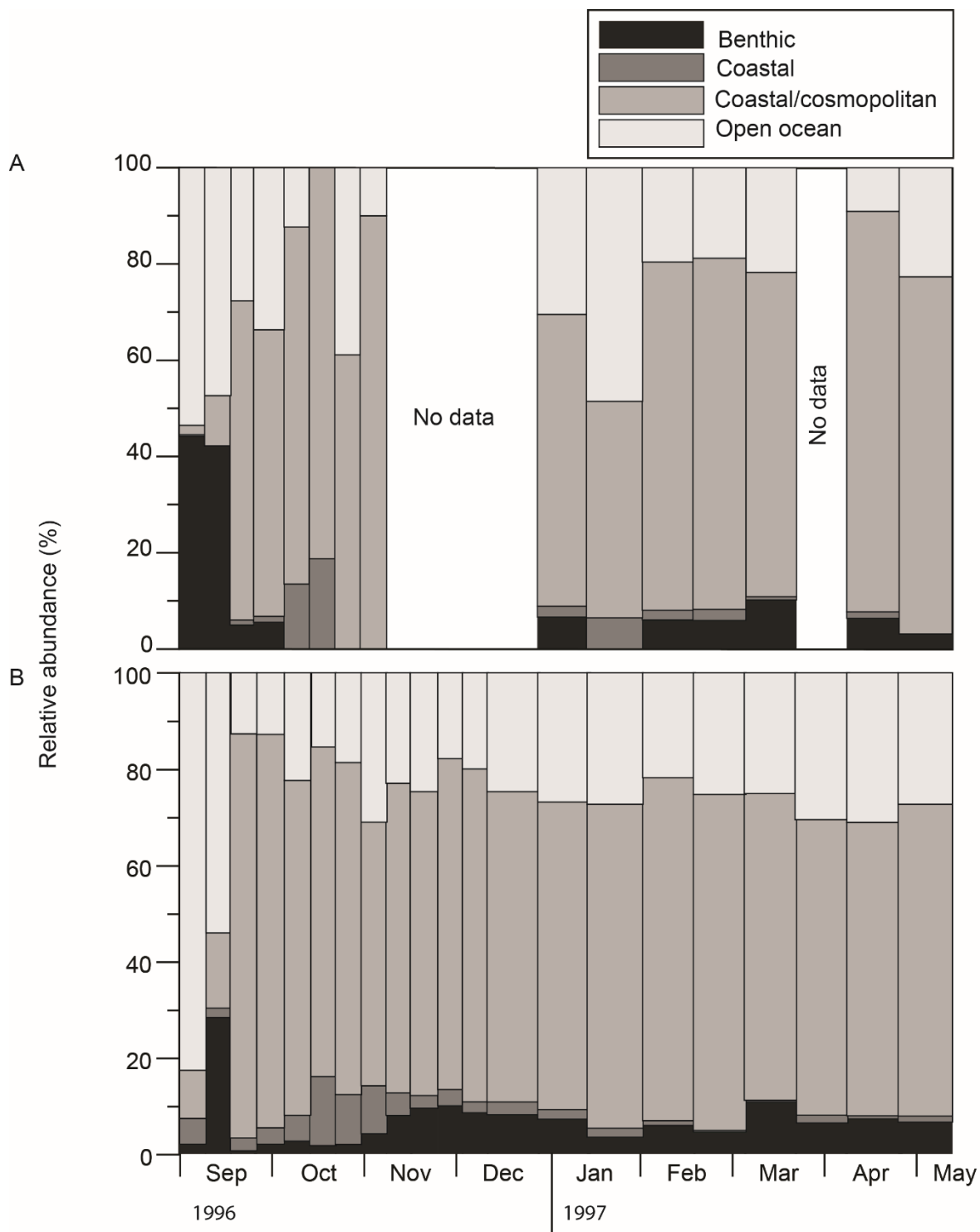
Figure 3. Diatom assemblages expressed as proportions of benthic, coastal, coastal and cosmopolitan, and open ocean taxa throughout the sampling period. A, NCR 300 m; B, NCR 1000 m.

Diatoms	NCR 300 m	NCR 1000 m	SCR 300 m	SCR 1000 m
Achtinoptichus senarius		0.4		
Bacteriastrum spp.	2.56	0.1		
Chaetoceros resting spores	44.8	64.7	0.1	1.4
Coscinodiscus spp.	0.4	0.3		
Delphineis minutissima	5.0	5.5		
Diploneis bombus		0.2		
Ditylum brightwellii	0.5	0.7		
Fragilariopsis kerguelensis		0.1		0.5
Fragilariopsis separanda	0.5	1.0		
Chaetoceros Hyalochaete spp.	9.8	0.6		
Lauderia annulata	6.1			
Navicula directa	1.2	0.2		
Nitzschia bicapitata	1.2	0.8	2.5	3.3
Odontella weissflogii		0.7		
Chaetoceros Phaeoceros spp.	5.7	0.3		
Psammodictyon panduriformis	0.5	0.6		
Pseudo-nitzschia australis	2.5			
Pseudo-nitzschia pungens	3.3	0.3	95.0	90.7
Rhizosolenia setigera	0.8	3.7		
Shionodiscus frenguellii group	1.2	2.6		
Shionodiscus oestrupii	0.4	2.6	0.5	
Shionodiscus poroseriatus	6.0	0.3		
Stephanopyxis orbicularis	1.2	2.8		
Thalassionema nitzschioides	0.6	2.4		
Thalassiosira ferelineata	0.3	0.2		
Centric <15 µm	1.3	0.6		
Coccolithophores				
Calcidiscus leptoporus	1.9	-	9.0	-
Coccolithus pelagicus	1.3	-		-
Emiliania huxleyi	65.7	-	76.7	-
Gephyrocapsa muellerae	2.4	-		-
Gephyrocapsa oceanica	3.8	-	-	-
Gephyrocapsa spp.	7.5	-	0.5	-
Gephyrocapsa spp. (< 3 µm)	11.0	-	11.3	-
Helicosphaera carteri	0.7	-		-
Umbellosphaera tenuis		-	1.7	-
Oolithotus spp.	0.5	-	0.3	-
Pontosphaera spp.	0.04	-		-
Syracosphaera spp.	1.3	-	0.1	-
Rhabdoliths	0.1	-		-
Reworked	0.1	-	-	-

344 ***Table 3***. List of diatom and coccolithophore species of over 1% weighted annual relative abundance at either depth (%).
345 Blank cells indicate values below 0.1. Dashes indicate no data.

346   At NCR 300 m, CCA plotted diatom species against two axes, with Axis 1 most strongly correlated
347   with SST, and Axis 2 with PAR (Table 4). The CCA showed two seasonal groupings of diatoms (Fig. 4A),
348   with taxa exhibiting peak relative abundance in spring clustered with the Chl-*a* vector, and
349   summer/autumn species associated with SST. *S. poroseriatus* and *S. frenguellii* also appeared to be
350   associated with PAR (Fig. 4A). Most of the major diatom species observed at NCR 300 m peaked in
351   relative abundance coinciding with the maximum spring peak in total diatom flux in early-October
352   (Figs. 2, 5), with peak abundances associated with highest mean Chl-*a* (Figs. 4A, 5). These spring-
353   peaking taxa were *Pseudo-nitzschia pungens, Psammodictyon panduriformis, Chaetoceros*
354   *Hyalochaete* and *Phaeoceros* spp., *Stephanopyxis orbicularis, Shionodiscus poroseriatus, Lauderia*
355   *annulata, Nitzschia bicapitata, Bacteriastrum* spp., and centric spp. < 15µm (Fig. 5). Taxa exhibiting
356   highest relative abundance in summer or autumn months formed a second grouping comprising
357   *Chaetoceros* spores, *Shionodiscus oestrupii, S. frenguellii* group, and *Rhizosolenia setigera*, with
358   peaks in abundance associated with higher SST (Fig. 4A). Note that many of these species also
359   showed high abundances in spring, but showed a strong resurgence later in the sampling period.
360   *Delphineis minutissima* was associated with this group, despite being most abundant in spring,
361   although a secondary peak in *D. minutissima* relative abundance occurred in autumn when SST was
362   near its warmest (Fig. 2C, 5). The correlation values between the vectors and axes are given in Table
363   4.

	NCR diatom fluxes		SCR diatom fluxes	
	Axis 1	Axis 2	Axis 1	Axis 2
SST	-0.73	-0.31	-0.27	0.21
Chl-*a*	0.57	-0.27	-0.38	-0.33
PAR	-0.05	-0.75	0.50	0.09
	NCR coccolith fluxes		SCR coccolith fluxes	
SST	-0.36	0.26	-0.68	-0.27
Chl-*a*	0.51	-0.26	-0.71	-0.10
PAR	0.30	0.31	-0.01	0.36

364   *Table 4.* Correlation between axes and vectors for SCR and NCR plotted in Figs. 4 and 8.
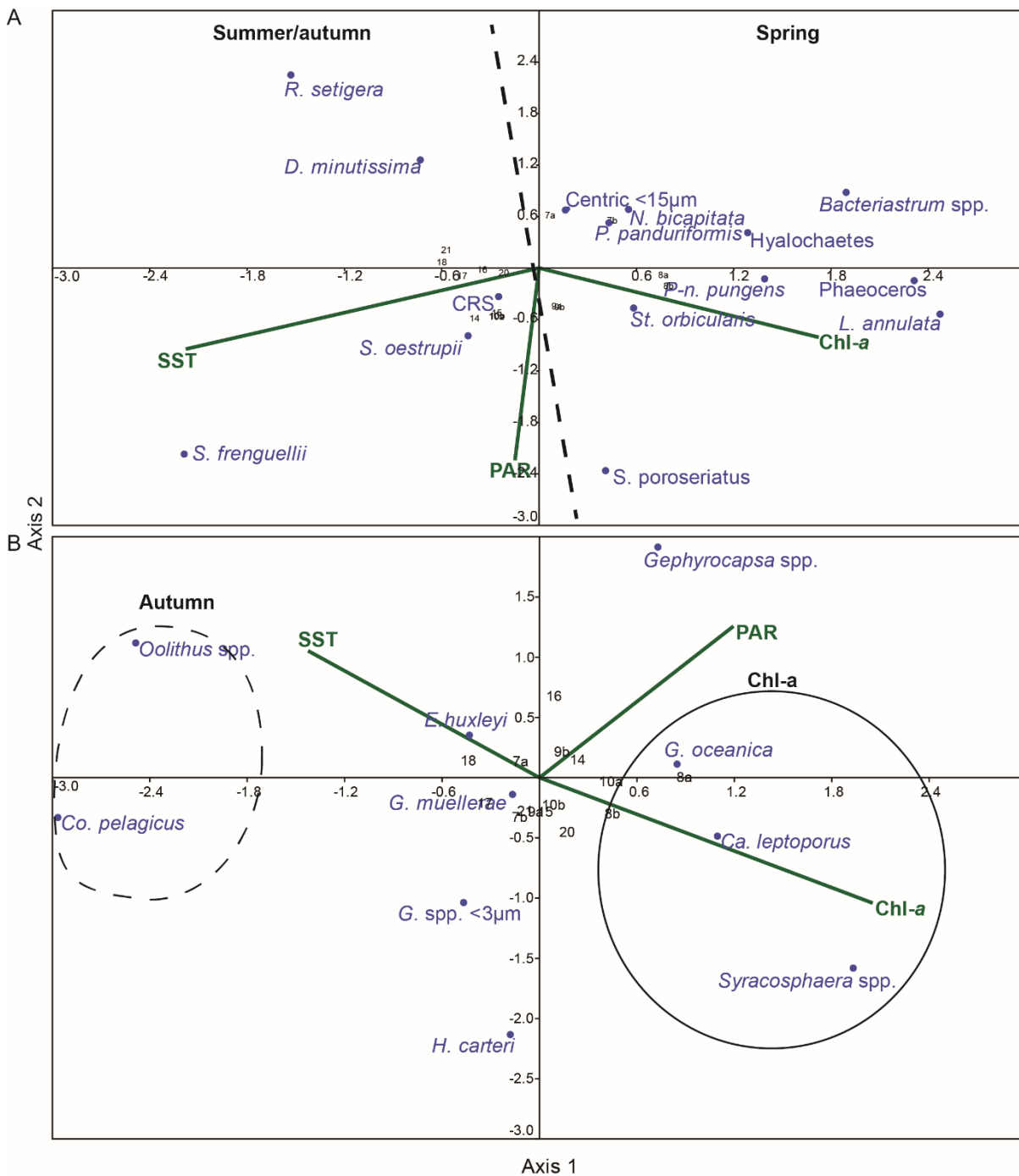
Figure 4. Canonical Correspondence Analysis (CCA) output for NCR 300 m. A, Diatoms ≥1% weighted annual RA and ≥5% RA in any cup, axis one = 71.3% of variation; B, coccolithophores present in more than one cup, axis one = 74.1% of variation. Vector lines are Sea Surface Temperature (SST), Photosynthetically Active Radiation (PAR) and Chlorophyll-a (Chl-a). Dashed line in A separates summer/autumn, and spring groupings. Dashed circle and solid circle in B highlights autumn and spring groupings, respectively. *Correlation values between the vectors and axes are given in Table 4.*
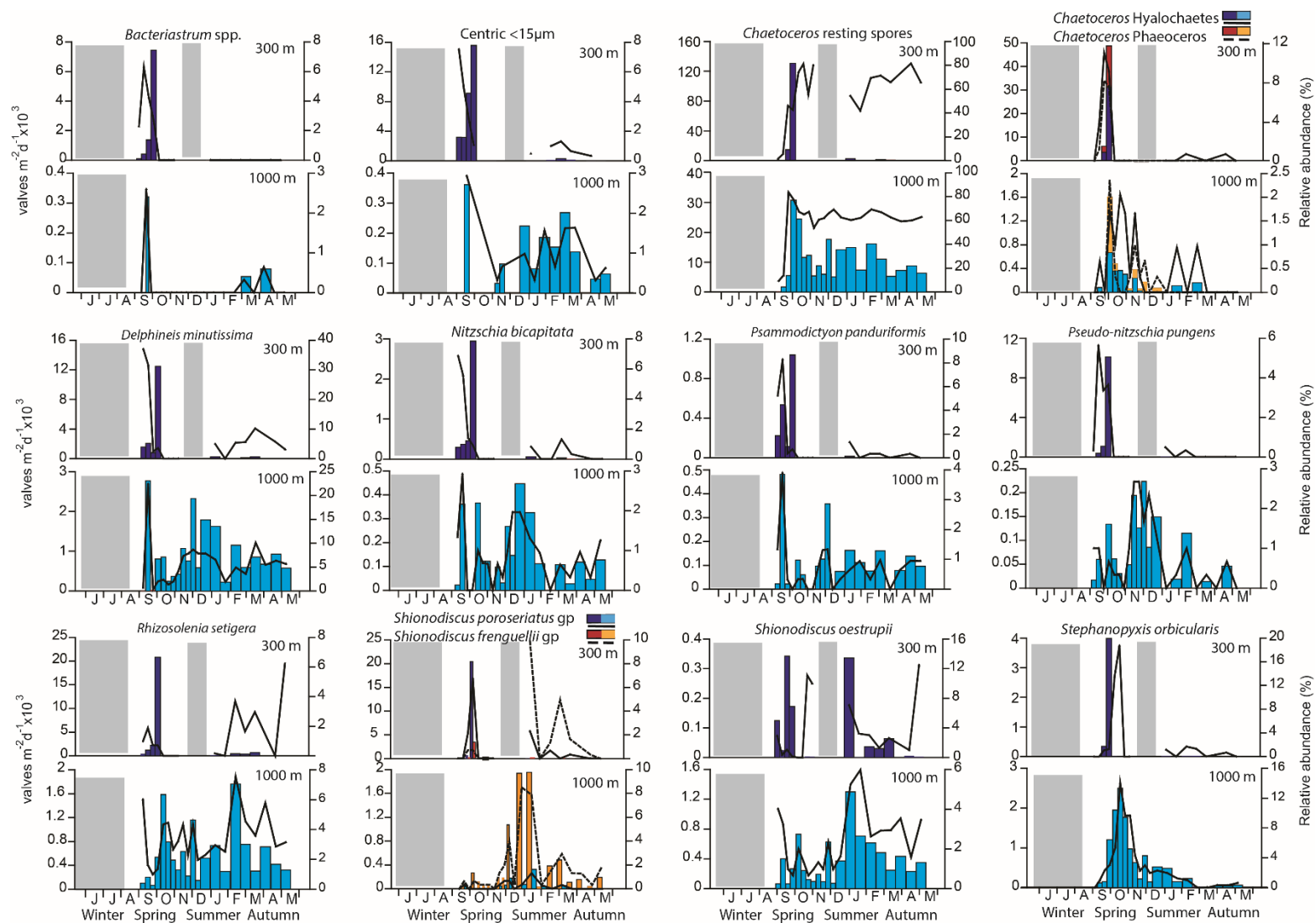
Figure 5. NCR 300 m (dark blue bars) and 1000 m (light blue bars) dominant diatom relative abundance (%; lines) and absolute abundance (valves m^2 d^{-1} × 10^3; bars). Diatom taxa over 1% weighted annual abundance and over 5% relative abundance in any cup. Grey vertical bars indicate no data collected.

374   Generally, species fluxes at 1000 m were lower and less strongly seasonal than at 300 m, except *S.*
375   *oestrupii*, which showed higher valve fluxes (but lower relative abundance) at the deeper trap,
376   peaking at ~1300 valves m^{-2} d^{-1} in late-December (Fig. 5). Other species which showed peak valve
377   flux in the summer months at 1000 m were *Nitzschia bicapitata, Shionodiscus poroseriatus* and *S.*
378   *frenguellii* group (Fig. 5).

379   The bulk of the coccolith spring peak at both sites was composed of *Emiliania huxleyi*, the most
380   abundant coccolithophore observed in this study, at 66% total integrated abundance. This taxon
381   dominated fluxes in all but one cup at NCR, with maximum abundances of 91% in October (Table 3,
382   Fig. 6). *Emiliania huxleyi* abundances were above 30% for the entire sampling period, except in early
383   October, when *G. muellerae* and *G.* spp. were co-dominant (Fig. 6). Small *Gephyrocapsa* spp. were
384   the next most significant group, and combined, the genus *Gephyrocapsa* comprised nearly 25% of
385   total coccolith flux at NCR (Table 3).
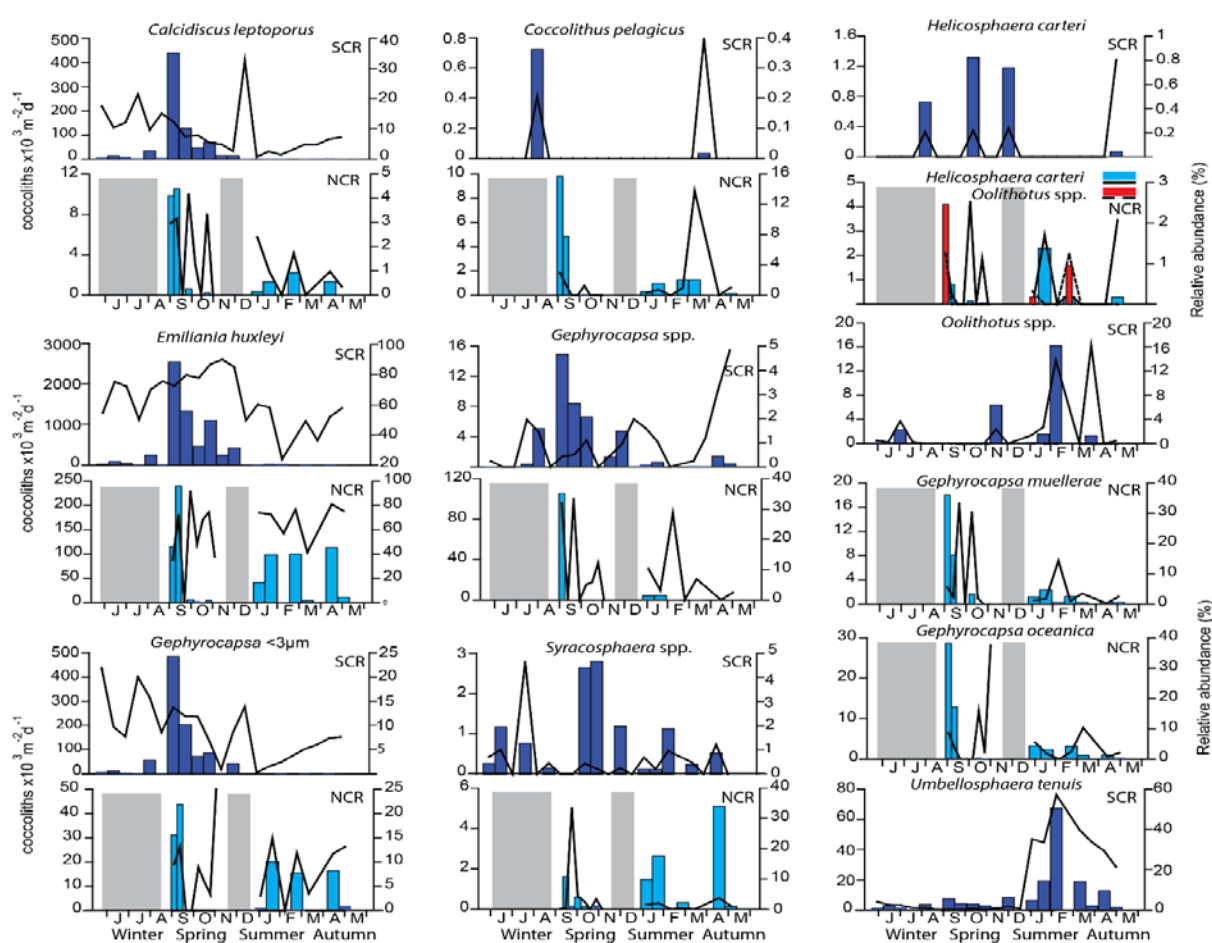
386

387   *Figure 6. NCR (light blue bars) and SCR (dark blue bars) coccolith relative abundance (%; lines) and absolute abundance*
388   *(coccoliths m^2 d^{-1} × 10^3; bars) of all coccoliths observed in more than one cup. Grey vertical bars indicate no data collected.*

389   Ten coccolithophore taxa were plotted on the CCA, and three main clusters were identified: Chl-*a*-
390   associated taxa, autumn taxa weakly related to SST, and taxa not related to any one environmental
391   variable, clustered towards the centre of the plot (Fig. 4B). *Gephyrocapsa* spp. appeared to be related
392   to the PAR vector (Fig. 4B). The Chl-*a* cluster included *Calcidiscus leptoporus, Gephyrocapsa oceanica*
393   and *Syracosphaera* spp., all of which showed highest absolute flux in the spring period (Fig. 6) *C.*
394   *leptoporus* and *Syracosphaera* spp. exhibited high relative abundances in winter (low Chl-*a*), while *G.*
395   *oceanica* showed greatest relative abundance in spring (high Chl-*a*; Fig. 6). The autumn-peaking taxa,
396   *Coccolithus pelagicus* and *Oolithotus* spp., exhibited relative abundance maxima in March (Fig. 6). It
397   should be noted that at low abundances (such as of the latter two species), the relationships
398   presented in the CCA may not be robust, making some of these groupings simply suggestions of
399   seasonality. The remaining coccolithophore taxa (*E. huxleyi, G. muellerae* and *G.* spp. <3µm, and
400   *Helicosphaera carteri*) were present to some extent throughout the sampling period. (Fig. 6).

401   *3.6 SCR phytoplankton assemblages*

402   The bulk of diatom flux at SCR was composed of *Pseudo-nitzschia* spp.*,* at 95% and 91% of annual
403   diatom fluxes at 300 and 1000 m, respectively (Table 3). *Pseudo-nitzschia* spp. formed a dense bloom
404   ("pulse") event, the sedimentation of which was captured in October-November (Fig. 7;
405   Supplementary Plate 1). The overwhelming flux of *Pseudo-nitzschia* caused the weighted annual
406   abundances of other species to appear low, so the CCA was expanded to include the top 13 diatom
407   taxa by relative abundance (Fig. 8). Axis 1 was most strongly related to PAR, while Axis 2 was
408   correlated, although weakly, to Chl-*a* (Table 4).
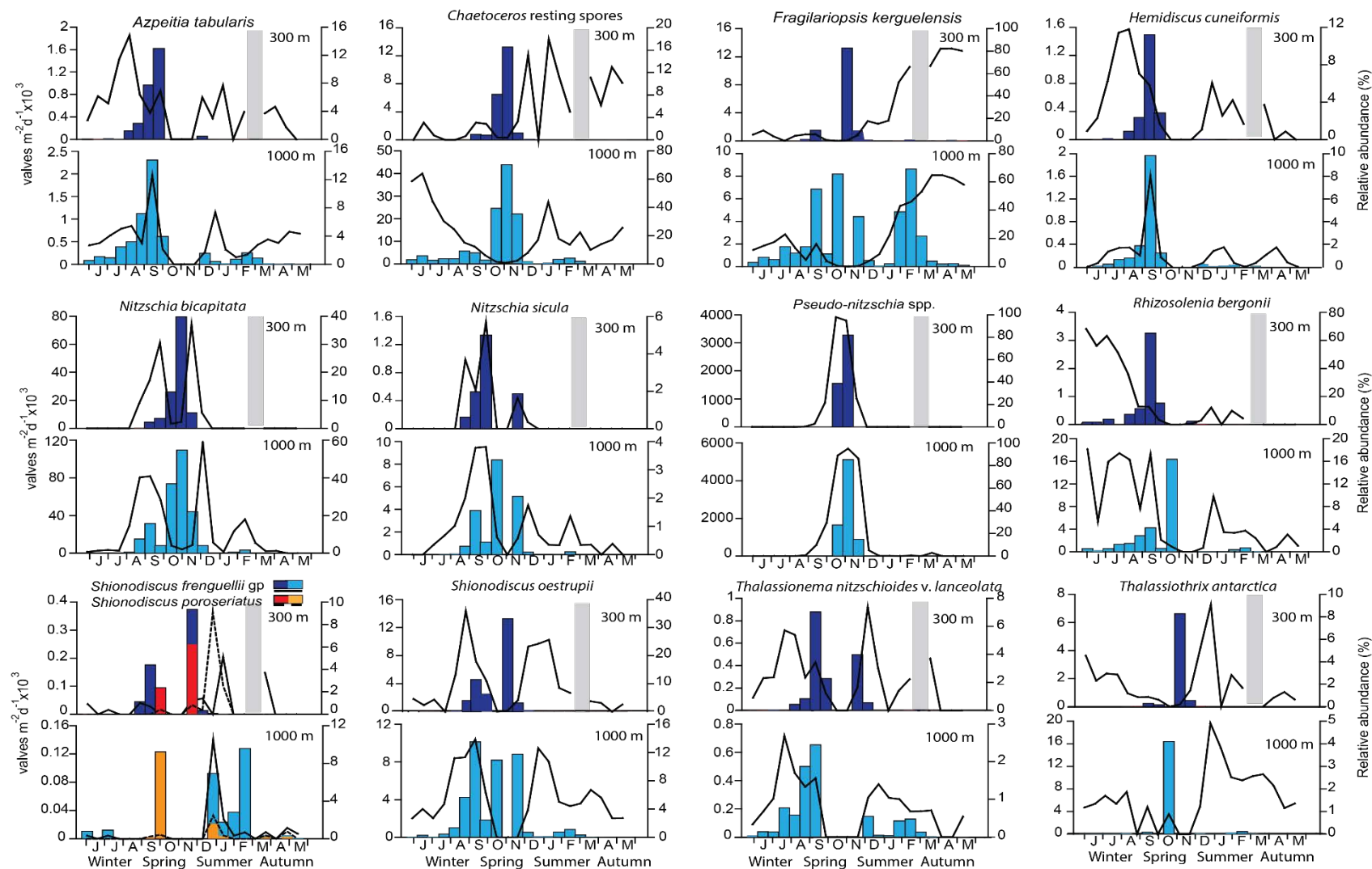
Figure 7. SCR 300 m (dark blue bars) and 1000 m (light blue bars) dominant diatom relative abundance (%; lines) and absolute abundance (valves $m^2\ d^{-1} \times 10^3$; bars). Diatom taxa over 1% weighted annual abundance and over 5% relative abundance in any cup. Grey vertical bars indicate no data collected.

A

Early-peaking/year-round

Late-peaking/PAR

4.0 — •S. poroseriatus

3.2 —

2.4 —

1.6 — Thalassiothrix spp.•

0.8 — SST CRS•

•R. bergonii
•F. kerguelensis

13

•P-n. spp.

PAR

10a 9a

20.3
47.316

-2.0 -1.5 -1.0 -0.55

12
6

1.01a 1.5 2.0 2.5

•A. tabularis

18

S. oestrupii

8a

•N. bicapitata

-0.8 — H. cuneiformis•
T. Nitzs. var. lance.

Chl-a

-1.6 —

-2.4 — •S. frenguellii gp. •N. sicula

Axis 2

B

PAR

•E. huxleyi

Oolithus spp.•

11a 10a

6 a
16

Chl-a

-3.0 -2.4 -1.8 -1.2 0.6
19

0.6 1.2 1.8 2.4
Ca. leptoporus

Syracosphaera spp.
SST U. tenuis

20 4
21

G. spp. <3µm

-1 —

-2 — Gephyrocapsa spp.•

Chl-a/SST related

-3 —

-4 —

-5 —

Low-abundance/Autumn

-6 —

-7 — •H. carteri

Co. pelagicus•

-8 —

Axis 1

412
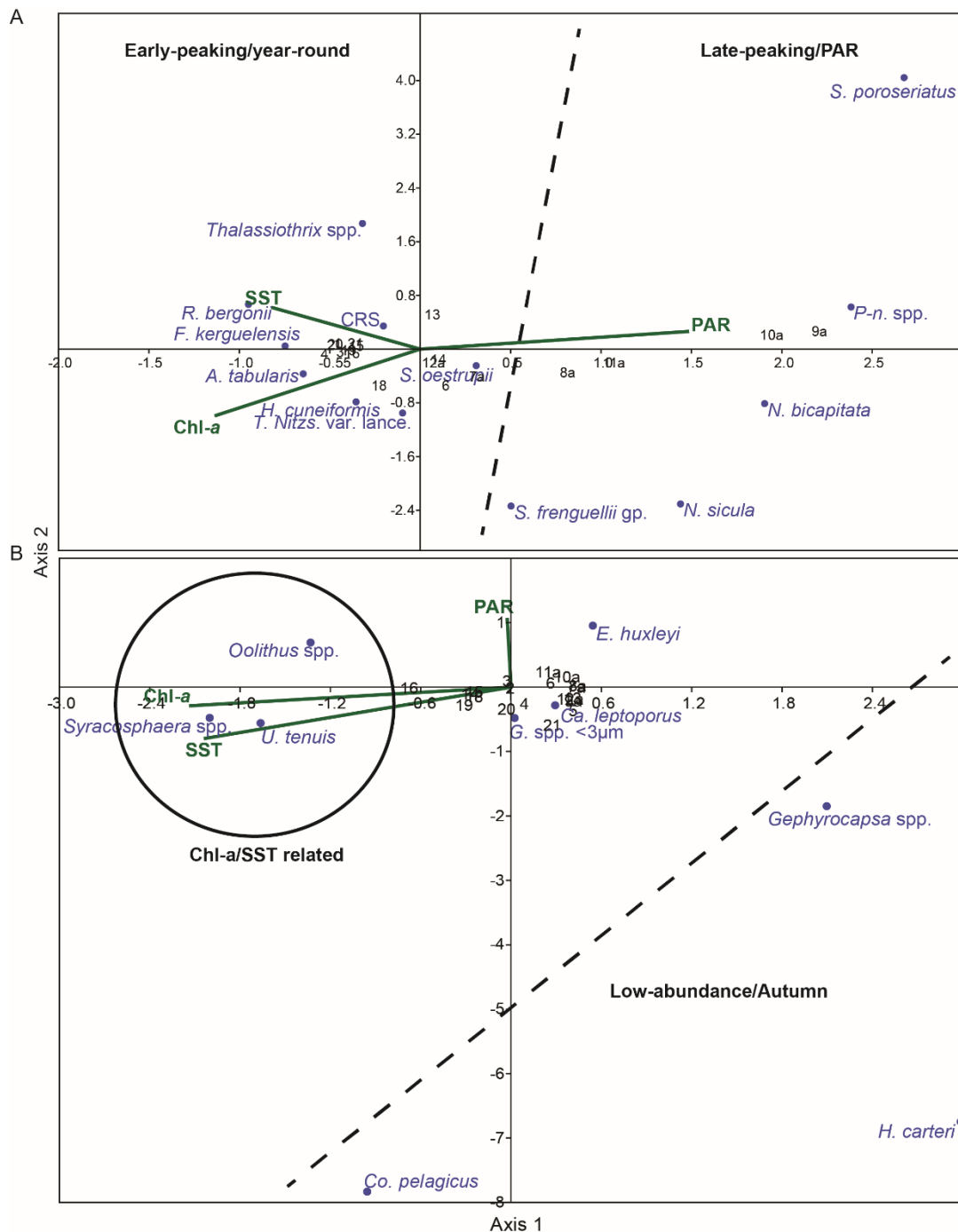
Figure 8. *Canonical Correspondence Analysis (CCA) output for site SCR 300 m. A) 13 most abundant diatoms by relative abundance, axis one = 87.6% of variation; B) coccolithophores present in more than one cup, axis one = 68.9% of variation. Vector lines are Sea Surface Temperature (SST), Photosynthetically Active Radiation (PAR) and Chlorophyll-a (Chl-a). Dashed line in A separates early-peaking/year-round from late-peaking/PAR groupings. Solid circle and dashed line in B highlights Chl-a/SST related, and Low-abundance/autumn groupings, respectively. Correlation values between the vectors and axes are given in Table 4.*

413
414
415
416
417
418

419   At SCR 300 m, the CCA identified taxa either peaking in relative abundance 'late' in the sample period
420   (i.e. during or after the main October total diatom flux peak in mid-spring or summer), peaking early
421   in the period (i.e. before the main October total diatom flux peak in winter to early-spring), or
422   present year-round (Fig. 8A). The late-peaking species included the dominant *Pseudo-nitzschia* spp.
423   (maximum relative abundance in spring), as well as *S. poroseriatus* (maximum in summer), *S.*
424   *frenguellii* group (summer) and *N. bicapitata* (late spring). These taxa were associated with
425   increasing PAR, and had maximum abundances from September to late January (Fig. 7, 8A). *N. sicula*
426   appeared with this grouping despite seeing peak relative abundance just before the main October
427   diatom flux peak, but was entirely absent after November, when PAR was highest (Figs. 2, 7).

428   SST and Chl-*a* were correlated in the CCA, with the first minor peak in Chl-*a* associated with the
429   beginning of SST warming in September, and the Chl-*a* maximum occurring with maximum SST in
430   February (Figs. 2, 8A). Diatom taxa that plotted near the SST and Chl-*a* vectors fell into two groups,
431   the first being early-peaking species showing highest relative abundances before the main spring
432   peak in October, when SST began to increase (*Rhizosolenia bergonii, Azpeitia tabularis, Hemidiscus*
433   *cuneiformis* and *Shionodiscus oestrupii*). The second group were those species with maximum
434   relative abundances in summer when Chl-*a* was highest (*Chaetoceros* resting spores, *Thalassionema*
435   *nitzschioides* var. *lanceolate* and *Fragilariopsis kerguelensis*; Fig. 7).

436   Flux patterns at 300 m were largely mirrored at 1000 m (Fig. 7). *Pseudo-nitzschia* spp*., Chaetoceros*
437   resting spores, *R. bergonii,* and *N. sicula* showed greater diatom flux at 1000 m than at 300 m. In
438   some cases, the disparity between flux captured in the 300 and 1000 m traps was substantial;
439   *Pseudo-nitzschia* fluxes at 1000 m were roughly 1.5 times those captured at 300 m, *N. bicapitata*
440   were 2 times higher, and spore fluxes were five times higher in the deeper trap (Fig. 7).

441   *Emiliania huxleyi* was the most abundant coccolithophore at SCR, forming 77% of the total integrated
442   assemblage (Table 3). As at NCR, *Gephyrocapsa* spp. were common in the sediment trap records,
443   with small *Gephyrocapsa* spp. <3 μm comprising >11% of the total capture, although other
444   *Gephyrocapsa* were rarer (Table 3).

445   The CCA plotted SCR coccolith species into three clusters; those species related to Chl-*a* and SST, the
446   low abundance or autumn-peaking taxa, and taxa with abundance patterns not related to the
447   environmental variables (Fig. 8B). Chl-*a* and SST vectors plotted close to one another, indicating
448   similar influences on *Oolithotus* spp., *Syracosphaera* spp., and *Umbellosphaera tenuis* (Fig. 8B).
449   *Syracosphaera* spp. were most abundant early in the sampling period when SST and Chl-*a* were
450   lowest in July, but was present at low abundances year-round (Fig. 6). *Oolithotus* spp. and *U. tenuis*
451   appeared at peak relative abundances later in the record when SST and Chl-*a* was high, with the
452   latter almost 60% of all coccoliths in late summer (Fig. 6). The taxa at the lower right of the plot,
453   *Gephyrocapsa* spp., *Coccolithus pelagicus,* and *H. carteri,* indicated no observable relationship to the
454   environmental vectors, but tended to be present at low abundances, and throughout autumn (Figs.
455   6, 8B).

456   The remaining coccolithophore species, and three most abundant taxa observed at SCR 300m, *E.*
457   *huxleyi, C. leptoporus* and *Gephyrocapsa* spp. <3 μm, showed complex abundance patterns that did
458   not relate to any individual environmental variable (Figs. 6, 8B). These taxa were a prominent

459   component of SCR sediment trap records for the time series, with *E. huxleyi* and *C. leptoporus*
460   showing peak abundance in summer, and *Gephyrocapsa* spp. <3 μm recorded with greatest
461   abundance in winter (Fig. 6).

462   **4. Discussion**

463   *4.1 Fluxes north and south of the Chatham Rise*
464   4.1.1 Siliceous phytoplankton
465   The magnitude of diatom fluxes at SCR was greater than at NCR, consistent with diatom flux results
466   from nearby traps, which reported diatom flux over seven times higher in the subantarctic (SAM,
467   1500 m) than Subtropical (STM, 1500 m) (Prebble et al. 2013) (Fig. 1). Deeper mixed layers at the
468   NCR site, allowing for greater microbial action on sinking particles, may have been a factor resulting
469   in lower fluxes at NCR, but this remains speculative. The annual diatom flux estimated for the SCR
470   300 m (8.2 x10^7 valves m^{-2} y^{-1}) was within the range observed in the Australian sector of the SAZ at
471   the same latitude (3 – 23 x 10^7, 500 to 1000 m; Rigual-Hernandéz et al. 2015a; Wilks et al. 2017). SCR
472   flux was, however, low relative to the nearest sediment trap deployments in the New Zealand sector,
473   (AESOPS site MS2, 56° 54'S, 170° 10'W, 982 m), where fluxes were calculated at 5 x10^9 m^{-2} y^{-1}
474   (Grigorov et al. 2014).

475   The strong correlation between POC flux with diatom and BSi fluxes at NCR (Table 2), paired with the
476   known significance of diatoms to cell carbon in surface waters of the STFZ off New Zealand (Bradford-
477   Grieve et al. 1997) together imply that diatoms likely played an important role in POC and BSi export
478   north of the Chatham Rise (Nodder and Northcote 2001, Sikes et al. 2005). At SCR, coccolith flux was
479   more strongly associated with POC flux than diatom flux, although BSi flux remained clearly diatom-
480   driven. Nonetheless, since the carrying capacity of POC per cell could not be quantified in this study,
481   the role of either group in organic carbon export at these sites remains hypothetical.

482   The potential significance of other silicifying groups is considered; silicoflagellates and radiolarians
483   were abundant at SCR, with fluxes at times almost as high as diatom flux (Supplementary Tables 1a
484   - 2b). The nearby STM and SAM moorings (1500 m trap depths) echo this finding, also indicating
485   higher silicoflagellate fluxes in the subantarctic than in the subtropical waters east of New Zealand
486   (though roughly equivalent radiolarian fluxes in the two water masses; Prebble et al. 2013). In the
487   Australian sector, silicoflagellates have been observed with increasing flux from the SAZ and south,
488   and comprise a significant proportion of silica exported in the Subantarctic Zone (Rigual-Hernández
489   et al. 2016a). Conversely, in the sediment record, radiolarians exhibited better preservation and
490   were more abundant at NCR than SCR (Hollis and Neil 2005), which has been attributed to lower
491   silicic acid concentrations relative to nitrate in subantarctic waters (Dugdale et al. 1995).

492   Over 90% of total diatom flux captured at SCR occurred during a 48-day pulse of *Pseudo-nitzschia*
493   spp. from mid-October to early-November (austral spring), with higher fluxes in the 1000 m than the
494   300 m trap (Fig. 7). This pulse corresponded with a spike in BSi flux into the traps (Nodder and
495   Northcote 2001), and a strong correlation was indicated between *Pseudo-nitzschia* flux and BSi at
496   300 m (0.92; Table 2). *Pseudo-nitzschia* spp. are generally regarded as opportunistic diatoms, and
497   iron fertilisation experiments result in rapid proliferation (with other pennate diatoms), with *Pseudo-*
498   *nitzschia* often dominating or co-dominating phytoplankton communities in the Southern Ocean

499   (Gall et al. 2001; Coale et al. 2004; De Baar et al. 2005) and elsewhere (Landry et al. 2000; Marchetti
500   et al. 2006; Trick et al. 2010).

501   The dense *Pseudo-nitzschia* spp. "mats" observed during the pulse event also entangled other large
502   pennate diatoms, such as *Thalassiothrix* spp., and diatoms with long spines such as *Chaetoceros*
503   (Phaeoceros) vegetative cells. It is likely that the formation of these mats facilitated the rapid export
504   and consequently good preservation of other taxa, evidenced by a simultaneous resurgence in
505   coccolith fluxes with the *Pseudo-nitzschia* pulse (Fig. 2). Interestingly, biomarker analysis in the same
506   sediment trap samples revealed a peak in alkenone abundance (signalling mainly *Emiliania huxleyi*)
507   coinciding with the *Pseudo-nitzschia* pulse (Sikes et al. 2005), providing compelling evidence of
508   enhanced export of other phytoplankton groups such as haptophytes at the same time. The
509   correlation between coccoliths and POC, TMF and BSi export at SCR 300 m (Table 2) may also be a
510   mat-associated phenomenon resulting from enhanced sedimentation (Kemp and Villareal 2013), and
511   the consequent co-sedimentation of different flux components.

512   Canonical Correspondence Analysis revealed a relationship between *Pseudo-nitzschia* and enhanced
513   light levels (PAR) (Fig. 8A), congruent with reports of increasing day length and light intensity as a
514   trigger for *Pseudo-nitzschia* blooms (Rhodes et al. 2013). On the other hand, *Pseudo-nitzschia* spp.
515   have been reported as important contributors to subsurface chlorophyll layers in several oceanic
516   systems (Revelante and Gilmartin 1995; Totti et al. 2000; Seegers et al. 2015), including the Southern
517   Ocean (Gomi et al. 2007). Deep-growing taxa may account for as much export production as the
518   spring bloom itself (Kemp et al. 2000) and such production is not necessarily detected by satellite
519   remote sensing of chlorophyll-*a*. Indeed, an 11-year sediment trap record from New Zealand
520   subantarctic waters recorded several years in which spring export was associated with subsurface
521   production and high BSi fluxes, undetected by chlorophyll-*a* accumulation in surface waters (Nodder
522   et al. 2016). Ocean colour data suggests the autumn bloom in subtropical waters in this region are
523   likely the result of wind-caused mixing of subsurface production to the upper layers (Chiswell et al.
524   2013), presumably followed by their sedimentation in autumn. Subsurface production may be a
525   common occurrence within the New Zealand SAZ, whether driven by deep-living *Pseudo-nitzschia*
526   spp., or other typical shade flora (e.g. *Rhizosolenia* or *Thalassiothrix*). Nonetheless, accompanying *in*
527   *situ* measurements of mixed layer depth and vertical distribution of nutrients and chlorophyll-*a* will
528   be required to identify with confidence the factors triggering the development and rapid export of
529   *Pseudo-nitzschia* blooms.

530   4.1.2 Coccolithophores
531   Spring coccolith flux was roughly an order of magnitude higher at SCR than NCR, but low relative to
532   other trap deployments in the Australian/New Zealand sector (Wilks et al. 2017; Rigual-Hernández
533   et al. 2018). High coccolith flux and diversity is typical in the SAZ in the open-ocean subantarctic
534   south Pacific region (Honjo et al. 2000; Gravalosa et al. 2008). East of New Zealand, seafloor
535   sediments in the SAZ are between 70 and 90% carbonate (Nodder et al. 2003), indicating high export
536   of calcareous phytoplankton and heterotrophic calcifying zooplankton, such as foraminifera and
537   pteropods. Sediment trap deployments in the SAZ typically capture calcium carbonate-rich material
538   (>50% of mass flux) (Honjo et al. 2000; Trull et al. 2001a; Rigual-Hernández et al. 2015a; Nodder et
539   al. 2016). Coccolithophores are more abundant than diatoms in subantarctic waters, both near SCR
540   (Malinverno et al. 2016), and in the Australian sector (Trull et al. 2018).

541 Annual coccolith flux estimates at the SCR 300 m trap (1.4 x 10^8 coccoliths m^{-2} y^{-1}) were three orders
542 of magnitude lower than coccolith fluxes estimated in the Australian sector at ~47°S (6.5 x10^{11}
543 coccoliths m^{-2} y^{-1}; Wilks et al. 2017), but comparable to estimates from sediment traps at 50°S, in the
544 Indian sector's Antarctic Zone (4.7 x10^7 coccoliths m^{-2} y^{-1}; Ternois et al. 1998). Lower coccolith fluxes
545 at SCR than in the corresponding Australian sector traps could be due simply to inter-annual
546 variability of fluxes. It is likely that the coccolith fluxes of Wilks et al. (2017) represented unusually
547 high coccolith sedimentation, though without multi-year data, this remains speculative.

548 *4.2 Phytoplankton community assemblages and seasonal succession on the Chatham Rise*

549 Phytoplankton community succession from coccolithophores to diatoms occurred at both sites (Fig.
550 2). In upwelling regions, diatoms typically bloom earlier in the season, declining after depleting the
551 surface waters of silicate, allowing coccolithophore proliferation (Hopkins et al. 2015; Balch et al.
552 2016). However, diatoms and coccolithophores can bloom synchronously (Hopkins et al. 2015).
553 Additionally, strong inter-annual variability in sediment trap fluxes has been observed in New
554 Zealand waters, especially in the SAZ (Nodder et al. 2016). The 1996-97 study year was particularly
555 warm (Sikes et al. 2005), with the Wairarapa Eddy intermittently delivering warmer waters over the
556 NCR study site, potentially influencing the timing of phytoplankton bloom development in this study
557 period. Further phytoplankton analysis on multi-year datasets (i.e. Nodder et al. 2016) in the study
558 region will be required to determine the typical phytoplankton successional regime in these waters.

559 Zooplankton grazing may cause sediment trap composition and seasonality to inaccurately mirror
560 surface production, for example via grazing-facilitated export due to incorporation of preferred prey
561 into aggregates and faecal pellets (Boyd et al. 1997). Grazing was not measured in this study, but
562 based on copepod faecal production rates, Zeldis et al. (2002) estimated faecal pellet export at half
563 to one third of SCR 300 m POC export, and therefore potentially highly significant to phytoplankton
564 fluxes. The potential impact of mesozooplankton grazing and faecal pellet flux on POC fluxes was
565 addressed by Nodder and Gall (1998), who estimated that faecal pellet export was highest in the
566 STFZ and STZ, compared to the SAZ, in spring while opposite trends were observed in winter.
567 Alkenone records from SCR and NCR indicated high winter zooplankton grazing at both sites, but
568 with zooplankton-related biomarker products dominating export production at NCR (Sikes et al.
569 2005). In the 1996-97 period, it is likely that grazing pressure was more pronounced at NCR. High
570 winter grazing can exaggerate the natural amplitude of phytoplankton population growth and
571 decline across a season in sediment trap records, with poor export efficiency due to particle recycling
572 in the upper water column (Nodder et al. 2005), and a lack of ballasting (Armstrong et al. 2001).

573 4.2.1 Diatoms
574 NCR and SCR traps contained largely distinct diatom communities, which are consistent with
575 previous reports on diatom assemblage composition in the surface waters (Chang and Gall 1998) and
576 sediments in the study region (Fenner et al. 1992; Romero et al. 2005; Cochran and Neil 2009).
577 Diatom floral composition at NCR was a typical subtropical open ocean assemblage characterised by
578 warm water taxa, such as *Thalassionema nitzschioides* and *Fragilariopsis doliolus*, but with a
579 substantial input of benthic (*Delphineis minutissima, Navicula directa, Melosira* spp.),
580 benthic/cosmopolitan (*Diploneis bombus*), and coastal/cosmopolitan (*Psammodictyon*
581 *panduriformis*) species (Table 3) (Hallegraeff et al. 2010).

582   Diatom assemblage diversity was the same at both the NCR and SCR sediment traps. The loss of
583   lightly silicified species at depth explains the slightly higher diversity index values resolved from the
584   shallower traps at each site (Supplementary Table 3). Diatom diversity at NCR was higher during the
585   spring/summer months, possibly attributable to enhanced aggregation rates and hence particle
586   export in the productive season (e.g. Rigual-Hernández et al. 2016b). In contrast, at SCR the lowest
587   diversity values were seen during the *Pseudo-nitzschia* pulse event (Supplementary Table 3), where
588   the high abundance of *Pseudo-nitzschia* spp. frustules overwhelmed the export flux, possibly causing
589   the under-estimation of the relative abundance of co-occurring species.

590   The observed seasonal pattern in the NCR and SCR sediment traps broadly follows the seasonal
591   succession scheme proposed by Quéguiner (2013) and Kemp et al. (2000) for colder and temperate
592   regions. Quéguiner (2013) outlines a basic diatom successional scheme whereby "group 1" taxa
593   (small, fast-growing, colonizing species) are seen first in assemblages, later succeeded by "group 2"
594   (slow-growing, persistent species). There is some evidence for such a succession of assemblages in
595   the Chatham Rise traps. Maximum abundances of the small pennates representing group 1, (e.g.
596   *Delphineis minutissima*) and centrics*,* were seen in late winter/early spring at NCR, while larger taxa
597   representing group 2 (*Shionodiscus* spp., *Rhizosolenia* spp.) reached their peak fluxes towards the
598   end of summer, and were associated with higher SST (Figs. 4, 5).

599   Cold water, subantarctic-associated species, such as *Thalassiothrix* spp., *Fragilariopsis rhombica* and
600   *Stellarima microtrias,* were occasionally observed at the NCR mooring (Table 3, Supplementary
601   Tables 1a-1b), providing evidence of the occasional advection of subantarctic waters across the
602   Chatham Rise. These occurrences did not appear to be linked to any obvious seasonal processes,
603   though mixing has been reported previously across the Chatham Rise (Chiswell et al. 2001), with
604   filaments of subantarctic waters found at least 150 km into the subtropical surface water mass
605   (Nodder 1997b). Mixing appeared to go in both directions over the rise, with the occasional input of
606   warm-water diatoms observed in the SCR trap (*F. doliolus* and *Roperia tesselata*; Supplementary
607   Tables 2a-b).

608   The ubiquitous *Fragilariopsis kerguelensis* occurred at higher abundances within SCR than NCR traps.
609   *F. kerguelensis* formed up to 80% of the winter assemblage at SCR; however on an annual scale, this
610   species was infrequent compared to its usual dominance in other Southern Ocean sediment trap
611   records, particularly those reported from higher latitudes (Rigual-Hernández et al. 2015a; Rigual-
612   Hernández et al. 2015b; Wilks et al. 2017).

613   Some taxa identified in the SCR and NCR sediment traps represent distributions not previously
614   recorded in regional phytoplankton surveys. For example, *Odontella mobiliensis* was only found in
615   the STFZ by Chang and Gall (1998), but was up to 5% of diatom sediment trap abundances at NCR,
616   highlighting the STFZ influence at this site. *O. mobiliensis* abundances were greatest in the deeper
617   trap, suggesting relative enrichment of this species due to enhanced dissolution of this more lightly
618   silicified taxa. Delicate species such as *L. annulata,* though more abundant in surface waters in winter
619   (Chang and Gall 1998), were only found in trap samples in spring and autumn. Particle sinking rates
620   (and hence preservation) are seasonal in the Southern Ocean (Berger and Wefer 1990), with greater
621   production leading to enhanced sinking rates in spring (Closset et al. 2015). This may explain the
622   higher prevalence of delicate forms such as *L. annulata* during periods of greater sedimentation.

623   *Chaetoceros Hyalochaete* vegetative cells and resting spores were a common feature at NCR, though
624   were also found at SCR (Table 3). The differential preservation of *Chaetoceros* resting spores relative
625   to less robust taxa may also play a role in the continued high spore fluxes at NCR, even after the
626   decline of the vegetative cells in October. The high, sustained presence of spores throughout the
627   decline of the main bloom was recorded in Australian sector sediment trap studies in the SAZ (Wilks
628   et al. 2017), signalling a transitional assemblage between early and late-successional taxa. Spore
629   formation is thought to be triggered by nutrient deficiency (Leventer 1991; Oku and Kamatani 1997),
630   and tends to occur later in the spring bloom progression in this region (Boyd et al. 1999; Ellwood et
631   al. 2015). Thus, the presence of spores reflects a mid/later stage of diatom bloom succession, after
632   the fast-growing, pioneer group 1 species (Quéguiner 2013).

633   Resting spores are adapted to dormancy during periods of low light and nutrient availability (Round
634   et al. 1990), so tend to be high in carbon (Kuwata et al. 1993), and resistant to zooplankton grazing
635   (Kuwata and Tsuda 2005). They have been identified as significant carbon exporters in the sub-polar
636   Atlantic (Rynearson et al. 2013), and near the subantarctic Kerguelen Plateau, where they were
637   responsible for >50% of POC export (Rembauville et al. 2015). The relative contribution of individual
638   taxa to carbon export was not estimated in this study. Nonetheless, resting spore abundances were
639   correlated with POC and BSi flux at both depths (Table 2) and when taken into consideration with
640   the observations of high year-round abundances and good frustule preservation, resting spores may
641   be major POC flux contributors at NCR. Further, *Chaetoceros* spp. tend to be coastal-associated
642   diatoms, as the germination of resting spores hinges upon them being mixed back into the photic
643   zone (i.e. not exported to great depth). A pulse in *Chaetoceros* spores might, then, be another
644   indicator of coastal water influence over the sediment traps.

645   At the SCR trap, patterns of seasonal succession are less clear, with spring assemblages containing
646   small species, typical of Quéguiner's group 1 (*Azpeitia tabularis* and *Nitzschia bicapitata*), and larger
647   taxa normally associated with Quéguiner's group 2 assemblage (*Hemidiscus cuneiformis*) (Fig. 7). As
648   at the NCR mooring, *Chaetoceros* spores were mostly present later in the year, as was *Fragilariopsis*
649   *kerguelensis,* a typical group 2 species (Quéguiner 2013). High abundances of these diatoms are likely
650   attributable to their robustness and selective preservation.

651   Peak abundances of *Rhizosolenia setigera* were observed in autumn/winter at the NCR site (Fig. 5),
652   and high contribution of *Rhizosolenia bergonii*, and *Thalassiothrix* spp. in winter assemblage at the
653   SCR trap (Fig. 7) could be due to a different ecological strategy of these species. Some members of
654   the genera *Rhizosolenia* and *Thalassiotrix* have been reported to belong to the so-called "shade
655   flora", i.e., living near the base of the mixed layer (Kemp et al. 2000), with peak export associated
656   with the breakdown of the seasonal stratification of the water column in autumn/winter. The
657   presence of deep-living taxa would certainly be expected at NCR, which had maximum winter mixed
658   layer depths almost twice as deep as SCR (Supp. Fig. 1). *R. bergonii* and *Thalassiothrix* spp. formed a
659   large portion of the winter assemblage within the SCR trap (Fig. 7), but were not reported by Chang
660   and Gall (1998) in the SAZ, prompting questions on the origin of *R. bergonii* frustules in these
661   sediment traps. *R. bergonii* may be involved in episodic particle flux events (Romero et al. 2000),
662   possibly related to sporadic nutrient supply, resulting in temporally and spatially patchy species
663   distributions (Sancetta et al. 1991). In addition, some *Rhizosolenia* spp. may adjust their buoyancy to

664   migrate vertically in the water column (Villareal et al. 1993), or exist at greatest abundances in
665   deeper layers (Kemp et al. 2000), and may elude shallow water sampling.

666   4.2.2 Coccolithophores
667   *Emiliania huxleyi*, the most abundant and widespread coccolithophore globally (Young et al. 2003),
668   was the most abundant coccolithophore found within sediment trap material at NCR and SCR, and
669   in surface waters in the New Zealand region (Chang and Northcote 2016). Considered a pioneer
670   species, *E. huxleyi* tends to reach peak abundances in late spring or early summer (Rost and Riebesell
671   2004). However, it can dominate assemblages year-round, due to its high tolerance to a range of
672   environmental conditions (Winter et al. 1994) including long day length (Balch 2004) and highly
673   stratified waters with low nutrients (Ziveri et al. 2000). Though highest abundances occurred in
674   spring at both Chatham Rise traps, *E. huxleyi* was overwhelmingly abundant in almost every sampling
675   cup, explaining its lack of correlation with any individual environmental factor in the CCA analysis
676   (Fig. 4B). *Emiliania huxleyi's* tendency to over-produce, and shed excess coccoliths (Paasche 2001)
677   could obscure real seasonal patterns in this species, and lead to overestimates of *E. huxleyi* fluxes in
678   sediments.

679   While 46 coccolithophore taxa were recovered in live assemblages east of New Zealand (Chang and
680   Northcote 2016), not all were identified in our sediment traps, though under light microscopy some
681   taxa, such as *Syracosphaera* spp., and are not discernible to species level. In this study,
682   coccolithophore diversity was greater at the NCR than SCR moorings (Table 2), and higher in spring
683   and summer, possibly due to enhanced export efficiency during these times. Seasonality of
684   coccolithophore diversity has been reported by Chang and Northcote (2016), who noted that during
685   *E. huxleyi* blooms, only four to six coccolithophore taxa were present, compared to 22 on average.
686   Coccolithophore assemblages are increasingly *E. huxleyi*-dominated towards the poles, eventually
687   becoming monospecific (Gravalosa et al. 2008; Malinverno et al. 2015; Rigual Hernández et al. 2018).
688   Lower abundances of *E. huxleyi* at NCR than SCR, as well as the presence of a wider variety of species
689   (13 and seven, respectively), accounts for the higher species diversity observed at NCR.

690   Notable exceptions to *E. huxleyi* dominance include early October at NCR, when *Gephyrocapsa* spp.
691   were the dominant taxa, and February at SCR, when *Umbellosphaera tenuis* peaked at 60% of
692   assemblages captured (Fig. 6). Notably, *U. tenuis* was a minor component of coccolithophores in
693   surface waters in the New Zealand SAZ (Malinverno et al. 2015). However, surface water
694   assemblages only provide a snapshot of phytoplankton standing stocks compared to sediment traps,
695   which provides an integration of the annual cycle, so discrepancies between these study types are
696   anticipated.

697   After *E. huxleyi*, small *Gephyrocapsa* spp. (<3 μm) were the next most abundant coccolithophore
698   species in the Chatham Rise sediment traps, and are known to be widely distributed in New Zealand
699   waters (Chang and Northcote 2016). *Gephyrocapsa* spp. diversity and abundance was greater at NCR,
700   with at least four groups identified (Table 3). Sediment core analysis in the Australian sector
701   identified *G. oceanica* as typical of a warmer-water assemblage usually north of the STF, while *G.*
702   *muellerae* was associated with a cooler-water assemblage (Findlay and Flores 2000). In the present
703   study, both *G. oceanica* and *G. muellerae* were more common at the subtropical site, suggesting
704   subantarctic water flow into the NCR trap region. *Calcidiscus leptoporus*, a warm-water associated

705 species, was 9% of SCR annual assemblages (Table 3), and is associated with high-productivity
706 environments (Boeckel et al. 2006), providing further evidence for frontal influence at the SCR trap
707 site.

708 Higher abundances of *Syracosphaera* spp. at NCR than SCR are consistent with a preference for
709 warmer water (Boeckel et al. 2006). *Syracosphaera* spp. were particularly diverse in a recent survey
710 of New Zealand surface waters (Chang and Northcote 2016), with an average 31% relative
711 abundance. In contrast, *Oolithotus* spp., which reached 16% of coccolith abundances in SCR sediment
712 traps (Fig. 6), were not found in surface waters in the New Zealand region (Chang and Northcote
713 2016). This could be explained by the depth preferences of *Oolithotus* spp. The common tropical to
714 temperate *Oolithotus fragilis*, also found in the Australian sector (Findlay and Flores 2000), inhabits
715 the mid-to-lower photic zone (50-200 m depths) (Okada and McIntyre 1977), thus the shallow near-
716 surface sampling of Chang and Northcote (2016) may have excluded taxa inhabiting deeper ocean
717 layers. *Oolithotus* spp. and *Helicosphaera carteri* tended to appear later in the season (summer and
718 autumn). Occurrences of *Oolithotus* spp. in the spring and summer months at NCR are followed by
719 its appearance in summer and autumn at SCR, possibly reflecting the delayed onset of southward-
720 migrating blooms (e.g. Chiswell et al. 2013).

721 *Syracosphaera* spp. were recorded in early spring at NCR, consistent with its relationship with Chl-*a*
722 in the CCA analysis (Fig. 4B), though at odds with its general acceptance as a late-succession taxon
723 (Dimiza et al. 2008). *Gephyrocapsa* spp. <3µm appeared in spring at NCR. This group tends to rapidly
724 respond to high nutrients, such as during upwelling conditions (Broerse et al. 2000; Andruleit et al.
725 2003). Both small *Gephyrocapsa* and *G. oceanica* are considered to exhibit a more pioneer, early-
726 blooming life strategy (Dimiza et al. 2008), hence high abundances of both species in early to mid-
727 spring at NCR. The seasonal appearance of small *Gephyrocapsa* spp. was more complex at SCR,
728 where maximum abundances occurred in the winter period.

729 *4.3 Influence of advection from coastal sites on oceanic diatom fluxes*
730 Diatom flux at NCR 1000 m was nearly constant throughout the trapping period and apparently
731 decoupled from seasonal production, raising the question of particle sources at this site (Fig. 2).
732 Nodder and Northcote (2001) previously reported higher mass flux and less pronounced seasonality
733 in the deeper traps at both sites. Normally, flux decreases with depth due to particle remineralization
734 (Buesseler and Boyd 2009), unless an additional particle source is present. Nodder and Northcote
735 (2001) partially attributed the higher mass flux at 1000 m to resuspension of material from the
736 Chatham Rise into the deeper traps, particularly as the deeper traps sit below the crest.

737 Diatom assemblage data at NCR support the resuspension hypothesis, but also suggest an additional
738 coastal particle origin not previously identified. Up to 40% of the assemblage at NCR was composed
739 of benthic (shelf/estuary) and coastal diatoms, derived from a coastal or continental shelf/slope via
740 advection. The East Cape Current (ECC) has the capacity to advect coastal material from the North
741 Island, feeding into the Wairarapa Eddy, the southern edge of which circulates over NCR (Chiswell et
742 al. 2015a; Fig. 1). Trace metal analyses also report material from the east coast becoming
743 incorporated into eddies shed eastwards off the continental margin (Ellwood et al. 2014), making
744 this a plausible source of coastal material to NCR. Seafloor sediment analyses around New Zealand
745 revealed 10% of diatom assemblages were coastally-derived, with STZ sediments having the greatest
746 percentage of coastal species, consistent with our findings (Cochran and Neil 2009). The presence of
747 coastal diatoms coincided with maximum LSi flux early in the sampling period at NCR, supporting the

748   conclusion that particle advection from a coastal/benthic system occurred at this time. Nodder and
749   Northcote (2001) estimated particle sources between 10 – 120 km away for the 300 m trap, though
750   possibly further due to the spatial extent of the Wairarapa Eddy, lending weight to this conclusion.

751   Benthic diatom capture at NCR indicates transport of sediments from a nearshore source, suggesting
752   a distant particle source such as the Cook Strait, where strong tidal flows may be capable of
753   resuspending and transporting sediment (Stevens 2014), which can then be advected out to near the
754   NCR trap site (Barnes 1985). Significant volumes of terrigenous material are shed into the sea by
755   rivers in the New Zealand region, particularly from the eastern coast of the North Island (Griffiths
756   and Glasby 1985; Hicks et al. 2011) and are transported to the open ocean by the ECC (see Fig. 1)
757   and perhaps entrained into offshore eddies (Ellwood et al. 2015). The transport of land-derived,
758   lithogenic material into sediment traps north of Chatham Rise is well-documented (Nodder et al.
759   2005; Nodder et al. 2016). In particular, the presence of the small pennate *D. minutissima* in the NCR
760   trap is a robust proxy for the advection of coastal sediments (Hallegraeff et al. 2010).

761   There is evidence for material input via resuspension at SCR too, with a relatively high correlation
762   between diatom flux and lithogenic particles (Table 2), as well as higher mass (Nodder and Northcote
763   2001) and higher diatom flux at 1000 m (Fig. 7). This is supported by Nodder et al. (2007), who
764   reported the deposition of seafloor sediments containing diatom frustules into sediment traps
765   deployed on the southern flank of the rise (2 m above seafloor), in the vicinity of the SCR site.
766   Furthermore, the relative enrichment of the STFZ in diatoms compared to the STZ and SAZ (Bradford-
767   Grieve et al. 1997; Chang and Gall 1998) may account for higher fluxes at SCR, given the proximity of
768   the site to the southern boundary of the STFZ (Fig. 1). This is considered a possibility, given that STFZ
769   waters are known to be advected to the SCR trap site (and even further south) in the form of deep
770   eddies (Uddstrom and Oien 1999; Williams 2004).

771   With the present data, it is difficult to conclusively identify particle sources at NCR or SCR, and this
772   region may benefit from a future dedicated study investigating particle pathways. Future sediment
773   trap studies of a year or longer in the region are needed to understand the inter-annual variability
774   of phytoplankton fluxes in this region, and to determine whether the present study's findings
775   represent typical export patterns east of New Zealand. Future studies would also benefit from the
776   existence of this seasonal dataset, and with it could assess the degree of change in phytoplankton
777   export patterns with climate change.

778   **5. Conclusions**

779   Baseline studies of phytoplankton assemblage composition and export seasonality from sediment
780   traps are vital to understand the direction, rate of change and adaptive capacity of key ecosystems
781   in a changing climate. Such data also allow a better understanding of which factors, environmental
782   or chemical, drive growth and export patterns, and how they may be changing. While bulk sediment
783   trap fluxes were published previously in Nodder and Northcote (2001), here we add valuable
784   information on species fluxes that may be employed in palaeoceanographic reconstructions and
785   export flux modelling. By understanding diatom and coccolithophore seasonality and preservation,
786   more insights may be gained from analysis of species deposition patterns in seafloor cores,
787   contributing to our knowledge of past climatic change.

788   We present the first record of seasonal variability of diatoms and coccolithophores in this region,
789   using sediment trap material from an approximately year-long record (1996-97) north and south of
790   the Subtropical Frontal Zone. From these findings we infer a complex array of potential particle
791   sources and processes that affect diatom and coccolith fluxes in the region, which are summarised
792   in Fig. 9.
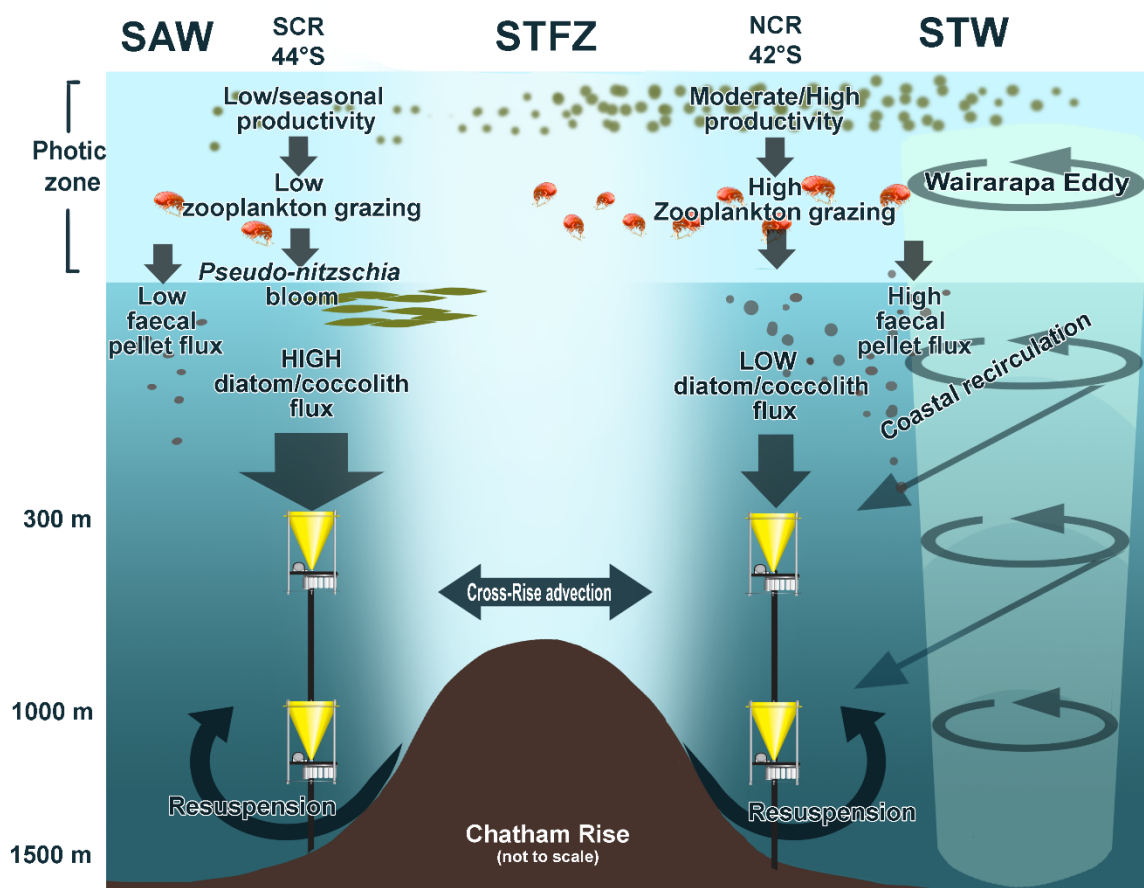
794   *Figure 9. Schematic (not to scale) of inferred particle sources into NCR and SCR sediment traps.*

795   •   Higher phytoplankton fluxes at SCR than at NCR likely reflected the proximity of the former
796   to the strong frontal gradients associated with the southern extent of the Subtropical Frontal Zone.
797   At NCR, diatom assemblages indicated coastal/benthic particle sources, suggesting this site was
798   sampling mainly from subtropical waters, including particles from waters that had a more
799   coastal/continental shelf origin. Occasional subantarctic input of diatoms at NCR was also evident
800   (cross-rise advection, Fig. 9).

801   •   Seasonal decoupling of diatom fluxes at the deep NCR 1000 m trap was probably due to
802   regular resuspension of Chatham Rise sediments into the trap, as well as "shedding" from the
803   Wairarapa Eddy (Fig. 9).

804   •   At the NCR mooring, the resting spores of the diatom *Chaetoceros* were likely significant in
805   POC export to the trap. At the SCR mooring, ~98% of annual diatom flux occurred during a *Pseudo-*
806   *nitzschia* spp. pulse event associated with high BSi flux. Co-sedimentation of other taxa with the
807   rapid-sinking mats may have enhanced the export of POC.

808 • Seasonal progression was observed among phytoplankton assemblages as a whole, with
809 diatoms preceded by coccolithophores. Within diatom and coccolithophore communities, some
810 classical succession was observed at NCR, with small-celled diatoms giving way to larger taxa, though
811 at SCR, size classes tended to be mixed. Succession amongst coccolithophore species generally
812 reflected the designation of taxa as pioneer or late-succession species.

813 **Acknowledgements**

829   **Supplementary Figures**

830

831   ***Supplementary Figure 1**. Mixed Layer Depth (m) at NCR and SCR for an annual series determined from Argo*
832   *float data (2001-2006) using the density difference criterion, data from Dong et al. (2008).*

833 **References**

834 Ajani P, Murray S, Hallegraeff G, Lundholm N, Gillings M, Brett S, Armand L (2013) The diatom
835 genus *Pseudo-nitzschia* (Bacillariophyceae) in New South Wales, Australia: morphotaxonomy,
836 molecular phylogeny, toxicity, and distribution. Journal of phycology 49:765-785.

837 Andruleit H, Stäger S, Rogalla U, Čepek P (2003) Living coccolithophores in the northern Arabian
838 Sea: ecological tolerances and environmental control. Marine Micropaleontology 49:157-181.

839 Armstrong RA, Lee C, Hedges JI, Honjo S, Wakeham SG (2001) A new, mechanistic model for
840 organic carbon fluxes in the ocean based on the quantitative association of POC with ballast
841 minerals. Deep-Sea Research 49:219-236.

842 Baker ET, Milburn HB, Tennant DA (1988) Field assessment of sediment trap efficiency under
843 varying flow conditions. Journal of Marine Research 46:573-592.

844 Balch WM (2004) Re-evaluation of the physiological ecology of coccolithophores. In: Thiersten HR,
845 Young, JR (eds) Coccolithophores. Springer, Germany, pp 165-190.

846 Balch WM, Bates NR, Lam PJ, Twining BS, Rosengard SZ, Bowler BC, Drapeau DT, Garley R,
847 Lubelczyk LC, Mitchell C, Rauschenberg S (2016) Factors regulating the Great Calcite Belt in the
848 Southern Ocean and its biogeochemical significance. Global Biogeochemical Cycles 30:1124-1144.
849 doi:10.1002/2016GB005414

850 Barnes EJ (1985) Eastern Cook Strait region circulation inferred from satellite-derived, sea-surface,
851 temperature data. New Zealand Journal of Marine and Freshwater Research 19:405-411.
852 doi:10.1080/00288330.1985.9516105

853 Belkin IM, Gordon AL (1996) Southern Ocean fronts from the Greenwich meridian to Tasmania.
854 Journal of Geophysical Research: Oceans 101: 3675-3696. doi10.1029/95JC02750

855 Belkin, IM (1988) Main hydrological features of the central South Pacific. In: ME Vinogradov, MV
856 Flint (eds) Pacific Subantarctic Ecosystems. Nauka, Moscow, pp 21–28.

857 Berger W, Wefer G (1990) Export production: seasonality and intermittency, and
858 paleoceanographic implications. Global and Planetary Change 3:245-254.

859 Bodén P (1991) Reproducibility in the random settling method for quantitative diatom analysis.
860 Micropaleontology 37:313-319.

861 Boeckel B, Baumann K-H, Henrich R, Kinkel H (2006) Coccolith distribution patterns in South
862 Atlantic and Southern Ocean surface sediments in relation to environmental gradients. Deep Sea
863 Research Part I: Oceanographic Research Papers 53:1073-1099.
864 doi:http://dx.doi.org/10.1016/j.dsr.2005.11.006

865 Bostock HC, Barrows TT, Carter L, Chase Z, Cortese G, Dunbar G, Ellwood M, Hayward B, Howard W,
866 Neil H (2013) A review of the Australian–New Zealand sector of the Southern Ocean over the last
867 30 ka (Aus-INTIMATE project). Quaternary Science Reviews 74:35-57.

868 Boyd P, Newton P, Rivkin RB, Legendre L, Deibel D, Tremblay J, Klein B, Crocker K, Roy S, Silverberg
869 N (1997) Measuring biogenic carbon flux in the ocean. Science 275:554-555.

870 Boyd P, LaRoche J, Gall M, Frew R, McKay RML (1999) Role of iron, light, and silicate in controlling
871 algal biomass in subantarctic waters SE of New Zealand. Journal of Geophysical Research: Oceans
872 104:13395-13408. doi:10.1029/1999JC900009

873 Boyd PW (2015) Toward quantifying the response of the oceans' biological pump to climate
874 change. Frontiers in Marine Science 2:77. doi:10.3389/fmars.2015.00077

875 Bradford-Grieve J, Chang F, Gall M, Pickmere S, Richards F (1997) Size‐fractionated phytoplankton
876 standing stocks and primary production during austral winter and spring 1993 in the Subtropical
877 Convergence region near New Zealand. New Zealand Journal of Marine and Freshwater Research
878 31:201-224.

879 Broecker W, Clark E (2009) Ratio of coccolith $CaCO_3$ to foraminifera $CaCO_3$ in late Holocene deep
880 sea sediments. Paleoceanography 24:PA3205. doi:10.1029/2009PA001731

881 Broerse AT, Ziveri P, van Hinte JE, Honjo S (2000) Coccolithophore export production, species
882 composition, and coccolith-$CaCO_3$ fluxes in the NE Atlantic (34° N, 21° W and 48° N, 21° W). Deep
883 Sea Research Part II: Topical Studies in Oceanography 47:1877-1905.

884 Buesseler KO, Antia AN, Chen M, Fowler SW, Gardner WD, Gustafsson O, Harada K, Michaels AF,
885 Rutgers van der Loeff M, Sarin M (2007) An assessment of the use of sediment traps for estimating
886 upper ocean particle fluxes. Journal of Marine Research 65:345-416.

887 Bull B, Livingston ME (2001) Links between climate variation and year class strength of New
888 Zealand hoki (Macruronus novaezelandiae): An update. New Zealand Journal of Marine and
889 Freshwater Research 35:871-880. doi:10.1080/00288330.2001.9517049

890 Chang FH (1983) winter phytoplankton and microzooplankton populations off the coast of
891 Westland, New Zealand, 1979. New Zealand Journal of Marine and Freshwater Research 17:279-
892 304.

893 Chang FH, Gall M (1998) Phytoplankton assemblages and photosynthetic pigments during winter
894 and spring in the Subtropical Convergence region near New Zealand. New Zealand Journal of
895 Marine and Freshwater Research 32:515-530. doi:10.1080/00288330.1998.9516840

896 Chang FH, Northcote L (2016) Species composition of extant coccolithophores including twenty six
897 new records from the southwest Pacific near New Zealand. Marine Biodiversity Records 9:75-XX.
898 doi:10.1186/s41200-016-0077-7

899 Chiswell SM (2001) Eddy energetics in the subtropical front over the Chatham Rise, New Zealand.
900 New Zealand Journal of Marine and Freshwater Research 35:1-15.
901 doi:10.1080/00288330.2001.9516975

902 Chiswell SM (2002) Temperature and salinity mean and variability within the subtropical front over
903 the Chatham Rise, New Zealand. New Zealand Journal of Marine and Freshwater Research 36:281-
904 298. doi:10.1080/00288330.2002.9517086

905 Chiswell SM (2005) Mean and variability in the Wairarapa and Hikurangi Eddies, New Zealand. New
906 Zealand Journal of Marine and Freshwater Research 39:121-134.
907 doi:10.1080/00288330.2005.9517295

908   Chiswell SM, Bradford‐Grieve J, Hadfield MG, Kennan SC (2013) Climatology of surface
909   chlorophyll *a*, Autumn‐Winter and spring blooms in the southwest Pacific Ocean. Journal of
910   Geophysical Research: Oceans 118:1003-1018. doi:10.1002/jgrc.20088

911   Chiswell SM, Bostock HC, Sutton PJH, Williams MJM (2015a) Physical oceanography of the deep
912   seas around New Zealand: a review. New Zealand Journal of Marine and Freshwater Research
913   49:286-317. doi:10.1080/00288330.2014.992918

914   Clark M (2001) Are deepwater fisheries sustainable?—the example of orange roughy (*Hoplostethus*
915   *atlanticus*) in New Zealand. Fisheries Research 51:123-135.

916   Coale KH, Johnson KS, Chavez FP, Buesseler KO, Barber RT, Brzezinski MA, Cochlan WP, Millero FJ,
917   Falkowski PG, Bauer JE (2004) Southern Ocean iron enrichment experiment: carbon cycling in high-
918   and low-Si waters. Science 304:408-414.

919   Cochran U, Neil H (2009) Diatom (< 63μm) distribution offshore of eastern New Zealand: Surface
920   sediment record and temperature transfer function. Marine Geology 270:257-271.

921   Currie KI, Hunter KA (1998) Surface water carbon dioxide in the waters associated with the
922   subtropical convergence, east of New Zealand. Deep Sea Research Part I: Oceanographic Research
923   Papers 45:1765-1777.

924   De Baar HJ, Boyd PW, Coale KH, Landry MR, Tsuda A, Assmy P, Bakker DC, Bozec Y, Barber RT,
925   Brzezinski MA (2005) Synthesis of iron fertilization experiments: from the iron age in the age of
926   enlightenment. Journal of Geophysical Research: Oceans 110:C09S16. doi:10.1029/2004JC002601.

927   De La Rocha CL, Passow U (2007) Factors influencing the sinking of POC and the efficiency of the
928   biological carbon pump. Deep Sea Research Part II: Topical Studies in Oceanography 54:639-658.
929   doi:https://doi.org/10.1016/j.dsr2.2007.01.004

930   Deppeler SL, Davidson AT (2017) Southern Ocean phytoplankton in a changing climate. Frontiers in
931   Marine Science 4:40. doi: 10.3389/fmars.2017.00040

932   Dimiza MD, Triantaphyllou MV, Dermitzakis MD (2008) Seasonality and Ecology of Living
933   Coccolithophores in Eastern Mediterranean Coastal Environment (Andros Island, Middle Aegean
934   Sea). Micropaleontology 54:159-175. doi:10.2307/30130910

935   Dong S, Sprintall J, Gille ST, Talley L (2008) Southern Ocean mixed-layer depth from Argo float
936   profiles. Journal of Geophysical Research: Oceans 113. doi:doi:10.1029/2006JC004051

937   Dugdale RC, Wilkerson FP, Minas HJ (1995) The role of a silicate pump in driving new production.
938   Deep Sea Research Part I: Oceanographic Research Papers 42:697-719.
939   doi:https://doi.org/10.1016/0967-0637(95)00015-X

940   Ellwood MJ, Nodder SD, King AL, Hutchins DA, Wilhelm SW, Boyd PW (2014) Pelagic iron cycling
941   during the subtropical spring bloom, east of New Zealand. Marine Chemistry 160:18-33.
942   doi:https://doi.org/10.1016/j.marchem.2014.01.004

943   Ellwood MJ, Hutchins DA, Lohan MC, Milne A, Nasemann P, Nodder SD, Sander SG, Strzepek R,
944   Wilhelm SW, Boyd PW (2015) Iron stable isotopes track pelagic iron cycling during a subtropical
945   phytoplankton bloom. Proceedings of the National Academy of Sciences 112:E15-E20.
946   doi:10.1073/pnas.1421576112

947   Fenner J, Carter L, Stewart R (1992) Late Quaternary paleoclimatic and paleoceanographic change
948   over northern Chatham Rise, New Zealand. Marine Geology 108:383-404.
949   doi:https://doi.org/10.1016/0025-3227(92)90206-W

950   Field CB, Behrenfeld MJ, Randerson JT, Falkowski P (1998) Primary Production of the Biosphere:
951   Integrating Terrestrial and Oceanic Components. Science 281:237-240.
952   doi:10.1126/science.281.5374.237

953   Findlay C, Flores J (2000) Subtropical front fluctuations south of Australia (45°09'S, 146°17'E) for
954   the last 130 ka years based on calcareous nannoplankton. Marine Micropaleontology 40:403-416

955   Flores J, Sierro F (1997) Revised technique for calculation of calcareous nannofossil accumulation
956   rates. Micropaleontology 43:321-324.

957   Gall M, Boyd P, Hall J, Safi K, Chang H (2001) Phytoplankton processes. Part 1: community structure
958   during the Southern Ocean iron release experiment (SOIREE). Deep Sea Research Part II: Topical
959   Studies in Oceanography 48:2551-2570.

960   Gomi Y, Taniguchi A, Fukuchi M (2007) Temporal and spatial variation of the phytoplankton
961   assemblage in the eastern Indian sector of the Southern Ocean in summer 2001/2002. Polar
962   Biology 30:817-827. doi:10.1007/s00300-006-0242-2

963   Gravalosa JM, Flores J-A, Sierro FJ, Gersonde R (2008) Sea surface distribution of coccolithophores
964   in the eastern Pacific sector of the Southern Ocean (Bellingshausen and Amundsen Seas) during the
965   late austral summer of 2001. Marine Micropaleontology 69:16-25.

966   Griffiths GA, Glasby GP (1985) Input of river-derived sediment to the New Zealand continental
967   shelf: I. Mass. Estuarine, Coastal and Shelf Science 21:773-787. doi:https://doi.org/10.1016/0272-
968   7714(85)90072-1

969   Grigorov I, Rigual-Hernandez AS, Honjo S, Kemp AE, Armand LK (2014) Settling fluxes of diatoms to
970   the interior of the Antarctic circumpolar current along 170 W. Deep Sea Research Part I:
971   Oceanographic Research Papers 93:1-13.

972   Hallegraeff GM, Bolch CJ, Hill D, Jameson I, LeRoi J, McMinn A, Murray S, de Salas MF, Saunders K
973   (2010) Algae of Australia: phytoplankton of temperate coastal waters. CSIRO Publishing,
974   Melbourne.

975   Heath RA (1985) A review of the physical oceanography of the seas around New Zealand - 1982.
976   New Zealand Journal of Marine and Freshwater Research 19:79-124.
977   doi:10.1080/00288330.1985.9516077

978   Hedges JI, Lee C, Wakeham SG, Hernes PJ, Peterson ML (1993) Effects of poisons and preservatives
979   on the fluxes and elemental compositions of sediment trap materials. Journal of Marine Research
980   51:651-668.

981   Hicks DM, Shankar U, McKerchar AI, Basher L, Lynn I, Page M, Jessen M (2011) Suspended
982   sediment yields from New Zealand rivers. Journal of Hydrology (New Zealand) 50:81.

983   Hollis C, Neil H (2005) Sedimentary record of radiolarian biogeography, offshore eastern New
984   Zealand. New Zealand Journal of Marine and Freshwater Research 39:165-192.

985   Honjo S (1997) The rain of ocean particles and Earth's carbon cycle. Oceanus 40:4-7.

986   Honjo S, Francois R, Manganini S, Dymond J, Collier R (2000) Particle fluxes to the interior of the
987   Southern Ocean in the Western Pacific sector along 170°W. Deep Sea Research Part II: Topical
988   Studies in Oceanography 47:3521-3548. doi:http://dx.doi.org/10.1016/S0967-0645(00)00077-1

989   Honjo S, Eglinton TI, Taylor CD, Ulmer KM, Sievert SM, Bracher A, German CR, Edgcomb V, Francois
990   R, Iglesias-Rodriguez MD (2014) Understanding the role of the biological pump in the global carbon
991   cycle: an imperative for ocean science. Oceanography 27:10-16.

992   Hopkins J, Henson SA, Painter SC, Tyrrell T, Poulton AJ (2015) Phenological characteristics of global
993   coccolithophore blooms. Global Biogeochemical Cycles 29:239-253.

994   Hopkins J, Shaw A, Challenor P (2010) The southland front, New Zealand: variability and ENSO
995   correlations. Continental Shelf Research 30:1535-1548.

996   Kemp AES, Pike J, Pearce RB, Lange CB (2000) The "Fall dump" - a new perspective on the role of a
997   "shade flora" in the annual cycle of diatom production and export flux. Deep Sea Research Part II:
998   Topical Studies in Oceanography 47:2129-2154. doi:https://doi.org/10.1016/S0967-
999   0645(00)00019-9

1000 Kemp AES, Villareal TA (2013) High diatom production and export in stratified waters - A potential
1001 negative feedback to global warming. Progress in Oceanography 119:4-23.
1002 doi:https://doi.org/10.1016/j.pocean.2013.06.004

1003 King AL, Howard WR (2001) Seasonality of foraminiferal flux in sediment traps at Chatham Rise, SW
1004 Pacific: implications for paleotemperature estimates. Deep Sea Research Part I: Oceanographic
1005 Research Papers 48:1687-1708.

1006 Klaas C, Archer DE (2002) Association of sinking organic matter with various types of mineral ballast
1007 in the deep sea: Implications for the rain ratio. Global Biogeochemical Cycles 16:1116.

1008 Kottmeier DM, Rokitta SD, Rost B (2016) H+-driven increase in CO_2 uptake and decrease in HCO^{3-}
1009 uptake explain coccolithophores' acclimation responses to ocean acidification. Limnology and
1010 Oceanography 61:2045-2057. doi:10.1002/lno.10352

1011 Kuwata A, Hama T, Takahashi M (1993) Ecophysiological characterization of two life forms, resting
1012 spores and resting cells, of a marine planktonic diatom, Chaetoceros pseudocurvisetus, formed
1013 under nutrient depletion. Marine Ecology Progress Series 102:245-255.

1014 Kuwata A, Tsuda A (2005) Selection and viability after ingestion of vegetative cells, resting spores
1015 and resting cells of the marine diatom, Chaetoceros pseudocurvisetus, by two copepods. Journal of
1016 experimental marine biology and ecology 322:143-151.

1017 Landry M, Ondrusek M, Tanner S, Brown S, Constantinou J, Bidigare R, Coale K, Fitzwater S (2000)
1018 Biological response to iron fertilization in the eastern equatorial Pacific (IronEx II). I. Microplankton
1019 community abundances and biomass. Marine Ecology Progress Series 201:27-42.

1020 Law CS, Bell JJ, Bostock HC, Cornwall CE, Cummings VJ, Currie K, Davy SK, Gammon M, Hepburn CD,
1021 Hurd CL, Lamare M, Mikaloff-Fletcher SE, Nelson WA, Parsons DM, Ragg NLC, Sewell MA, Smith
1022 AM, Tracey DM (2017) Ocean acidification in New Zealand waters: trends and impacts. New
1023 Zealand Journal of Marine and Freshwater Research 52:155-195.
1024 doi:10.1080/00288330.2017.1374983

1025 Lefebvre SC, Benner I, Stillman JH, Parker AE, Drake MK, Rossignol PE, Okimura KM, Komada T,
1026 Carpenter EJ (2012) Nitrogen source and pCO_2 synergistically affect carbon allocation, growth and

morphology of the coccolithophore *Emiliania huxleyi*: potential implications of ocean acidification for the carbon cycle. Global Change Biology 18:493-503. doi:10.1111/j.1365-2486.2011.02575.x

Leventer A (1991) Sediment trap diatom assemblages from the northern Antarctic Peninsula region. Deep Sea Research Part A. Oceanographic Research Papers 38:1127-1143. doi:http://dx.doi.org/10.1016/0198-0149(91)90099-2

Locarnini R, Mishonov A, Antonov J, Boyer T, Garcia H, Baranova O, Zweng M, Johnson D (2010)

World Ocean Atlas 2009, Volume 1: Temperature US Government Printing Office, Washington, DC.

Malinverno E, Triantaphyllou MV, Dimiza MD (2015) Coccolithophore assemblage distribution along a temperate to polar gradient in the West Pacific sector of the Southern Ocean (January 2005). Micropaleontology 61:489-506.

Malinverno E, Maffioli P, Gariboldi K (2016) Latitudinal distribution of extant fossilizable phytoplankton in the Southern Ocean: Planktonic provinces, hydrographic fronts and palaeoecological perspectives. Marine Micropaleontology 123:41-58. doi:http://dx.doi.org/10.1016/j.marmicro.2016.01.001

Marchetti A, Sherry ND, Kiyosawa H, Tsuda A, Harrison PJ (2006) Phytoplankton processes during a mesoscale iron enrichment in the NE subarctic Pacific: Part I—Biomass and assemblage. Deep Sea Research Part II: Topical Studies in Oceanography 53:2095-2113. doi:https://doi.org/10.1016/j.dsr2.2006.05.038

Murphy R, Pinkerton M, Richardson K, Bradford-Grieve J, Boyd P (2001) Phytoplankton distributions around New Zealand derived from SeaWiFS remotely‐sensed ocean colour data. New Zealand Journal of Marine and Freshwater Research 35:343-362.

Nodder SD (1997a) Short-term sediment trap fluxes from Chatham Rise, southwest Pacific Ocean. Limnology Oceanography 42:783-788.

Nodder, SD (1997b) Particulate fluxes in the subtropical convergence region and other marine environments of New Zealand. Dissertation, University of Waikato.

Nodder SD, Alexander BL (1998) Sources of variability in geographical and seasonal differences in particulate fluxes from short-term sediment trap deployments, east of New Zealand. Deep Sea Research Part I: Oceanographic Research Papers 45:1739-1764. doi:http://dx.doi.org/10.1016/S0967-0637(98)00040-5

Nodder S, Gall M (1998) Pigment fluxes from the Subtropical Convergence region, east of New Zealand: Relationships to planktonic community structure. New Zealand Journal of Marine and Freshwater Research 32:441-465. doi:10.1080/00288330.1998.9516836

Nodder SD, Northcote LC (2001) Episodic particulate fluxes at southern temperate mid-latitudes (42–45°S) in the Subtropical Front region, east of New Zealand. Deep Sea Research Part I: Oceanographic Research Papers 48:833-864. doi:http://dx.doi.org/10.1016/S0967-0637(00)00062-5

Nodder SD, Pilditch CA, Probert PK, Hall JA (2003) Variability in benthic biomass and activity beneath the Subtropical Front, Chatham Rise, SW Pacific Ocean. Deep Sea Research Part I: Oceanographic Research Papers 50:959-985. doi:https://doi.org/10.1016/S0967-0637(03)00094-3

Nodder SD, Boyd PW, Chiswell SM, Pinkerton MH, Bradfor-Grieve JM, Greig MJ (2005) Temporal coupling between surface and deep ocean biogeochemical processes in contrasting subtropical and subantarctic water masses, southwest Pacific Ocean. Journal of Geophysical Research: Oceans 110:12017.

Nodder SD, Duineveld GC, Pilditch CA, Sutton PJ, Probert PK, Lavaleye MS, Witbaard R, Chang FH, Hall JA, Richardson KM (2007) Focusing of phytodetritus deposition beneath a deep‐ocean front, Chatham Rise, New Zealand. Limnology and Oceanography 52:299-314

Nodder SD, Bowden DA, Pallentin A, Mackay K (2012) 56 - Seafloor Habitats and Benthos of a Continental Ridge: Chatham Rise, New Zealand A2 - Harris, Peter T. In: Baker EK (ed) Seafloor Geomorphology as Benthic Habitat. Elsevier, London, pp 763-776

Nodder SD, Chiswell SM, Northcote LC (2016) Annual cycles of deep-ocean biogeochemical export fluxes in subtropical and subantarctic waters, southwest Pacific Ocean. Journal of Geophysical Research: Oceans 121:2405-2424. doi:10.1002/2015JC011243

Northcote LC, Neil HL (2005) Seasonal variations in foraminiferal flux in the Southern Ocean, Campbell Plateau, New Zealand. Marine Micropaleontology 56:122-137.

Okada H, McIntyre A (1977) Modern coccolithophores of the Pacific and north Atlantic Oceans. Micropaleontology 23:PP-PP. doi:10.2307/1485309

Oku O, Kamatani A (1997) Resting spore formation of the marine planktonic diatom *Chaetoceros anastomosans* induced by high salinity and nitrogen depletion. Marine Biology 127:515-520.

Paasche E (2001) A review of the coccolithophorid *Emiliania huxleyi* (Prymnesiophyceae), with particular reference to growth, coccolith formation, and calcification-photosynthesis interactions. Phycologia 40:503-529. doi:10.2216/i0031-8884-40-6-503.1

Prebble J, Crouch E, Carter L, Cortese G, Nodder S (2013) Dinoflagellate cysts from two sediment traps east of New Zealand. Marine Micropaleontology 104:25-37.

Quéguiner B (2013) Iron fertilization and the structure of planktonic communities in high nutrient regions of the Southern Ocean. Deep Sea Research Part II: Topical Studies in Oceanography 90:43-54. doi:http://dx.doi.org/10.1016/j.dsr2.2012.07.024

Rembauville M, Blain S, Armand L, Quéguiner B, Salter I (2015) Export fluxes in a naturally iron-fertilized area of the Southern Ocean–Part 2: Importance of diatom resting spores and faecal pellets for export. Biogeosciences 12:3171-3195.

Revelante N, Gilmartin M (1995) The relative increase of larger phytoplankton in a subsurface chlorophyll maximum of the northern Adriatic Sea. Journal of Plankton Research 17:1535-1562. doi:10.1093/plankt/17.7.1535

Rhodes L, Jiang W, Knight B, Adamson J, Smith K, Langi V, Edgar M (2013) The genus *Pseudo-nitzschia* (Bacillariophyceae) in New Zealand: analysis of the last decade's monitoring data. New Zealand Journal of Marine and Freshwater Research 47:490-503.

Rigual-Hernández A, Trull T, Bray S, Cortina A, Armand L (2015a) Latitudinal and temporal distributions of diatom populations in the pelagic waters of the Subantarctic and Polar Frontal Zones of the Southern Ocean and their role in the biological pump. Biogeosciences 12:5309–5337. doi:10.5194/bg-12-5309-2015

1106   Rigual-Hernández AS, Trull TW, Bray SG, Closset I, Armand LK (2015b) Seasonal dynamics in diatom
1107   and particulate export fluxes to the deep sea in the Australian sector of the southern Antarctic
1108   Zone. Journal of Marine Systems 142:62-74. doi:http://dx.doi.org/10.1016/j.jmarsys.2014.10.002

1109   Rigual-Hernández AS, Trull TW, McCartney K, Ballegeer A-M, Lawler K-A, Bray SG, Armand LK
1110   (2016a) Indices based on silicoflagellate assemblages offer potential for paleo-reconstructions of
1111   the main oceanographic zones of the Southern Ocean. Geo-Marine Letters 36:271-280.
1112   doi:10.1007/s00367-016-0444-8

1113   Rigual-Hernández AS, Trull TW, Bray SG, Armand LK (2016b) The fate of diatom valves in the
1114   Subantarctic and Polar Frontal Zones of the Southern Ocean: Sediment trap versus surface
1115   sediment assemblages. Palaeogeography, Palaeoclimatology, Palaeoecology 457:129-143.
1116   doi:http://dx.doi.org/10.1016/j.palaeo.2016.06.004

1117   Rigual Hernández AS, Flores JA, Sierro FJ, Fuertes MA, Cros L, Trull TW (2018) Coccolithophore
1118   populations and their contribution to carbonate export during an annual cycle in the Australian
1119   sector of the Antarctic Zone. Biogeosciences Discuss. 2017:1-40. doi:10.5194/bg-2017-523

1120   Roemmich D, Sutton PJH (1998) The mean and variability of ocean circulation past northern New
1121   Zealand: determining the representativeness of hydrographic climatologies. Journal of Geophysical
1122   Research 103: 13041-13054. doi:10.1029/98JC00583

1123   Romero O, Lange C, Fischer G, Treppke U, Wefer G (1999) Variability in export production
1124   documented by downward fluxes and species composition of marine planktic diatoms:
1125   Observations from the tropical and equatorial Atlantic. In: Fischer G, Wefer G (eds) Use of Proxies
1126   in Paleoceanography: examples from the south Atlantic. Springer, Berlin, pp 365-392.

1127   Romero O, Fischer G, Lange C, Wefer G (2000) Siliceous phytoplankton of the western equatorial
1128   Atlantic: sediment traps and surface sediments. Deep Sea Research Part II: Topical studies in
1129   Oceanography 47:1939-1959

1130   Romero O, Armand L, Crosta X, Pichon J-J (2005) The biogeography of major diatom taxa in
1131   Southern Ocean surface sediments: 3. Tropical/Subtropical species. Palaeogeography,
1132   Palaeoclimatology, Palaeoecology 223:49-65

1133   Rost B, Riebesell U (2004) Coccolithophores and the biological pump: responses to environmental
1134   changes. In: Thiersten HR, Young JR (eds) Coccolithophores-From Molecular Processes to Global
1135   Impact: Springer, Berlin, pp 76-99.

1136   Round FE, Crawford RM, Mann DG (1990) Diatoms: biology and morphology of the genera.
1137   Cambridge University Press, New York.

1138   Rynearson T, Richardson K, Lampitt R, Sieracki M, Poulton A, Lyngsgaard MM, Perry M (2013)
1139   Major contribution of diatom resting spores to vertical flux in the sub-polar North Atlantic. Deep
1140   Sea Research Part I: Oceanographic Research Papers 82:60-71.

1141   Saavedra-Pellitero M, Baumann K-H, Flores J-A, Gersonde R (2014) Biogeographic distribution of
1142   living coccolithophores in the Pacific sector of the Southern Ocean. Marine Micropaleontology
1143   109:1-20.

1144   Sancetta C, Calvert SE (1988) The annual cycle of sedimentation in Saanich Inlet, British Columbia:
1145   implications for the interpretation of diatom fossil assemblages. Deep Sea Research Part A.
1146   Oceanographic Research Papers 35:71-90.

1147   Sancetta C, Villareal T, Falkowski P (1991) Massive fluxes of rhizosolenid diatoms: A common
1148   occurrence? Limnology and Oceanography 36:1452-1457. doi:10.4319/lo.1991.36.7.1452

1149   Schlitzer R, (2016) Ocean Data View Software. http://odv.awi.de

1150   Seegers BN, Birch JM, Marin R, Scholin CA, Caron DA, Seubert EL, Howard MDA, Robertson GL,
1151   Jones BH (2015) Subsurface seeding of surface harmful algal blooms observed through the
1152   integration of autonomous gliders, moored environmental sample processors, and satellite remote
1153   sensing in southern California. Limnology and Oceanography 60:754-764. doi:10.1002/lno.10082

1154   Shannon CE, Weaver W (1949) The mathematical theory of communication. Illinois Press, Urbana.

1155   Sikes EL, O'Leary T, Nodder SD, Volkman JK (2005) Alkenone temperature records and biomarker
1156   flux at the subtropical front on the Chatham Rise, SW Pacific Ocean. Deep Sea Research Part I:
1157   Oceanographic Research Papers 52:721-748.

1158   Smith RO, Vennell R, Bostock HC, Williams MJM (2013) Interaction of the Subtropical Front with
1159   topography around southern New Zealand. Deep Sea Research Part I: Oceanographic Research
1160   Papers 76:13-26. doi:http://dx.doi.org/10.1016/j.dsr.2013.02.007

1161   Stanton BR, Ridgway NM (1988) An oceanographic survey of the subtropical convergence zone in
1162   the Tasman Sea. New Zealand Journal of Marine and Freshwater Research 22:583-593.
1163   doi:10.1080/00288330.1988.9516328

1164   Stevens C (2014) Residual flows in Cook Strait, a large tidally dominated strait. Journal of Physical
1165   Oceanography 44:1654-1670.

1166   Sutton P (2001) Detailed structure of the Subtropical Front over Chatham Rise, east of New
1167   Zealand. Journal of Geophysical Research: Oceans 106:31045-31056.

1168   Sutton PJ (2003) The Southland Current: a subantarctic current. New Zealand Journal of Marine and
1169   Freshwater Research 37:645-652.

1170   Ternois Y, Sicre M-A, Boireau A, Beaufort L, Miquel J-C, Jeandel C (1998) Hydrocarbons, sterols and
1171   alkenones in sinking particles in the Indian Ocean sector of the Southern Ocean. Organic
1172   Geochemistry 28:489-501.

1173   Tomas CR (1997) Identifying marine phytoplankton. Academic press, San Diego.

1174   Totti C, Civitarese G, Acri F, Barletta D, Candelari G, Paschini E, Solazzi A (2000) Seasonal variability
1175   of phytoplankton populations in the middle Adriatic sub-basin. Journal of Plankton Research
1176   22:1735-1756.

1177   Trick CG, Bill BD, Cochlan WP, Wells ML, Trainer VL, Pickell LD (2010) Iron enrichment stimulates
1178   toxic diatom production in high-nitrate, low-chlorophyll areas. Proceedings of the National
1179   Academy of Sciences 107:5887-5892.

1180   Trimborn S, Thoms S, Brenneis T, Heiden JP, Beszteri S, Bischof K (2017) Two Southern Ocean
1181   diatoms are more sensitive to ocean acidification and changes in irradiance than the
1182   prymnesiophyte *Phaeocystis antarctica*. Physiologia Plantarum 160:155-170.
1183   doi:10.1111/ppl.12539

1184   Trull T, Bray S, Manganini S, Honjo S, Francois R (2001a) Moored sediment trap measurements of
1185   carbon export in the Subantarctic and Polar Frontal Zones of the Southern Ocean, south of
1186   Australia. Journal of Geophysical Research: Oceans (1978–2012) 106:31489-31509.

1187   Trull T, Rintoul SR, Hadfield M, Abraham ER (2001b) Circulation and seasonal evolution of polar
1188   waters south of Australia: Implications for iron fertilization of the Southern Ocean. Deep Sea
1189   Research Part II: Topical Studies in Oceanography 48:2439-2466.

1190   Trull TW, Passmore A, Davies DM, Smit T, Berry K, Tilbrook B (2018) Distribution of planktonic
1191   biogenic carbonate organisms in the Southern Ocean south of Australia: a baseline for ocean
1192   acidification impact assessment. Biogeosciences 15:31-49.

1193   Uddstrom MJ, Oien NA (1999) On the use of high-resolution satellite data to describe the spatial
1194   and temporal variability of sea surface temperatures in the New Zealand region. Journal of
1195   Geophysical Research: Oceans 104:20729-20751. doi:10.1029/1999JC900167

1196   Villareal TA, Altabet MA, Culver-Rymsza K (1993) Nitrogen transport by vertically migrating diatom
1197   mats in the North Pacific Ocean. Nature 363:709-712

1198   Wilks JV, Rigual-Hernández AS, Trull TW, Bray SG, Flores J-A, Armand LK (2017) Biogeochemical flux
1199   and phytoplankton succession: a year-long sediment trap record in the Australian sector of the
1200   Subantarctic Zone. Deep Sea Research Part I: Oceanographic Research Papers 121:143-159.
1201   doi:http://dx.doi.org/10.1016/j.dsr.2017.01.001

1202   Williams MJM (2004) Analysis of quasi‐synoptic eddy observations in the New Zealand
1203   subantarctic. New Zealand Journal of Marine and Freshwater Research 38:183-194.
1204   doi:10.1080/00288330.2004.9517227

1205   Winter A, Jordan R, Roth PH (1994) Biogeography of coccolithophores in oceanic waters. In: winter
1206   A, Siesser WG (eds) Coccolithophores. Cambridge University Press, New York, pp 290.

1207   Young J, Geisen M, Cros L, Kleijne A, Sprengel C, Probert I, Østergaard J (2003) A guide to extant
1208   coccolithophore taxonomy. Journal of Nannoplankton Research Special 1:1-124

1209   Zeldis J, James MR, Grieve J, Richards L (2002) Omnivory by copepods in the New Zealand
1210   Subtropical Frontal Zone. Journal of Plankton Research 24:9-23. doi:10.1093/plankt/24.1.9

1211   Ziveri P, Rutten A, De Lange G, Thomson J, Corselli C (2000) Present-day coccolith fluxes recorded in
1212   central eastern Mediterranean sediment traps and surface sediments. Palaeogeography,
1213   Palaeoclimatology, Palaeoecology 158:175-195
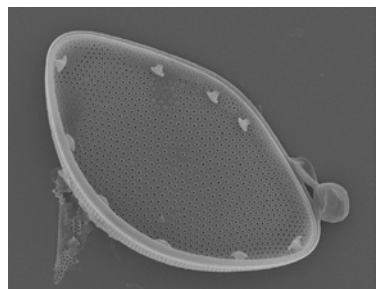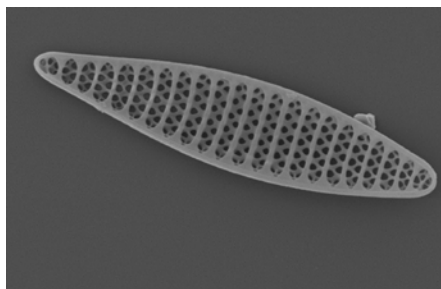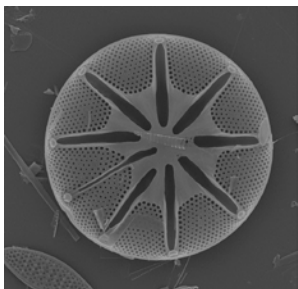
Chapter Four
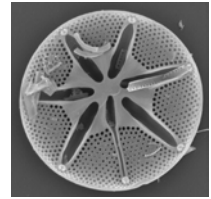
Reviews and syntheses: diatom and coccolith fluxes
from temperate to polar Southern Hemisphere sediment traps.

The following chapter is in preparation for publication, and is presented in the format requested
by Biogeosciences.

1 **Reviews and syntheses: Diatom and coccolithophore fluxes from temperate to**

2 **polar Southern Hemisphere sediment traps.**

3 Jessica V. Wilks[1], Andrés Rigual-Hernández[2] and Leanne K. Armand[3].

4 [1]Department of Biological Sciences, Macquarie University, North Ryde, NSW 2109, Australia.

5 [2]Department of Geology. Universidad de Salamanca, Salamanca 37008, Spain.

6 [3]Research School of Earth Sciences, The Australian National University, Canberra, ACT 2601,

7 Australia.

8 *Correspondence to:* Jessica V. Wilks (jessicavwilks@gmail.com)

9 **Abstract**

10 Sediment trap studies since the 1970s have been instrumental in developing knowledge of oceanic

11 particle flux and export drivers. In the Southern Hemisphere, sediment traps have been in use since

12 the 1970s, and have revealed the significance of the Southern Ocean as a major carbon sink, driven

13 by seasonally high phytoplankton production. The strength of this carbon sink may be reduced in

14 the Southern Ocean under future climate scenarios, making baseline studies of phytoplankton

15 fluxes highly valuable. Yet, deployments are clustered, leaving some regions neglected.

16 Furthermore, studies that calculate fluxes and assemblages of diatoms and coccolithophores are

17 comparatively rare. In this study, sediment trap deployment data was compiled from publications

18 since 1977, spanning 126 mooring sites from 30° S to the Antarctic coast. Diatom flux data were

19 available for 49 trap deployments, while coccolith flux data exist for only seven. Diatom fluxes were

20 mapped along with the major hydrological zones, revealing a general trend of increasing diatom

21 flux from the Polar Front to the Antarctic coast. Exceptions to this trend were found in the Antarctic

22 Peninsula and Ross Sea region, possibly driven by differences in exported phytoplankton

23 assemblage and/or methodological disparities. Linear models are used to relate diatom fluxes to

24 eight physical, biological and chemical variables that may influence flux magnitudes. The models

25 reveal surface nitrate concentration as the single most significant driver of diatom flux, contrary to

26 expectations that key diatom nutrients silicate and iron would be the strongest flux predictors.

27 Coccolith fluxes were also mapped, however, data points were too sparse to derive meaningful

28 trends. Future trap studies that calculate phytoplankton fluxes at the species level will be

29 invaluable in determining potential regional changes in the functioning of the biological pump, and

30 in palaeoreconstructions from seafloor sediment assemblages.

31 **1. Introduction**

32 The biological pump (BP) describes the process by which primary organic material synthesised in

33 the photic zone of the ocean by photosynthetic phytoplankton is transferred to the deep sea via

34 the seasonal export of particles (i.e. marine snow) (Volk and Hoffert, 1985). This process lowers

35 the partial pressure of CO_2 in the photic zone, and is driven by non-calcifying autotrophs, such as

36 diatoms. The BP drives the transfer of CO_2 to the deep ocean (Honjo, 2004). In contrast, the

37 Carbonate Counter Pump (CCP) describes the release of CO_2 associated with the production of

38 calcium carbonate skeletons in organisms such as coccolithophores and foraminifera

39 (Frankignoulle et al., 1994). The relative strength of either pump, in combination with the physical

40 processes of CO_2 dissolution and movement in the water column, will influence whether an oceanic

41 region is a net sink or source for CO_2 (Balch, 2018). Future climate scenarios indicate that

42 phytoplankton assemblages are likely to change. For example, increasing CO_2 content of water may

43 favour diatom photosynthetic rates (Hopkinson et al. 2011). Nitrate deficiency paired with ocean

44 acidification may place coccolithophores under increased pressure due to carbonate dissolution

45 and growth rates, possibly reducing their contribution to carbon export (Feng et al., 2017). At any

46 rate, the effects will be complex, with flow-on implications for atmospheric CO_2 levels (Heinze et

47 al., 2015).

48 Carbon export may be quantified chronologically using sediment traps; moored or free-floating

49 receptacles that capture and compartmentalise a time series (by days or weeks) of particulate

50 export. In this study, data from sediment trap deployments reporting diatom and/or coccolith

51 fluxes in the subtropical to polar Southern Hemisphere were compiled and mapped. Linear models

52 were derived for diatom flux using eight environmental variables implicated to influence particle

53 transfer efficiency in terms of potential production (nitrate, phosphate, silicate, iron and sea ice

54 cover), actual production (chlorophyll-*a* concentration), dissolution rates (sea surface

55 temperature) and ballast availability (particulate inorganic carbon concentration).

56 Over the last 50 years, sediment trap deployments across the Earth's oceans have revealed that

57 the volume, composition, and manner in which particles are exported is highly spatially and

58 temporally variable (Lampitt and Antia, 1997; Honjo et al., 2008). Sediment traps are not without

59 problems; high current speeds, trap tilt, trap shape (cylindrical or funnel shaped), or the entry of

60 swimming zooplankton into traps ("swimmers") may all adversely influence particle capture and

61 skew results (Gardner, 1985; Asper, 1996; Buesseler et al., 2007; McDonnell et al., 2015). Despite

62 these limitations, significant advances in understanding particle export in the oceans have resulted,

63 allowing the construction of global oceanic carbon budgets (Lampitt and Antia, 1997; Honjo et al.,

64 2008).

65 A strength of sediment trap studies over other tools is that not only can the total quantity of export

66 be determined, but also the seasonal composition of planktonic organisms. Relative to seafloor

67 sediment analyses, which provide information on export over centennial to millennial scales,

68 sediment traps studies capture seasonality of exported assemblages. Sediment trap data can also

69 be used by micropaleotologists to understand how the seasonal phytoplankton record may be

70 represented in the sediments (Rigual-Hernández et al., 2016).

71 The assumption that particle flux is directly related to magnitude of production is increasingly being

72 challenged (Maiti et al., 2013). Recent studies have revealed that physical features such as ocean

73 temperature and oxygen concentration may significantly alter particle export rates via particle

74 remineralisation (Cram et al., 2017), as may the types of ballasting particles present (Weber et al.,

75 2016). However, these studies have exclusively focused on identifying environmental drivers that

76 explain bulk carbon flux, and the composition of the phytoplankton component has been largely

77 ignored or underestimated. Phytoplankton assemblages in a given system likely determine the

78 magnitude of export.

79 Recently, sediment trap data have challenged the traditionally-held paradigm that larger diatoms

80 contribute the bulk of carbon exported, suggesting previously-overlooked pico- and nano-sized

81 diatoms may be more important carbon exporters in some systems (Leblanc et al., 2018). Often,

82 high organic carbon export regimes are characterised by small cells and high abundances of

83 calcium-carbonate producers such as coccolithophores (Lam et al., 2011; Maiti et al., 2013; Leblanc

84 et al., 2018). Despite the importance of characterising phytoplankton assemblage fluxes on

85 seasonal timescales, most sediment trap studies are limited to bulk component analysis

86 (Particulate Organic Carbon (POC), Particulate Inorganic Carbon (PIC), Biogenic Silica (BSi),

87 Particulate Nitrogen and Particulate Phosphorus, etc.).

88 *1.2 Regional setting*

89 In the Southern Hemisphere from 30° S to Antarctica there are several distinct

90 oceanographic/hydrological regions (Supp. Fig. 1).The major part of this study region is the

91 Southern Ocean, which is the water mass encircling Antarctica from ~40° S, and is bounded on the

92 north by the Subtropical Front (STF), the meeting place of Subtropical and Subantarctic water

93 masses (Ardnt et al. 2013). North of the STF, the Subtropical Zone consists of relatively warm, saline

94 waters that tend to be low in nitrate (Supp. Fig. 1).

95 The major current of the Southern Ocean, the Antarctic Circumpolar Current (ACC), consists of

96 those waters south of the STF. It is banded by several major water masses, each with distinct

97 hydrological properties (Sokolov and Rintoul, 2009) that significantly influence the phytoplankton

98   species, and hence the export regimes, observed in the region (Pollard et al., 2002). Nitrate, silicate

99   and iron all tend to increase south of the STF, towards the pole, while salinity decreases (Supp. Fig.

100   1).

101   South of the STF is the Subantarctic Zone (SAZ), the northernmost and largest belt of the Southern

102   Ocean. The SAZ is bounded on the south by the Subantarctic Front (SAF), followed by the Polar

103   Frontal Zone (PFZ) and the Antarctic Zone (AZ), between which is the Polar Front (PF). The AZ is

104   divided further by Sokolov and Rintoul (2009) with the identification of two additional fronts

105   between the PF and the Antarctic coastline- the Southern ACC Front (SACCF) and the Southern

106   Boundary of the ACC (SB). The meridional positions of the Southern Ocean fronts varies due to

107   local bathymetry (Gordon et al., 1978): for example, the SAF meanders considerably and is found

108   as far north as ~42° S east of Argentina, but sits around 60° S at the Drake Passage (Fig. 1).

109   In the Southern Hemisphere, latitudinal gradients of nutrient availability constrain the locations of

110   carbonate-export (e.g. coccolithophores, foraminifera) and silicate-export (e.g. diatoms and

111   radiolarians) regions. North of the Polar Front (PF), export is suggested to be principally related to

112   carbonate particle flux and is known as the "Carbonate Ocean" (Honjo et al. 2008). South of the

113   PF, siliceous phytoplankton make up a significant proportion of flux (the "Silicate Ocean"; Honjo,

114   2004; Honjo et al., 2008), corresponding with high surface water silicate concentrations between

115   the PF and the Antarctic continent (Supp. Fig. 1) (Bostock et al., 2013). Carbonate is regarded as a

116   better ballast for the export of particulate matter compared to silicate (Klaas and Archer, 2002).

117   Because of the latitudinal differences in the types of exported material (see above), there is an

118   expectation that regional variation in ballasted particle sinking speeds, and therefore biological

119   pump efficiency, occurs in the Southern Ocean (Jin et al., 2006). Studies of phytoplankton fluxes

120   should consider regional differences in ballast availability in explaining flux patterns.

121   Sediment trap deployments would ideally be well-spread, sampling a diversity of oceanographic

122   regimes. This is not the case, and sediment trap deployments have been clustered in some regions,

123   leaving others unsampled (Romero and Armand, 2010; Fig. 1). In part this is the result of

124   remoteness and inherent difficulty of access in some regions (for example regions that are distal

125   from countries with oceanographic programs), and the cost of deployment and retrieval. Of the

126   sediment trap publications in the temperate and Subantarctic, few report fluxes of coccoliths

127   and/or diatoms (red dots in Fig. 1). Even fewer studies determine fluxes of individual species, even

128   though it is increasingly evident that the floristic composition of the phytoplankton community

129   largely determines biological pump efficiency in oceanic ecosystems (Assmy et al., 2013; Balch,

130   2018; Leblanc et al., 2018).
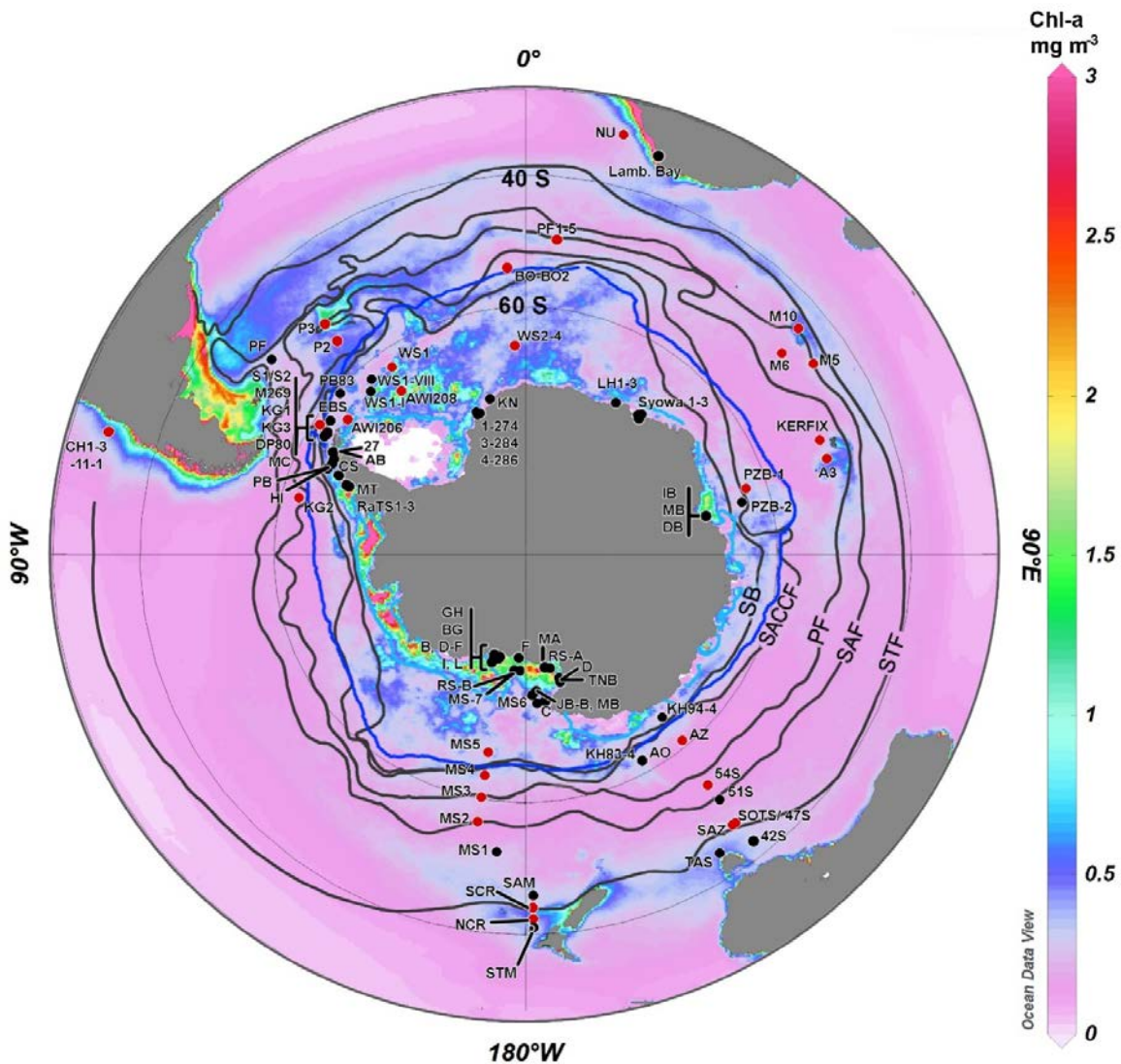
Figure 1. Map of Southern Hemisphere from 30° S with annual time-averaged Chlorophyll-*a* concentration (mg/m^{-3}) indicated by colour (https://giovanni.gsfc.nasa.gov). Sediment trap moorings shown by dots. Sediment trap mooring locations for which diatom and/or coccolith flux was available are identified by red dots. Station identifiers in Supp. Table 1. Fronts from Orsi et al. 1995. STF= Subtropical Front, SAF = Subantarctic Front, PF= Polar Front, SACCF= South Antarctic Circumpolar Current Front, SB= Southern Boundary (of the ACC). Map created with Ocean Data View 4 (http://odv.awi.de; Schlitzer 2016). Dark blue line indicates maximum winter sea ice extent.

Investigations reporting both diatom and coccolith fluxes from the same deployments have been principally undertaken for the Northern Hemisphere. Of these, one study collected an exceptional 19 years of export histories in the Bering Sea and central subarctic Pacific (Takahashi et al., 2012), although shorter duration trap studies have also been undertaken (e.g. 2 years in the Gulf of California; Ziveri and Thunell, 2000). Several annual trap deployments, and studies examining both diatom and coccolith fluxes have been published from the Mediterranean (Bárcena et al., 2004; Hernández-Almeida et al., 2011; Rigual-Hernández et al., 2013; Malinverno et al., 2014). In the

146 Southern Hemisphere, diatoms and coccolith fluxes from the same trap deployment have been

147 reported from single-year trap deployments within the Benguela Upwelling System (Romero et al.,

148 2002), the Australian sector of the Subantarctic Zone (Wilks et al., 2017), and from locations within

149 the subtropical and subantarctic marine systems surrounding New Zealand (Wilks et al., in review).

150 Studies calculating both diatom and coccolith fluxes from the same trap are valuable because as

151 the main phytoplankton silicate and carbonate producers, respectively, both are needed to

152 decipher the mechanisms driving organic matter export.

153 *1.3 Review aims*

154 General reviews of global or sector-based particle flux have been undertaken in the past (e.g.

155 Lampitt and Antia, 1997; Honjo et al., 2008; Romero and Armand, 2010; Rigual-Hernández et al.,

156 2018b), but, no specific review comparing results from sediment trap-derived diatom and coccolith

157 fluxes across the subtropical (from 30° S) to polar Southern Hemisphere has been attempted. The

158 aims of this semi-quantitative review are twofold;

159 1) compile an exhaustive spatial record of Southern Ocean to subtropical diatom and coccolith

160 fluxes from sediment trap records in order to identify large scale patterns in phytoplankton fluxes,

161 and

162 2) identify possible relationships between Southern Hemisphere diatom fluxes from the

163 Subtropical to Polar regions from existing sediment trap reports and environmental parameters.

164 Based on these observations, recommendations for future sediment trap research specific to the

165 Subtropical, Subantarctic and Southern Ocean regions of the Southern Hemisphere are proposed.

166 **2. Methodology**

167 *2.1 Compilation of sediment trap data*

168 A comprehensive survey of published data from moored sediment traps and other types of free-

169 drifting and surface tethered deployments south of 30° S since 1977 (to our knowledge the first

170 trap deployment in this region) are used as the basis of this review. Although the bulk of the

171 publications compiled report on Southern Ocean (generally defined as south of 50° S) traps, this

172 study expanded its focus to 30° S to enable inclusion of several subtropical studies. Publications

173 were included based on diatom and/or coccolithophore flux data from a sediment trap

174 deployment. Data compiled included diatom and coccolithophore fluxes, site coordinates,

175 deployment years and deployment depths. Each published survey was provided with a station

176 identifier (Supp. Table 1) to facilitate analysis and graphic representation.

177   With respect to diatom or coccolith fluxes documented, flux estimates were extracted from

178   original publications or supplementary material and recorded as diatom frustules/valves or

179   coccoliths m^{-2} y^{-1}. Coccosphere fluxes were not considered in this study. Where flux values were

180   provided as an annual value, these data were left unchanged. In instances where a sediment trap

181   was deployed for more than 200 days, the annual flux was calculated from reported daily fluxes

182   via normalisation to account for the missing sampling days (indicated in Table 1 in italics). For some

183   studies, trapping duration was too short (less than 200 days), or daily fluxes for sampling duration

184   were not provided, making extrapolation to an annual flux impossible. In these cases, fluxes are

185   given as originally published. In some instances, annual flux could not be determined. For example,

186   although diatoms were counted from the two moorings east of New Zealand (Prebble et al., 2013),

187   and the deployment time was in total sufficient to estimate annual flux, sampling was

188   discontinuous, making annual estimate too inaccurate.

189   *2.2 Considerations of sediment trap methodologies*

190   There are considerable methodological barriers to comparing sediment trap records. Studies have

191   compared particle capture from different trap mooring techniques (i.e. surface tethered, free-

192   floating/neutrally-buoyant and bottom-tethered) finding considerable differences in the volume

193   of material captured with each technique, and even different particle composition (Buesseler et

194   al., 2000). Theoretically, neutrally-buoyant drifting traps, such as those utilised in Leventer (1991)

195   are the most free of hydrodynamic bias, as they may match ambient current speeds (Buesseler et

196   al., 2007), though these are disadvantaged by not being deployable for as long as a typical moored

197   trap. The degree of trap tilt may depend on both the trap type and shape (cylindrical vs. conical)

198   (Gust et al., 1994), and deployment depth (Buesseler et al., 2007). Issues of collection efficiency

199   are likely of greater concern for earlier sediment trapping efforts, because some early trap designs

200   simply comprised PVC cylinders without preservatives (McMinn, 1996; Schloss et al., 1999). Even

201   in contemporary, and widely used Parflux traps, the clogging of trap baffles during highly

202   productive periods causes inaccuracies in sediment capture (Honjo et al., 2000).

203   In this review, all publications for which diatom or coccolith fluxes were reported are included.

204   Deployments were mainly of the moored type, although some were under-ice deployments

205   (Leventer and Dunbar, 1987; Leventer 1991).

206   "Swimmers" (organisms that enter the trap actively and die) are not considered part of the

207   passively sinking flux, but may comprise a significant portion of the organic carbon captured by

208   traps (Hargrave et al., 1989; Buesseler et al., 2007). Typically, swimmers are removed by sieving,

209   and/or picked by hand, usually under magnification. A 1.0 mm screen is most commonly used,

210   sometimes also paired with hand-picking (Abelmann and Gersonde, 1991; Fischer et al., 2002;

211   Salter et al., 2012). Hand-picking of swimmers is considered the most reliable way to distinguish

212   active from passive entrance into the trap to determine mass fluxes without risk of material loss

213   (Chiarini, 2013), and several studies in this compilation used hand-picking alone rather than

214   screening trap material (Leventer and Dunbar, 1987; Suzuki et al., 2001; Rembauville et al., 2015a).

215   Again, in this review, processing methods varied, and should be considered when interpreting the

216   flux results.

217   *2.3 Environmental and oceanographic data analysis*

218   Data on eight variables previously suggested to influence diatom flux were obtained for each

219   sediment trap deployment site. The variables included four key nutrients and minerals; phosphate

220   (PO^{3-}_4; µmol L^{-1}), nitrate (NO_{3^-}; µmol L^{-1}), silicate (SiO^{4-}_4; µmol L^{-1}), iron (Fe; nmol L^{-1}), which are

221   necessary for diatom growth. Sea Surface Temperature (SST; °C) was chosen as it can influence

222   both phytoplankton growth and dissolution rate, and hence export efficiency (Laufkötter et al.,

223   2017). Phosphate, nitrate, silicate and SST data was retrieved from the World Ocean Atlas 2009,

224   from the National Centres for Environmental Information

225   https://www.nodc.noaa.gov/OC5/WOA09/pr_woa-09-html.

226   Chlorophyll-*a* concentration (Chl-*a*; mg m^{-3}) was included as a measure of actual mean primary

227   production. Finally, Particulate Inorganic Carbon (PIC; mol m^{-3}) concentration was included as a

228   proxy for abundance of calcifying phytoplankton, as well as ballast availability, which has been

229   identified as a key export efficiency-related variable (Weber et al., 2016; see also Appendix 1).

230   Annual time-averaged (2009- 2014) mean Chl-*a* (4 km resolution, MODIS-Aqua satellite), time-

231   averaged (2009-2014) mean iron (0.67 x 1.25° resolution, NOBM model), time-averaged (2009-

232   2014) mean % annual sea ice cover (NOBM model), and time-averaged (2009-2014) PIC

233   concentration (4 km resolution, MODIS-Aqua satellite) was obtained from the Goddard Earth

234   Sciences Data and Information Services Centre (GES DISC) for the region 25° S to the South pole

235   (see https://giovanni.gsfc.nasa.gov; Appendix 1). This particular 5-year window was selected

236   because it was the most recent time interval for which data exists for the three environmental

237   parameters obtained from GES DISC. Since many of the trap deployments pre-date satellite data

238   for this region, it was not feasible to obtain data spanning the actual trap deployment years.

239   *2.4 Modelling diatom and coccolith flux using oceanographic data*

240   Diatom and coccolith annual and maximum fluxes were log transformed for mapping and

241   modelling, to improve model interpretation. A linear model was fitted for log_{10} maximum diatom

242   flux against seven variables chosen as potential predictors of diatom flux using R's lm function.

243   Predictive values of each variable was tested using R's step function (backwards and forwards). All

244   analyses were conducted in R version 3.5.0 (R Core Team, 2018). Silicate was $\log_{10}$ transformed to

245   improve linearity of data. A Pearson's product-moment correlation matrix was also constructed to

246   visualise potential relationships between predictors and $\log_{10}$ max diatom flux.

247   *2.5 Mapping diatom and coccolith flux*

248   Diatom and coccolith maximum and annual fluxes varied by several orders of magnitude between

249   studies, so $\log_{10}$-transformed fluxes were plotted using Ocean Data View (ODV) (Schlitzer, 2016).

250   Data points are extrapolated via weighted-average gridding. Oceanic fronts follow Orsi et al.

251   (1995). Plotted data are provided in Supplementary Tables 2-3. Oceanic sectors are defined thus:

252   Atlantic and eastern Pacific sector from 80° W to 25° E, the Indian sector from 25° E to 150° E, and

253   the Pacific sector from 150° E to 80° W. Abbreviations for the oceanic zones spanned by this study

254   are given in Figure 1 caption.

255   **3. Results**

256   *3.1 Summary of sediment trap compilation*

257   Since 1977 there have been 76 publications documenting observations from 126 moored sediment

258   trap sites between the Antarctic coast and 30° S (Fig. 1; Supp. Table 1). Deployments are highly

259   clustered, with the most comprehensively studied regions being the Antarctic Peninsula/Drake

260   Passage, Weddell and Ross Seas (Fig. 1). The majority of deployments are in shallow, shelf or

261   coastal regions. In the Weddell Sea, most of the 15 mooring deployments were undertaken in the

262   1980s, with a recent deployment in 2012 in the northern Weddell Sea near South Georgia

263   (Rembauville et al., 2016; Supp. Table 1). The densely-monitored Ross Sea has 24 mooring sites,

264   providing observations through to the late 1990s, while the Antarctic Peninsula (19 moorings) was

265   sampled into the early 2000s (Supp. Table 1). The most systematically and recently-sampled area

266   is the Australian/ New Zealand sector, with sediment trap deployments spanning all major

267   hydrological zones, and deployments from 1996 up to as recently as 2012 east of Tasmania

268   (Nodder et al., 2016; Fig. 1, Supp. Table 1). There is a notable absence of data in the southeast

269   Indian sector between the Kerguelen Islands and Tasmanian deployments south of Australia.

270   Conversely, the southern Pacific sector, from ~170° W to 70° W has had no sediment trap deployed

271   and constitutes the largest gap in the sediment trap record of the Southern Hemisphere.

272   Generally, sediment trap deployments in the subtropical to polar Southern Hemisphere occur in

273   the more-productive regions, as indicated by mean chl-*a* concentration, for example in the Ross

274   Sea (Fig. 1). However, there are some high productivity regions that have not been studied such as

275   the on the western Antarctic continental margin (Bellingshausen/Amundsen Sea region), where

276   there has been no sediment trap mooring, possibly due to year-round inaccessibility due to sea ice

277   (Fig. 1). One of the highest productivity regions by areal extent is found along the southeast coast

278   of Argentina, for which no sediment trap data are available.

279   In this review, 25 documented diatom and coccolithophore observations from an additional 65

280   free-drifting, tethered and moored sediment traps at various depths. Amongst these studies, 21

281   calculated only diatom fluxes, two determined only coccolith fluxes, and three studies recorded

282   both diatom and coccolith fluxes (Table 1).

283   Most of the deployments for which phytoplankton fluxes were determined presented daily and

284   annual fluxes in the text or figures, though there were exceptions for which neither annual nor

285   maximum fluxes were published. For example, the Syowa Station deployments in Lützow-Holm

286   Bay, Antarctica (Ishikawa et al., 2001; Ichinomiya et al., 2008) reported the fluxes separately for

287   dominant pennate and centric diatom taxa only (*Fragilariopsis kerguelensis, Pseudo-nitzschia*

288   *turgiduloides, Chaetoceros* spp., *Porosira pseudodenticulata* and *Thalassiosira australis*).

289   Rembauville et al. (2015b and 2018; Kerguelen plateau), and Wefer et al. (1988; Bransfield Strait,

290   Antarctica) reported on traps of longer duration (322, 337 and 330 days, respectively), but did not

291   present annual flux data. Suzuki et al. (2001) reported short deployments in the Australian sector

292   of the Antarctic Zone, but did not provide fluxes of the whole diatom component, only separate

293   fluxes for fast and slow-sinking fractions.

294   *3.2 Southern Hemisphere diatom flux*

295   Maximum diatom flux was published for 49 trap deployments south of 30° S, while annual flux was

296   provided for 28 (Fig. 2, Table 1). With the exception of the central Pacific and southeast Indian

297   sectors, diatom fluxes in the Southern Ocean are generally well-represented by trapping efforts to

298   date (Table 1), and some generalisations are possible. Diatom flux tends to increase towards the

299   pole, and diatom flux is highest, with a few exceptions, south of the Polar Front (PF; Fig. 2).
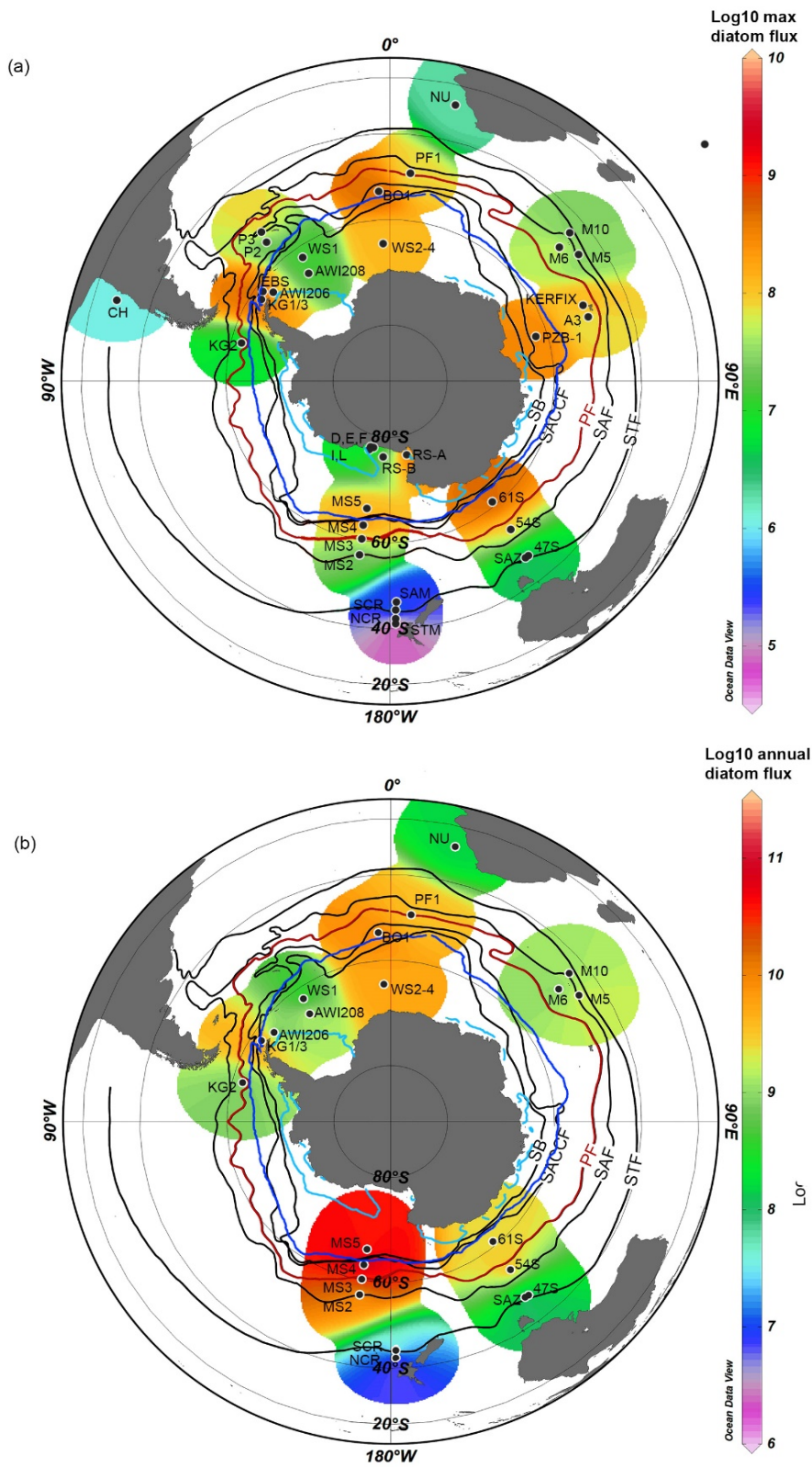
Figure 2. (a) Log$_{10}$ maximum (m^{-2} d^{-1}), and (b) annual (m^{-2} y^{-1}) diatom flux for sediment trap studies in the subtropical to polar Southern Hemisphere for which data was available. Magnitude of fluxes indicated by colour bars. White-ringed black circles indicate trap site. Oceanic abbreviations and trap identifiers are the same as Fig. 1. Dark blue and light blue lines indicate maximum winter, and minimum summer sea ice extent, respectively.

306   In several instances, a sharp differentiation between diatom flux magnitudes are seen north and south

307   of the PF, with noticeably higher fluxes to the south, consistent with the identification of Honjo (2004)

308   as a region of high silica export. This trend is particularly evident in the systematic trapping efforts in

309   the Australian and New Zealand regions, such as between trap stations MS2 and MS3 (Grigorov et al.,

310   2014), and between the Polar Frontal Zone (PFZ) and Antarctic Zone (AZ) traps (Rigual-Hernández et

311   al., 2015a; Rigual-Hernández et al., 2015b; Fig. 2, Table 1). The sharp demarcation between low fluxes

312   north of the PF, and high fluxes south is also visible between the Crozet Plateau (M5, M6 and M10 in

313   Fig. 2; Salter et al., 2012) and Kerguelen Plateau (A3 in Fig. 2, KERFIX; Rembauville et al., 2015b; 2018).

314   While the Crozet and Kerguelen traps occupy a similar latitude, the latter sit south of the PF, and have

315   correspondingly higher maximum diatom fluxes (~1 order of magnitude, Fig. 2a). Similarly, in the

316   Atlantic sector, the KG2 site, north of the PF, captured lower diatom flux than the similar-latitude

317   Antarctic Peninsula traps, which sit south of the PF in this sector (Fig. 2a).

318 **Table 1.** Compilation of sediment trap studies of diatom or coccolithophore fluxes in the subtropics (30°S) to the Antarctic coast. Annual flux estimates annualized by

319 normalization are indicated in italics. Where the same site was published in more than one publication, the publication in which the fluxes were stated is given here. *

320 indicates discontinuous sampling spanning 300 days (Prebble et al., 2013).

Region/ Trap ID	Latitude, Longitude	Trap depth (m)	Water column depth (m)	No. days	Diatom flux	Coccolith flux	Reference
Southeast Pacific sector							
CH	30° S, 73°11' W	2300	4700	~669	-	3.5×10^5-$1.2 \times 10^8 \ m^{-2} \ d^{-1}$	González et al., 2004
CH3-1	30°01.5' S, 73°11.0' W	2333	4360	180	2.3-$69.8 \times 10^5 \ m^{-2} \ d^{-1}$	-	Romero et al., 2001
CH4-1	30°00.3' S, 73°10.3' W	2303	4330	160	0.2-$1.6 \times 10^5 \ m^{-2} \ d^{-1}$	-	Romero et al., 2001
CH10-1	29°59.9' S, 73°16.8' W	1492	4500	260	1.2-$28.2 \times 10^5 \ m^{-2} \ d^{-1}$	-	Romero et al., 2001
CH10-2	29°59.9' S, 73°16.8' W	2578	4500	260	0.6-$15.8 \times 10^5 \ m^{-2} \ d^{-1}$	-	Romero et al., 2001
CH11-1	29°58.8' S, 73°18.1' W	2526	4442	228	0.2-$3.6 \times 10^5 \ m^{-2} \ d^{-1}$	-	Romero et al., 2001
Drake Passage/ Antarctic Peninsula							
KG1	62°15.4' S, 57°31.7' W	494	1952	348	$>26.6 \times 10^9 \ m^{-2} \ y^{-1}$	-	Abelmann and Gersonde, 1991
"	62°15.4' S, 57°31.7' W	1588	1952	360	$2.6 \times 10^{11} \ m^{-2} y^{-1}$	-	Abelmann and Gersonde, 1991
KG2	62°20.1' S, 75°28.3' W	700	1650	344	$0.8 \times 10^9 \ m^{-2} y^{-1}$	-	Abelmann and Gersonde, 1991
KG3	62°22.0' S, 57°59.9' W	687	1992	162	$2.2 \times 10^9 \ m^{-2} y^{-1}$	-	Abelmann and Gersonde, 1991
EBS	61°45.8' S, 54°59.1' W	1000	2134	364	Max $2.4 \times \times 10^9 \ m^{-2} \ d^{-1}$	-	Kang et al., 2003
R13	63°25' S, 62°23' W	100-200	n/a	4-5	13.33-$66.68 \times 10^7 \ m^{-2} \ d^{-1}$	-	Leventer, 1991
R20	61°55' S, 62°00' W		n/a	"	1.26 to $5.32 \times 10^7 \ m^{-2} \ d^{-1}$	-	Leventer, 1991
R39	62°30' S, 61°32' W		n/a	"	3.71 to $70.89 \times 10^7 \ m^{-2} \ d^{-1}$	-	Leventer, 1991
R43	64°17' S, 61°17' W		n/a	"	6.24 to $978.5 \times 10^7 \ m^{-2} \ d^{-1}$	-	Leventer, 1991
R48	63°14' S, 60°55' W		n/a	"	0.42 to $183.25 \times 10^7 \ m^{-2} \ d^{-1}$	-	Leventer, 1991

Weddell Sea

WS-1	62°26.5' S, 34°45.5' W	443	3880	418	~10^6 to 10^7 m^{-2}d^{-1}	-	Fischer et al., 1988
WS1	62°26.5' S, 34°45.4' W	863	3880	418	0.26 x10^9 m^{-2}y^{-1}	-	Abelmann and Gersonde, 1991
WS2	64°55.0' S, 2°30.0' W	4454	5053	304	8.8 x10^9 m^{-2}y^{-1}	-	Abelmann and Gersonde, 1991
WS3	64°53.1' S, 2°33.7' W	360	5053	385	1.0 x10^{10} m^{-2}y^{-1}	-	Abelmann and Gersonde, 1991
WS4	64°55.5' S, 2°35.5' W	352	5044	360	>1.8 x10^9 m^{-2}y^{-1}	-	Abelmann and Gersonde, 1991
PF1	50°09.0' S, 5°43.8' E	700	3779	421	5.5 x10^9 m^{-2}y^{-1}	-	Abelmann and Gersonde, 1991
AWI206	63°29.6' S, 52°07.4' W	500	946	233	166.1 x10^6 m^{-2} sampling period^{-1} (=*2.6 x10^8 m^{-2} y^{-1}*)	-	Gersonde and Zielinksi, 2000
AWI208	65°36.3' S, 36°29.9' W	1000	4768	345	1722.0 x10^6 m^{-2} sampling period^{-1} (=*1.8 x10^9 m^{-2} y^{-1}*)	-	Gersonde and Zielinksi, 2000
P2	55°11.99' S, 41°7.42' W	1500	3200	230	Max 1.4 x10^7 m^{-2} d^{-1}	-	Rembauville et al., 2016
P3	52°43.40' S, 40°8.83' W	2000	3800	292	Max 1.2 x10^8 m^{-2} d^{-1}	-	Rembauville et al., 2016

East Atlantic sector

BO1	54°20.3' S, 3°22.6' W	450	2734	368	21049 x10^6 m^{-2} sampling period^{-1} (=*2.1 x10^{10} m^{-2} y^{-1}*)	-	Gersonde and Zielinski, 2000, Fischer et al., 2002
BO2	54°20.8' S, 3°23.6' W	456	2695	200	1906.9 m^{-2} sampling period^{-1} (=3.5 x10^9 m^{-2} y^{-1})	-	Gersonde and Zielinski, 2000
PF1	50°09.0' S, 5°43.8' E	700	3779	421	5.5 x10^9 m^{-2}y^{-1}	-	Abelmann and Gersonde, 1991
PF3	50°07.6' S, 5°50.0' E	614	3785	378	12163.8 m^{-2} sampling period^{-1} (=1.2 x10^{10} m^{-2} y^{-1})	-	Gersonde and Zielinski, 2000
PF5	50°06.0' S, 5°55.4' E	654	3804	200	322.8 m^{-2} sampling period^{-1} (=5.9 x10^8 m^{-2} y^{-1})	-	Gersonde and Zielinski, 2000
NU	29°12' S, 13°07' E	2516	3055	~365	1.5 x10^8 m^{-2} yr^{-1}	1.6 x10^{12} m^{-2} yr^{-1}	Romero et al. 2002

Southwest Indian sector

KERFIX	50°40' S, 68°25' E	280	2300	337	<1 x10^6-1.3 x10^8 m^{-2} d^{-1}	-	Rembauville et al., 2018

"	50°40' S, 68°25' E	200	1700	290	-	0.1 to 137.6 x10^6 m^{-2} d^{-1}	Ternois et al., 1998
A3	50°38.30' S, 72°02.6' E	289	527	322	<5 x10^6-6.1 x10^7 m^{-2} d^{-1}	-	Rembauville et al., 2015b
PZB-1	62°28.6' S, 72°58.6' E	1400	4000	366	<3 x10^6 to >270 x10^6 m^{-2} d^{-1}	-	Pilskaln et al., 2004; Rigual-Hernández et al., 2018b
M10	44°29.95' S, 49°59.9' E	2000	2935	352	1.3 x10^9 m^{-2} yr^{-1}	-	Salter et al., 2012
M5	46°00' S, 56°05.0' E	3195	4277	361	2.0 x10^9 m^{-2} yr^{-1}	-	Salter et al., 2012
M6	49°00.03'S, 51°30.6' E	3160	4221	361	8.3 x10^8 m^{-2} yr^{-1}	-	Salter et al., 2012
Australian/New Zealand Sector							
MS2	56°54' S, 170°10' W	982	4924	425	5.0 x10^9 m^{-2} y^{-1}	-	Grigorov et al., 2014
MS3	60°17' S, 170°03' W	1003	3957	425	2.9 x10^{10} m^{-2} y^{-1}	-	Grigorov et al., 2014
MS4	63°09' S, 169°54' W	1031	2885	425	1.8 x10^{11} m^{-2} y^{-1}	-	Grigorov et al., 2014
MS5	66°10' S, 169°40' W	937	3015	425	2.6 x10^{10} m^{-2} y^{-1}	-	Grigorov et al., 2014
NCR	44°37' S 178°37' E	300	1500	178	5.5 x 10^5 m^{-2} yr^{-1}	1.0 x10^7 m^{-2} yr^{-1}	Wilks et al., under review
"		1000	"	243	1.5 x10^6 m^{-2} yr^{-1}	-	Wilks et al., under review
SCR	42°42' S 178°38' E	300	1500	340	8.2 x10^7 m^{-2} yr^{-1}	1.4 x10^8 m^{-2} yr^{-1}	Wilks et al., under review
"		1000	"	340	1.4 x10^8 m^{-2} yr^{-1}	-	Wilks et al., under review
STM	41°15' S, 178°33' E	1500	3100	>300*	Max 3.4 x10^4 m^{-2} d^{-1}	-	Prebble et al., 2013
SAM	46°33' S, 178°33' E	1500	2700	>300*	1.2 x10^5 m^{-2} d^{-1}	-	Prebble et al., 2013
SAZ	46°46' S, 142°40' E	1060	4540	790	0.5 ± 0.4 x10^8 m^{-2} yr^{-1}	-	Rigual-Hernández et al., 2015a
47S	46°46' S, 142°4' E	500	4540	364	2.3 x10^8 m^{-2} yr^{-1}	6.5 x10^{11} m^{-2} yr^{-1}	Wilks et al., 2017
PFZ	53°45' S, 141°45' E	830	2280	1894	3.1 ± 5.5 x10^9 m^{-2} yr^{-1}	-	Rigual-Hernández et al., 2015a
AZ	60°44.4' S, 139°54.0' E	2000	4393	309	2.4 x10^{10} m^{-2} yr^{-1}	1.03 ×10^{11} m^{-2} yr^{-1}	Rigual-Hernández et al., 2015b; 2018a
"		3700	"	172	2.3 x10^{10} m^{-2} yr^{-1}	1.2 x10^{11} m^{-2} yr^{-1}	Rigual-Hernández et al., 2015b; 2018a
Ross Sea							
B-F, I, L	76°56'-77°52' S, 163°46'-166°37' W	15-685	41-715	~61	<1 x10^5 to >4 x10^7 m^{-2} d^{-1}	-	Leventer and Dunbar, 1987
RS-A	76°30.1' S, 167°30.3' E	250	not stated	357	Max 5.5 x 10^8 m^{-2} d^{-1}	-	Leventer and Dunbar, 1996
RS-B	76°30.3' S, 74°59.1' W	250	not stated	363	Max 9.5 x10^7 m^{-2} d^{-1}	-	Leventer and Dunbar, 1996

321

322   3.2.1 Southeast Pacific and Atlantic sector traps

323   Sediment trap deployments in the Southeast Pacific and Atlantic sector are well scattered between

324   the Antarctic Peninsula/Bransfield Strait and Weddell Sea, with a total of 13 mooring sites for

325   which diatom fluxes were reported (Fig. 3). Sediment trapping in this region was mainly

326   undertaken in the mid-1980s to 1990s (Supp. Table 1), with the exception of two sites, P2 and P3

327   in the northern Weddell Sea region downstream of South Georgia, which had sediment trap

328   deployments in 2012 (Rembauville et al., 2016). The Drake Passage was the site of the first

329   sediment trap deployed in the Antarctic region (site DP80-81) between 1980 and 81, although

330   diatom fluxes were not determined for this deployment (Fig. 1; Supp. Table 1). The steep gradient

331   in diatom flux magnitude north and south of the PF breaks down around the Antarctic Peninsula/

332   Weddell Sea traps, with lower fluxes seen in the central Weddell Sea (especially WS1 and AWI208

333   (Abelmann and Gersonde, 1991; Gersonde and Zielinski, 2000) than in surrounding moorings.

334   Traps to the west, on the Antarctic Peninsula/ Bransfield Strait (EBS, AWI206, KG1 and 3), and in

335   the eastern Weddell Sea (PF1, BO1 and WS2-4) reported some of the highest diatom fluxes in the

336   focus region (Fig. 2a; Table 1). The central Benguela site NU, at the eastern edge of the Atlantic

337   sector, was also a relatively low diatom flux site, with annual fluxes of 1.5 x10^8 valves m^{-2} yr^{-1} (Table

338   1; Romero et al., 2002).
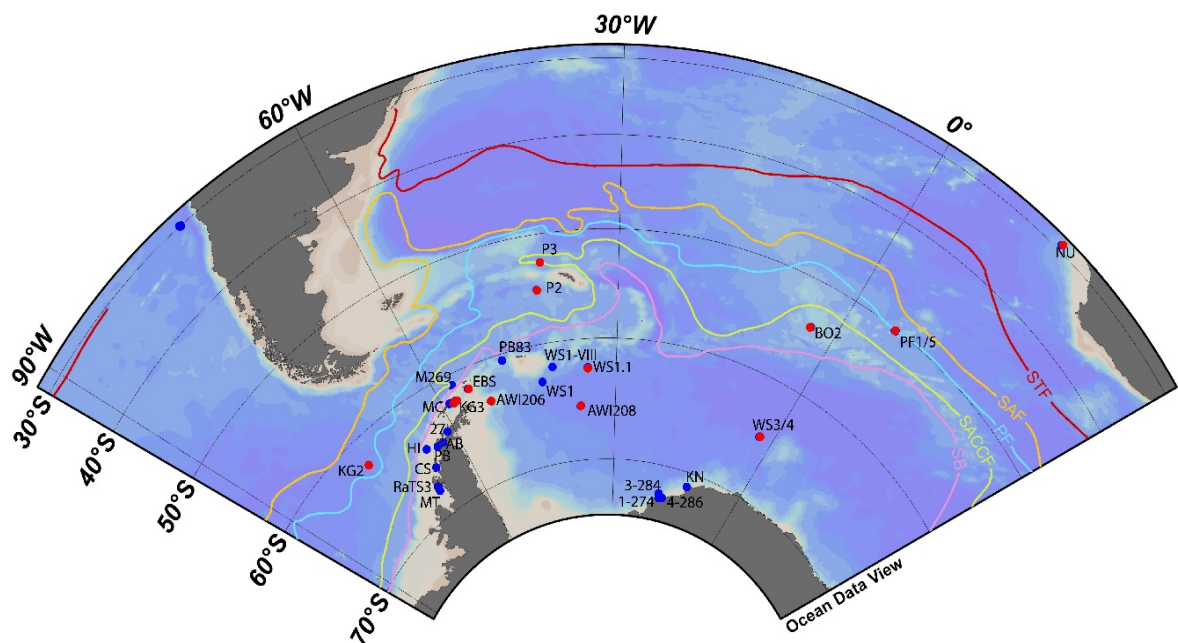
339

340   **Figure 3.** Atlantic sector sediment trap moorings. Red circles indicate moorings for which diatom flux data is

341   available. Oceanic abbreviations and trap identifiers are the same as Fig. 1.

342 The seasonally ice-covered sites in the Bransfield Strait and Antarctic Peninsula reported high
343 fluxes of *Fragilariopsis curta* and *F. cylindrus*, typical sea-ice species. At EBS, *F. cylindrus* was also
344 present, but fluxes were dominated by *Minidiscus chilensis* (87% of total flux), a diatom not
345 reported in other trap studies in this region, as well as *Pseudo-nitzschia heimii* and *Thalassiosira*
346 *Antarctica* (Kang et al., 2003) (Table 2).

347 *Fragilariopsis kerguelensis* was highly abundant at the Weddell Sea sites WS2-4 (up to 90% of
348 winter assemblages at WS3), and at PF1 (60-85%) (Abelmann and Gersonde 1991). At P2 and P3,
349 *F. kerguelensis* was 46% and 31% of total assemblages, respectively (Rembauville et al. 2016).
350 *Fragilariopsis curta* was usually in excess of 20% of total flux at the Weddell Sea AWI, BO and WS
351 sites, and up to 50% at BO1, while *F. cylindrus* was 70% of the winter assemblage at WS1 (Abelmann
352 and Gersonde, 1991; Gersonde and Zielinski, 2000). The ice-free PF1 traps overwhelmingly
353 captured *F. kerguelensis* (60-85%) and *Thalassionema nitzschioides* (5-15%) (Abelmann and
354 Gersonde 1991).

355 Low diatom fluxes were captured off the coast of Chile in the Subtropical Humbolt Current System
356 (CH traps), between 1993-94 (CH1-3; normal year) and 1997-98 (CH11-1; El Niño year). Total
357 annual diatom flux in the El Niño year was 75% lower than in the normal year, and spring flux
358 maxima were 15.8 x10^5 m^{-2} d^{-2} in 1997-98, compared to 69.8 valves x10^5 m^{-2} d^{-2} in 1993-94 (Romero
359 et al., 2001). Both normal and El Niño years saw high abundances of *Chaetoceros* resting spores
360 and *F. doliolus*, although assemblage diversity was higher in the El Niño year, and taxa such as
361 *Rhizosolenia* and *Chaetoceros* vegetative cells were more abundant (Romero et al. 2001). At the
362 other subtropical station NU (non El Niño deployment years 1992-93), assemblages were also rich
363 in *F. doliolus* (34% total), as well as *Azpeitia* spp. And *Thalassionema nitzschioides* (Table 2; Romero
364 et al., 2002).

Table 2. Top diatom taxa at sediment trap deployments in the study region for which data are available. Guide to abbreviations: *F.* = *Fragilariopsis*, *T.* = *Thalassiosira*, CRS = *Chaetoceros* resting spores, *A.* = *Azpeitia*, *P-n.* = *Pseudo-nitzschia, N. = Nitzschia.*

Region/ Trap ID	Deployment years	Trap depth (m)	Most abundant taxa	References
Southeast Pacific sector				
CH3-1	1993-1994	2300	CRS, *F. doliolus, A. curvulatus*	Romero et al., 2001
CH10-1	1997	2578	CRS, *Rhizosolenia* spp., *Chaetoceros* spp.	Romero et al., 2001
Drake Passage/ Antarctic Peninsula				
KG1	1983-1984	494	*Chaetoceros* spp. (50-70%), *T. antarctica*, *F. kerguelensis*	Abelmann and Gersonde, 1991
KG2	1984-1985	700	*Chaetoceros* spp. (50-60%)	Abelmann and Gersonde, 1991
KG3	1983	687	*T. antarctica* (30-80%), *Chaetoceros* spp. (10-35%)	Abelmann and Gersonde, 1991
EBS	1998-1999	1000	*Minidiscus chilensis* (max 87%), *P-n. heimii, T. antarctica*	Kang et al., 2003
DP80/81	1980-1981	965	*F. curta* (25.3%), *F. cylindrus* (8.4%), *Chaetoceros* spp. (0.5%)	Gersonde and Zielinski, 2000
PB83	1983	1660	*F. cylindrus* (48.7%), *F. curta* (4.2%), *Chaetoceros* (6.2%)	Gersonde and Zielinski, 2000
Weddell Sea				
WS1	1985-1986	863	*F. curta* (33.2%), *F. cylindrus* (24.3%), *T. gracilis* (20-40%)	Abelmann and Gersonde, 1991
WS2	1987	4454	*F. kerguelensis* (90%)	Abelmann and Gersonde, 1991
WS3	1988-1989	360	*F. kerguelensis* (30-60%), *F. cylindrus* (12.5%), *F.curta* (5-20%)	Abelmann and Gersonde, 1991
WS4	1989-1990	400	*F. kerguelensis* (30-40%), *F. cylindrus* (25.6%), *F. curta* (14.1%)	Abelmann and Gersonde, 1991
PF1	1987-1988	700	*F. kerguelensis* (60-85%), *T. nitzschioides* (5-15%)	Abelmann and Gersonde, 1991
AWI208	1990-1992	500	*F. cylindrus* (10.6%), *F. curta* (17.7%), *F. sublinearis* (17.9%)	Abelmann and Gersonde, 1991
AWI206	1989-1990	1000	*F. cylindrus* (9%), *F. curta* (47.8%), *F. obliquecosta* (1.3%)	Abelmann and Gersonde, 1991
P2	2012	1500	*F. kerguelensis* (45.7%), *F. separanda* (15.6%), *T. gracilis* (8.9%)	Rembauville et al., 2016
P3	2012	2000	*F. kerguelensis* (31.4%), CRS (42.7%), *T. nitzschioides* (8.9%)	Rembauville et al., 2016
East Atlantic sector				
BO1	1990-1991	450	*F. curta* (37%), *F. kerguelensis* (28.7%), *T. gracilis* (7%)	Gersonde and Zielinski, 2000, Fischer et al., 2002
BO2	1992	456	*F. cylindrus* (max 38%), *F. curta* (max 30%)	Gersonde and Zielinski, 2000

PF1	1987-1988	700	*F. kerguelensis* (60-85%), *T. nitzschioides* (5-15%)	Gersonde and Zielinski, 2000
PF3	1989-1990	614	*F. kerguelensis* (40.4%), *T. nitzschioides* (25.7%), *T. lentiginosa* (6.5%)	Gersonde and Zielinski, 2000, Fischer et al., 2002
NU	1992-1993	2516	*F. doliolus* (34%), *A. tabularis, A. neocrenulata, T. nitzschioides*	Romero et al. 2002
Southwest Indian sector				
KERFIX	1994-1995	280	*F. kerguelensis* (59.8%), CRS (5.6%), *P-n. lineola* (5.4)	Rembauville et al., 2017
A3	2011-2012	289	*Chaetoceros* spp., *E. antarctica* var. *antarctica, P-n. spp.*	Rembauville et al., 2015b
PZB-1	1998-1999	1400	*Fragilariopsis cylindrus* (25%), *F. kerguelensis* (24%), *P-n. spp.* (10%)	Rigual-Hernández et al., 2018
M10	2004-2005	2000	*E. antarctica* var. *antarctica* (58%), *F. kerguelensis* (40%)	Salter et al., 2012
M5	2004-2005	3195	*E. antarctica* var. *antarctica* (28%), *F. kerguelensis* (67%)	Salter et al., 2012
M6	2005-2006	3160	*F. kerguelensis* (83%), *Rhizosolenia* spp. (0.3%), *Thalassiothrix* spp. (0.3%)	Salter et al., 2012
Australian/New Zealand Sector				
MS2	1996-1998	1000	*F. kerguelensis* (58.5%), *N. bicapitata* (6.5%), *T. lentiginosa* (4.4%)	Grigorov et al., 2014
MS3	1996-1998	1000	*F. kerguelensis* (67.1%), *T. gracilis* (6.9%), *F. cylindrus* (3.2%)	Grigorov et al., 2014
MS4	1996-1998	1000	*F. kerguelensis* (34.7%), *T. gracilis* (8.3%), *F. separanda* (7.9%),	Grigorov et al., 2014
MS5	1996-1998	1000	*F. curta* (31.7%), *F. cylindrus* (23.3), *F. kerguelensis* (22.2%)	Grigorov et al., 2014
SCR	1996-1997	300	*P-n.* spp. (95%), *N. bicapitata* (2.5%), *S. oestrupii* (0.5%)	Wilks et al., under review
NCR	1996-1997	300	CRS (44.8%), *Chaetoceros* spp. (9.8%), *L. annulata* (5.1%)	Wilks et al., under review
SAZ	2003-2004	500	*F. kerguelensis* (24.8%), *A. tabularis* (10.8%), CRS (7.2%)	Wilks et al., 2017
PFZ	1997-1998, 1999- 2000, 2002- 2007	830	*F. kerguelensis* (60%), *P-n. lineola* (10%),*T. gracilis* (6%)	Rigual-Hernández et al., 2015a
AZ	2001-2002	2000	*F. kerguelensis* (72%), *T. lentiginosa* (5%), *T. gracilis* (6%)	Rigual-Hernández et al., 2015b
Ross Sea				
B	1984	25-103	*N. stellata, F. curta, Amphiprora* spp., *Fragilaria islandica*	Leventer and Dunbar, 1987
D	1984	28-161	*Amphipropra* spp., *Thalassiosira* spp., *F. curta*	Leventer and Dunbar, 1987
F	1984	32-238	*Pinnularia quardatarea, Amphiprora* spp., *Pleurosigma* spp.	Leventer and Dunbar, 1987
RS-A	1991-1992	250	*F. curta* (92%), *F. cylindrus*	Leventer and Dunbar, 1996
RS-B	1991-1992	250	*F. curta, F. cylindrus, Fragilariopsis* spp., *Thalassiosira* spp.	Leventer and Dunbar, 1996

367

368   3.2.2 The Indian sector

369   In the Indian sector, diatom flux data was available from six moorings; the three Crozet Island

370   moorings (M5, M6 and M10; Salter et al. 2012), the Kerguelen Island and Plateau moorings (KERFIX

371   and A3; Rembauville et al., 2015b; Rembauville et al., 2018), and the Prydz Bay site PZB-1 (Pilskaln

372   et al., 2004; Rigual-Hernández et al., 2018b) (Fig. 4). Studies of diatom fluxes in this sector report

373   on traps deployed as early as 1993 (KERFIX), to the Crozet Island deployments retrieved as recently

374   as 2006 (Supp. Table 1; Salter et al. 2012). The Crozet Plateau and A3 deployments were each one

375   year, while KERFIX was sampled for 2 years (Supp. Table 1). In the case of the PZB traps, although

376   they were deployed between 1998 and 2001, phytoplankton analyses were not undertaken on

377   these records until very recently (Rigual-Hernández et al., 2018b). North of the PF, the Crozet Island

378   traps had moderate diatom fluxes (maximum 5.6 x 10^7 valves m^{-2} d^{-1} at M6), comparable in

379   magnitude to fluxes at a similar latitude in the Australian sector (SAZ and 47° S; Fig. 2). KERFIX, A3

380   and PZB-1, south of the PF, showed increasing diatom flux towards the Antarctic continent.
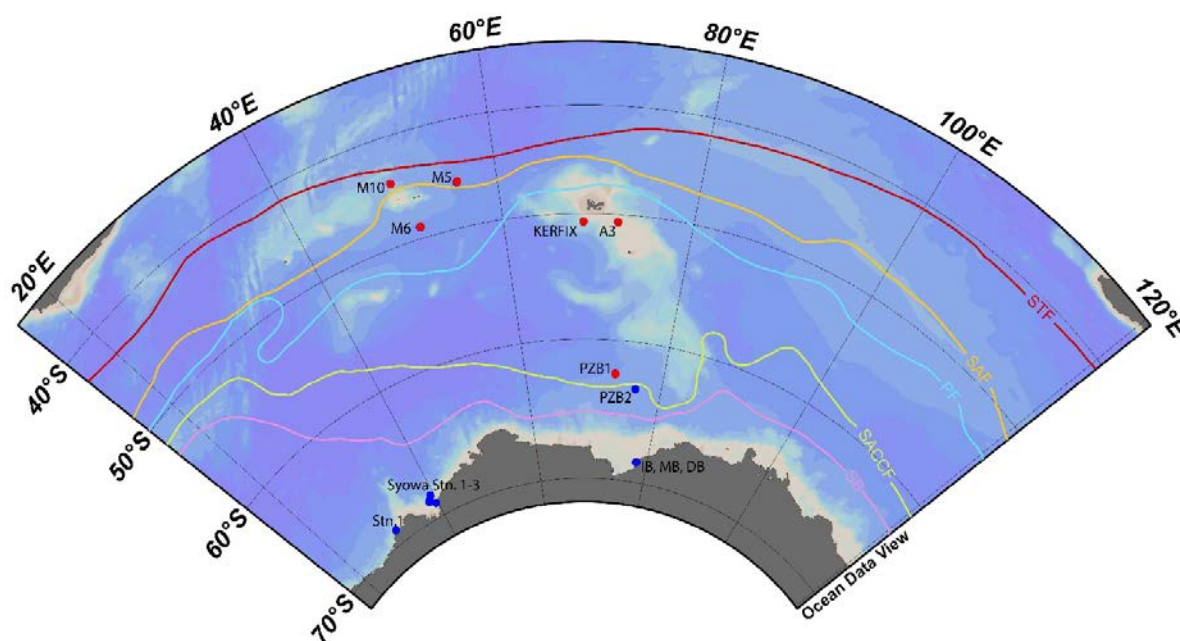
381

382   **Figure 4.** Indian sector sediment trap moorings. Red circles indicate moorings for which diatom flux data is

383   available. Oceanic abbreviations and trap identifiers are the same as Fig. 1.

384   At the two naturally iron-fertilized Crozet sites M10 and M5, two taxa, *Eucampia antarctica* var.

385   *antarctica* and *Fragilariopsis kerguelensis* together comprised over 92% of total diatom fluxes

386   (Table 2). However, *E. antarctica* was absent from the non-iron fertilised trap at M6 (Salter et al.,

387   2012). *F. kerguelensis* was also highly abundant at KERFIX (59.8% total flux) (Rembauville et al.,

388   2017), but less so at the nearby site A3, where it made up only 11.8% (Rembauville et al., 2015b).

389   Instead, *Chaetoceros* Hyalochaete cells were the bulk of diatom flux at A3, followed by *E. antarctica*

390 var. *antarctica*, and *Pseudo-nitzschia* spp. Further south, at the PZB station, *F. kerguelensis* and *F.*

391 *curta* were roughly a quarter of total fluxes each, while *Pseudo-nitzschia* were also a significant

392 component at 10% of total flux (Rigual-Hernández et al., 2018b).

393 3.2.3 The Australian and New Zealand sector and Ross Sea

394 The Australian and New Zealand sectors (southeast Indian Ocean to southwest Pacific Ocean) are

395 arguably the most comprehensively-studied in the Southern Hemisphere in terms of

396 phytoplankton flux and community characterisation, with moorings spanning all major zones

397 between the subtropics and the Antarctic coast (Fig. 5). The Australian and New Zealand sectors

398 contain the longest and second-longest sediment trap deployments in the Southern Ocean,

399 respectively. The longest mooring is the Southern Ocean Time Series located in the Australian

400 sector at 140° E, 47° S (SOTS; 1998-present), under the management of Tom Trull and Eric Schulz

401 (Integrated Marine Observing System, University of Tasmania). Most recently, surface

402 phytoplankton assemblages were determined from a one-year sediment trap deployment at SOTS

403 (Eriksen et al., 2018). Other sediment trap deployments south of Australia represent every main

404 hydrological zone of the Southern Ocean (Bray et al., 2000; Trull et al., 2001a), with intermittent

405 sediment trap deployments over the last decade (Table 1).
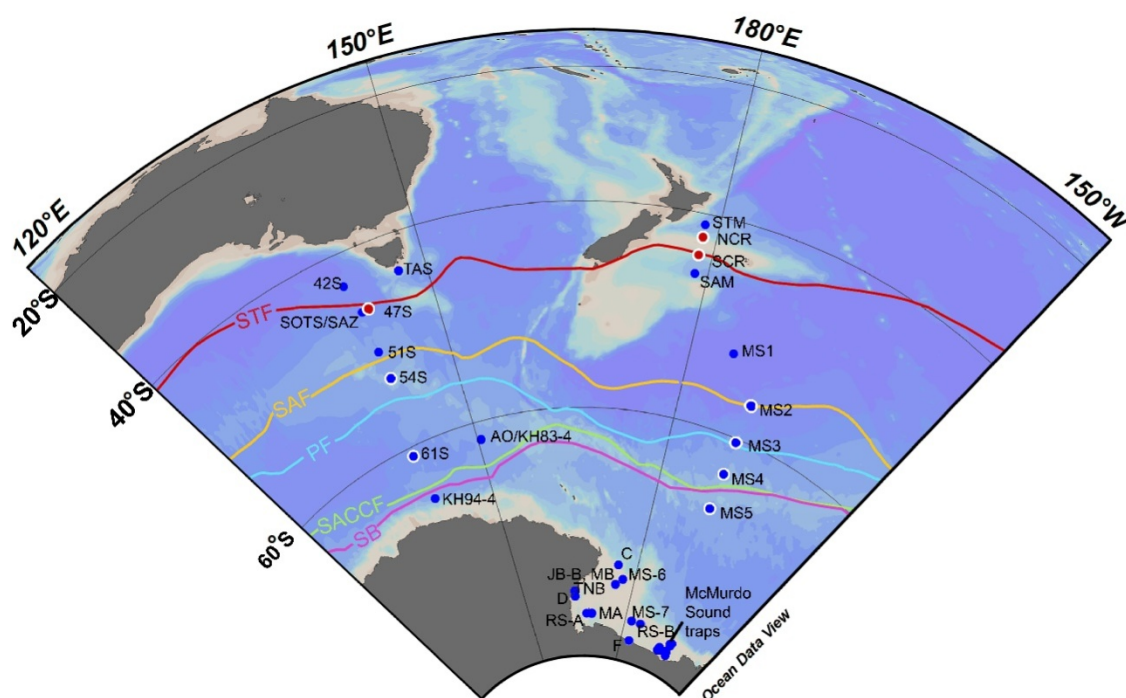
406

407 **Figure 5.** Summary map of all sediment trap moorings in the Australian and New Zealand sector. Sediment

408 trap moorings are indicated with blue circles. Circles with white rings have calculated annual records of

409 diatom and/or coccolith flux. Red circles represent the study locations for which both diatom and coccolith

410 fluxes are available. Abbreviations defined in Fig. 1 caption. Oceanic abbreviations and trap identifiers are

411 the same as Fig. 1.

412 East of New Zealand, the STM and SAM mooring sites represent the second longest sediment trap

413 time series in the Southern Ocean (2000-2012), managed by the National Institute of Water and

414 Atmospheric research, New Zealand (NIWA) (Nodder et al., 2016). Of the moorings managed by

415 NIWA, the NCR and SCR deployments are the first for which annual diatom and coccolith flux, as

416 well as assemblage seasonality, has been calculated (Wilks et al., in review). Southeast of New

417 Zealand, in the Southwestern Pacific sector, US JGOFS-Antarctic Environment and Southern Ocean

418 Process Study (AESOPS) program deployments extend from the SAZ (MS1) to below the Southern

419 Boundary (SB) of the ACC (MS5), with trap coverage from 1996-98 (Supp. Table 1, Fig. 5) (Honjo et

420 al., 2000). Of the AESOPS moorings, diatom assemblages and fluxes between MS2-5 have been

421 characterised to species level (Grigorov et al., 2014).

422 The SAZ Project and AESOPS deployments again represent rare trapping efforts for which diatoms

423 and/or coccolith fluxes have been determined over an annual cycle, in addition to the bulk

424 compounds usually measured (i.e. POC, biogenic silica, PIC etc.) (Honjo et al., 2000; Grigorov et al.,

425 2014; Rigual-Hernández et al., 2015a; Rigual-Hernández et al., 2015b; Wilks et al., 2017).

426 Exceptionally, seafloor sediment and phytoplankton standing stock analyses have also been

427   undertaken at or near the NIWA moorings (Bradford-Grieve et al., 1997; Nodder et al., 2007; Chang

428   and Northcote, 2016), SAZ Project moorings (Hutchins et al., 2001; Rigual-Hernández et al., 2016)

429   and AESOPS mooring sites, making these deployments comprehensive in terms of complete

430   surface to seafloor characterisation.

431   East of New Zealand, *Fragilariopsis kerguelensis* dominated diatom flux between MS-2, MS-3, and

432   MS-4, averaging 58.5 %, 67.1 % and 34.7 % of diatom flux across the study period, respectively

433   (Grigorov et al., 2014). At MS-5, the dominance of *F. kerguelensis* was replaced by higher

434   abundances of sea ice taxa *F. curta* and *F. cylindrus*, though *F. kerguelensis* still accounted for

435   22.2 % of average flux. High fluxes of *Chaetoceros* resting spores were captured at the Subtropical

436   station NCR off New Zealand (44.8 %), along with high proportions of coastal and benthic taxa,

437   whereas the SCR station to the south saw diatom flues overwhelmingly dominated by *Pseudo-*

438   *nitzschia* spp. (95 %) (Wilks et al., under review). In the Australian sector, *F. kerguelensis* was about

439   a quarter of total flux at the 2003-04 SAZ station deployment, followed by *Azpeitia tabularis*

440   (10.2 %) and *Chaetoceros* spores (7.2 %) (Wilks et al., 2017). For the 1999-2000 deployment the

441   same site, *F. kerguelensis* was even more abundant (48 %), with *A. tabularis* again 10 % (Rigual-

442   Hernández et al., 2015a). Finally, *F. Kerguelensis* abundances increased southwards at the PFZ and

443   AZ sites, comprising 60 % and 72 % of annual assemblages, respectively (Rigual-Hernández et al.,

444   2015a, b).

445   In the Ross Sea, diatom fluxes at mooring RS-A was an order of magnitude higher than RS-B and

446   the short-term under-ice McMurdo Sound Deployments (D, E, F, I-L) (Fig. 2a). The McMurdo Sound

447   mooring sites each saw several deployments of several days in length, and at various depths

448   (ranging from 15 – 685 m (Leventer and Dunbar, 1987). Although fluxes from the McMurdo Sound

449   traps have been plotted for the sake of completion, the short deployment times and inconsistent

450   conditions make comparisons with other sediment trap deployments difficult. Common taxa

451   sampled in McMurdo Sound were *Amphiprora* spp., *Pleurosigma* spp. and *Nitzschia stellate* (Table

452   2; Leventer and Dunbar., 1987). RS-A and RS-B sampled for over a continuous year each, and

453   *Fragilariopsis curta* was the dominant diatom at both moorings (Leventer and Dunbar 1996).

454   3.3 Diatom flux model

455   Four key nutrients were used as predictors in linear models (nitrate, phosphate, iron and silicate),

456   as well as Chl-*a* (indicator of total algal biomass accumulation), SST, sea ice cover (%) and

457   Particulate Inorganic Carbon (PIC). A correlation matrix was created to summarise the relationships

458   between each of the eight variables and $\log_{10}$ diatom flux. Most of the environmental variables

459   appeared to co-vary and were strongly and significantly correlated (Table 3). Notable exceptions

460   include iron, which showed weakly negative correlations with all variables except SST (and

461   significant only for sea ice), and a weakly positive (significant) correlation with SST (p= 0.02; Table

462   3).

463   **Table 3.** Pearson's product-moment correlation matrix of environmental predictors of $\log_{10}$ maximum

464   diatom flux (valves m^{-2} d^{-1}). Values in bold are significant (p value given in brackets).

	$\log_{10}$ max diatom flux	Phosphate	Nitrate	$\log_{10}$ Silicate	SST	Chl-*a*	Iron	Sea ice cover	PIC
$\log_{10}$ max diatom flux	-								
Phosphate	**0.76 (<0.001)**	-							
Nitrate	**0.78 (<0.001)**	**0.97 (<0.001)**	-						
$\log_{10}$ Silicate	**0.63 (<0.001)**	**0.92 (<0.001)**	**0.85 (<0.001)**	-					
SST	**-0.67 (<0.001)**	**-0.96 (<0.001)**	**-0.92 (<0.001)**	**-0.96 (<0.001)**	-				
Chl-*a*	-0.10	0.14	-0.02	**0.34 (0.02)**	**-0.30 (0.04)**	-			
Iron	-0.09	-0.25	-0.27	-0.27	**0.35 (0.02)**	-0.19	-		
Sea ice cover	0.19	**0.49 (<0.001)**	**0.36 (0.01)**	0.74	-0.64	0.61	**-0.29 (0.04)**	-	
PIC	0.20	0.18	0.15	**0.32 (0.03)**	**-0.30 (0.04)**	**0.47 (<0.001)**	-0.18	0.57	-

465

466   SST demonstrated significant correlation with all variables except sea ice. The strongest

467   relationships were observed between phosphate and nitrate (positive, r = 0.97), and $\log_{10}$Silicate

468   and SST (negative, r = -0.96; Table 3). There was a positive relationship between diatom flux and

469   the nutrients phosphate and nitrate (r > 0.76), diatom flux and silicate (r = 0.63), and negatively

470   with SST (R = -0.67) (Table 3). PIC was weakly positively correlated with $\log_{10}$ silicate and

471   chlorophyll-*a*, and weakly negatively correlated with SST (Table 3).

472   A stepwise regression test was performed to determine which of the eight variables were the best

473   potential predictors of $\log_{10}$ max diatom flux (Figs. 6a-d; only models for which r^2> 0.4 included).

474   Backwards (subtractive) and forwards (additive) stepwise regressions were undertaken to

475   determine which of the variables best predicted variation in $\log_{10}$ diatom flux. The backwards

476   stepwise model identified phosphate, iron and sea ice in combination as the most significant

477   predictors of $\log_{10}$ diatom flux (AIC= -28.35), predicting 63 % of $\log_{10}$ max diatom flux in this dataset

478   (p< 0.001). The forwards stepwise model identified the most important predictors as nitrate and

479   iron (AIC= -28.28), explaining 62 % of variation in $\log_{10}$ max diatom flux (p< 0.001). Given that

480   phosphate and nitrate are extremely well correlated (0.97; Table 3), and nitrate alone explains

481   most of the variation in $\log_{10}$ diatom flux (adjusted r^2= 0.60, p< 0.001), nitrate concentration was

482   identified as the single most important variable controlling $\log_{10}$ max diatom flux in this dataset,

483   followed by phosphate, SST, and $\log_{10}$ silicate (r^2= 0.57, 0.44 and 0.38, respectively; Fig. 6a-d).

484   Nitrate concentration tends to increase between the PF and the Antarctic coast (Fig. 7), consistent

485   with the observed trend of increasing diatom fluxes south of the PF.

486
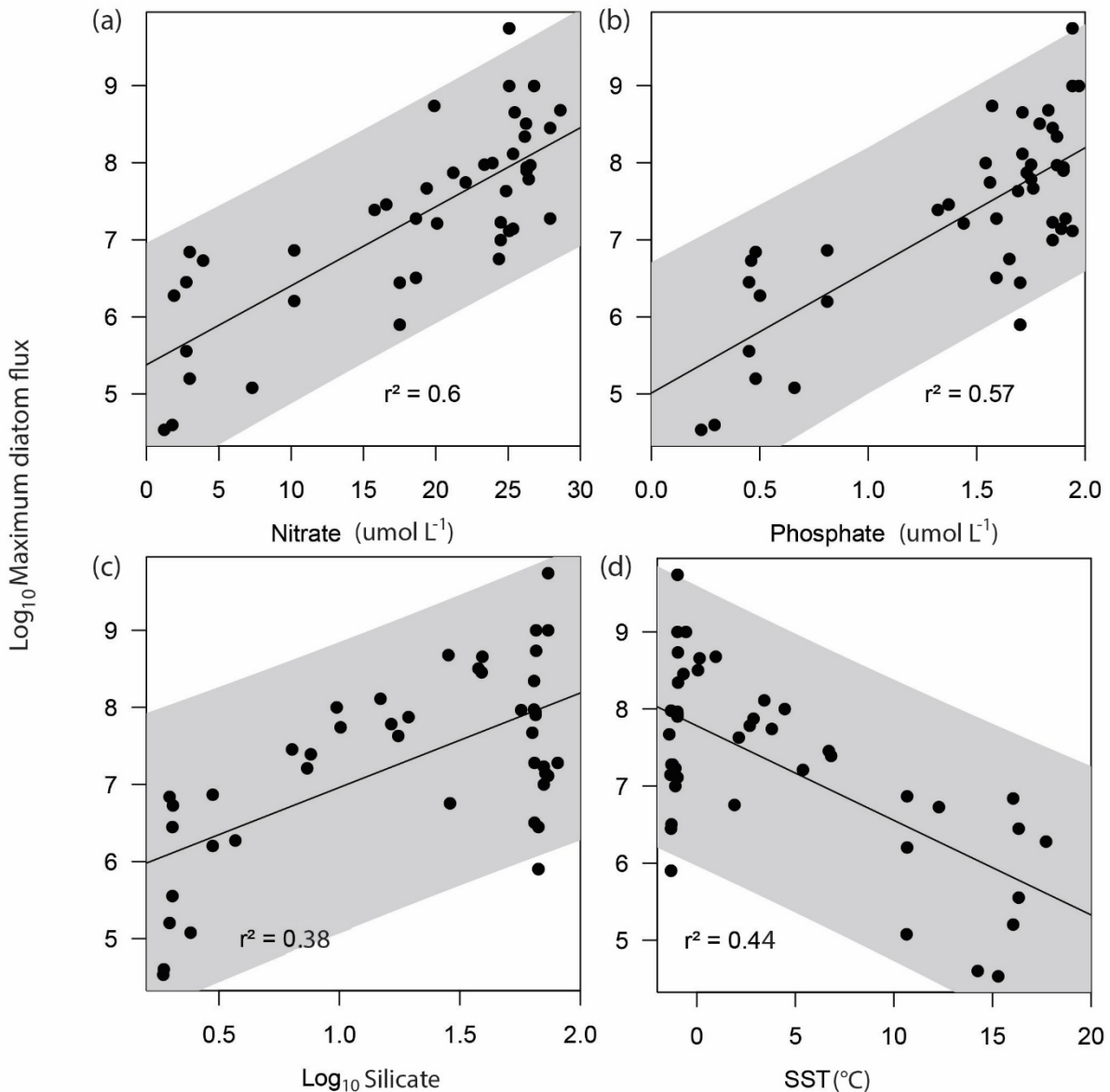
Figure 6. Linear models visualising individual parameters: (a) Nitrate; (b) Phosphate; (c) $\log_{10}$ Silicate; (d) SST, as predictors of $\log_{10}$ maximum diatom flux. Adjusted r^2 value given on plot. Grey bars represent 95% prediction confidence intervals.
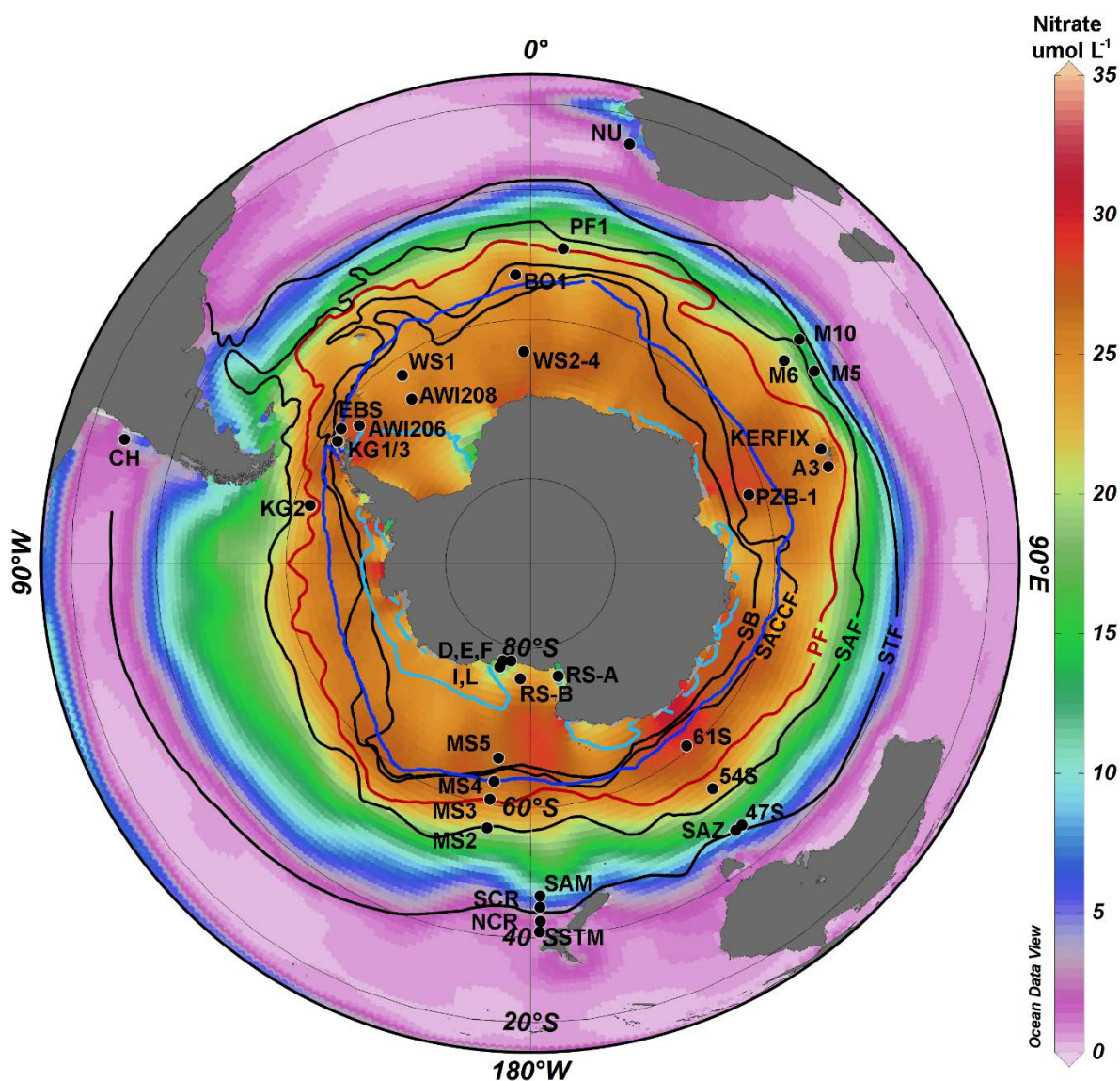
Figure 7. Map of Subtropical to Antarctic Southern Hemisphere with annual average nitrate concentration (μmol.L^{-1}) indicated by colour (https://www.nodc.noaa.gov/OC5/WOA09/pr_woa09.html). Oceanic abbreviations and trap identifiers are the same as Fig. 1. Dark blue and light blue lines indicate maximum winter, and minimum summer sea ice extent, respectively.

3.4 Southern Hemisphere coccolith flux

Of the studies that calculated coccolith flux, two were just within the scope of this study, between ~29 and 30° S off southwest South America (González et al., 2004), and southwest Africa (Romero et al., 2002). The other four studies detailing coccolith fluxes were at the KERFIX (Kerguelen Island) station (Ternois et al., 1998) at ~50° S, the subtropical and subantarctic New Zealand sites (NCR and SCR; Wilks et al., in review), and south of Australia at the SAZ (Wilks et al., 2017) and AZ deployments (Rigual-Hernández et al., 2018a). Thus, despite the known extent of carbonate

502   production in the Southern Ocean (Balch et al., 2016), knowledge on the seasonality of coccolith

503   fluxes is relatively limited.

504   Seven data points for sediment trap-derived coccolith fluxes were available to map $\log_{10}$ maximum

505   coccolith fluxes, and five data points for annual coccolith flux (Fig. 8). Highest annual coccolith flux

506   was observed in the central Benguela system (NU) at 1.6×10^{12} coccoliths m^{-2} yr^{-1}, with daily maxima

507   of $\sim 2.3 \times 10^{8}$ coccoliths m^{-2} d^{-1} (Romero et al., 2002). Similarly high coccolith fluxes were observed

508   at the SAZ site at 6.5×10^{11} m^{-2} yr^{-1} (Table 1; Wilks et al., 2017). Surprisingly, site CH, occupying a

509   similar latitude to the productive NU site, showed only moderate coccoliths fluxes comparable to

510   KERFIX (Fig. 8). The lowest coccolith fluxes in the study region occur at the NCR site east of New

511   Zealand at 1.0×10^{7} coccoliths m^{-2} yr^{-1} (Wilks et al., in review) (Fig. 8b). All studies reported

512   *Emiliania huxleyi* as the dominant coccolithophore in trap records, with minor contributions from

513   taxa such as *Coccolithus pelagicus, Gephyrocapsa* spp. and *Calcidiscus leptoporus*.
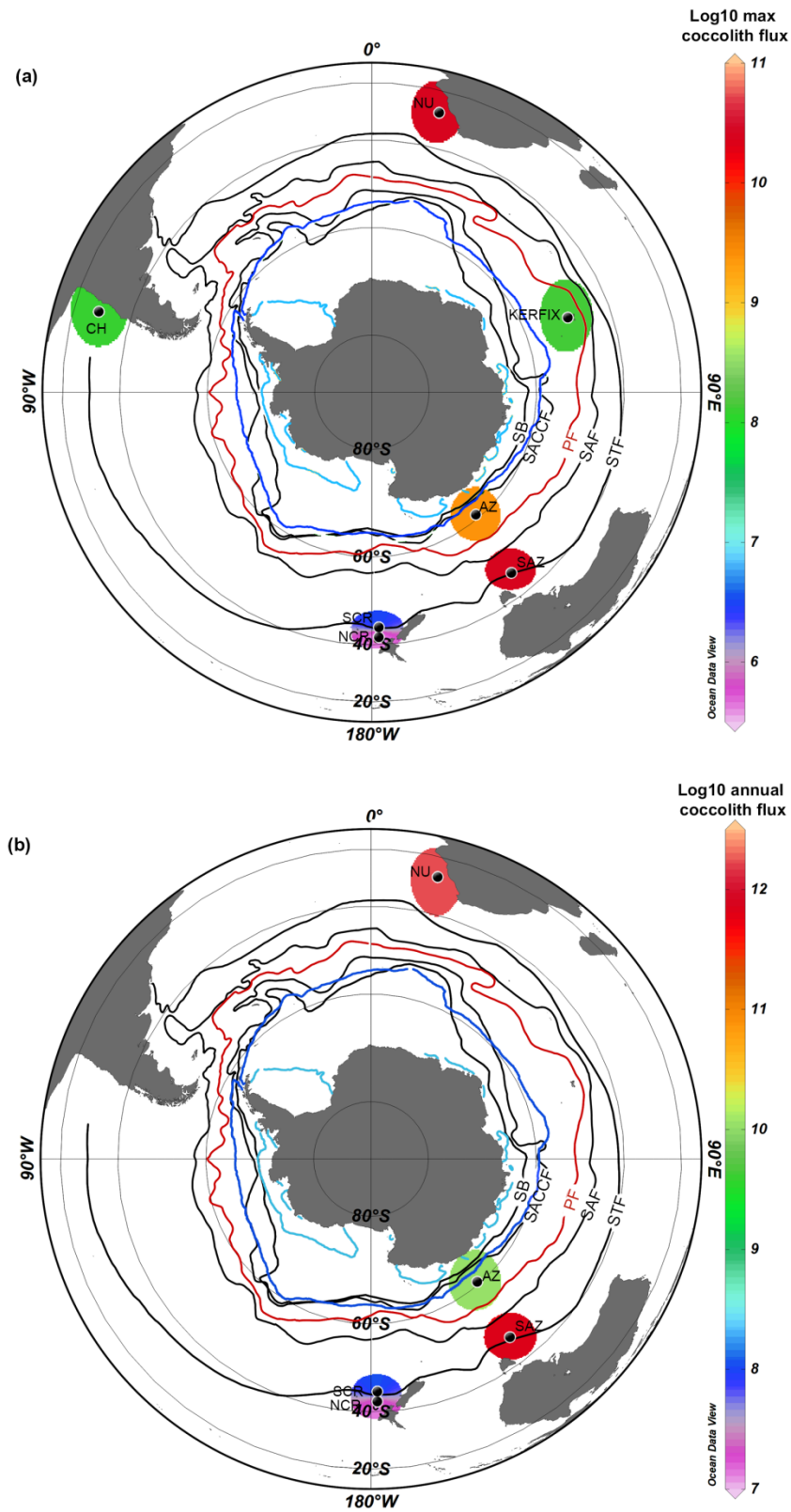
Figure 8. (a) Log$_{10}$ maximum and (b) annual coccolith flux for sediment trap studies in the subtropical to polar Southern Hemisphere. Magnitude of fluxes indicated by colour bars. Oceanic abbreviations and trap identifiers are the same as Fig. 1. Dark blue and light blue lines indicate maximum winter and minimum summer winter sea ice extent, respectively.

519 **4. Discussion**

520 *4.1 Spatial trends in diatom flux*

521 To address aim one, log_{10} maximum and log_{10} annual diatom fluxes derived from sediment trap

522 deployments in the Southern Hemisphere were mapped with the major oceanic fronts, revealing

523 some broad regional trends. Diatom flux is highest, with a few exceptions, south of the Polar Front

524 (PF; Fig. 2a). A review of 27 sediment traps by Antia et al. (2001) reported increasing carbon export

525 flux towards the poles, while Honjo (2004) found the PF to be the boundary between calcium-

526 carbonate-driven export to the north, and biogenic silica-driven export to the south.

527 One of the recurring discoveries of multi-year sediment trapping has been variability in both the

528 timing and magnitude of fluxes between years (e.g. Gersonde and Zielinski, 2000; Romero et al.,

529 2001; Rigual-Hernández et al., 2015a; Nodder et al., 2016). This needs to be kept in mind as a

530 potential cause of variability in the broader diatom flux trends. At high latitudes, annual primary

531 production is highly seasonal due to light limitation (Harrison et al., 2018). Further, in some regions

532 the start date of spring diatom bloom can vary by a month (Broekhuizen et al., 1998). Short term,

533 and even whole-year sediment trap records, may be less readily extrapolated to typical seasonality

534 and flux than multi-year trap studies. However, short-term trapping studies may still be of great

535 value. Studies such as those of Ichinomiya et al. (2008) under sea ice at Syowa Station (38 days),

536 or the Drake Passage traps DP80/81 (52 days; Gersonde and Zielinski, 2000) are undertaken during

537 productive seasons, and may provide excellent data about the magnitude of spring export flux, as

538 well as contributing species composition (Ichinomiya et al., 2008).

539 The preservation potential of different diatom taxa may account for differences in fluxes between

540 sediment trap deployments, and may also be influenced by sea ice and proximity to land. In the

541 Antarctic Peninsula, high abundances of resting spore-forming taxa are suggested as a "seeding"

542 strategy in neritic and sea-ice regions (Bodungen et al., 1986). Sediment trap deployments in the

543 Antarctic Peninsula (e.g. EBS, KG1-3, AWI206) and seasonally ice-covered Weddell Sea (AWI208,

544 WS1) traps do tend to report a high presence of spore forming taxa, which are resistant to

545 dissolution and appear as a strong signal in sediment traps. Despite this, total fluxes at AWI206

546 and 208 were relatively low, possibly because both sites were ice-free for only 2-3 months of the

547 year (Gersonde and Zielinski, 2000). Traps WS1 and KG1 in the Antarctic Peninsula region collected

548 data in the same year (1985-86) and for roughly the same duration, but diatom fluxes were an

549 order of magnitude higher at KG1 (Table 1). Higher fluxes in the region of the Antarctic Peninsula

550 could be the result of higher sediment input due to resuspension or lateral transport because of

551 the proximity of the KG1 mooring site to the coast (Abelmann and Gersonde, 1991). Abelmann and

552 Gersonde (1991) reported high fluxes of dissolution-resistant *Chaetoceros* resting spores in KG1

553 (up to 80% of fluxes) and *Thalassiosira antarctica* (including its spores) at KG3 (80 %). WS1

554 contained more lightly-silicified taxa, but still a large contribution from resting spores (up to 60 %;

555 Abelmann and Gersonde, 1991).The open-ocean site WS2, on the other hand, also captured higher

556 flux than WS1 (Fig. 2a), but these authors attributed this to the year-round resuspension of

557 material from the adjacent Maud Rise.

558 The proximity of land masses may also influence the assemblages captured by sediment traps. For

559 example, high iron conditions may be found close to continental shelves where upwelling occurs

560 (Graham et al., 2015), allowing the growth of large, heavily silicified taxa such as *Eucampia*, or

561 *Fragilariopsis kerguelensis*, (Salter et al., 2012; Rembauville et al., 2016). These heavily silicified

562 taxa often preserve better, and could result in higher flux capture by sediment traps. *Chaetoceros*

563 taxa also tend to be associated with coastal systems (Tomas, 1997), and spores of *Chaetoceros*

564 form a significant proportion of high-nutrient coastal and upwelling assemblages. *Chaetoceros*

565 spores were also present in seafloor sediments near the Humbolt Current upwelling system (CH)

566 traps (Romero et al., 2001). The Island Mass Effect is also evident north of the Weddell Sea, (P2

567 and P3, Rembauville et al., 2016). P3, downstream of South Georgia, where influence from the

568 island causes high nutrient concentrations, captured diatom fluxes an order of magnitude higher

569 than the upstream trap, P2 (Fig. 2). Further, assemblages at P3 were rich in *Chaetoceros* spores

570 (43 % integrated annual flux), consistent with the influence of island-derived water masses, while

571 P2 traps captured mainly *Fragilariopsis kerguelensis* (~40 %; Rembauville et al., 2016).

572 In the Indian sector, diatom resting spores comprised significant portions of fluxes at both Crozet

573 and Kerguelen, both naturally iron-fertilized regions. At Crozet, resting spores of *Eucampia*

574 *antarctica* var. *antarctica* were strongly correlated with POC export (Salter et al., 2012), while at

575 A3, 60% of POC flux was attributable to *Chaetoceros* Hyalochaete spores and *Thalassiosira*

576 *antarctica* resting spores (Rembauville et al., 2015a). In contrast, *Chaetoceros* resting spores were

577 a relatively minor contribution to flux at KERFIX, attributable to deeper waters at KERFIX than A3

578 preventing spore recirculation after sinking, and higher silicic acid availability inhibiting spore

579 formation (Rembauville et al., 2018). At the seasonally ice-covered Prydz Bay site (PZB-1),

580 assemblages were dominated by *Fragilariopsis kerguelensis*, which was identified as key to

581 biogenic silica export in this trap record, and a typically well-preserved taxon (Rigual-Hernández et

582 al., 2018b).

583 The ubiquitous and dissolution-resistant *Fragilariopsis kerguelensis* also dominated in the New

584 Zealand sector traps between MS-2 and MS-4. At M-5, which is covered by sea ice for over 50% of

585 the year (Supp. Table 2), the dominance of *F. kerguelensis* was replaced by higher abundances of

586   other *Fragilariopsis* taxa, *F. curta* and *F. cylindrus* (Grigorov et al., 2014). In the Australian sector,

587   decreasing diatom diversity between the SAZ and AZ was accompanied by flux assemblages

588   increasingly dominated by the robust *F. kerguelensis* (up to 96 % of assemblages at the AZ site, and

589   80 % of the annual integrated flux; Rigual-Hernández et al., 2015b; Rigual-Hernández et al., 2016).

590   The site of maximum *F. kerguelensis* flux in the Australian sector (AZ), and in the New Zealand

591   sector (MS-3), sit at nearly the same latitude (Fig. 5). *F. kerguelensis* is generally considered a

592   silicon-sinking, rather than a carbon-sinking diatom (Assmy et al., 2013). So, a bloom of *F.*

593   *kerguelensis* may not export as much carbon as a typical carbon-sinking group (such as

594   *Chaetoceros*). It is thus of merit to understand the way diatom assemblage fluxes change

595   throughout the ocean, as this has a bearing on the composition of exported material. This type of

596   comparison of latitudinal gradients in diatom assemblages is made possible as a result of the

597   systematic Australian/New Zealand sector trapping efforts.

598   *4.2 Can environmental parameters explain diatom flux patterns?*

599   Collectively, phosphate (or nitrate), iron and % annual sea ice cover were the best predictors of

600   diatom flux in this dataset. Nitrate, phosphate, silicate and iron are the major nutrients required

601   by diatoms, although co-limitation by silicate and iron often limits diatom growth in the Southern

602   Ocean (De Baar et al., 1995; Boyd et al., 1999). The Southern Ocean is commonly described as

603   HNLC (High-Nitrate, Low-Chlorophyll), and in HNLC systems nitrate and phosphate may not be fully

604   utilized by phytoplankton due to iron limitation, resulting in large phytoplankton blooms when iron

605   is seasonally, or artificially, enriched (Martin, 1990; Martin et al., 1994). Since the preservation and

606   flux of diatom frustules is often enhanced in bloom conditions due to higher sinking rates

607   (Smetacek, 1985), iron and phosphate are logical predictors of diatom flux.

608   The seasonal presence and absence of sea ice is known to affect diatom sedimentation at very high

609   latitudes (Abelmann and Gersonde, 1991; Armand et al., 2005). In fact, some of the highest

610   maximum daily rates of primary productivity of the Southern Ocean occurs at the retreating ice

611   edge in spring/summer (Arrigo et al., 2008), because of high nutrient upwelling and more stable,

612   stratified waters at the edges of melting ice (Smith and Nelson, 1986).

613   Several recent studies have attempted to determine the factors controlling the efficiency of

614   particulate organic carbon export flux in the global ocean (Henson et al., 2012; Weber et al., 2016;

615   Cram et al., 2017). Although these factors remain contentious, there is agreement that flux is

616   controlled not only by the amount of production, but also the degree to which particles are

617   changed while in the water column, such as by microbial degradation (which can be affected by

618   SST; Cram et al., 2017)), as well as by zooplankton grazing. Microbial remineralization affects

619   organic fluxes, but does not affect the flux of the siliceous remains of diatoms, so was not

620   considered in this review. Rather, diatom frustules are at greatest risk of dissolution before

621   reaching export depths; an estimated 50% of biogenic silica dissolves in the upper 100m of the

622   ocean, but may be slower at lower water temperatures (Nelson et al., 1995). SST was significantly

623   negatively correlated with $\log_{10}$ diatom flux (-0.67; Table 3), and slower rates of silica dissolution is

624   incited as a possible reason, though as SST co-varies with iron concentration (one of the three main

625   predictors of diatom flux), this remains speculative.

626   The correlations between diatom flux, chlorophyll-*a*, and PIC are best interpreted with care. The

627   lack of any significant relationship between diatom flux and Chl-*a* does not, intuitively, sit well with

628   the high correlation between diatom flux and key nutrients (except iron) unless a large proportion

629   of the production observed via Chl-*a* is not attributable to diatoms. This conclusion is possible;

630   other autotrophs such as *Phaeocystis* spp., dinoflagellates and picoeukaryotes may be regionally

631   significant Chl-*a* producers (Boyd et al., 2000; Alvain et al., 2008). *Phaeocystis* spp., for example,

632   are highly abundant in Southern Ocean waters (Arrigo et al., 1999). Another alternative is the

633   decoupling of fluxes from surface production, which is not uncommonly observed from sediment

634   trap deployments, and may occur if sinking particles are very rapidly remineralized or dissolved

635   before reaching traps (Buesseler, 1998). This phenomenon has been observed in the New Zealand

636   sector (Nodder et al., 2005). Decoupling may also be the result of stochastic "pulse" bloom events

637   (for example of *Rhizosolenid* diatoms), whereby particles are drawn down together with sinking

638   fluxes, and surface production thus does not reflect flux capture (Sancetta et al. 1991).

639   Zooplankton grazing may be another cause of decoupling of production from export, with

640   zooplankton grazing reported to exceed new production under some conditions (James and Hall,

641   1998). The extent to which surface-export decoupling occurs is unknown, and this question alone

642   certainly warrants further sediment trap investigations.

643   The correlation between Chl-*a* and PIC might suggest calcifying organisms as key producers, except

644   that in coastal regions or shallow waters, particulate resuspension is known to affect the accuracy

645   of PIC concentration estimates via remotely sensed ocean colour (Daniels et al., 2012). Given that

646   most of the trap deployments are in such regions, the Chl-*a* and PIC correlation may be an artefact.

647   Further, remotely-sensed Chlorophyll-*a* data does not account for sub-surface chlorophyll

648   production, which is not remotely detectable and may account for a significant proportion of

649   annual flux (Kemp et al., 2000; Nodder et al., 2016). The significance of sub-surface production is

650   not well known, but may vary between years (Nodder et al., 2016), possibly limiting attempts to

651   draw relationships between flux and remotely-sensed Chlorophyll-*a.*

652 The model applied in this study must be viewed with a degree of caution, because a simple linear

653 model cannot account for factors such as community composition, grazing, or the influence of

654 microbial dynamics (Laurenceau et al., 2015). Additionally, since environmental data were not

655 obtained at the time of trapping in most instances, they should be regarded only as indicative of

656 general patterns of nutrient distribution, rather than recording local conditions at the time of

657 sampling. Unfortunately, with so few trap deployments that calculated coccolith flux, it was not

658 possible to derive a relationship between coccolith flux and any environmental parameter.

659 *4.3 Methodological considerations*

660 In the Ross Sea, the generalised pattern of increasing diatom flux towards the poles is confounded

661 by McMurdo Sound traps D, E, F, I, L (Leventer and Dunbar, 1987) and RS-B (Leventer and Dunbar,

662 1996). Relative low fluxes in McMurdo Sound contrast with a global database of diatom

663 abundance, which reported highest abundances of diatoms in the water column (cells L^{-1}) in the

664 Ross Sea region (Leblanc et al., 2012), though as previously discussed, this does not necessarily

665 mean higher flux. The McMurdo Sound traps utilised a conical single-cup sediment trap design,

666 suspended beneath sea ice for up to 61 days, with either 1950 or 400 cm^2 capture area (Leventer

667 and Dunbar, 1987). The RS-B and RS-A traps were longer and deeper-deployed, time-incremental

668 traps anchored to the seafloor with 500 cm^2 capture area (Dunbar et al., 1998).

669 As a result of the different methodologies employed, perhaps the ~2 month duration McMurdo

670 Sound trap record should not be compared with the annual RS-A and RA-B traps. Though

671 speculative, the lower fluxes at McMurdo Sound could be the result of disturbance to under-ice

672 plankton communities caused by the deployment method itself (ice-drilling). Other authors have

673 reported that algae are very easily detached from the underside of the ice during trap deployment

674 (McMinn, 1996), even coming loose by the currents caused by scuba divers (Sasaki and Watanabe,

675 1984), thus it is possible that the act of drilling and deploying early under-ice traps may have

676 disturbed natural flux patterns.

677 Material processing after trap retrieval may also affect flux results, and the ways material was

678 processed by studies included in this review should be considered. Prebble et al. (2013) hand-

679 picked swimmers, then sieved at 200 and 6 µm, and the 6-200 µm fraction was used in

680 phytoplankton analysis. In this instance, it is possible that very small taxa (e.g. *Delphineis*

681 *minutissima*) and very large diatoms (such as long *Thalassiothrix antarctica* or *Pseudo-nitzschia*

682 spp. chains), all of which have been observed at or near STM and SAM sites in New Zealand (Wilks

683 et al., in review), may have been omitted from those counts. Leventer (1991) used short-term

684   Racer trap material filtered through a 20 μm screen, and counted the >20 μm fraction only, again
685   leading to the possibility of underrepresentation of small size fractions.

686   Sediment trap practice has evolved considerably since the earliest deployments, and although
687   methodologies have greatly improved with time, some methodological disparities between studies
688   are unavoidable. The strengths and weaknesses of sediment trap deployment methods and
689   designs have been reviewed elsewhere (Buesseler et al., 2007; McDonnell et al., 2015). The
690   differences in trap deployment and processing methodology in the present compilation are
691   acknowledged, but efforts to map diatom and coccolith fluxes from sediment trap records are
692   clearly of great value. For the most part, nearby trap deployments, despite utilising different
693   methodologies and deployment times, tended to calculate fluxes of a similar magnitude, and this
694   broadly demonstrates data comparability. For example, traps WS1 (1985-86) (Fischer et al., 1988)
695   and AWI208 (1989-90) (Gersonde and Zielinski, 2000) reported similar maximum diatom fluxes, as
696   did the Bransfield Strait/Antarctic Peninsula traps EBS (1998-1999; Kang et al., 2003), AWI206
697   (1989-90; Gersonde and Zielinski, 2000) and KG1/3 (1983-84, and 1985-86; Abelmann and
698   Gersonde, 1991) (Fig. 2a).

699   Methodologically, the NIWA, AESOPS and SAZ Project trap results are readily comparable, having
700   employed similar deployment types and processing methods. Each deployment used McLane^{TM}
701   Parflux conical sediment traps, though different trap preservatives were employed; $HgCl_2$ for the
702   SAZ Project traps, buffered formalin for the AESOPS traps, and either buffered formalin or $HgCl_2$ in
703   the NZ traps. The NIWA, AESOPS, and SAZ Project deployments also used a minimum 1.0 mm
704   screen to remove swimmers prior to flux calculation. The consistency between the Australian and
705   New Zealand sector deployments, and their ease of comparability, should be considered the aim
706   of all future deployments.

707   *4.4 Spatial trends in coccolith fluxes*

708   Coccolith flux was also mapped relative to oceanographic fronts, but only seven data points were
709   available for log_{10} maximum coccolith flux, while five were available for log_{10} annual coccolith flux
710   (Table 1; Fig. 8). Highest coccolith flux at the Namibia Upwelling (NU) and Tasmanian (SAZ) sites is
711   supported by reports of calcium carbonate-dominated export flux (maximum 74 % and 82 % of
712   total flux, respectively) (Romero et al,. 2002; Wilks et al., 2017). Relatively high annual and
713   maximum coccolith fluxes were recorded at the AZ trap (Rigual-Hernández et al., 2018a), in which
714   calcium carbonate comprised up to 30 % of total flux into the traps.

715   Calcium carbonate was also the major component of trap material at the Chilean site (CH), but
716   coccolith fluxes were relatively low (González et al., 2004). This disparity cannot easily be

717   attributed to methodological differences, since all three mooring sites used conical traps (either

718   Parflux or Kiel, 0.5m^2 aperture) and HgCl$_2$ poisoning methods. It is difficult to explain this distinct

719   difference without more comparative deployment data. Coccolith fluxes at the KERFIX site were

720   determined from a near-annual record obtained between April 1993 and January 1994 (290 days)

721   (Ternois et al., 1998). This record may not have captured a peak in export in late summer, as minor

722   coccolith flux peaks in February and March have been observed elsewhere in the Southern Ocean

723   (Romero et al. 2002; González et al. 2004), though with only one record this also remains

724   speculation.

725   All sites recorded *Emiliania huxleyi* as the most abundant coccolithophore captured in sediment

726   traps. Highest abundances of *E. huxleyi* were found within the southernmost AZ traps, where the

727   annual integrated abundance of the taxon was >99 % of coccolith flux captured at both depths,

728   and with minor occurrences of *C. leptoporus* (Rigual-Hernández et al., 2018a). Comparatively, the

729   annual integrated abundance of *E. huxleyi* at the SAZ trap in the same sector was only 59.3 % of

730   coccolith flux (500 m trap depth), followed by *Gephyrocapsa* spp. < 3 μm (37.9 %) with other taxa

731   below 2% abundance each (Wilks et al., 2017). Coccolithophore assemblage are known to become

732   increasingly *E. huxleyi-* dominated at high latitude in the Southern Ocean, and are more or less

733   monospecific south of ~60 °S (Gravalosa et al., 2008; Malinverno et al., 2015). Seafloor sediment

734   composition has been examined more widely than either coccolith or diatom flux (see Dutkiewicz

735   et al., 2016), making further studies of coccolith fluxes warranted in the Southern Hemisphere.

736   *4.5 Priority regions in sediment trapping*

737   Despite the scattered distribution of sediment traps in the Southern Hemisphere, the Southern

738   Ocean zones exhibit relatively homogenous chemical and physical water column properties

739   (Lutjeharms et al., 1993), meaning that a deployment may be representative of a relatively broad

740   area. For example, the SAZ moorings were determined to be representative of the region from 90°

741   to 145° E based on satellite data and oceanographic observations of the region (Trull et al., 2001b).

742   The exception is near island masses, where upwelling and runoff induce increased nutrient

743   concentrations and productivity (Blain et al., 2001). So, while sediment trap deployments in the

744   pelagic Southern Ocean may be representative of a relatively large region, coastal and shelf regions

745   may need to be more densely sampled in order to capture potential regional variability. Sediment

746   trapping in the central Indian and central Pacific sectors of the Southern Ocean is lacking (Fig. 1),

747   and should be considered priority regions for future sediment trap deployments.

748   Co-ordinated time series investigations with well-defined coverage, sufficient length of

749   deployment (minimum 200 days for an annual extrapolation to be estimated, and preferably one

750   year or longer), and standardised method of analysis will be key. The Argentinian shelf region

751   would greatly benefit from sediment trap work, given the high productivity of the region. The Ross

752   Sea region, while densely trapped, saw most interest in the 1980s and 1990s, and would benefit

753   from trapping using modern deployment methodologies (e.g. Parflux traps) and for longer

754   duration. Existing trap records, archival or modern, would be well used to calculate phytoplankton

755   fluxes, where preservation allows. A broad knowledge of phytoplankton flux magnitude, and

756   species composition, is ideal in order to predict how large scale carbon export may change, and

757   which taxa are likely to drive export in the future.

5. Conclusions

758

759 Comparing sediment trap data needs to be treated with some caution due to methodological and

760 oceanographic/biological variability, but these pelagic records provide highly valuable data for

761 developing understanding of the contribution of different phytoplankton taxa to global carbon

762 export. In this systematic review, major sediment trapping efforts is mapped and modelled in

763 subtropical to the polar oceans of the Southern Hemisphere over the last 40 years. The region is

764 mostly well-trapped (e.g. the Ross and Weddell Seas, Antarctic Peninsula, and Australian/New

765 Zealand sector), though there remain extensive un-trapped zones for which we may only estimate

766 diatom fluxes (e.g. the Pacific sector).

767 Diatom fluxes were available for 49 trap deployments. Log_{10} maximum diatom flux tended to

768 increase south of the Polar Front and to the Antarctic continent. This pattern was not observed in

769 all regions, such as the central Weddell Sea and McMurdo Sound, Ross Sea. In the Weddell Sea,

770 the factors controlling spatial differences in diatom fluxes are complex and are not resolved, but

771 may relate to local oceanography (e.g. upwelling from Maud Rise at WS2), or the preservability of

772 assemblages at the different sites. In McMurdo Sound, diatom flux was more difficult to interpret

773 due to seasonal nutrient variability associated with continental run-off and differences in

774 methodologies employed to capture pelagic data.

775 Coccolith fluxes were available for only seven deployments, and too few data points were available

776 to make any generalizations about flux patterns. Given the well-known importance of carbonates

777 in Southern Ocean sedimentary processes, the dearth of coccolith flux studies is both surprising

778 and unfortunate. Future efforts to characterise coccolith fluxes from a range of deployments will

779 be vital in attempts to weigh the relative influence of the biological and carbonate counter pumps

780 in this region.

781 Diatom fluxes were also compared to time-averaged data including nutrient concentration (nitrate,

782 phosphate, silicate and iron), productivity (chlorophyll-*a*),variables that affect production and

783 export (sea ice, SST) and ballast concentration (PIC) to determine which, if any, of these factors

784 best predicted flux. The linear model suggests that the majority of diatom flux could be correlated

785 with nitrate/phosphate concentration, iron and sea ice. These data should be considered with care

786 given that the diatom flux, and environmental parameter datasets were extracted for different

787 time intervals by necessity.

788 Phytoplankton community structure has great bearing on export efficiency and magnitude of

789 carbon fluxes throughout the ocean (Lam et al., 2011). Climate change-related increases in sea

790 surface temperature are expected to influence plankton size classes, and hence the transfer

791   efficiency of particles in the future (Cram et al., 2017). This review has demonstrated the value of

792   phytoplankton flux calculations from sediment trap deployments, and particularly those for which

793   species flux data is available. The need for systematic, multi-year sediment trap deployments

794   employing consistent, best-practice methodologies in under-sampled regions of the global ocean,

795   followed by both bulk compound and phytoplankton flux analyses will lead to a better

796   understanding of global ocean productivity and oceanographic processes.

801   **References**

802   Abelmann, A., and Gersonde, R.: Biosiliceous particle flux in the Southern Ocean, Mar. Chem., 35,

803   503-536, 1991.

804   Alvain, S., Moulin, C., Dandonneau, Y., and Loisel, H.: Seasonal distribution and succession of

805   dominant phytoplankton groups in the global ocean: A satellite view, Global Biogeochemical

806   Cycles, 22, GB3001, 10.1029/2007GB003154, 2008.

807   Antia, A. N., Wolfgang, K., Gerhard, F., Thomas, B., Detlef, S.-B., Jan, S., Susanne, N., Klaus, K.,

808   Joachim, K., Rolf, P., Dirk, H., Ulrich, B., Maureen, C., Uwe, F., and B., Z.: Basin-wide particulate

809   carbon flux in the Atlantic Ocean: Regional export patterns and potential for atmospheric CO2

810   sequestration, Global Biogeochem. Cycles, 15, 845-862, doi:10.1029/2000GB001376, 2001.

811   Armand, L. K., Crosta, X., Romero, O., and Pichon, J.-J.: The biogeography of major diatom taxa in

812   Southern Ocean sediments: 1. Sea ice related species, Palaeogeography, Palaeoclimatology,

813   Palaeoecology, 223, 93-126, 2005.

814   Arndt, J. E., Schenke, H. W., Jakobsson, M., Nitsche, F. O., Buys, G., Goleby, B., Rebesco, M.,

815   Bohoyo, F., Hong, J., and Black, J.: The International Bathymetric Chart of the Southern Ocean

816   (IBCSO) Version 1.0—A new bathymetric compilation covering circum‐Antarctic waters,

817   Geophys. Res. Lett., 40, 3111-3117, 2013.

818   Arrigo, K. R., Robinson, D. H., Worthen, D. L., Dunbar, R. B., DiTullio, G. R., VanWoert, M., and

819   Lizotte, M. P.: Phytoplankton Community Structure and the Drawdown of Nutrients and CO_2 in

820   the Southern Ocean, Science, 283, 365-367, 10.1126/science.283.5400.365, 1999.

821   Arrigo, K. R., van Dijken, G. L., and Bushinsky, S.: Primary production in the Southern Ocean,

822   1997–2006, Journal of Geophysical Research: Oceans, 113, 2008.

823   Assmy, P., Smetacek, V., Montresor, M., Klaas, C., Henjes, J., Strass, V. H., Arrieta, J. M., Bathmann,

824   U., Berg, G. M., and Breitbarth, E.: Thick-shelled, grazer-protected diatoms decouple ocean carbon

825   and silicon cycles in the iron-limited Antarctic Circumpolar Current, P. Natl. Acad. Sci., 110, 20633-

826   20638, 2013.

827   Balch, W. M., Drapeau, D. T., Bowler, B. C., Lyczskowski, E., Booth, E. S., and Alley, D.: The

828   contribution of coccolithophores to the optical and inorganic carbon budgets during the Southern

829   Ocean Gas Exchange Experiment: New evidence in support of the "Great Calcite Belt" hypothesis,

830   J. Geophys. Res.: Oceans (1978–2012), 116, 10.1029/2011JC006941, 2011.

831   Balch, W. M., Bates, N. R., Lam, P. J., Twining, B. S., Rosengard, S. Z., Bowler, B. C., Drapeau, D. T.,

832   Garley, R., Lubelczyk, L. C., Mitchell, C., and Rauschenberg, S.: Factors regulating the Great Calcite

833   Belt in the Southern Ocean and its biogeochemical significance, Global Biogeochem. Cycles, 30,

834   1124-1144, 10.1002/2016GB005414, 2016.

835   Balch, W. M.: The Ecology, Biogeochemistry, and Optical Properties of Coccolithophores, Ann. Rev.

836   Mar. Sci., 10, 2018.

837   Bárcena, M., Flores, J., Sierro, F., Pérez-Folgado, M., Fabres, J., Calafat, A., and Canals, M.:

838   Planktonic response to main oceanographic changes in the Alboran Sea (Western Mediterranean)

839   as documented in sediment traps and surface sediments, Mar. Micropaleontol., 53, 423-445, 2004.

840   Blain, S., Tréguer, P., Belviso, S., Bucciarelli, E., Denis, M., Desabre, S., Fiala, M., Jézéquel, V. M., Le

841   Fèvre, J., and Mayzaud, P.: A biogeochemical study of the island mass effect in the context of the

842   iron hypothesis: Kerguelen Islands, Southern Ocean, Deep Sea Res. Part I: Oceanogr. Res. Pap., 48,

843   163-187, 2001.

844   Bodungen, B.: Phytoplankton growth and krill grazing during spring in the Bransfield Strait,

845   Antarctica — Implications from sediment trap collections, Pol. Biol., 6, 153-160,

846   10.1007/bf00274878, 1986.

847   Bostock, H. C., Barrows, T. T., Carter, L., Chase, Z., Cortese, G., Dunbar, G., Ellwood, M., Hayward,

848   B., Howard, W., and Neil, H.: A review of the Australian–New Zealand sector of the Southern Ocean

849   over the last 30 ka (Aus-INTIMATE project), Quat. Sci. Rev., 74, 35-57, 2013.

850   Boyd, P., LaRoche, J., Gall, M., Frew, R., and McKay, R. M. L.: Role of iron, light, and silicate in

851   controlling algal biomass in subantarctic waters SE of New Zealand, J. Geophys. Res.: Oceans, 104,

852   13395-13408, 10.1029/1999JC900009, 1999.

853   Boyd, P. W., Watson, A. J., Law, C. S., Abraham, E. R., Trull, T., Murdoch, R., Bakker, D. C. E., Bowie,

854   A. R., Buesseler, K. O., Chang, H., Charette, M., Croot, P., Downing, K., Frew, R., Gall, M., Hadfield,

855   M., Hall, J., Harvey, M., Jameson, G., LaRoche, J., Liddicoat, M., Ling, R., Maldonado, M. T., McKay,

856   R. M., Nodder, S., Pickmere, S., Pridmore, R., Rintoul, S., Safi, K., Sutton, P., Strzepek, R.,

857   Tanneberger, K., Turner, S., Waite, A., and Zeldis, J.: A mesoscale phytoplankton bloom in the polar

858   Southern Ocean stimulated by iron fertilization, Nature, 407, 695-702, 2000.

859   Boyer, T. P., Antonov, J. I., Baranova, O. K., Garcia, H. E., Johnson, D. R., Locarnini, R. A., Mishonov,

860   A. V., O'Brien, T. D., Seidov, D., Smolyar, I., Zweng, M. M. World Ocean Database 2009. U.S. Gov.

861   Printing Office, Washington, D. C., 2009.

862   Bradford-Grieve, J., Chang, F., Gall, M., Pickmere, S., and Richards, F.: Size-fractionated

863   phytoplankton standing stocks and primary production during austral winter and spring 1993 in

864 the Subtropical Convergence region near New Zealand, N. Z. J. Mar. Freshwater Res., 31, 201-224,

865 1997.

866 Bray, S., Trull, T., Manganini, S., and Antarctic, C.: SAZ project moored sediment traps: results of

867 the 1997-1998 deployments, Antarctic CRC, 2000.

868 Broekhuizen, N., Hadfield, M., and Taylor, A. H.: Seasonal photoadaptation and diatom dynamics

869 in temperate waters, Mar. Ecol. Prog. Ser., 227-239, 1998.

870 Buesseler, K. O.: The decoupling of production and particulate export in the surface ocean, Global

871 Biogeochemical Cycles, 12, 297-310, doi:10.1029/97GB03366, 1998.

872 Buesseler, K. O., Steinberg, D. K., Michaels, A. F., Johnson, R. J., Andrews, J. E., Valdes, J. R., and

873 Price, J. F.: A comparison of the quantity and composition of material caught in a neutrally buoyant

874 versus surface-tethered sediment trap, Deep Sea Res. Part I: Oceanogr. Res. Pap., 47, 277-294,

875 2000.

876 Buesseler, K. O., Antia, A. N., Chen, M., Fowler, S. W., Gardner, W. D., Gustafsson, O., Harada, K.,

877 Michaels, A. F., Rutgers van der Loeff, M., and Sarin, M.: An assessment of the use of sediment

878 traps for estimating upper ocean particle fluxes, J. Mar. Res., 65, 345-416, 2007.

879 Chang, F. H., and Northcote, L.: Species composition of extant coccolithophores including twenty

880 six new records from the southwest Pacific near New Zealand, Mar. Biodivers. Rec., 9, 75,

881 10.1186/s41200-016-0077-7, 2016.

882 Chiarini, F.: Study of the inter-annual variability of particle vertical fluxes in two moorings in the

883 Ross Sea (Antarctica), dissertation, alma, 2013.

884 Cram, J. A., Weber, T., Leung, S. W., McDonnell, A. M., Liang, J. H., and Deutsch, C.: The role of

885 particle size, ballast, temperature, and oxygen in the sinking flux to the deep sea, Global

886 Biogeochem. Cycles, 2017.

887 Daniels, C. J., Tyrrell, T., Poulton, A. J., and Pettit, L.: The influence of lithogenic material on

888 particulate inorganic carbon measurements of coccolithophores in the Bay of Biscay, Limnol.

889 Oceanogr., 57, 145-153, 2012.

890 De Baar, H. J., De Jong, J. T., Bakker, D. C., Löscher, B. M., Veth, C., Bathmann, U., and Smetacek,

891 V.: Importance of iron for plankton blooms and carbon dioxide drawdown in the Southern Ocean,

892 Nature, 373, 412, 1995.

893 Dunbar, R. B., Leventer, A. R., and Mucciarone, D. A.: Water column sediment fluxes in the Ross

894 Sea, Antarctica: Atmospheric and sea ice forcing, J. Geophys. Res.: Oceans, 103, 30741-30759,

895 doi:10.1029/1998JC900001, 1998.

896   Dutkiewicz, A., O'Callaghan, S., and Müller, R.: Controls on the distribution of deep-sea sediments,
897   Geochem., Geophy., Geosy., 17, 3075-3098, 2016.

898   Eriksen, R., Trull, T. W., Davies, D., Jansen, P., Davidson, A. T., Westwood, K., and van den Enden,
899   R.: Seasonal succession of phytoplankton community structure from autonomous sampling at the
900   Australian Southern Ocean Time Series (SOTS) observatory, Mar. Ecol. Prog. Ser., 589, 13-31, 2018.

901   Feng, Y., Roleda, M. Y., Armstrong, E., Boyd, P. W., and Hurd, C. L.: Environmental controls on the
902   growth, photosynthetic and calcification rates of a Southern Hemisphere strain of the
903   coccolithophore Emiliania huxleyi, Limnol. Oceanogr., 62, 519-540, 2017.

904   Fischer, G., Fütterer, D., Gersonde, R., Honjo, S., Ostermann, D., and Wefer, G.: Seasonal variability
905   of particle flux in the Weddell Sea and its relation to ice cover, Nature, 335, 426-428, 1988.

906   Fischer, G., Gersonde, R., and Wefer, G.: Organic carbon, biogenic silica and diatom fluxes in the
907   marginal winter sea-ice zone and in the Polar Front Region: interannual variations and differences
908   in composition, Deep Sea Res. Part II: Top. Stud. Oceanogr., 49, 1721-1745, 2002.

909   Frankignoulle, M., Canon, C., and Gattuso, J. P.: Marine calcification as a source of carbon dioxide:
910   Positive feedback of increasing atmospheric CO_2, Limnol. Oceanogr., 39, 458-462, 1994.

911   Garcia, H. E., Locarnini, R. A., Boyer, T. P., Antonov, J. I., Baranova, O. K., . Zweng, M. M, and
912   Johnson, D. R.: World Ocean Atlas 2009, Volume 3: Dissolved Oxygen, Apparent Oxygen Utilization,
913   and Oxygen Saturation. S. Levitus, Ed. NOAA Atlas NESDIS 70, U.S. Government Printing Office,
914   Washington, D.C., 344 pp, 2010.

915   Garcia, H. E., Locarnini, R. A., Boyer, T. P., Antonov, J. I., Zweng, M. M., Baranova, O. K., and
916   Johnson, D. R.: World Ocean Atlas 2009, Volume 4: Nutrients (phosphate, nitrate, and silicate), S.
917   Levitus, Ed., NOAA Atlas NESDIS 71, U.S. Government Printing Office, Washington, D.C., 398 pp,
918   2010.

919   Gardner, W. D.: The effect of tilt on sediment trap efficiency, Deep Sea Res. Part I.: Oceanogr. Res.
920   Pap., 32, 349-361, 1985.

921   Gersonde, R., and Zielinski, U.: The reconstruction of late Quaternary Antarctic sea-ice
922   distribution—the use of diatoms as a proxy for sea-ice, Palaeogeogr., Palaeoclimatol., Palaeoecol.,
923   162, 263-286, https://doi.org/10.1016/S0031-0182(00)00131-0, 2000.

924   González, H. E., Hebbeln, D., Iriarte, J. L., and Marchant, M.: Downward fluxes of faecal material
925   and microplankton at 2300m depth in the oceanic area off Coquimbo (30 S), Chile, during 1993–
926   1995, Deep Sea Res. Part II: Top. Stud. Oceanogr., 51, 2457-2474, 2004.

927   Gordon, A., Molinelli, E., and Baker, T.: Large‐scale relative dynamic topography of the Southern
928   Ocean, J. Geophys. Res.: Oceans, 83, 3023-3032, 1978.

929   Graham, R. M., De Boer, A. M., van Sebille, E., Kohfeld, K. E., and Schlosser, C.: Inferring source
930   regions and supply mechanisms of iron in the Southern Ocean from satellite chlorophyll data, Deep
931   Sea Res. Part I: Oceanogr. Res. Pap., 104, 9-25, https://doi.org/10.1016/j.dsr.2015.05.007, 2015.

932   Gravalosa, J. M., Flores, J.-A., Sierro, F. J., and Gersonde, R.: Sea surface distribution of
933   coccolithophores in the eastern Pacific sector of the Southern Ocean (Bellingshausen and
934   Amundsen Seas) during the late austral summer of 2001, Marine Micropaleontology, 69, 16-25,
935   2008.

936   Grigorov, I., Rigual-Hernandez, A. S., Honjo, S., Kemp, A. E., and Armand, L. K.: Settling fluxes of
937   diatoms to the interior of the Antarctic circumpolar current along 170 W, Deep Sea Res. Part I:
938   Oceanogr. Res. Pap., 93, 1-13, 2014.

939   Gust, G., Michaels, A. F., Johnson, R., Deuser, W. G., and Bowles, W.: Mooring line motions and
940   sediment trap hydromechanics: in situ intercomparison of three common deployment designs,
941   Deep Sea Res. Part I: Oceanogr. Res. Pap., 41, 831-857, https://doi.org/10.1016/0967-
942   0637(94)90079-5, 1994.

943   Hargrave, B. T., von Bodungen, B., Conover, R. J., Fraser, A. J., Phillips, G., and Vass, W. P.: Seasonal
944   changes in sedimentation of particulate matter and lipid content of zooplankton collected by
945   sediment trap in the Arctic Ocean off Axel Heiberg Island, Polar Biol., 9, 467-475,
946   10.1007/bf00443235, 1989.

947   Harrison, C. S., Long, M. C., Lovenduski, N. S., and Moore, J. K.: Mesoscale Effects on Carbon Export:
948   A Global Perspective, Global Biogeochem. Cycles, 32, 680-703, 10.1002/2017GB005751, 2018.

949   Heinze, C., Meyer, S., Goris, N., Anderson, L., Steinfeldt, R., Chang, N., Le Quere, C., and Bakker, D.
950   C.: The ocean carbon sink–impacts, vulnerabilities and challenges, Earth Syst. Dynam., 6, 327-358,
951   2015.

952   Henson, S. A., Sanders, R., and Madsen, E.: Global patterns in efficiency of particulate organic
953   carbon export and transfer to the deep ocean, Global Biogeochem. Cycles, 26, 2012.

954   Hernández-Almeida, I., Bárcena, M. A., Flores, J. A., Sierro, F. J., Sanchez-Vidal, A., and Calafat, A.:
955   Microplankton response to environmental conditions in the Alboran Sea (Western
956   Mediterranean): One year sediment trap record, Mar. Micropaleontol., 78, 14-24,
957   https://doi.org/10.1016/j.marmicro.2010.09.005, 2011.

958   Honjo, S., Francois, R., Manganini, S., Dymond, J., and Collier, R.: Particle fluxes to the interior of
959   the Southern Ocean in the Western Pacific sector along 170°W, Deep Sea Res. Part II: Top. Stud.
960   Oceanogr., 47, 3521-3548, http://dx.doi.org/10.1016/S0967-0645(00)00077-1, 2000.

961   Honjo, S.: Particle export and the biological pump in the Southern Ocean, Antarct. Sci., 16, 501-
962   516, 2004.

963   Honjo, S., Manganini, S. J., Krishfield, R. A., and Francois, R.: Particulate organic carbon fluxes to
964   the ocean interior and factors controlling the biological pump: A synthesis of global sediment trap
965   programs since 1983, Prog. Oceanogr., 76, 217-285, 2008.

966   Hopkinson, B. M., Dupont, C. L., Allen, A. E., and Morel, F. M. M.: Efficiency of the CO_2 concentrating
967   mechanism of diatoms, Proc. Natl. Acad. Sci., 108, 3830-3837, 10.1073/pnas.1018062108, 2011.

968   Hutchins, D. A., Sedwick, P. N., DiTullio, G. R., Boyd, P. W., Quéguiner, B., Griffiths, F. B., and
969   Crossley, C.: Control of phytoplankton growth by iron and silicic acid availability in the subantarctic
970   Southern Ocean: Experimental results from the SAZ Project, J. Geophys. Res.: Oceans, 106, 31559-
971   31572, 10.1029/2000JC000333, 2001.

972   Ichinomiya, M., Gomi, Y., Nakamachi, M., Honda, M., Fukuchi, M., and Taniguchi, A.: Temporal
973   variations in the abundance and sinking flux of diatoms under fast ice in summer near Syowa
974   Station, East Antarctica, Polar Sci., 2, 33-40, 2008.

975   Ishikawa, A., Washiyama, N., Tanimura, A., and Fukuchi, M.: Variation in the diatom community
976   under fast ice near Syowa Station, Antarctica, during the austral summer of 1997/98, 2001.

977   James, M. R., and Hall, J. A.: Microzooplankton grazing in different water masses associated with
978   the subtropical convergence round the south island, New Zealand, Deep Sea Res. Part I: Oceanogr.
979   Res. Pap., 45, 1689-1707, https://doi.org/10.1016/S0967-0637(98)00038-7, 1998.

980   Jin, X., Gruber, N., Dunne, J., Sarmiento, J., and Armstrong, R.: Diagnosing the contribution of
981   phytoplankton functional groups to the production and export of particulate organic carbon,
982   CaCO3, and opal from global nutrient and alkalinity distributions, Glob. Biogeochem. Cycles, 20,
983   2006.

984   Kang, J.-S., Kang, S.-H., Kim, D., and Kim, D.-Y.: Planktonic centric diatom Minidiscus chilensis
985   dominated sediment trap material in eastern Bransfield Strait, Antarctica, Mar. Ecol. Prog. Ser.,
986   255, 93-99, 2003.

987   Kemp, A. E. S., Pike, J., Pearce, R. B., Lange, C. B.: The "Fall dump" - a new perspective on the role
988   of a "shade flora" in the annual cycle of diatom production and export flux, Deep Sea Res. Part II:
989   Top. Stud. Oceanogr., 47, 2129-2154, doi:https://doi.org/10.1016/S0967-0645(00)00019-9, 2000.

990 Klaas, C., and Archer, D. E.: Association of sinking organic matter with various types of mineral
991 ballast in the deep sea: Implications for the rain ratio, Glob. Biogeochem. Cycles, 16, 63-61-63-14,
992 2002.

993 Lam, P. J., Doney, S. C., and Bishop, J. K.: The dynamic ocean biological pump: Insights from a global
994 compilation of particulate organic carbon, CaCO3, and opal concentration profiles from the
995 mesopelagic, Glob. Biogeochem. Cycles, 25, 2011.

996 Lampitt, R., and Antia, A.: Particle flux in deep seas: regional characteristics and temporal
997 variability, Deep Sea Res. Part I: Oceanogr. Res. Pap., 44, 1377-1403, 1997.

998 Laurenceau, E., Trull, T., Davies, D., Bray, S., Doran, J., Planchon, F., Carlotti, F., Jouandet, M.-P.,
999 Cavagna, A.-J., and Waite, A.: The relative importance of phytoplankton aggregates and
1000 zooplankton fecal pellets to carbon export: insights from free-drifting sediment trap deployments
1001 in naturally iron-fertilised waters near the Kerguelen plateau, Biogeosci. Discuss., 11, 2015.

1002 Leblanc, K., Arístegui, J., Kopczynska, E., Marshall, H., Peloquin, J., Piontkovski, S., Poulton, A.,
1003 Quéguiner, B., Schiebel, R., and Shipe, R.: A global diatom database–abundance, biovolume and
1004 biomass in the world ocean, 2012.Leblanc, K., Quéguiner, B., Diaz, F., Cornet, V., Michel-Rodriguez,
1005 M., de Madron, X. D., Bowler, C., Malviya, S., Thyssen, M., and Grégori, G.: Nanoplanktonic diatoms
1006 are globally overlooked but play a role in spring blooms and carbon export, Nat. Commun., 9, 953,
1007 2018.

1008 Leventer, A., and Dunbar, R. B.: Diatom flux in McMurdo Sound, Antarctica, Mar. Micropaleontol.,
1009 12, 49-64, http://dx.doi.org/10.1016/0377-8398(87)90013-2, 1987.

1010 Leventer, A.: Sediment trap diatom assemblages from the northern Antarctic Peninsula region,
1011 Deep Sea Res. Part I: Oceanogr. Res. Pap., 38, 1127-1143, http://dx.doi.org/10.1016/0198-
1012 0149(91)90099-2, 1991.

1013 Leventer, A., and Dunbar, R. B.: Factors influencing the distribution of diatoms and other algae in
1014 the Ross Sea, J. Geophys. Res.: Oceans, 101, 18489-18500, doi:10.1029/96JC00204, 1996.

1015 Locarnini, R. A., A. V. Mishonov, J. I. Antonov, T. P. Boyer, H. E. Garcia, O. K. Baranova, M. M. Zweng,
1016 and Johnson. D. R.: World Ocean Atlas 2009, Volume 1: Temperature. S. Levitus, Ed. NOAA Atlas
1017 NESDIS 68, U.S. Government Printing Office, Washington, D.C., 184 pp, 2010.

1018 Lutjeharms, J., Valentine, H., and Vanballegooyen, R.: On the Subtropical Convergence in the
1019 South-Atlantic Ocean, South African Journal of Science, 89, 552-552, 1993.

1020 Maiti, K., Charette, M. A., Buesseler, K. O., and Kahru, M.: An inverse relationship between
1021 production and export efficiency in the Southern Ocean, Geophys. Res. Lett., 40, 1557-1561,
1022 10.1002/grl.50219, 2013.

1023 Malinverno, E., Maffioli, P., Corselli, C., and De Lange, G. J.: Present-day fluxes of coccolithophores
1024 and diatoms in the pelagic Ionian Sea, J. Mar. Syst., 132, 13-27,
1025 https://doi.org/10.1016/j.jmarsys.2013.12.009, 2014.

1026 Malinverno, E., Triantaphyllou, M. V., and Dimiza, M. D.: Coccolithophore assemblage distribution
1027 along a temperate to polar gradient in the West Pacific sector of the Southern Ocean (January
1028 2005), Micropaleontolog., 61, 489-506, 2015.

1029 Marchant, M., Hebbeln, D., and Wefer, G.: Seasonal flux patterns of planktic foraminifera in the
1030 Peru–Chile Current, Deep Sea Res, Part I: Oceanogr. Res. Pap., 45, 1161-1185, 1998.

1031 Marchant, M., Hebbeln, D., Giglio, S., Coloma, C., and González, H. E.: Seasonal and interannual
1032 variability in the flux of planktic foraminifera in the Humboldt Current System off central Chile
1033 (30°S), Deep Sea Res. Part II: Top. Stud. Oceanogr., 51, 2441-2455,
1034 https://doi.org/10.1016/j.dsr2.2004.08.013, 2004.

1035 Martin, J. H.: Glacial‐interglacial CO_2 change: The iron hypothesis, Paleoceanogr., 5, 1-13, 1990.

1036 Martin, J. H., Coale, K., Johnson, K., Fitzwater, S., Gordon, R., Tanner, S., Hunter, C., Elrod, V.,
1037 Nowicki, J., and Coley, T.: Testing the iron hypothesis in ecosystems of the equatorial Pacific Ocean,
1038 Nature, 371, 123, 1994.

1039 McDonnell, A. M., Lam, P. J., Lamborg, C. H., Buesseler, K. O., Sanders, R., Riley, J. S., Marsay, C.,
1040 Smith, H. E., Sargent, E. C., and Lampitt, R. S.: The oceanographic toolbox for the collection of
1041 sinking and suspended marine particles, Prog. Oceanogr., 133, 17-31, 2015.

1042 McMinn, A.: Preliminary investigation of the contribution of fast-ice algae to the spring
1043 phytoplankton bloom in Ellis Fjord, eastern Antarctica, Polar Biol., 16, 301-307, 1996.

1044 Nelson, D. M., Tréguer, P., Brzezinski, M. A., Leynaert, A., and Quéguiner, B.: Production and
1045 dissolution of biogenic silica in the ocean: revised global estimates, comparison with regional data
1046 and relationship to biogenic sedimentation, Glob. Biogeochem. Cyc., 9, 359-372, 1995.

1047 Nodder, S. D., Boyd, P. W., Chiswell, S. M., Pinkerton, M. H., Bradford‐Grieve, J. M., and Greig, M.
1048 J.: Temporal coupling between surface and deep ocean biogeochemical processes in contrasting
1049 subtropical and subantarctic water masses, southwest Pacific Ocean, J. Geophys. Res.: Oceans,
1050 110, 2005.

1051 Nodder, S. D., Duineveld, G. C., Pilditch, C. A., Sutton, P. J., Probert, P. K., Lavaleye, M. S., Witbaard,
1052 R., Chang, F. H., Hall, J. A., and Richardson, K. M.: Focusing of phytodetritus deposition beneath a
1053 deep-ocean front, Chatham Rise, New Zealand, Limnol. Oceanogr., 52, 299-314, 2007.

1054 Nodder, S. D., Chiswell, S. M., and Northcote, L. C.: Annual cycles of deep-ocean biogeochemical
1055 export fluxes in subtropical and subantarctic waters, southwest Pacific Ocean, J. Geophys. Res.:
1056 Oceans, 121, 2405-2424, 10.1002/2015JC011243, 2016.

1057 Orsi, A. H., Whitworth, T., and Nowlin, W. D.: On the meridional extent and fronts of the Antarctic
1058 Circumpolar Current, Deep Sea Res. Part I: Oceanogr. Res. Pap., 42, 641-673, 1995.

1059 Pilskaln, C. H., Manganini, S. J., Trull, T. W., Armand, L., Howard, W., Asper, V. L., and Massom, R.:
1060 Geochemical particle fluxes in the Southern Indian Ocean seasonal ice zone: Prydz Bay region, East
1061 Antarctica,   Deep   Sea   Res.   Part   I: Oceanogr.   Res.   Pap.,   51,   307-332,
1062 https://doi.org/10.1016/j.dsr.2003.10.010, 2004.

1063 Pollard, R., Lucas, M., and Read, J.: Physical controls on biogeochemical zonation in the Southern
1064 Ocean, Deep Sea Res. II: Top. Stud. Oceanogr., 49, 3289-3305, 2002.

1065 Pollard, R. T., Salter, I., Sanders, R. J., Lucas, M. I., Moore, C. M., Mills, R. A., Statham, P. J., Allen, J.
1066 T., Baker, A. R., Bakker, D. C. E., Charette, M. A., Fielding, S., Fones, G. R., French, M., Hickman, A.
1067 E., Holland, R. J., Hughes, J. A., Jickells, T. D., Lampitt, R. S., Morris, P. J., Nédélec, F. H., Nielsdóttir,
1068 M., Planquette, H., Popova, E. E., Poulton, A. J., Read, J. F., Seeyave, S., Smith, T., Stinchcombe, M.,
1069 Taylor, S., Thomalla, S., Venables, H. J., Williamson, R., and Zubkov, M. V.: Southern Ocean deep-
1070 water carbon export enhanced by natural iron fertilization, Nature, 457, 577,
1071 10.1038/nature07716, 2009.

1072 Prebble, J., Crouch, E., Carter, L., Cortese, G., and Nodder, S.: Dinoflagellate cysts from two
1073 sediment traps east of New Zealand, Mar. Micropaleontol., 104, 25-37, 2013.

1074 Pudsey, C. J., and King, P.: Particle fluxes, benthic processes and the palaeoenvironmental record
1075 in the Northern Weddell Sea, Deep Sea Res. Part I: Oceanogr. Res. Pap., 44, 1841-1876,
1076 https://doi.org/10.1016/S0967-0637(97)00064-2, 1997.

1077 R Core Team: R: A language and environment for statistical computing. R Foundation for Statistical
1078 Computing, Vienna, Austria, https://www.R-project.org/, 2018.

1079 Rembauville, M., Blain, S., Armand, L., Quéguiner, B., and Salter, I.: Export fluxes in a naturally iron-
1080 fertilized area of the Southern Ocean–Part 2: Importance of diatom resting spores and faecal
1081 pellets for export, Biogeosci., 12, 3171-3195, 2015a.

1082   Rembauville, M., Salter, I., Leblond, N., Gueneugues, A., and Blain, S.: Export fluxes in a naturally

1083   iron-fertilized area of the Southern Ocean-Part 1: Seasonal dynamics of particulate organic carbon

1084   export from a moored sediment trap, Biogeosci., 12, 3153, 2015b.

1085   Rembauville, M., Manno, C., Tarling, G. A., Blain, S., and Salter, I.: Strong contribution of diatom

1086   resting spores to deep-sea carbon transfer in naturally iron-fertilized waters downstream of South

1087   Georgia, Deep Sea Res. Part I: Oceanogr. Res. Pap., 115, 22-35,

1088   https://doi.org/10.1016/j.dsr.2016.05.002, 2016.

1089   Rembauville, M., Salter, I., Dehairs, F., Miquel, J.-C., and Blain, S.: Annual particulate matter and

1090   diatom export in a high nutrient, low chlorophyll area of the Southern Ocean, Polar Biol., 41, 25-

1091   40, 10.1007/s00300-017-2167-3, 2018.

1092   Rigual-Hernández, A. S., Bárcena, M. A., Jordan, R. W., Sierro, F. J., Flores, J. A., Meier, K. J. S.,

1093   Beaufort, L., and Heussner, S.: Diatom fluxes in the NW Mediterranean: evidence from a 12-year

1094   sediment trap record and surficial sediments, J. Plankton Res., 35, 1109-1125,

1095   10.1093/plankt/fbt055, 2013.

1096   Rigual-Hernández, A., Trull, T., Bray, S., Cortina, A., and Armand, L.: Latitudinal and temporal

1097   distributions of diatom populations in the pelagic waters of the Subantarctic and Polar Frontal

1098   Zones of the Southern Ocean and their role in the biological pump, Biogeosci., 12, 5309-5337,

1099   2015a.

1100   Rigual-Hernández, A. S., Trull, T. W., Bray, S. G., Closset, I., and Armand, L. K.: Seasonal dynamics

1101   in diatom and particulate export fluxes to the deep sea in the Australian sector of the southern

1102   Antarctic Zone, J. Mar. Sys., 142, 62-74, http://dx.doi.org/10.1016/j.jmarsys.2014.10.002, 2015b.

1103   Rigual-Hernández, A. S., Trull, T. W., Bray, S. G., and Armand, L. K.: The fate of diatom valves in the

1104   Subantarctic and Polar Frontal Zones of the Southern Ocean: Sediment trap versus surface

1105   sediment assemblages, Palaeogeogr., Palaeoclimatol., Palaeoecol., 457, 129-143,

1106   http://dx.doi.org/10.1016/j.palaeo.2016.06.004, 2016.

1107   Rigual-Hernández, A. S., Flores, J. A., Sierro, F. J., Fuertes, M. A., Cros, L., and Trull, T. W.:

1108   Coccolithophore populations and their contribution to carbonate export during an annual cycle in

1109   the Australian sector of the Antarctic zone, Biogeosciences, 15, 1843-1862,

1110   https://doi.org/10.5194/bg-15-1843-2018, 2018a.

1111   Rigual-Hernández, A., Pilskaln, C., Cortina, A., Abrantes, F., and Armand, L.: Diatom species fluxes

1112   in the seasonally ice-covered Antarctic Zone: New data from offshore Prydz Bay and comparison

1113   with other regions from the eastern Antarctic and western Pacific sectors of the Southern Ocean,

1114   Deep Sea Res. Part II: Top. Stud. Oceanogr., 2018b.

1115 Romero, O. E., Hebbeln, D., and Wefer, G.: Temporal and spatial variability in export production in
1116 the SE Pacific Ocean: evidence from siliceous plankton fluxes and surface sediment assemblages,
1117 Deep Sea Res. Part I: Oceanogr. Res. Pap., 48, 2673-2697, 2001.

1118 Romero, O., Boeckel, B., Donner, B., Lavik, G., Fischer, G., and Wefer, G.: Seasonal productivity
1119 dynamics in the pelagic central Benguela System inferred from the flux of carbonate and silicate
1120 organisms, J. Mar. Sys., 37, 259-278, 2002.

1121 Romero, O. and Armand, L. K.: Marine diatoms as indicators of modern changes in oceanographic
1122 conditions, in: The diatoms: applications for the environmental and earth sciences edited by: Smol,
1123 J. P., and Stoermer, E. F., Cambridge University Press, New York, 373-400, 2010.

1124 Salter, I., Kemp, A. E., Moore, C. M., Lampitt, R. S., Wolff, G. A., and Holtvoeth, J.: Diatom resting
1125 spore ecology drives enhanced carbon export from a naturally iron-fertilized bloom in the Southern
1126 Ocean, Global Biogeochem. Cycles, 26, 2012.

1127 Salter, I., Schiebel, R., Ziveri, P., Movellan, A., Lampitt, R., and Wolff, G. A.: Carbonate counter pump
1128 stimulated by natural iron fertilization in the Polar Frontal Zone, Nature Geosci., 7, 885-889, 2014.

1129 Sancetta, C., Villareal, T., and Falkowski, P.: Massive fluxes of rhizosolenid diatoms: A common
1130 occurrence?, Limnolog. Oceanogr., 36, 1452-1457, 10.4319/lo.1991.36.7.1452, 1991.

1131 Sasaki, H., and Watanabe, K.: Underwater observations of ice algae in Lutzow-Holm Bay,
1132 Antarctica, 1984.

1133 Schlitzer, R., (2016) Ocean Data View Software. http://odv.awi.de 1185

1134 Schloss, I. R., Ferreyra, G. A., Mercuri, G., and Kowalke, J.: Particle flux in an Antarctic shallow
1135 coastal environment: a sediment trap study, Scientia Marina, 63, 99-111, 1999.

1136 Smetacek, V. S.: Role of sinking in diatom life-history cycles: ecological, evolutionary and geological
1137 significance, Mar. Biol., 84, 239-251, 10.1007/bf00392493, 1985.

1138 Smith, W. O., and Nelson, D. M.: Importance of Ice Edge Phytoplankton Production in the Southern
1139 Ocean, BioSci., 36, 251-257, 10.2307/1310215, 1986.

1140 Sokolov, S., and Rintoul, S. R.: Circumpolar structure and distribution of the Antarctic Circumpolar
1141 Current fronts: 1. Mean circumpolar paths, J. Geophys. Res.: Oceans, 114, 2009.

1142 Suzuki, H., Sasaki, H., and Fukuchi, M.: Short-term variability in the flux of rapidly sinking particles
1143 in the Antarctic marginal ice zone, Polar Biol., 24, 697-705, 10.1007/s003000100271, 2001.

1144 Takahashi, K., Asahi, H., Okazaki, Y., Onodera, J., Tsutsui, H., Ikenoue, T., Kanematsu, Y., Tanaka, S.,
1145 and Iwasaki, S.: Museum archives of the 19 years long time-series sediment trap samples collected

1146   at central subarctic Pacific Station SA and Bering Sea Station AB during 1990–2010, Memoirs of the

1147   Faculty of Sciences, Kyushu University, Series D, Earth and Planetary Sciences 32, 1-38, 2012.

1148   Ternois, Y., Sicre, M.-A., Boireau, A., Beaufort, L., Miquel, J.-C., and Jeandel, C.: Hydrocarbons,

1149   sterols and alkenones in sinking particles in the Indian Ocean sector of the Southern Ocean, Org.

1150   Geochem., 28, 489-501, 1998.

1151   Tomas, C. R.: Identifying marine phytoplankton, Academic press, San Diego, 1997.

1152   Trull, T., Sedwick, P., Griffiths, F., and Rintoul, S.: Introduction to special section: SAZ Project, J.

1153   Geophys. Res.: Oceans (1978–2012), 106, 31425-31429, 2001a.

1154   Trull, T., Bray, S., Manganini, S., Honjo, S., and Francois, R.: Moored sediment trap measurements

1155   of carbon export in the Subantarctic and Polar Frontal Zones of the Southern Ocean, south of

1156   Australia, J. Geophys. Res.: Oceans, 106, 31489-31509, 2001b.

1157   Volk, T., and Hoffert, M. I.: Ocean carbon pumps: Analysis of relative strengths and efficiencies in

1158   ocean-driven atmospheric CO_2 changes, in: The Carbon Cycle and Atmospheric CO: Natural

1159   Variations Archean to Present edited by: Sundquist, E. T., and Broecker, W. S., American Gephysical

1160   Union; Geophysical Monograph 32, 99-110, 1985.

1161   Weber, T., Cram, J. A., Leung, S. W., DeVries, T., and Deutsch, C.: Deep ocean nutrients imply large

1162   latitudinal variation in particle transfer efficiency, P. Natl. Acad. Sci., 113, 8606-8611,

1163   10.1073/pnas.1604414113, 2016.

1164   Wefer, G., Fischer, G., Füetterer, D., and Gersonde, R.: Seasonal particle flux in the Bransfield Strait,

1165   Antartica, Deep Sea Res. Part I: Oceanogr. Res. Pap., 35, 891-898, 1988.

1166   Wilks, J. V., Rigual-Hernández, A. S., Trull, T. W., Bray, S. G., Flores, J.-A., and Armand, L. K.:

1167   Biogeochemical flux and phytoplankton succession: a year-long sediment trap record in the

1168   Australian sector of the Subantarctic Zone, Deep Sea Res. Part I: Oceanogr. Res. Pap.,

1169   http://dx.doi.org/10.1016/j.dsr.2017.01.001, 2017.

1170   Wilks, J. V., Nodder, S., Rigual-Hernández, A. S., Brock, G., and Armand, L. K.: Diatom and

1171   coccolithophore flux assemblages from the Subtropical Frontal region, east of New Zealand, Deep

1172   Sea Res. Part I: Oceanogr. Res. Pap., in review.

1173   Ziveri, P., Thunell, R. C.: Coccolithophore export production in Guaymas Basin, Gulf of California:

1174   response to climate forcing. Deep Sea Res. Part II: Top. Stud. Oceanogr., 47:2073-2100.

1175   doi:https://doi.org/10.1016/S0967-0645(00)00017-5, 2000.

Supplementary Information 2

Diatom flux, coccolith flux, environmental data and additional references
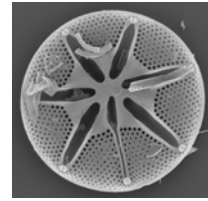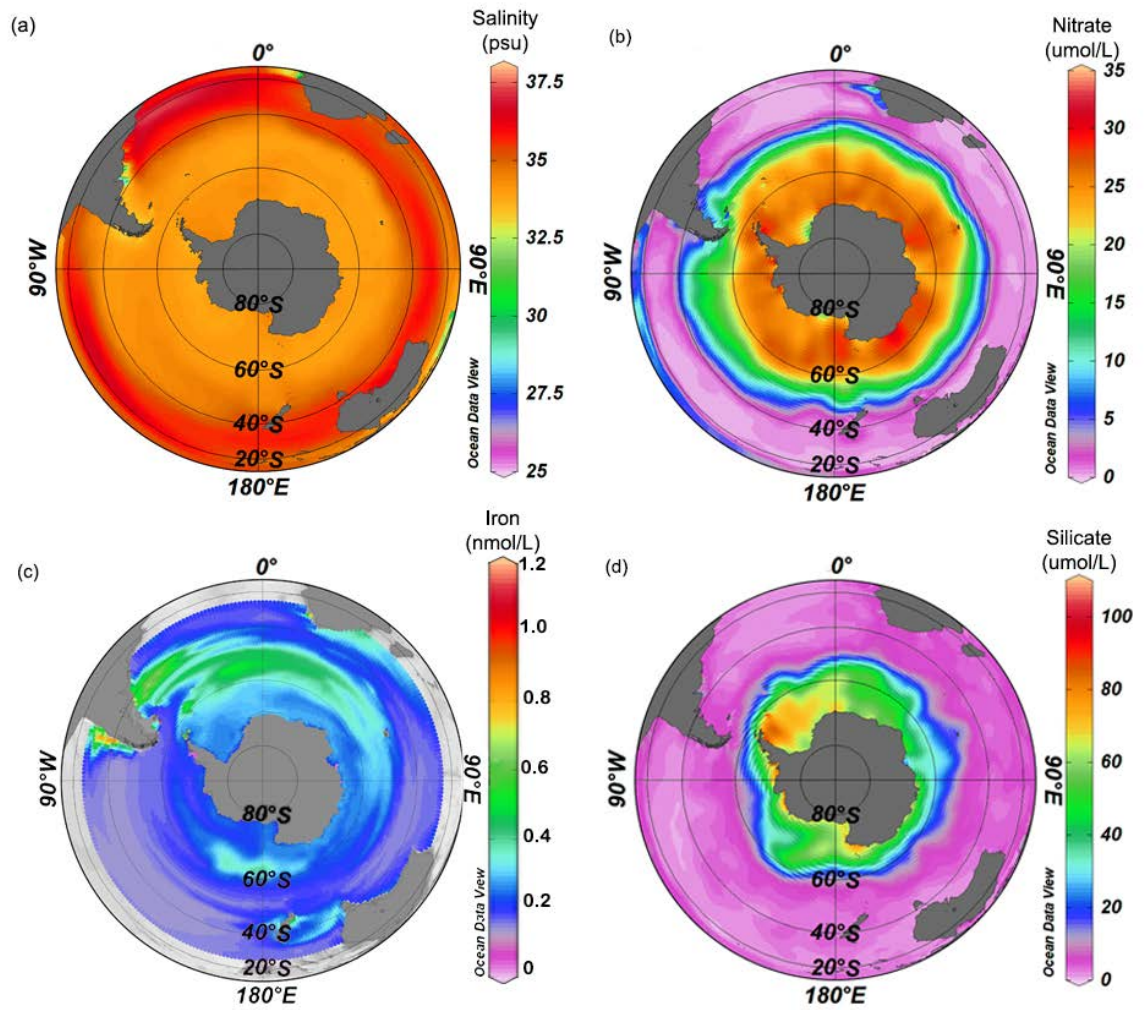
Supplementary Figure 1. Physical and chemical hydrology of the Southern Hemisphere from 30° S to the pole. a) Salinity (psu); b) Nitrate (umol.L^{-1}); c) Iron (nmol.L^{-1}); d) Silicate (umol.L^{-1}).

Supplementary Table 1. List of mooring sites in subtropical to polar Southern Hemisphere and associated publications covered in Chapter Five.

Region	Trap ID[#]	coordinates	Depths	Years	Sources
Weddell Sea	WS1	62°26.5' S, 34°45.5' W	863	1985-1986	Abelmann Gersonde 1991, Fischer et al., 1988, Gersonde and Zielinski 2000, Pudsey and King, 1997, Wefer et al. 1988, Wefer et al. 1990, Wefer and Fischer 1991
	WS2	64°55.0' S, 2°30.0' W	4454	1987	Wefer and Fischer 1991, Wefer et al. 1988, Wefer et al. 1990, Abelmann Gersonde 1991
	WS3	64°53.1' S, 2°33.7' W	360	1988-1989	Wefer and Fischer 1991, Abelmann and Gersonde 1991, Gersonde and Zielinski 2000
	WS4	64°55.5' S, 2°35.5' W	352, 400	1989-1990	Wefer and Fischer 1991, Abelmann and Gersonde 1991
	PF1	50°09.0' S, 5°43.8' E	700	1987-1988	Wefer and Fischer 1991, Abelmann and Gersonde 1991
	WS1-I	63°11' S, 42°43' W	2971, 3777	1988-1990	Pudsey and King 1997
	WS1-VIII	62°05' S, 40°36' W	2971, 3777	1990-1992	Pudsey and King 1997
	AWI208	63°29.6' S, 52°07.4' W	500	1989-1990	Gersonde and Zielinski 2000
	AWI206	65°36.3' S, 36°29.9' W	1000	1989-1990	Gersonde and Zielinski 2000
	KN	71°07' S, 12°12' W	250	1988	Bathman et al. 1991
	1-274	72°35' S, 18°09' W	80	1985	Nöthig and Bodungen 1989
	3-284	72°15' S, 18°21' W	80	1985	Nöthig and Bodungen 1989
	4-286	72°31' S, 17°17' W	80	1985	Nöthig and Bodungen 1989
	P2	55°11.99' S, 41°07.42' W	1500	2012	Rembauville et al. 2016
	P3	52°43.40' S, 40°08.83' W	2000	2012	Rembauville et al. 2016

Bransfield Strait/Drake Passage/ Antarctic Peninsula	KG1	62°16.3' S, 57°22.8' W	323, 494, 539, 963, 1410, 1588, 1835	1983-1984	Liebezeit and Bodungen 1987, Wefer et al. 1990, Wefer et al. 1998, Wefer and Fischer 1991,
	KG2	62°20.1' S, 75°28.3' W	700	1984-1985	Wefer et al. 1988, Abelmann and Gersonde 1991
	KG3/ KG83	62°16.3 S, 57°22.8 W	323, 539, 687, 963, 1410, 1835	1983, 1985-1986	von Bodungen et al. 1986, Gersonde and Wefer 1987, Wefer et al. 1988, Abelmann and Gersonde 1991, Abelmann 1991
	EBS	61°45.8' S, 54°59.1' W	1000	1998-1999	Kang et al. 2003
	AB	64°46.58' S, 62°49.68' W	279, 379, 416	2001-2003	Berger et al. 2009
	27	64°13.25' S, 61°14.48' W	447, 531, 573	2001-2003	Berger et al. 2009
	MC	62°13' S, 58°47' W	30	1998-2000	Khim et al. 2007
	S1	62°14' S, 58°38' W	30-40	1991-1994	Schloss et al. 1999
	S2	62°14' S, 58°38' W	30-41	1991-1992	Schloss et al. 1999
	M269	60°54.6' S 57°06.0' W	965, 2540	1980-1981	Wefer et al. 1982, Müller et al. 1986
	DP80/81	60°54.6 S 57°06.0 W	965, 2540	1980-1981	Gersonde and Wefer 1987, Gersonde and Zielinski 2000
	PB83	60°32.0' S, 48°18.8' W	1660	1983	Gersonde and Wefer 1987, Gersonde and Zielinski 2000
	HI	~64°30' S, 66°00' W	350	1992-2006	Ducklow et al. 2008
	CS	66°10.5' S, 66°25.17' W	350	1992-2006	Ducklow et al. 2008
	PB	64°50.11' S, 64°8.36' W	350	1992-2006	Ducklow et al. 2008
	RaTS1	67°34.02' S, 68°14.02' W	200, 420	2005-2006	Weston et al. 2013
	RaTS2	67°33.97' S, 68°14.06' W	200, 420	2006	Weston et al. 2013

	RaTS3	67°34.01' S, 68°14.00' W	200, 420	2006-2007	Weston et al. 2013
	MT	67°55.39' S, 68°24.15' W	123, 735	2005-2006	Weston et al. 2013
Ross Sea	B/EIT	77°42' S, 166°21' W	25, 51, 77, 103	1984	Leventer and Dunbar 1987, Dunbar et al. 1989
	D/HP1	77°52' S, 166°30' W	28, 57, 109, 161	1984	Leventer and Dunbar 1987, Dunbar et al. 1989
	E/NH1	77°40' S, 163°36' W	47, 99, 151, 203, 255	1984	Leventer and Dunbar 1987, Dunbar et al. 1989
	F/NH3	77°38' S, 163°46' W	32, 84, 186, 238	1984	Leventer and Dunbar 1987, Dunbar et al. 1989
	I/GH	76°56' S, 163°13' W	34, 127, 220, 313, 406, 499, 592, 685	1984	Leventer and Dunbar 1987, Dunbar et al. 1989
	L/HP2	77°51' S, 166°37' W	15, 37	1984	Leventer and Dunbar 1987, Dunbar et al. 1989
	NH2	77°41' S, 163°29' W	210	1986	Dunbar et al. 1989
	TI	77°42' S, 166°12' W	313	1986-1987	Dunbar et al. 1989
	BG	77°36' S, 166°11' W	345	1986-1987	Dunbar et al. 1989
	DG1	77°7' S, 163°20' W	181	1986-1987	Dunbar et al. 1989
	DG2	77°1' S, 163°35' W	464	1986-1987	Dunbar et al. 1989
	GH	77°56' S, 163°13' W	715	1984	Dunbar et al. 1989
	MS	77° 46' S, 165°39' W	500	1986	Dunbar et al. 1989
	MS-6	73°33' S, 176°53' E	200, 465	1996-1998	Collier et al. 2000
	MS-7	76°30' S, 178°1' W	200	1996-1998	Collier et al. 2000

	TNB	74°41.9' S, 164°07.5' E	40	1993-1994	Fabiano et al. 1997
	JB-B	74°01.50'S, 175°05.55'E	200	1994-1996	Langone et al. 2000
	D	75°06' S, 164°13' E	95, 180, 868	1995-1997	Accornero et al. 2003
	F	77°59' S, 177°01' W	423	1995-1996	Accornero et al. 1999
	C	72°29.55' S, 175°08.10' E	200, 416	1994-1996	Cerchierini et al. 2004
	K	74°42.00' S, 164°14.82' E	200, 514	1996-1998	Cerchierini et al. 2004
	RS-A	76°30.1' S, 167°30.3' E	250, 659	1991-1992	DeMaster et al. 1992; Leventer and Dunbar 1996, Dunbar et al. 1998
	RS-B	76°30.3' S, 174°59.1' W	250, 469	1991-1992	DeMaster et al. 1992; Leventer and Dunbar 1996, Dunbar et al. 1998
	RS-C	72°30' S, 172°30' W	250, 443	1990-1992	DeMaster et al. 1992; Leventer and Dunbar 1996, Dunbar et al. 1998
	MA	76°41' S , 169°02' E	370, 780	2008	Chiarini et al. 2013
	MB	74°00' S, 175°05' E	235, 550	2008	Chiarini et al. 2013
East Atlantic sector	BO1	54°20.3' S, 3°22.6' W	450	1990-1991	Gersonde and Zielinski 2000, Fischer et al. 2002
	BO2	54°20.8' S, 3°23.6' W	456	1992	Gersonde and Zielinski 2000
	PF1	50°09.0' S, 5°43.8' E	700	1987-1988	Gersonde and Zielinski 2000
	PF3	50°07.6' S, 5°50.0' E	614	1989-1990	Gersonde and Zielinski 2000, Fischer et al. 2002
	PF5	50°06.0' S, 5°55.4' E	654	1992	Gersonde and Zielinski 2000
	M269	60°54.6' S 57°06.0' W	965	1980-1981	Wefer and Fischer 1991,
	Lambert Bay	32°05.02' S, 18°16.01' E	20	1984, 2002-2005	Pitcher 1986, Pitcher and Joyce 2009

	NU	29°12' S, 13°07' E	2516	1992-1993	Romero et al. 2002
Australian/New Zealand Sector	MS1	53°02' S, 174°44' W	982, 1981, 3381, 4741	1996-1998	Honjo et al. 2000, Grigorov et al. 2014, Pollard et al. 2009
	MS2	56°54' S, 170°10' W	982, 1976, 2966, 4224	1996-1998	Honjo et al. 2000, Grigorov et al. 2014, Pollard et al. 2009
	MS3	60°17' S, 170°03' W	1003, 1997, 3257	1996-1998	Honjo et al. 2000, Grigorov et al. 2014, Pollard et al. 2009
	MS4	63°09' S, 169°54' W	1031, 2026, 2182	1996-1998	Honjo et al. 2000, Grigorov et al. 2014, Pollard et al. 2009
	MS5	66°10' S, 169°40' W	937, 1033, 1842, 2311	1996-1998	Honjo et al. 2000, Grigorov et al. 2014, Pollard et al. 2009
	SCR	42°42' S 178°38' E	300, 1000	1996-1997	Nodder and Northote 2001, Wilks et al. 2018, in press, Sikes et al. 2005, King and Howard 2001
	NCR	44°37' S 178°37' E	300, 1000	1996-1997	Nodder and Northote 2001, Wilks et al. 2018, in press, Sikes et al. 2005, King and Howard 2001
	STM	41°15' S, 178°33' E	1500	2000-2012	Prebble et al. 2013, Nodder et al. 2016
	SAM	46°33' S, 178°33' E	1500	2000-2012	Prebble et al. 2013, Nodder et al. 2016
	TAS	44°12.25'5, 147°5.35' E	305, 952	1992-1993	Parslow et al. 1995
	SAZ A/42S	42° 7.3' S, 141°45.3' E	1000, 4250	1997-1998,	Bray et al. 2000
	SAZ B/ 47S	46°46' S, 142°40' E	500, 1060, 2050, 3850	1997-1998, 1999-2001, 2003-2004	Bray et al. 2000, Trull et al. 2001, Rigual-Hernández et al. 2015b, Wilks et al. 2017
	SAZ E/ 51S	53°45' S, 141°45' E	830, 3080, 3300	1997-1998,	Bray et al. 2000, Trull et al. 2001, Rigual-Hernández et al. 2015b
	SAZ C/ PFZ/ 54S	53°45' S, 141°45' E	800, 1580	1997-1998, 1999-2000,2002-2004, 2005-2007	Bray et al. 2000, Trull et al. 2001, Rigual-Hernández et al. 2015
	61S/AZ	60°44.4' S, 139°54.0' E	1000, 2000, 3700	2001-2002	Rigual-Hernández et al. 2015a, Rigual-Hernández et al., 2018a

	KH83-4	61°33' S, 150°27' E	690, 930, 1330, 2330, 3130	1983-1984	Harada and Tsugonai 1986
	KH94-4	64°42'S, 139°59'E	537, 796, 1259, 1722, 2727	1994-1995	Suzuki et al. 2001
	AO	61°30' S, 150°30' E	520, 770, 1200, 2260, 3110	1984-1984	Noriki and Tsugonai 1986
	A.Stn.3	61°34.1' S, 150°23.3' E	630, 1430, 3230	1983-1984	Matsueda and Handa 1986
Southeast Pacific sector	CH1-3	29°59.27' S, 73°11.05' W	3700	1991-1992	Marchant et al. 1998, Hebbeln et al. 2000, Romero et al. 2001, González et al. 2004
	CH3-1	30°1.05' S, 73°11.0' W	2300	1993-1994	Romero et al. 2001, Marchant et al. 1998
	CH3-2	30°1.05' S, 73°11.0' W	3700	1993-1994	Marchant et al. 1998
	CH4-1	30°0.3' S, 73°10.27' W	2300	1994	Romero et al. 2001, Marchant et al. 1998
	CH5-2	29°59.61', 73°13.23'	2407	1994-1995	Marchant et al. 2004
	CH6-2	29°57.30', 73°17.21'	2393	1995	Marchant et al. 2004
	CH7-2	29°57.40', 73°17.30'	2498	1995-1996	Marchant et al. 2004
	CH8-2	29°54.80', 73°17.97'	2508	1996	Marchant et al. 2004
	CH10-2	29°59.90', 73°16.75'	2578	1997	Romero et al. 2001, Marchant et al. 2004
	CH11-1	29°58.80', 73°18.10'	2526	1997-1998	Romero et al. 2001, Marchant et al. 2004
Southwest Indian sector/Lützow-Holm Bay	Syowa Stn.I	68°37.2' S 38°47.5' E	50, 100, 150	1977	Fukuchi and Sasaki 1981
	Syowa Stn.II	68°41.1' S 38°35.8' E	50, 100, 150	1977	Fukuchi and Sasaki 1981
	Syowa Stn.III	68°41.5' S 38°39.0' E	50, 100, 150	1977	Fukuchi and Sasaki 1981

Syowa Stn.1	68°20.3' S 39°21.2' E	0.3, 10, 30,50, 100, 150	1979, 1983	Fukuchi and Sasaki 1981, Sasaki and Hoshiai 1986
Syowa Stn.2	69°00' S, 39°35' E	5, 25	1984-1985	Matsuda et al. 1987
Syowa Stn.3	69°0' S, 39°37.12' E	1.6, 5, 5.6, 20, 25	1982, 1997-1998, 2005-2006	Sasaki and Hoshiai 1986, Matsuda et al. 1987, Ishikawa et al. 2001, Ichinomiya et al. 2008
KERFIX	50°40' S, 68°25' E	280	1993-1994, 1994-1995	Ternois et al. 1998, Miquel et al. 1998, Rembauville et al. 2018, Jeandel et al. 1998
A3	50°38.30' S, 72°02.6' E	289	2011-2012	Rembauville et al. 2014, 2015a, 2015b, 2016
PZB-1	62°28.6' S, 72°58.6' E	1400, 2400, 3400	1998-2000, 2000-2001	Pilskaln et al. 2004, Rigual-Hernández et al. 2018
PZB-2	63°27.7' S, 76°09.5' E	3300	1998-2000, 2000-2001	Pilskaln et al. 2004
IB	~68°35' S, 78° E	5	1992	McMinn et al. 1996
MB	~68°35' S, 78°2' E	5	1992	McMinn et al. 1996
DB	~68°35' S, 78°4' E	5	1992	McMinn et al. 1996
M10	44°29.95' S, 49°59.9' E	2000	2004-2005	Pollard et al. 2009, Salter et al. 2012
M5	46°00' S, 56°05.0' E	3195	2004-2005	Pollard et al. 2009, Salter et al. 2012
M6	49°00.03'S, 51°30.6' E	3160	2005-2006	Pollard et al. 2009, Salter et al. 2012

= trap reference used in Figure 1.

Supplementary Table 2. Diatom annual and maximum flux from sediment trap deployments, and eight environmental. parameters. Phosphate, nitrate, silicate and SST from World Ocean Atlas 2009 (https://www.nodc.noaa.gov/OC5/WOA09/pr_woa09.html). Time-averaged (2009-2014) mean Chl-a (4km resolution, MODIS-Aqua satellite), time-averaged (2009-2014) mean iron (0.67 x 1.25° resolution, NOBM model), and time-averaged (2009-2014) PIC concentration (4km resolution, MODIS-Aqua satellite) was obtained from the via the Goddard Earth Sciences Data and Information Services Centre (GES DISC) for the region 25° S to the pole (accessible at https://giovanni.gsfc.nasa.gov).

Author	Station	LAT.	LONG.	Annual diatom flux	max diatom flux	silicate umol/L	log10 silicate	phosphate	nitrate	iron	Annual mean sea ice	PIC	SST	chl-a
				m2/y	m2/d	L		umol/L	umol/L	nmol/L	%	mol/m3	°C	mg/m3
Abelmann Gersonde 1991	KG1	-62.3	-57.5	2.7E+10	5.6E+09	73.38	1.87	1.94	25.07	0.27	24.6	0.00012	-0.98	0.52
Abelmann Gersonde 1991	KG2	-62.3	-75.5	8.0E+08	5.7E+06	28.78	1.46	1.65	24.36	0.18	0.7	0.00031	1.90	0.15
Abelmann Gersonde 1991	KG3	-62.4	-58.0	2.2E+09	1.3E+07	73.38	1.87	1.94	25.07	0.27	24.6	0.00012	-0.98	0.52
Abelmann Gersonde 1991	WS1	-62.4	-34.8	2.6E+08	1.7E+07	70.47	1.85	1.85	24.49	0.32	61.1	0.00041	-1.08	0.26
Abelmann Gersonde 1991	WS3	-64.9	-2.6	1.0E+10	2.2E+08	64.27	1.81	1.87	26.14	0.29	55.3	0.00046	-0.95	0.35
Abelmann Gersonde 1991	WS4	-64.9	-2.6	1.8E+09	8.7E+07	65.12	1.81	1.90	26.27	0.29	55.3	0.00046	-0.98	0.39
Abelmann Gersonde 1991	WS2	-64.9	-2.5	8.8E+09	8.0E+07	65.12	1.81	1.90	26.27	0.29	57	0.00035	-0.98	0.35
Abelmann Gersonde 1991	PF1	-50.2	5.7	5.5E+09	7.5E+07	19.35	1.29	1.73	21.21	0.44	0	0.00025	2.88	0.30
Fischer et al1998	WS1.1	-62.4	-34.8		1.0E+07	70.47	1.85	1.85	24.49	0.32	66.2	0.00041	-1.08	1.51
Gersonde Zielinski 2000	AWI206	-63.5	-52.1	2.6E+08	1.9E+07	80.37	1.91	1.91	27.89	0.26	71.3	0.00017	-1.22	0.44
Gersonde Zielinski 2000	AWI208	-65.6	-36.5	1.8E+09	1.4E+07	71.46	1.85	1.89	25.34	0.29	73.1	0.00046	-1.33	0.63
Gersonde Zielinski 2000	BO1	-54.3	-3.4	2.1E+10	4.6E+08	39.18	1.59	1.71	25.45	0.47	1.6	0.00016	0.14	0.21
Gersonde Zielinski 2000	BO2	-54.3	-3.4	3.5E+09		39.18	1.59	1.71	25.45	0.47	1.6	0.00016	0.14	0.21

Gersonde Zielinski 2000	PF3	-50.1	5.8	1.2E+10		19.35	1.29	1.73	21.21	0.44	0	0.00027	2.88	0.30
Gersonde Zielinski 2000	PF5	-50.1	5.9	5.9E+08		19.35	1.29	1.73	21.21	0.44	0	0.00027	2.88	0.30
Grigorov et al. 2014	MS5	-66.2	-169.7	2.6E+10	9.3E+07	56.76	1.75	1.87	26.54	0.25	56.1	0.00045	-0.99	0.30
Grigorov et al. 2014	MS4	-63.2	-169.9	1.8E+11	3.2E+08	37.65	1.58	1.79	26.24	0.35	17.3	0.00073	0.06	0.35
Grigorov et al. 2014	MS3	-60.3	-170.1	2.9E+10	4.3E+07	17.54	1.24	1.69	24.86	0.25	0.1	0.00035	2.12	0.25
Grigorov et al. 2014	MS2	-56.9	-170.2	5.0E+09	1.6E+07	7.35	0.87	1.44	20.08	0.18	0	0.00020	5.38	0.16
Kang et al. 2003	EBS	-61.8	-55.0		1.0E+09	65.35	1.82	1.97	26.79	0.28	21.8	0.00010	-0.55	0.37
Leventer and Dunbar 1987	D	-77.9	-166.5		3.2E+06	64.43	1.81	1.59	18.61	0.21	74.6	0.00053	-1.29	1.53
Leventer and Dunbar 1987	E	-77.7	-163.6		2.8E+06	66.95	1.83	1.70	17.50	0.21	75	0.00037	-1.30	3.54
Leventer and Dunbar 1987	F	-77.6	-163.8		8.0E+05	66.95	1.83	1.70	17.50	0.21	75	0.00037	-1.30	3.54
Leventer and Dunbar 1987	I	-76.9	-163.2		4.7E+07	63.05	1.80	1.76	19.36	0.21	80	0.00049	-1.40	1.49
Leventer and Dunbar 1987	L	-77.9	-166.6		1.9E+07	64.43	1.81	1.59	18.61	0.21	74.6	0.00035	-1.29	1.53
Leventer and Dunbar 1996	RS-A	-76.5	167.5		5.5E+08	65.35	1.82	1.57	19.88	0.23	76.8	0.00204	-0.97	2.69
Leventer and Dunbar 1996	RS-B	-76.5	-175.0		9.5E+07	64.06	1.81	1.75	23.34	0.24	71.8	0.00044	-1.31	1.06
Pilskaln et al. 2004	PZB1	-62.5	73.0		2.9E+08	38.92	1.59	1.85	27.89	0.23	45	0.00032	-0.68	0.30
Prebble et al. 2013	STM	-41.3	178.6		3.4E+04	1.86	0.27	0.23	1.21	0.18	0	0.00021	15.28	0.34
Prebble et al. 2013	SAM	-46.6	178.6		1.2E+05	2.41	0.38	0.66	7.31	0.21	0	0.00026	10.64	0.31
Rembauville et al. 2015b	A3	-50.6	72.0		6.1E+07	16.43	1.22	1.75	26.42	0.28	0	0.00033	2.68	0.85
Rembauville et al. 2016	P2	-55.2	-41.1		1.4E+07	23.19	1.37	1.57	23.56	0.26	0.2	0.00033	1.50	0.45

Reference	ID													
Rembauville et al. 2016	P3	-52.7	-40.2		1.2E+08	12.45	1.10	1.60	22.61	0.28	0	0.00016	2.56	1.37
Rembauville et al. 2017	KERFIX	-50.7	68.4		1.3E+08	14.81	1.17	1.71	25.34	0.30	0	0.00020	3.43	0.27
Rigual-Hernández et al. 2015a	SAZ	-46.8	142.7	4.0E+07	1.6E+06	2.98	0.47	0.81	10.21	0.15	0	0.00029	10.66	0.25
Rigual-Hernández et al. 2015a	PFZ	-53.8	141.8	5.5E+09	1.0E+08	9.73	0.99	1.54	23.90	0.18	0	0.00017	4.46	0.14
Rigual-Hernández et al. 2015b	AZ	-60.7	139.9	2.4E+09	4.8E+08	28.35	1.45	1.83	28.61	0.22	4.6	0.00021	0.96	0.17
Romero et al. 2001	CH3-1	-30.0	-73.2		7.0E+06	1.97	0.29	0.48	2.98	0.68	0	0.00016	16.04	0.47
Romero et al. 2001	CH4-1	-30.0	-73.2		1.6E+05	1.97	0.29	0.48	2.98	0.68	0	0.00016	16.04	0.47
Romero et al. 2001	CH10-1	-30.0	-73.3		2.8E+06	2.03	0.31	0.45	2.74	0.60	0	0.00018	16.32	0.48
Romero et al. 2001	CH11-1	-30.0	-73.3		3.6E+05	2.03	0.31	0.45	2.74	0.60	0	0.00018	16.32	0.48
Romero et al. 2002	NU	-29.2	13.1	1.5E+08	1.9E+06	3.70	0.57	0.50	1.90	0.22	0	0.00014	17.71	0.26
Salter et al. 2012	M10	-44.5	50.0	1.3E+09	2.5E+07	7.59	0.88	1.32	15.77	0.27	0	0.00032	6.82	0.46
Salter et al. 2012	M5	-46.0	56.1	2.0E+09	2.9E+07	6.37	0.80	1.37	16.57	0.27	0	0.00020	6.69	0.36
Salter et al. 2012	M6	-49.0	51.5	8.3E+08	5.6E+07	10.11	1.00	1.56	22.06	0.34	0	0.00018	3.81	0.17
Wefer et al. 1988	KG1.0	-62.3	-57.5		1.0E+09	73.38	1.87	1.94	25.07	0.27	37.3	0.00012	-0.98	0.24
Wilks et al. 2017	47S	-46.8	142.1	2.3E+08	7.4E+06	2.98	0.47	0.81	10.21	0.15	0	0.00024	10.66	0.26
Wilks et al. 2018, in press	SCR	-44.6	178.6	1.4E+08	5.4E+06	2.04	0.31	0.46	3.91	0.32	0	0.00026	12.28	0.48
Wilks et al. 2018, in press	NCR	-42.7	178.6	1.5E+06	4.0E+04	1.87	0.27	0.29	1.77	0.19	0	0.00017	14.25	0.42

Supplementary Table 3. Coccolith annual and maximum fluxes from sediment trap deployments.

Author	Station	LAT	LONG	Annual coccolith flux m2/y	Maximum coccolith flux m2/d
González et al. 2004	HCS	-30	-73.2		1.2E+08
Romero et al. 2002	NU	-29.2	13.1	1.6E+12	2.3E+10
Ternoise et al. 1998	KERFIX	-50.7	68.417		1.4E+08
Wilks et al. 2017	47S	-46.8	142.1	6.5E+11	2.3E+10
Wilks et al. 2018	SCR	-44.6	178.6	1.4E+08	3.5E+06
Wilks et al. 2018	NCR	-42.7	178.6	1.0E+07	3.3E+05
Rigual-Hernández et al. 2018	AZ	-60.7	139.9	1.0E+10	2.2E+09

Supplementary References

Abelmann, A., and Gersonde, R.: Biosiliceous particle flux in the Southern Ocean, Mar. Chem., 35, 503-536, 1991.

Bathmann, U., Fischer, G., Müller, P. J., and Gerdes, D.: Short-term variations in particulate matter sedimentation off Kapp Norvegia, Weddell Sea, Antarctica: relation to water mass advection, ice cover, plankton biomass and feeding activity, Polar Biol., 11, 185-195, 10.1007/bf00240207, 1991.

Berger, G. W., Ante, S., and Domack, E. W.: Seasonal and water-depth variations in sediment luminescence and in sedimentation from sediment trap samples at Gerlache Strait, Antarctic Peninsula, Antarct. Sci., 21, 483-499, 10.1017/S0954102009990186, 2009.

Cerchiarini, M., Langone, L., and Ravaioli, M.: Sediment trap particle fluxes in the northwestern Ross Sea, Antarctica, Proc. Ital. Assoc. Oceanol. Limnol., 17, 13-24.

Collier, R., Dymond, J., Honjo, S., Manganini, S., Francois, R., and Dunbar, R.: The vertical flux of biogenic and lithogenic material in the Ross Sea: moored sediment trap observations 1996–1998, Deep Sea Res. Part II: Top. Stud. Oceanogr., 47, 3491-3520, 2000.

DeMaster, D. J., Dunbar, R. B., Gordon, L. I., Leventer, A. R., Morrison, J. M., Nelson, D. M., Nittrouer, C. A., and Smith, W. O.: Cycling and accumulation of biogenic silica and organic matter in high-latitude environments: the Ross Sea. Oceanogr., 5, 146-153, 1992.

Ducklow, H. W., Erickson, M., Kelly, J., Montes-Hugo, M., Ribic, C. A., Smith, R. C., Stammerjohn, S. E., and Karl, D. M.: Particle export from the upper ocean over the continental shelf of the west Antarctic Peninsula: a long-term record, 1992–2007, Deep Sea Res. Part II: Top. Stud. Oceanogr., 55, 2118-2131, 2008.

Dunbar, R. B., Leventer, A. R., and Stockton, W. L.: Biogenic sedimentation in McMurdo Sound, Antarctica, Mar. Geol., 85, 155-179, https://doi.org/10.1016/0025-3227(89)90152-7, 1989.

Fabiano, M., Chiantore, M., Povero, P., Cattaneo-Vietti, R., Pusceddu, A., Misic, C., and Albertelli, G.: Short-term variations in particulate matter flux in Terra Nova Bay, Ross Sea, Antarct. Sci., 9, 143-149, 1997.

Fischer, G., Fütterer, D., Gersonde, R., Honjo, S., Ostermann, D., and Wefer, G.: Seasonal variability of particle flux in the Weddell Sea and its relation to ice cover, Nature, 335, 426-428, 1988.

Gersonde, R., and Wefer, G.: Sedimentation of biogenic siliceous particles in Antarctic waters from the Atlantic sector, Mar. Micropaleontol., 11, 311-332, https://doi.org/10.1016/0377-8398(87)90004-1, 1987.

Gersonde, R., and Zielinski, U.: The reconstruction of late Quaternary Antarctic sea-ice distribution—the use of diatoms as a proxy for sea-ice, Palaeogeogr., Palaeoclimatol., Palaeoecol., 162, 263-286, https://doi.org/10.1016/S0031-0182(00)00131-0, 2000.

Jeandel, C., Ruiz-Pino, D., Gjata, E., Poisson, A., Brunet, C., Charriaud, E., Dehairs, F., Delille, D., Fiala, M., and Fravalo, C.: KERFIX, a time-series station in the Southern Ocean: a presentation, J. Mar. Sys., 17, 555-569, 1998.

Kang, J.-S., Kang, S.-H., Kim, D., and Kim, D.-Y.: Planktonic centric diatom Minidiscus chilensis dominated sediment trap material in eastern Bransfield Strait, Antarctica, Mar. Ecol. Prog. Ser., 255, 93-99, 2003.

Khim, B. K., Shim, J., Yoon, H. I., Kang, Y. C., and Jang, Y. H.: Lithogenic and biogenic particle deposition in an Antarctic coastal environment (Marian Cove, King George Island): Seasonal patterns from a sediment trap study, Estuar. Coast. Mar. Sci., 73, 111-122, https://doi.org/10.1016/j.ecss.2006.12.015, 2007.

Langone, L., Frignani, M., Ravaioli, M., and Bianchi, C.: Particle fluxes and biogeochemical processes in an area influenced by seasonal retreat of the ice margin (northwestern Ross Sea, Antarctica), J. Mar. Sys., 27, 221-234, https://doi.org/10.1016/S0924-7963(00)00069-5, 2000.

Leventer, A., and Dunbar, R. B.: Diatom flux in McMurdo Sound, Antarctica, Mar. Micropaleontol., 12, 49-64, http://dx.doi.org/10.1016/0377-8398(87)90013-2, 1987.

Liebezeit, G., and von Bodungen, B.: Biogenic fluxes in the Bransfield Strait: planktonic versus macroalgal sources, Mar. Ecol. Prog. Ser., 23-32, 1987.

McMinn, A.: Preliminary investigation of the contribution of fast-ice algae to the spring phytoplankton bloom in Ellis Fjord, eastern Antarctica, Polar Biol., 16, 301-307, 1996.

Miquel, J., Carroll, M., and Jeandel, C.: Seasonal trend in particulate carbon flux at the time-series site Kerfix in the Southern Ocean, Ann. Geophys., 16, 549, 1998.

Müller, P. J., Suess, E., and AndréUngerer, C.: Amino acids and amino sugars of surface particulate and sediment trap material from waters of the Scotia Sea, Deep Sea Res. Part I. Oceanogr. Res. Pap., 33, 819-838, 1986.

Nöthig, E.-M., and von Bodungen, B.: Occurrence and vertical flux of faecal pellets of probably protozoan origin in the southeastern Weddell Sea (Antarctica), Mar. Ecol. Prog. Ser., 281-289, 1989.

Pilskaln, C. H., Manganini, S. J., Trull, T. W., Armand, L., Howard, W., Asper, V. L., and Massom, R.: Geochemical particle fluxes in the Southern Indian Ocean seasonal ice zone: Prydz Bay region, East Antarctica, Deep Sea Res. Part I. Oceanogr. Res. Pap., 51, 307-332, https://doi.org/10.1016/j.dsr.2003.10.010, 2004.

Pollard, R. T., Salter, I., Sanders, R. J., Lucas, M. I., Moore, C. M., Mills, R. A., Statham, P. J., Allen, J. T., Baker, A. R., Bakker, D. C. E., Charette, M. A., Fielding, S., Fones, G. R., French, M., Hickman, A. E., Holland, R. J., Hughes, J. A., Jickells, T. D., Lampitt, R. S., Morris, P. J., Nédélec, F. H., Nielsdóttir, M., Planquette, H., Popova, E. E., Poulton, A. J., Read, J. F., Seeyave, S., Smith, T., Stinchcombe, M., Taylor, S., Thomalla, S., Venables, H. J., Williamson, R., and Zubkov, M. V.: Southern Ocean deep-water carbon export enhanced by natural iron fertilization, Nature, 457, 577, 10.1038/nature07716, 2009.

Pudsey, C. J., and King, P.: Particle fluxes, benthic processes and the palaeoenvironmental record in the Northern Weddell Sea, Deep Sea Res. Part I. Oceanogr. Res. Pap., 44, 1841-1876, https://doi.org/10.1016/S0967-0637(97)00064-2, 1997.

Rembauville, M., Blain, S., Armand, L., Quéguiner, B., and Salter, I.: Export fluxes in a naturally iron-fertilized area of the Southern Ocean–Part 2: Importance of diatom resting spores and faecal pellets for export, Biogeosci., 12, 3171-3195, 2015a.

Rembauville, M., Salter, I., Leblond, N., Gueneugues, A., and Blain, S.: Export fluxes in a naturally iron-fertilized area of the Southern Ocean-Part 1: Seasonal dynamics of particulate organic carbon export from a moored sediment trap, Biogeosci., 12, 3153, 2015b.

Rembauville, M., Meilland, J., Ziveri, P., Schiebel, R., Blain, S., and Salter, I.: Planktic foraminifer and coccolith contribution to carbonate export fluxes over the central Kerguelen Plateau, Deep Sea Res. Part I. Oceanogr. Res. Pap., 111, 91-101, http://dx.doi.org/10.1016/j.dsr.2016.02.017, 2016.

Rembauville, M., Salter, I., Dehairs, F., Miquel, J.-C., and Blain, S.: Annual particulate matter and diatom export in a high nutrient, low chlorophyll area of the Southern Ocean, Polar Biol., 41, 25-40, 10.1007/s00300-017-2167-3, 2018.

Rigual-Hernández, A., Pilskaln, C., Cortina, A., Abrantes, F., and Armand, L.: Diatom species fluxes in the seasonally ice-covered Antarctic Zone: New data from offshore Prydz Bay and comparison

with other regions from the eastern Antarctic and western Pacific sectors of the Southern Ocean, Deep Sea Res. Part II: Top. Stud. Oceanogr., 2018.

Salter, I., Kemp, A. E., Moore, C. M., Lampitt, R. S., Wolff, G. A., and Holtvoeth, J.: Diatom resting spore ecology drives enhanced carbon export from a naturally iron-fertilized bloom in the Southern Ocean, Global Biogeochem. Cycles, 26, 2012.

Schloss, I. R., Ferreyra, G. A., Mercuri, G., and Kowalke, J.: Particle flux in an Antarctic shallow coastal environment: a sediment trap study, Sci. Mar., 63, 99-111, 1999.

von Bodungen, B.: Phytoplankton growth and krill grazing during spring in the Bransfield Strait, Antarctica — Implications from sediment trap collections, Polar Biol., 6, 153-160, 10.1007/bf00274878, 1986.

Wefer, G., Suess, E., Balzer, W., Liebezeit, G., Müller, P. J., Ungerer, C. A., and Zenk, W.: Fluxes of biogenic components from sediment trap deployment in circumpolar waters of the Drake Passage, Nature, 299, 145, 1982.

Wefer, G., Fischer, G., Füetterer, D., and Gersonde, R.: Seasonal particle flux in the Bransfield Strait, Antartica, Deep Sea Res. Part I. Oceanogr. Res. Pap., 35, 891-898, 1988.

Wefer, G., Fischer, G., Fütterer, D., Gersonde, R., Honjo, S., and Ostermann, D.: Particle sedimentation and productivity in Antarctic waters of the Atlantic sector, in: Geological history of the polar oceans: Arctic versus Antarctic, Springer, 363-379, 1990.

Wefer, G., and Fischer, G.: Annual primary production and export flux in the Southern Ocean from sediment trap data, Mar. Chem., 35, 597-613, 1991.

Weston, K., Jickells, T. D., Carson, D. S., Clarke, A., Meredith, M. P., Brandon, M. A., Wallace, M. I., Ussher, S. J., and Hendry, K. R.: Primary production export flux in Marguerite Bay (Antarctic Peninsula): Linking upper water-column production to sediment trap flux, Deep Sea Res. Part I. Oceanogr. Res. Pap., 75, 52-66, https://doi.org/10.1016/j.dsr.2013.02.001, 2013.
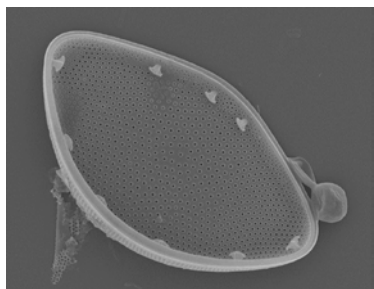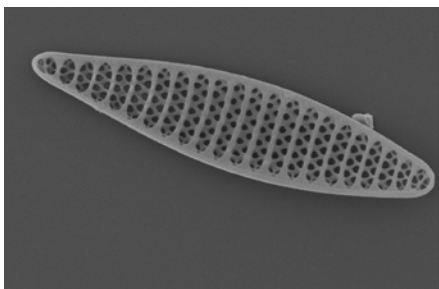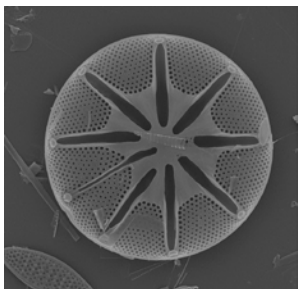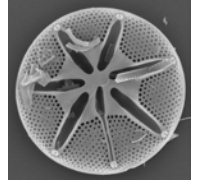
Chapter Five

Diversity and taxonomic identification of *Shionodiscus* spp. in the Australian sector of the Subantarctic Zone

The following chapter is presented in the format in which it was published.

Taylor & Francis
Taylor & Francis Group

Check for updates

Diversity and taxonomic identification of *Shionodiscus* spp. in the Australian sector of the Subantarctic Zone

JESSICA V. WILKS ⓘ* & LEANNE K. ARMAND

MQ Marine Research Centre and Department of Biological Sciences, Macquarie University, North Ryde, NSW 2109, Australia

Diatoms are siliceous phytoplankton that play a major role in global carbon fixation, as well as forming the basis of most marine food webs. In the Southern Ocean, diatoms are responsible for significant volumes of carbon export and sequestration in the deep sea. Diatoms are unicellular and microscopic, thus diatom taxonomy has naturally progressed as imaging and molecular technologies have developed. Despite recent advancements, some aspects of diatom taxonomy remain unclear. The genus *Shionodiscus* was separated from *Thalassiosira* in 2006, and possesses, as a group, internal extensions of the marginal strutted processes as well as a labiate process on the valve face, usually distant from the margin. The features distinguishing *Shionodiscus* from *Thalassiosira*, and *Shionodiscus* spp. from each other, are difficult to examine under light microscopy, and most taxonomists will group similar *Shionodiscus* species together when encountered, rather than discriminating species. As a result, the full extent of *Shionodiscus* diversity is rarely examined in individual studies. In this study, sediment trap material captured in the Australian sector of the Subantarctic Zone was examined using both light and scanning electron microscopy, and compared to known measurements on *Shionodiscus* species and varieties. This study had two aims; to catalogue for the first time the diversity of *Shionodiscus* spp. within the Australian sector, and to create a formalized set of criteria for grouping *Shionodiscus* species, when only light microscopy analysis is possible. By documenting *Shionodiscus* diversity in the Australian sector and establishing a standard identification protocol, researchers will be better able to determine the ecological significance of the genus in diatom assemblages.

Keywords: *diatom,* Shionodiscus*, taxonomy, Southern Ocean, sediment traps*

Introduction

Diatoms are an extremely diverse and widespread group of unicellular phytoplankton that exist in both marine and freshwater habitats worldwide. Marine diatoms are central to the global carbon and silica cycles, due to their siliceous cell-covering (frustule) and export of carbon from the water column to the deep ocean (Treguer et al. 1995, Jin et al. 2006). While marine phytoplankton as a whole account for nearly half of global net primary production (Field et al. 1998), the diatoms alone are thought to be responsible for approximately 20% of global net primary production (Nelson et al. 1995).

Thalassiosira Cleve is the third most abundant and widespread of the diatom genera with over 100 different species (Hasle & Syvertsen 1997, Malviya et al. 2016), and both marine and freshwater species (Hallegraeff 1984). *Thalassiosira* is not a monophyletic group, and the characters discriminating *Thalassiosira* from the Thalassiosirales as a whole remain unclear. Despite the complexity in the current state of the phylogeny of Thalassiosirales, diatoms classified as *Thalassiosira* have both strutted processes (fultoportulae) and at least one labiate process

(rimoportula), and possess spines or occluded processes at the valve margin (Theriot & Serieyssol 1994). Species are identified by a suite of morphological features such as cell shape, location and number of strutted and labiate processes, pattern of areolation and areola size, and anatomy of the girdle band, although many of these features are not distinguishable without scanning electron microscopy (SEM) (Fryxell & Hasle 1972, Hasle 1972, 1978, Fryxell 1975, Hasle & Fryxell 1977).

Hasle (1968) separated the genus *Thalassiosira* into two morphological groups, 'A' and 'B'. Hasle's group 'A' contained *Thalassiosira* spp. with strutted processes extending mainly outwards and the labiate process on the valve mantle, while group 'B' displayed mostly inward extensions of the strutted processes and the labiate process on the valve face (Hasle 1968, Hasle & Syvertsen 1997). A study by Alverson et al. (2006) reviewed the two morphological groups, placing many of the former group 'B' species in a new genus, *Shionodiscus* Alverson, Kang & Theriot. Diatoms of *Shionodiscus* possess the derived trait of a labiate process on the valve face rather than the mantle (usually distant from the valve margin) and

---

296   Wilks & Armand

marginal strutted processes with longer inward extensions, and with reduced or absent outward extensions (Alverson et al. 2006).

  Shionodiscus is common and relatively abundant in the Southern Ocean, a band of water that encircles Antarctica from approximately 40–70°S (Orsi et al. 1995). Within the Subantarctic Zone (SAZ) (the largest Southern Ocean water mass), both *Thalassiosira* and *Shionodiscus* spp. comprise a significant proportion of the diatom assemblages as spring bloom-forming taxa, but are also present year-round (Johansen & Fryxell 1985, Kopczyńska et al. 2007, Rigual-Hernández et al. 2015a). From sediment trapping and seafloor sediment studies they are also observed to make up a large component of the diatom fluxes in the SAZ (Zielinski & Gersonde 1997, Crosta et al. 2005, Romero et al. 2005, Rigual-Hernández et al. 2015a, Wilks et al. 2017). In the last study, sediment traps were deployed in the Australian Sector of the SAZ, south of Tasmania (46°46′S, 142°4′E) as part of the Antarctic Cooperative Research Centre's Subantarctic Zone (SAZ) Project (Trull et al. 2001b). Analysis of trap material revealed the presence of several *Shionodiscus* spp., which were not discriminated under LM and were combined, for convenience of analysis, into the 'Shionodiscus frenguellii group' (Wilks et al. 2017). Wilks et al. (2017) found that the *S. frenguellii* group formed 1.3% of total diatom relative abundance in sediment traps, and up to ∼4% relative abundance at their peak in the summer months. Other studies at the same site have found the same group (designated the 'Thalassiosira trifulta group') to be even more abundant, making up ∼2% to ∼3.5% relative diatom abundance at 1000 m (Rigual-Hernández et al. 2015a, 2016).

  Due to the fine structure and overlapping size and distributional ranges of *S. frenguellii* (Kozlova) Alverson, Kang & Theriot and related species, positive identifications under LM are usually impossible. Preliminary SEM analyses of the SAZ Project samples indicated that this grouping included *S. frenguellii*, *Shionodiscus trifultus* (Fryxell) Alverson, Kang & Theriot, and possibly *Shionodiscus frenguelliopsis* (Fryxell & Johansen) Alverson, Kang & Theriot (J.V. Wilks et al., unpub.).

  In the absence of SEM studies of diatom assemblages in this region, the precise contribution of *Shionodiscus* spp. to diatom diversity in the SAZ was until now unknown. In this study, sediment trap samples from the SAZ Project deployment at 47°S were revisited using SEM in order to determine the extent of the presence of the *S. frenguellii* group and similar species in the Australian sector of the SAZ. This study aims to provide a new description, separating four *S. frenguellii* group diatoms based on observations from this region, as well as outlining a formalized grouping convention for species difficult to differentiate based on light microscopy (LM) analysis alone. These suggested groupings are proposed as a starting point for LM-based studies that encounter indistinguishable *Shionodiscus* species, prior to (or in place of, if not possible) the use
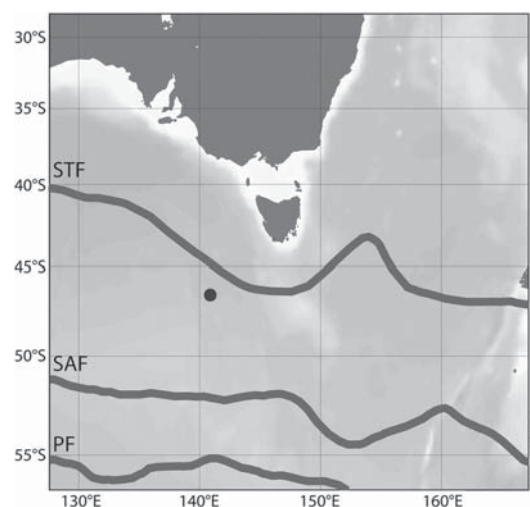

Fig. 1. Map of mooring site of sediment traps at 47°S in context of regional fronts. STF = Subtropical Front; SAF = Subantarctic Front; PF = Polar Front. Front locations from Orsi et al. (1995). Map created using Ocean Data View, available at http://odv.awi.de.

of additional identification techniques. While molecular research on *Shionodiscus* is needed, more rigorous naming conventions and detailed taxonomic identifiers will help researchers to better understand the ecological significance of these ambiguous species.

Methods

Oceanographic setting

The Antarctic Circumpolar Current (ACC) circulates uninterrupted around the globe, making up the region known as the Southern Ocean. The ACC is banded by several major zones that flow westerly (Orsi et al. 1995). Each zone is designated by several uniform properties that determine phytoplankton assemblages and are roughly homogeneous throughout (Pollard et al. 2002, Sokolov & Rintoul 2002) (Fig. 1). The transition from one hydrological zone to another is called a front, where the physical and biological characteristics of the water masses change sharply. The Subantarctic Zone (SAZ) is the region between the Subtropical Front (STF) to the north, occurring at around 44.5–45.6°S in the Australian region, and the Subantarctic Front (SAF) to the south, the strongest front within the ACC, occurring at 50–53°S (Sokolov & Rintoul 2002). In the SAZ, hydrological masses are strongly stratified, with this stratification controlled mainly by temperature (Pollard et al. 2002). In this study the front locations defined in Orsi et al. (1995) are used.

  The trap deployment site (46°48′S, 142°6′E) (Fig. 1) is low in silica and iron year-round but replete in nitrate, making it hydrologically typical of the SAZ (Rintoul & Trull 2001). The SAZ between 90° and 145°E is homogeneous,

171

so the trap deployment site is considered representative of this wider region (Trull et al. 2001a). The winter mixed layer can be as deep as 600, 75–100 m in summer (Rintoul & Trull 2001, Trull et al. 2001b).

Field experiment

Detailed methods on sediment trap deployment may be found in Trull et al. (2001b) and Wilks et al. (2017). Briefly, two sediment traps were deployed at 46°48′S, 142°6′E between September 2003 and October 2004, at 500 and 2000 m depth. Each trap operated on a 14 or 35-day rotation capture cycle, with 21 cups in total at each depth. After retrieval, each cup was poisoned with mercuric chloride, sieved to remove 'swimmers', and divided into ten splits.

Sample cleaning and preparation

The sample cleaning protocol is described in Wilks et al. (2017). Glass slides for SEM were prepared using the random settling first developed by Flores & Sierro (1997) and modified as per Wilks et al. (2017). Once prepared, slides were gold coated and observed using a JEOL JSM-6480LA SEM at 10 kV.

Diatom identification

Slides known to contain the target species were systematically observed along transects under SEM until the entire slide had been searched. The target number of specimens of each species was 20 to capture the full range of morphological diversity, however, 20 individuals could not be found for all species. Taxonomic identifications followed Fryxell & Hasle (1979a), Hallegraeff (1984), Johansen & Fryxell (1985) and Hasle & Syvertsen (1997). Measurements taken and morphological features observed were valve diameter, areolae in 10 μm at the centre and margin, number and arrangement of central strutted processes, number of marginal strutted processes in 10 μm, number of struts on strutted processes, presence of occluded processes, placement of labiate process, valve convexity and

areolation pattern on valve face. Girdle band width and ornamentation was recorded where possible. The degree of dissolution was also noted.

Helicon Focus© software was used to stack 3 LM images at different focal planes for Figs 7 and 9 in order to increase clarity (purchased from www.heliconsoft.com).

Results

LM and SEM were used to analyse material collected from sediment traps placed in the SAZ as part of the SAZ Project. Fourteen samples, spanning ten collecting months and three sediment trap depths, were systematically searched for *Shionodiscus* spp. Four different *Shionodiscus* spp. (and their varieties) were observed; *S. frenguellii*, *Shionodiscus gracilis* var. *gracilis* (Karsten) Alverson, Kang & Theriot, *S. gracilis* var. *expectus* (VanLandingham) Alverson, Kang & Theriot, *Shionodiscus oestrupii* var. *oestrupii* (Ostenfeld) Alverson, Kang & Theriot, *S. oestrupii* var. *venrickae* (Fryxell & Hasle) Alverson, Kang & Theriot and *S. trifultus*. Specimen measurements are given in Table 1.

Within the samples, six specimens of *S. frenguellii*, and only two specimens of *S. trifultus* were observed. The two varieties of *S. gracilis* (var. *gracilis* and var. *expectus*) and of *S. oestrupii* (var. *oestrupii* and var. *venrickae*) were relatively common in the samples (Table 1).

Species observations

Shionodiscus frenguellii (Kozlova) Alverson, Kang & Theriot (Figs 2–6)

Basionym: *Thalassiosira frenguellii*. Kozlova (1967, fig. 6)

Species descriptions are based upon six individual specimens of *S. frenguellii* observed in samples taken between July and September (winter to spring) (Table 1). Cells were 15.6–22.6 μm in diameter. Valve areolae hexagonal under LM, arranged in irregularly linear to sublinear array (Figs. 2, 4), eight to nine areolae in 10 μm at valve centre, 10–14 at margin. Two trifultate central strutted processes and one ring of marginal strutted processes, placed roughly

Table 1. Morphological measurements of *Shionodiscus* spp. and varieties found in the Australian sector of the SAZ.

Species name	Specimens #	Diameter μm	CSPs #	Distance CSP to LP μm	Distance CSP to LP # areolae	Distance between MSPs μm	Areolae in 10 μm Centre	Areolae in 10 μm Margin
S. oestrupii v. *oestrupii*	23	12–23.6 (16.6)	1	2.4–6.7 (4.6)	2–4 (2.6)	1.3–3.4 (1.9)	7–12 (9.0)	8–17 (12.2)
S. oestrupii v. *venrickae*	15	15.3–26.6 (22.1)	1	4.4–8.9 (7.1)	3–6 (4.7)	3.3–5.7 (4.8)	7–12 (8.8)	9–24 (12.4)
S. gracilis v. *gracilis*	21	7.4–23.1 (14.4)	1	2–7.8 (4.9)	2–6 (4.1)	2.2–3.8 (2.9)	9–24 (13.5)	20–36 (28.3)
S. gracilis v. *expectus*	15	12.8–24.4 (17.9)	1	2.6–6.5 (4.5)	2–5 (3.8)	3.2–5 (3.7)	10–14 (11.5)	14–26 (19.4)
S. frenguellii	6	15.6–22.6 (19.3)	2	4.7–7.2 (5.7)	2–4 (3.4)	4.7–5	8–9 (8.2)	10–14 (11.8)
S. trifultus	2	38.8–39	2–3	12–14.3	7–9	4–4.8	7	9.5–10

Notes: Values given in parentheses are averages. CSP = central strutted process. MSP = marginal strutted process. LP = labiate process.

298   Wilks & Armand
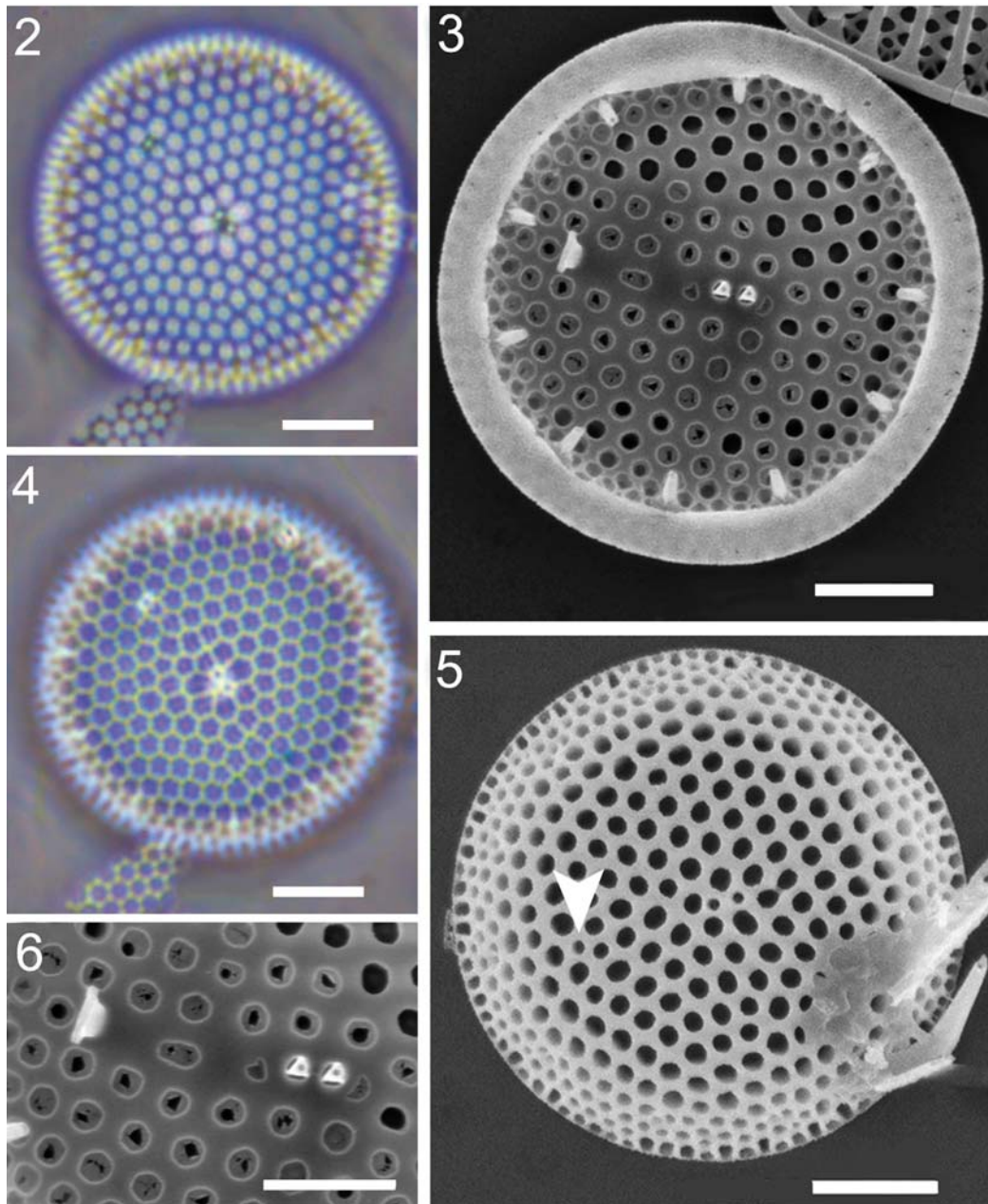
Figs 2–6. *Shionodiscus frenguellii* in light (Figs 2, 4) and SEM (Figs 3, 5–6). Figs 2, 4. The same cell in two planes of focus, with marginal strutted processes visible. Fig. 3. Internal valve view, showing strutted and labiate processes. Fig. 5. External valve view. Note central strutted processes and labiate process are visible from the outside as apparently wider areolae (arrowed). Fig. 6. Close-up internal valve view of central strutted and labiate processes. Note trifultate structure of central strutted processes. Scale bars represent 5 μm.

5 μm apart (Figs 3, 5–6). Marginal strutted processes have internal extensions and are difficult to see under LM. Labiate process is on valve face, with two to four areolae (4.7–7.2 μm) between it and the central strutted processes (Fig. 6).

***Shionodiscus gracilis* var. *gracilis* (Karsten) Alverson, Kang & Theriot (Figs 7–8)**

Basionym: *Coscinodiscus gracilis.* Karsten (1905, pl. 3, fig. 4)
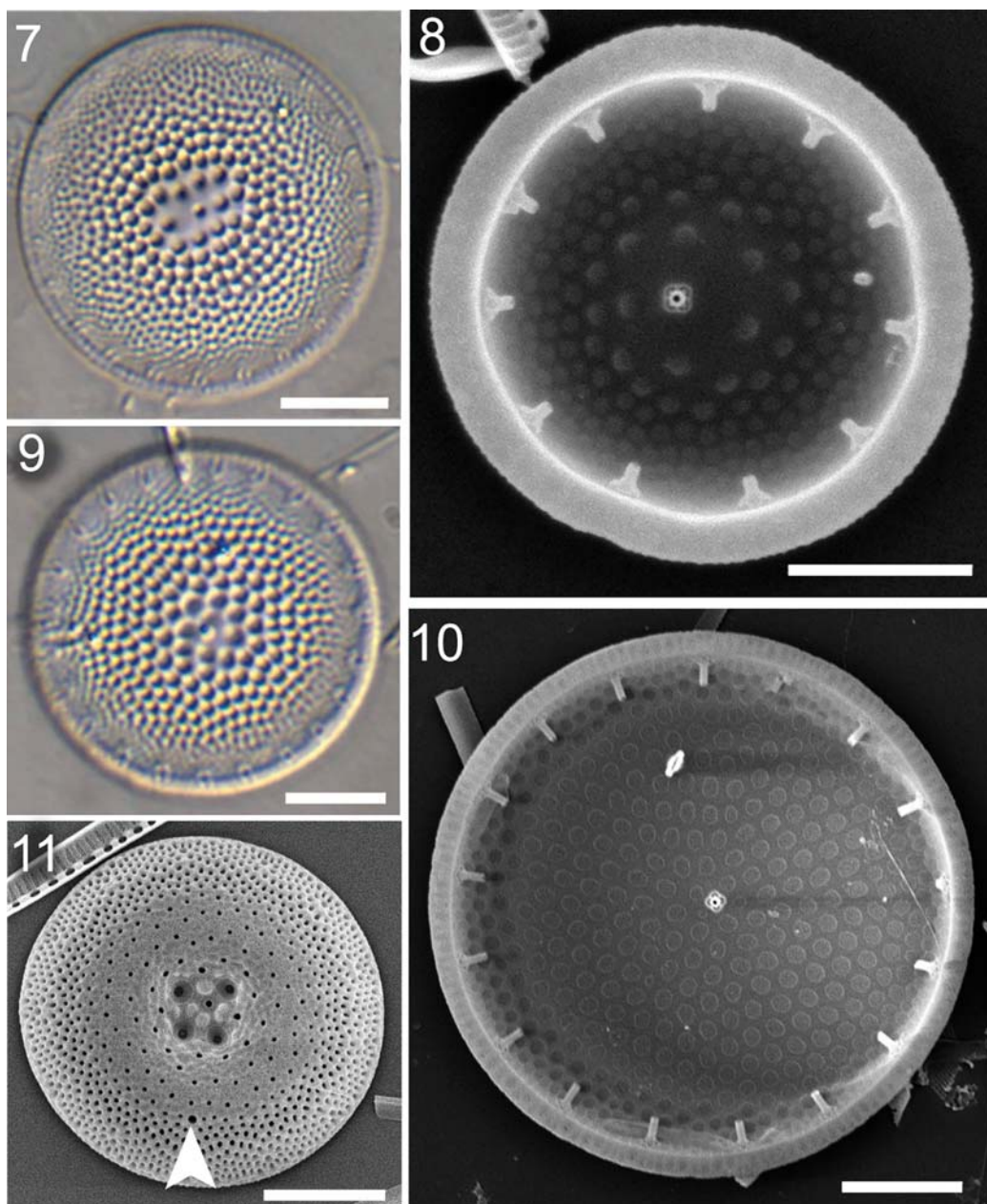
Figs 7–11. *Shionodiscus gracilis* with light (Figs 7, 9) and SEM (Figs 8, 10, 11). Fig. 7. *Shionodiscus gracilis* v. *gracilis*; Fig. 9. *Shionodiscus gracilis* v. *expectus*. Fig. 8. Internal valve view of *S. gracilis* var. *gracilis*. Note the pore-free space surrounding the operculate central strutted process. Fig. 10. Internal valve view of *S. gracilis* var. *expectus* showing strutted and labiate processes. Fig. 11. External view of *S. gracilis* valve. Note depressed central region, and labiate process visible as a large areola approximately halfway between the centre and margin (arrowed). Scale bars represent 5 μm.

Synonym: *Thalassiosira gracilis* (Karsten) Hustedt var. *gracilis* Hustedt (1958, pl. 3, figs 4–7)

Twenty one individual specimens of *S. gracilis* var. *gracilis* were measured, with the majority of specimens taken from late winter/early spring samples (August–November)

(Table 1). Cell diameter ranged from 7.4 to 23.1 μm. Areolae are distinctly larger in the centre (9–24 in 10 μm) than at the valve margin (20–36 in 10 μm). Areolae at the centre surrounded by depressed hyaline region, distinct under both LM and SEM (Figs 7, 8). Cells possess one operculate strutted process positioned in either a central or subcentral

position, and one labiate process placed two to five areolae (3.6–8 μm; though sometimes as little as 2 μm) apart on the valve face (Fig. 8). Marginal strutted processes are operculate, 2.2–3.8 μm apart.

Shionodiscus gracilis var. *expectus* (VanLandingham) Alverson, Kang & Theriot (Figs 9–10)

Basionym: *Thalassiosira expecta* VanLandingham
Synonym: *Thalassiosira gracilis* var. *expecta* Fryxell, & Hasle

Fifteen specimens of *S. gracilis* var. *expectus* were measured, tending to occur in spring and summer (October–December) (Table 1). Cells ranged from 12.8 to 22.5 μm in diameter. Areolae in the centre are smaller than at margin (10–14, and 14–26 in 10 μm, respectively), though not as distinctively different as in *S. gracilis* var. *gracilis* (Fig. 10). One subcentral operculate strutted process, with a labiate process two to five areolae (2.6–6.5 μm) away. Areolae at centre may appear slightly thick-rimmed under LM (Fig. 9). Marginal strutted processes tend to be more widely spaced than in *S. gracilis* var. *gracilis*; 3.2–5 μm apart. External valve view shown in Fig. 11.

Shionodiscus oestrupii var. *oestrupii* (Ostenfeld) Alverson, Kang & Theriot (Figs 12–14)

Basionym: *Coscinodiscus oestrupii* Ostenfeld
Synonym: *Thalassiosira oestrupii* var. *oestrupii* Fryxell & Hasle (1980, figs 1–10).

Twenty three specimens of *S. oestrupii* var. *oestrupii* were measured, with specimens found in greatest abundance in late spring/summer (November–December) (Table 1). Valves range from 9.2 to 23.6 μm in diameter; areolation is sublinear, but the areolation pattern may not be visible in smaller specimens. This species can appear heavily silicified under LM, with bubble-shaped areolae (Fig. 12), 7–12 in 10 μm at the centre, and 8–17 in 10 μm at the margin. Usually two (or up to four) areolae between the trifultate central strutted process and labiate process (Fig. 13). Marginal strutted processes are closely spaced, 1.3–3.4 μm apart (Figs 13–14).

Shionodiscus oestrupii var. *venrickae* (Fryxell & Hasle) Alverson, Kang & Theriot (Figs 15–16)

Basionym: *Thalassiosira oestrupii* var. *venrickae* Fryxell & Hasle (1980, figs 11–19)

Shionodiscus oestrupii var. *venrickae*, like *S. oestrupii* var. *oestrupii*, was found predominantly between late spring and early summer, with 15 specimens measured (Table 1). Cells 15.3–28.6 μm in diameter, with areolation ranging from sublinear to eccentric (Fig. 15). Areolae in the centre are 7–10 in 10 μm, and at the margin 9–24 in 10 μm. Usually four or five (can be only three or up to six) areolae between the central trifultate strutted process and the labiate process (Figs 15, 16). Marginal strutted processes more widely spaced than in *S. oestrupii* var. *oestrupii*; 3.3–5.7 μm apart.

Shionodiscus trifultus (Fryxell) Alverson, Kang & Theriot (Figs 17–21)

Basionym: *T. trifulta* Fryxell. Fryxell & Hasle (1979b, figs 1–24)

Only two specimens of *S. trifultus* were observed, both occurring in winter/spring samples (July–September) (Table 1). Cells 38–39 μm in diameter. Areolation is sublinear in pattern, with seven areolae in 10 μm at the centre, and 9.5–10 at the margin. Areolae appear hexagonal under LM; central strutted processes usually visible and marginal processes sometimes visible under LM (Figs 17, 19). Two or three trifultate central strutted processes, arranged in a line when more than two, and with labiate process 12–14.3 μm (7–9 areolae) away (Figs 18, 20–21). Marginal strutted processes are 4–4.8 μm apart.

Discussion

Shionodiscus *spp. in the Australian sector*

In the Australian sector of the SAZ, the diversity and morphology of *Shionodiscus* spp. have not previously been documented. Previous workers have assessed diatom species diversity in both surface waters (Kopczyńska et al. 2001, 2007, de Salas et al. 2011), sediment traps (Rigual-Hernández et al. 2015a, 2016, Wilks et al. 2017) and seafloor sediment (Crosta et al. 2004) in this area, although the full diversity of *Shionodiscus* was not the focus of these studies. In the sediment trap studies (Rigual-Hernández et al. 2015a, 2016, Wilks et al. 2017), the two *S. oestrupii* varieties and the two *S. gracilis* varieties were grouped together for statistical analyses.

The *Shionodiscus* specimens identified in this study were for the most part consistent with previous descriptions and measurements. With the exception of *S. gracilis* var. *expectus*, the specimens tended to be at the lower size ranges of the respective species. It is not known whether *Shionodiscus* of the Australian sector are simply small specimens, or whether the sizes found reflect some sort of cell transformation (e.g., dissolution and breakage of larger cells, leaving smaller cells) between surface and sediment trap, or during sample processing. Despite this, the results confirm the presence of previously undifferentiated species within the Australia sector of the SAZ.

Shionodiscus gracilis

This study confirmed the presence of both varieties of *S. gracilis* in the Australian sector of the SAZ. The largest specimens of *S. gracilis* var. *expectus* observed exceeded previously recorded cell diameters (Fryxell & Hasle 1979a,
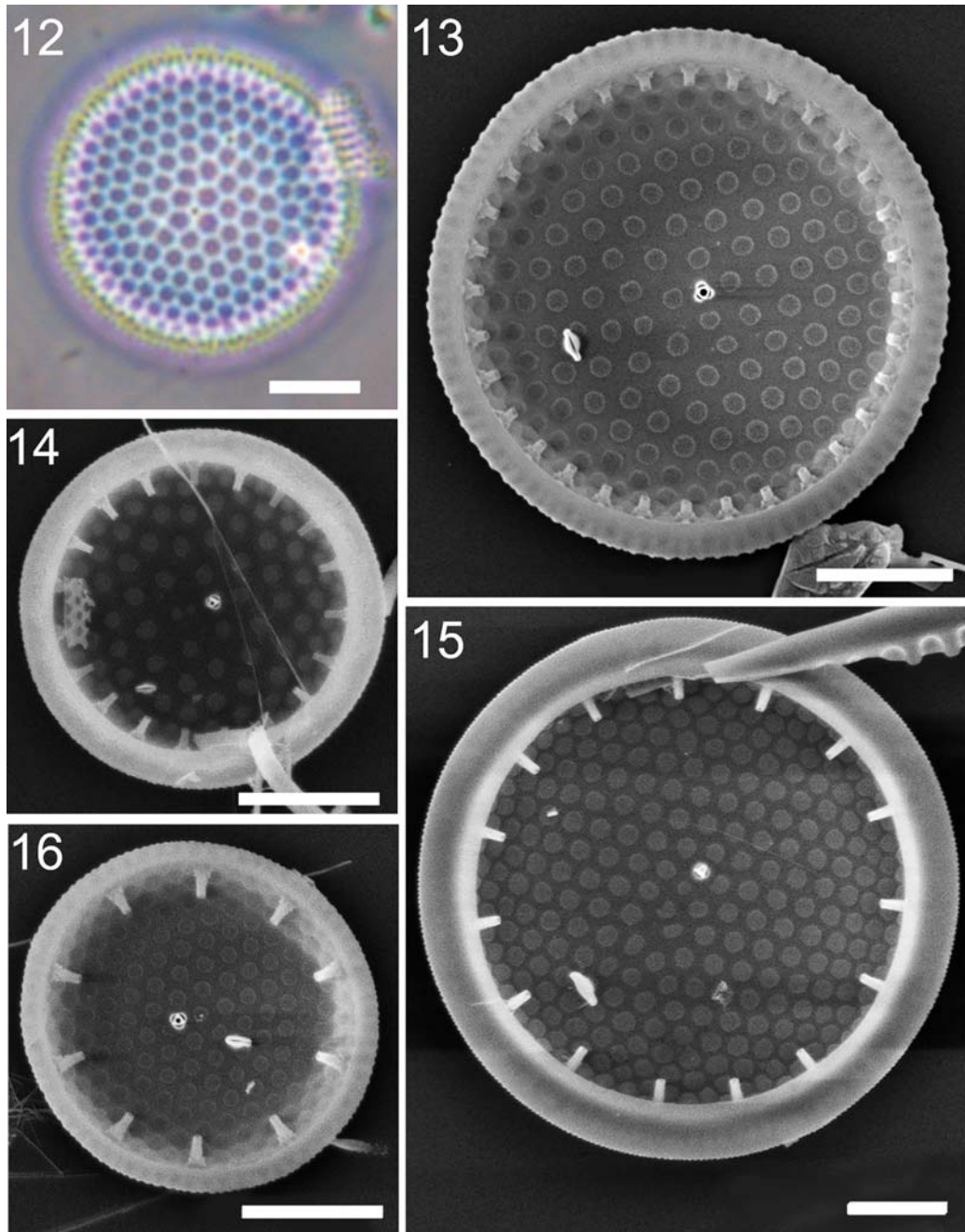
Figs 12–16. *Shionodiscus oestrupii* in light (Fig. 12) and SEM (Figs 13–16). Fig. 12. *Shionodiscus oestrupii* group, marginal processes not visible. Figs 13, 14. Internal valve views of *S. oestrupii* var. *oestrupii*, note more closely spaced marginal strutted processes. Figs 15, 16. Internal valve views of *S. oestrupii* var. *venrickae*. Note that placement of the labiate process relative to the trifultate central strutted process is variable. Scale bars represent 5 μm.

Hasle & Syvertsen 1997), with cell diameters of over 24 μm found (Table 1).

In addition to being difficult to identify under LM, the varieties of *S. gracilis* have not generally been considered worth separating taxonomically, as they most likely represent different growth stages of the same species (Fryxell 1994, Crosta et al. 2005). The nominate form, *S. gracilis* var. *gracilis*, is significantly more heavily silicified than

302   Wilks & Armand
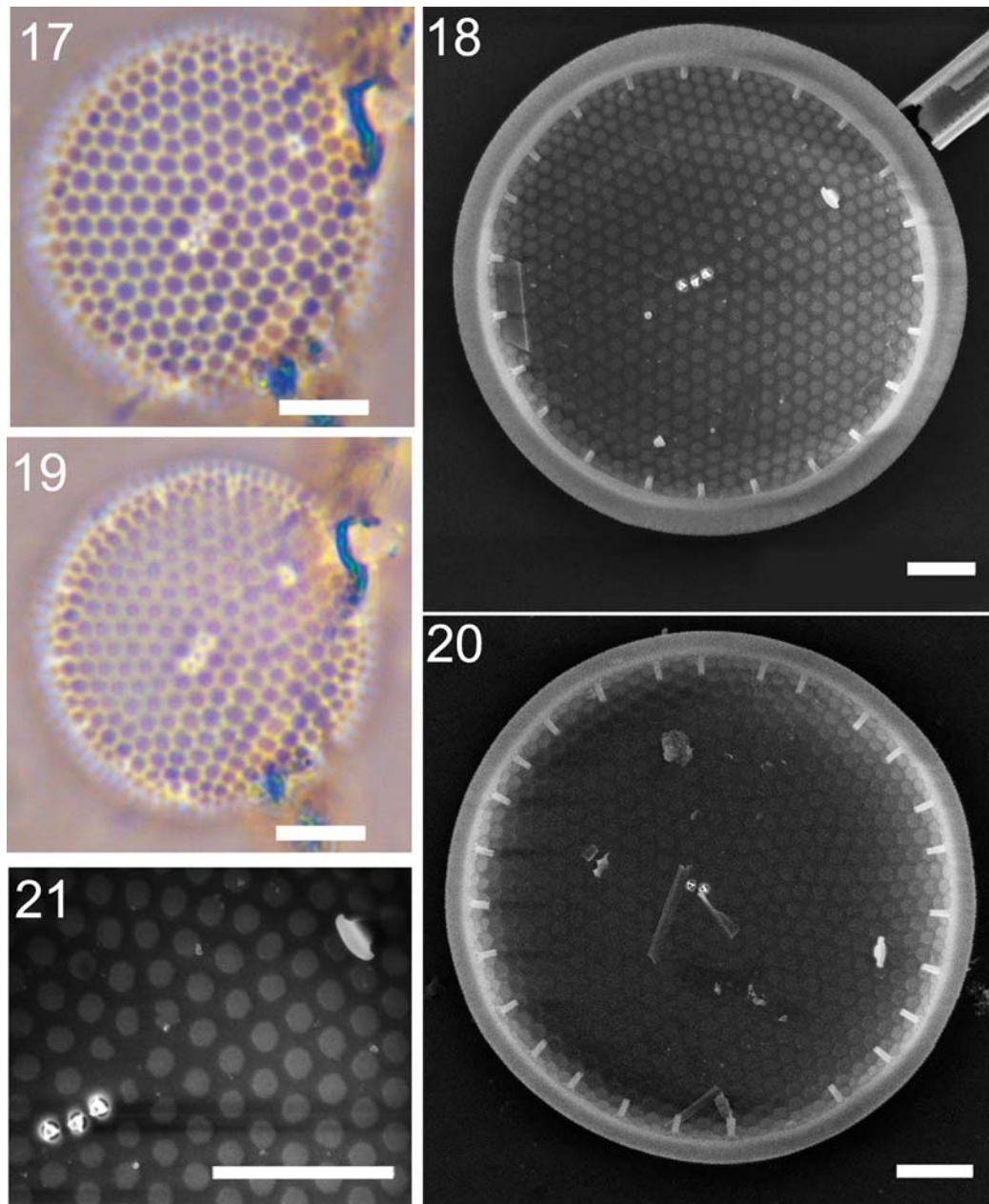
Figs 17–21. *Shionodiscus trifultus* in light (Figs 17, 19) and SEM (Figs 18, 20, 21). Figs 17, 19. *S. trifultus*. Figs 18, 20. Internal valve views of *S. trifultus* with three and two central strutted processes, respectively. Fig. 21. Close-up view of trifultate central strutted processes and labiate process. Scale bars represent 5 μm.

the finer *S. gracilis* var. *expectus*, and represents the winter variant of this species. Due to its robustness, the winter stage, *S. gracilis* var. *gracilis*, is likely to appear in greater abundances within surface waters and sediments than its summer counterpart (Fryxell 1994). This is certainly consistent with the reports of Johansen & Fryxell (1985), who

noted that *S. gracilis* var. *expectus* is less abundant than *S. gracilis* var. *gracilis*, although the two varieties have similar distributions. Aside from the tendency of the robust winter form to be better represented in sediments, and the potential over-estimation of its abundances as a result, the summer variety may be difficult to distinguish from other

morphologically similar species under LM. With LM, the fine structure of the strutted processes are not discernible, thus, given that *S. gracilis* var. *expectus* lacks the easily-distinguishable hyaline section seen in *S. gracilis* var. *gracilis*, to the less trained eye it is a potential mimic of, for example, *S. oestrupii* var. *venrickae*. This problem is solved by the use of SEM, with which the operculate process of *S. gracilis* is easily distinguished from the trifultate processes of *S. oestrupii*. If the two varieties of *S. gracilis* can be reliably discriminated, they would likely be of ecological use in paleo-reconstructions, as the ratio of summer and winter forms is indicative of the amount of growth occurring during winter periods (Fryxell 1994).

Shionodiscus oestrupii

Both *S. oestrupii* var. *oestrupii* and *S. oestrupii* var. *venrickae* were found in sediment trap records from the Australian sector of the SAZ. As with *S. gracilis*, the specimens of *S. oestrupii* observed in this study were small relative to existing size ranges reported south of the Antarctic Convergence Zone, where *S. oestrupii* var. *oestrupii* reached 60 μm diameter and *S. oestrupii* var. *venrickae* 39 μm diameter (Johansen & Fryxell 1985). A study of *Thalassiosira* diversity in tropical Australian waters also found only small *S. oestrupii* cells in water samples, with maximum diameters of 25 μm (Hallegraeff 1984).

As is the case for *S. gracilis* varieties, due to the high overlap of other distinguishing traits (Hasle & Syvertsen 1997), *S. oestrupii* varieties are difficult to differentiate under LM if the marginal processes are not visible. *Shionodiscus oestrupii* varieties have been grouped together in previous studies (Romero et al. 2005, Rigual-Hernández et al. 2015b, 2016). When visible, however, the spacing of the marginal strutted processes remains the most consistent morphological distinction between the two varieties. It is of ecological interest to distinguish the two varieties as, while they have not been confirmed as seasonal, they do appear to have different, though overlapping, distribution patterns (Fryxell & Hasle 1980). Fryxell & Hasle (1980) described *S. oestrupii* var. *oestrupii* as more cosmopolitan in distribution than *S. oestrupii* var. *venrickae*, with the former found in oceanic regions, while the latter is related to shelf and inshore environments and has been found in tropical and subtropical waters. Hallegraeff (1984) found only *S. oestrupii* var. *venrickae* in the Australian tropics. If *S. oestrupii* var. *venrickae* is linked to warm waters, then its presence in the Subantarctic could indicate the southward movement of warm, coastal waters. Hence, discrimination of the two varieties in the Subantarctic Zone could provide insights into the movement of water masses.

Shionodiscus frenguellii *and* S. trifultus

Shionodiscus frenguellii and *S. trifultus* are virtually indistinguishable under LM, and only reliably distinguishable under SEM, when the valves are viewed from the inside and both strutted and labiate processes are visible. For this reason, studies using LM diatom counts have traditionally grouped the two species together for convenience, and because species abundances were not great enough to make discriminating the two worthwhile (Wilks et al. 2017). Further, both *S. frenguellii* and *S. trifultus* may possess just one central strutted process, making them very similar to other species (e.g., *S. oestrupii* var. *venrickae*), so that the single central process forms may not even be included within the '*Shionodiscus trifultus* group'. Thus, the abundance of this species is likely to be underestimated in LM studies. The most consistent distinguishing trait between these two species, assuming the overlap of other features such as size and number of central processes, is the number of areolae between the central strutted process and labiate process. In *S. frenguellii* specimens, the labiate process is placed closer to the central strutted processes than *S. trifultus* (2–4 areolae, and 7–9 areolae apart, respectively) (Table 1; Figs 2, 18).

Both *S. frenguellii* and *S. trifultus* are typically present in cool, fresh, stratified waters (Sancetta 1983, Medlin & Priddle 1990). In this study we have confirmed, for the first time, the presence of both *S. frenguellii* and *S. trifultus* within the Australian sector of the SAZ. Although previous studies within the Australian sector have reported low relative abundances of this group, (Rigual-Hernández et al. 2015a, 2016), studies from other regions revealed a more significant presence. A sediment trap study in the Bering Sea found the *S. trifultus* group to be among the most dominant diatom group observed (Stroynowski et al. 2015).

Defining* Shionodiscus *groupings under LM

Given the difficulties in distinguishing *Shionodiscus* species, even under SEM, the use of molecular techniques to clarify the taxonomy of this genus is surely warranted. Some molecular analyses of *Shionodiscus* species have been undertaken in the northern hemisphere. Alverson et al. (2007) constructed a phylogenetic tree of 78 species in the Thalassiosirales, including *Shionodiscus ritscheri* (Hustedt) Alverson, Kang & Theriot and *S. oestrupii* var. *venrickae*. Several studies have identified *Shionodiscus bioculatus* (Grunow) Alverson, Kang & Theriot using DNA/RNA analysis techniques (Hamsher et al. 2013, Malviya et al. 2016, Balzano et al. 2017), though none within the Australian Sector. Despite this work, the majority of *Shionodiscus* species have received no attention from a molecular perspective, and there has been no molecular analysis of Southern Ocean *Shionodiscus* species. Distinguishing *Shionodiscus* species at the DNA level will be of merit in the future. Nevertheless, there is still merit in LM studies of this genus, with a more clearly defined grouping system in place for those species indistinguishable under LM. To that end, four groupings of SAZ *Shionodiscus* taxa

Table 2. *Shionodiscus* spp. groupings based on shared characteristics visible under LM.

Group name	Species/varieties included	Group features visible under LM	Group notes
Frenguellii group	*S. frenguellii* *S. frenguelliopsis* *S. trifultus* (with 1–2 CSPs)	• (12) 16–25 μm diameter • 1–2 CSPs • 1–2 MSPs in 10 μm • 7–13 + areolae in 10 μm at valve centre • Sublinear – irregularly linear areolation	Specimens matching this description, but with more than two CSPs, and/or fewer than seven areolae in 10 μm at the valve centre, are most likely *S. trifultus.*
Gracilis group	*S. gracilis* var. *gracilis* *S. gracilis* var. *expectus*	• 7–17 μm diameter • 3–4 MSPs in 10 μm • 8–20 areolae in 10 μm at valve centre	Variety *expectus* specimens tend to have much a less pronounced hyaline region at the valve centre.
Oestrupii group	*S. oestrupii* var. *oestrupii* *S. oestrupii* var. *venrickae*	• 7–39 μm diameter • 1 CSP • 6–11 areolae in 10 μm at valve centre	MSPs tend to be invisible under LM, but when visible are the main feature distinguishing the two varieties, with var. *oestrupii* having five to ten MSPs in 10 μm, and var. *venrickae* having two or three. Very small specimens with significantly larger areolae at the centre of the valve than the margin and with CSP only one or two areolae from the LP are likely var. *oestrupii*.

Note: CSP = central strutted process; MSP = marginal strutted process; LP = labiate process.

are suggested, based on taxonomic features visible under LM (Table 2). Given the current complexity of Thalassiosirales phylogeny, these groupings are likely not monophyletic, and may change as molecular work on *Shionodiscus* is undertaken. However, the groupings provide a convenient and consistent starting point to assist the separation of taxa into ecological groupings for statistical analyses in LM-based studies. The groupings presented (Table 2) are based on measurements shared by all species or varieties within the grouping. Specimens that fall outside the given ranges are deemed to be identifiable to species level.

The name '*trifultus/trifulta*' group has been used in several ways, to capture the former group 'B' species (Shiono & Koizumi 2000, Stroynowski et al. 2015), and in other studies to include only the species commonly confused with *S. trifultus* (in particular *S. frenguellii*, *S. frenguelliopsis* and *S. trifultus*) (Onodera et al. 2014, Rigual-Hernández et al. 2016). We propose that the grouping containing *S. frenguellii*, *S. frenguelliopsis* and *S. trifultus* be called the *S. frenguellii* group. Since the features that overlap under LM more reliably discriminate *S. trifultus* from the other two species, than *S. frenguelli* from *S. frenguelliopsis*, it seems more sensible to name the group in this way. Specimens matching the description of *S. frenguellii* and *S. frenguelliopsis* under LM, but with more than two central strutted processes, can be designated as *S. trifultus*, particularly if the specimens are also > 25 μm in diameter. Under SEM this group's diagnosis begins with the discernment of an operculate (e.g., *S. frenguelliopsis*), or trifultate (*S. frenguellii* and *S. trifultus*) central strutted process. Thus, '*S. frenguellii* group' is suggested to be

valid only for LM-based studies, since *S. frenguellii* and *S. frenguelliopsis* are phylogenetically distant.

As outlined earlier, the two varieties of *S. gracilis* are most likely to be different seasonal forms of the same species. They are not always impossible to distinguish under LM, however, reliable diagnoses are difficult due to overlapping diagnostic measurements of the two varieties, possibly due to the presence of intermediate forms. The hyaline central region is more pronounced in *S. gracilis* var. *gracilis*, although it is not easy to quantify this feature. Thus for more intermediary forms a *S. gracilis* group is recommended. Where possible, the varieties should be counted separately to enable the possibility of linking the ratio of the varieties to seasonal and ecological processes.

The two varieties of *S. oestrupii* are easily identified using SEM. Once the presence of a single trifultate central strutted process is confirmed, the distance between marginal strutted processes will reliably differentiate *S. oestrupii* var. *oestrupii* from *S. oestrupii* var. *venrickae*, with the former having more closely spaced marginal processes. In very small specimens particularly, the marginal processes are often not visible under LM and given the overlap between other diagnostic measurements, the only option is a broader *S. oestrupii* group.

A key to **Shionodiscus** *spp. of the Australian sector of the SAZ*

The following key has been constructed from observations and measurements made using LM and SEM analysis of *Shionodiscus* spp. in the Australian sector of the SAZ,

1a	One central or subcentral strutted process	2
1b	More than one central or subcentral strutted process	6
2a	Central strutted process is trifultate	3
2b	Central strutted process is operculate	4
3a	One or two marginal strutted processes in 10 µm	5
3b	Five to ten marginal strutted processes in 10 µm	*S. oestrupii* var. *oestrupii*
4a	One or two marginal strutted processes in 10 µm	*S. frenguelliopsis*
4b	Three or four marginal strutted processes in 10 µm	7
5a	Areolae at valve centre 1.5 or 2 times larger than at valve margin	*S. oestrupii* var. *venrickae*
5b	Areolae at valve centre not significantly larger than at valve margin	*S. frenguellii*
6a	Central strutted processes arranged in a cluster, with labiate process subcentral or halfway between valve centre and margin	*S. ritscheri*
6b	Central strutted processes arranged in one or two rows	8
7a	Areolae at valve centre surrounded by hyaline region	*S. gracilis* var. *gracilis*
7b	Areolae at valve centre not surrounded by hyaline region	*S. gracilis* var. *expectus*
8a	Labiate process four or five areolae distant from central strutted process	*S. frenguellii*
8b	Labiate process more than five areolae distant from central strutted process	9
9a	11–16 areolae in 10 µm at valve centre	*Shionodiscus poroseriatus*
9b	5–7 areolae in 10 µm at valve centre	*S. trifultus*

taken from sediment trap samples and from data within Hasle & Syvertsen (1997).

Specimens with labiate process on valve face and marginal strutted processes with internal extensions.

Conclusions

Thalassiosira is one of the most diverse and widespread diatom genera. In recent years, morphological and molecular studies have confirmed that *Thalassiosira* is a polyphyletic grouping (Alverson et al. 2007) and efforts continue to improve species characterization within the genus. *Shionodiscus*, recently separated from *Thalassiosira*, contains several morphologically similar Southern Ocean species, which are difficult to distinguish using LM alone, and are often placed in more inclusive groupings. In the Australian sector, *Shionodiscus* spp. make up a seasonally significant component of total diatom fluxes, yet the ecological significance of the genus is not well known, in part due to the difficulty of distinguishing closely related *Shionodiscus* species.

In this study, we analysed sediment trap samples from the Australian sector of the SAZ, using both LM and SEM, and described the *Shionodiscus* spp. found. Using these measurements, a new taxonomic key and three new *Shionodiscus* spp. groupings (the *S. frenguellii*, *S. gracilis* and *S. oestrupii* groups) were defined to enable future workers in the region to better identify these species using the technologies available to them.

Acknowledgements

Funding

ORCID

Jessica V. Wilks http://orcid.org/0000-0001-6217-4952

References

ALVERSON A.J., KANG S-H. & THERIOT E.C. 2006. Cell wall morphology and systematic importance of *Thalassiosira ritscheri* (Hustedt) Hasle, with a description of *Shionodiscus* gen. nov. *Diatom Research* 21: 251–262. doi:10.1080/0269249X.2006.9705667

ALVERSON A.J., JANSEN R.K. & THERIOT E.C. 2007. Bridging the Rubicon: phylogenetic analysis reveals repeated colonizations of marine and fresh waters by Thalassiosiroid diatoms. *Molecular Phylogenetics and Evolution* 45: 193–210.

BALZANO S., PERCOPO I., SIANO R., GOURVIL P., CHANOINE M., MARIE D., VAULOT D. & SARNO D. 2017. Morphological and genetic diversity of Beaufort Sea diatoms with high contributions from the *Chaetoceros*

neogracilis species complex. *Journal of Phycology* 53: 161–187.

CROSTA X., STURM A., ARMAND L. & PICHON J-J. 2004. Late Quaternary sea ice history in the Indian sector of the Southern Ocean as recorded by diatom assemblages. *Marine Micropaleontology* 50: 209–223. doi:10.1016/S0377-8398(03)00072-0

CROSTA X., ROMERO O., ARMAND L.K. & PICHON J-J. 2005. The biogeography of major diatom taxa in Southern Ocean sediments: 2. Open ocean related species. *Palaeogeography, Palaeoclimatology, Palaeoecology* 223: 66–92.

DE SALAS M.F., ERIKSEN R., DAVIDSON A.T. & WRIGHT S.W. 2011. Protistan communities in the Australian sector of the Sub-Antarctic Zone during SAZ-Sense. *Deep Sea Research Part II: Topical Studies in Oceanography* 58: 2135–2149. doi:10.1016/j.dsr2.2011.05.032

FIELD C.B., BEHRENFELD M.J., RANDERSON J.T. & FALKOWSKI P. 1998. Primary production of the biosphere: integrating terrestrial and oceanic components. *Science* 281: 237–240. doi:10.1126/science.281.5374.237

FLORES J.A. & SIERRO F.J. 1997. Revised technique for calculation of calcareous nannofossil accumulation rates. *Micropaleontology* 43: 321–324.

FRYXELL G. 1975. Three new species of *Thalassiosira*, with observations on the occluded process, a newly observed structure of diatom valves. *Beihefte zur Nova Hedwigia* 53: 57–81.

FRYXELL G. 1994. Planktonic marine diatom winter stages: Antarctic alternatives to resting spores. In: *Proceedings of the 11th International Diatom Symposium 1990* (Ed. by J.P. KOCIOLEK), pp. 437–448. California Academy of Sciences, San Francisco.

FRYXELL G. & HASLE G.R. 1972. *Thalassiosira eccentrica* (Ehrenb.) Cleve, *T. symmetrica* sp. nov., and some related centric diatoms. *Journal of Phycology* 8: 297–317.

FRYXELL G. & HASLE G.R. 1979a. The genus *Thalassiosira*: species with internal extensions of the strutted processes. *Phycologia* 18: 378–393.

FRYXELL G. & HASLE G. 1979b. The genus *Thalassiosira*: *T. trifulta* sp. nova and other species with tricolumnar supports on strutted processes. *Beihefte zur Nova Hedwigia* 64: 13–10.

FRYXELL G. & HASLE G. 1980. The marine diatom *Thalassiosira oestrupii*: structure, taxonomy and distribution. *American Journal of Botany* 67: 804–814.

HALLEGRAEFF G. 1984. Species of the diatom genus *Thalassiosira* in Australian waters. *Botanica Marina* 27: 495–514.

HAMSHER S.E., LEGRESLEY M.M., MARTIN J.L. & SAUNDERS G.W. 2013. A comparison of morphological and molecular-based surveys to estimate the species richness of *Chaetoceros* and *Thalassiosira* (Bacillariophyta), in the Bay of Fundy. *PLoS One* 8: e73521.

HASLE G.R. 1968. The valve processes of the centric diatom genus *Thalassiosira*. *Nytt Magasin for Botanik* 15: 193–201.

HASLE G.R. 1972. *Thalassiosira subtilis* (Bacillariophyceae) and two allied species. *Norwegian Journal of Botany* 19: 111–137.

HASLE G.R. 1978. Some *Thalassiosira* species with one central process (Bacillariophyceae). *Norwegian Journal of Botany* 25: 77–110.

HASLE G.R. & FRYXELL G.A. 1977. Genus *Thalassiosira*: some species with a linear areola array. *Beihefte zur Nova Hedwigia* 54: 15–66.

HASLE G.R. & SYVERTSEN E.E. 1997. *Identifying marine phytoplankton*. Academic Press, San Diego. 858 pp.

HUSTEDT F. 1958. Diatomeen aus der Antarktis und dem Südatlantik. *Deutsche Antarktische Expedition 1938/39* 2: 103–191.

JIN X., GRUBER N., DUNNE J., SARMIENTO J. & ARMSTRONG R. 2006. Diagnosing the contribution of phytoplankton functional groups to the production and export of particulate organic carbon, $CaCO_3$, and opal from global nutrient and alkalinity distributions. *Global Biogeochemical Cycles* 20: 1–17.

JOHANSEN J.R. & FRYXELL G. 1985. The genus *Thalassiosira* (Bacillariophyceae): studies on species occurring south of the Antarctic Convergence Zone. *Phycologia* 24: 155–179.

KARSTEN G. 1905. Das Phytoplankton des Antarktischen Meeres nach dem Material der deutschen Tiefsee-Expedition 1898–1899. *Deutsche Tiefsee-Expedition* 2: 1–136.

KOPCZYŃSKA E.E., DEHAIRS F., ELSKENS M. & WRIGHT S. 2001. Phytoplankton and microzooplankton variability between the subtropical and polar fronts south of Australia: thriving under regenerative and new production in late summer. *Journal of Geophysical Research: Oceans (1978–2012)* 106: 31597–31609.

KOPCZYŃSKA E.E., SAVOYE N., DEHAIRS F., CARDINAL D. & ELSKENS M. 2007. Spring phytoplankton assemblages in the Southern Ocean between Australia and Antarctica. *Polar Biology* 31: 77–88.

KOZLOVA O.G. 1967. De speciebus Bacillariophytorum novis e partibus Antarcticis Oceanorum Indici et Pacifici. *Novitates Systematicae Plantarum Non Vascularium* 1967: 54–62.

MALVIYA S., SCALCO E., AUDIC S., VINCENT F., VELUCHAMY A., POULAIN J., WINCKER P., IUDICONE D., DE VARGAS C. & BITTNER L. 2016. Insights into global diatom distribution and diversity in the world's ocean. *Proceedings of the National Academy of Sciences* 113: 1516–1525.

MEDLIN L.K. & PRIDDLE J. 1990. *Polar marine diatoms*. Lubrecht & Cramer Ltd, Cambridge. 214 pp.

NELSON D.M., TRÉGUER P., BRZEZINSKI M.A., LEYNAERT A. & QUÉGUINER B. 1995. Production and dissolution of biogenic silica in the ocean: revised global estimates, comparison with regional data and relationship to biogenic sedimentation. *Global Biogeochemical Cycles* 9: 359–372.

ONODERA J., OHASHI A., TAKAHASHI K. & HONDA M. 2014. Time-series variation of diatom valve fluxes at Station K2 in the western Subarctic Pacific. *Diatom* 30: 104–121. doi:10.11464/diatom.30.104.

ORSI A.H., WHITWORTH T. & NOWLIN W.D. 1995. On the meridional extent and fronts of the Antarctic Circumpolar Current. *Deep Sea Research Part I: Oceanographic Research Papers* 42: 641–673.

POLLARD R., LUCAS M. & READ J. 2002. Physical controls on biogeochemical zonation in the Southern Ocean. *Deep Sea Research Part II: Topical Studies in Oceanography* 49: 3289–3305.

RIGUAL-HERNÁNDEZ A., TRULL T., BRAY S., CORTINA A. & ARMAND L. 2015a. Latitudinal and temporal distributions of diatom populations in the pelagic waters of the Subantarctic and Polar Frontal Zones of the Southern Ocean and their role in the biological pump. *Biogeosciences* 12: 5309–5337.

RIGUAL-HERNÁNDEZ A.S., TRULL T.W., BRAY S.G., CLOSSET I. & ARMAND L.K. 2015b. Seasonal dynamics in diatom and particulate export fluxes to the deep sea in the Australian sector of the southern Antarctic Zone. *Journal of Marine Systems* 142: 62–74. doi:10.1016/j.jmarsys.2014.10.002

RIGUAL-HERNÁNDEZ A.S., TRULL T.W., BRAY S.G. & ARMAND L.K. 2016. The fate of diatom valves in the Subantarctic and Polar Frontal Zones of the Southern Ocean: sediment trap versus surface sediment assemblages. *Palaeogeography, Palaeoclimatology, Palaeoecology* 457: 129–143. doi:10.1016/j.palaeo.2016.06.004

RINTOUL S.R. & TRULL T.W. 2001. Seasonal evolution of the mixed layer in the Subantarctic Zone south of Australia. *Journal of Geophysical Research: Oceans* 106: 31447–31462.

ROMERO O., ARMAND L., CROSTA X. & PICHON J-J. 2005. The biogeography of major diatom taxa in Southern Ocean surface sediments: 3. Tropical/Subtropical species. *Palaeogeography, Palaeoclimatology, Palaeoecology* 223: 49–65.

SANCETTA C. 1983. Effect of Pleistocene glaciation upon oceanographic characteristics of the North Pacific Ocean and Bering Sea. *Deep Sea Research Part A. Oceanographic Research Papers* 30: 851–869.

SHIONO M. & KOIZUMI I. 2000. Taxonomy of the *Thalassiosira trifulta* group in late Neogene sediments from the northwest Pacific Ocean. *Diatom Research* 15: 355–382.

SOKOLOV S. & RINTOUL S.R. 2002. Structure of Southern Ocean fronts at 140°E. *Journal of Marine Systems* 37: 151–184.

STROYNOWSKI Z., RAVELO A.C. & ANDREASEN D. 2015. A Pliocene to recent history of the Bering Sea at Site U1340A, IODP Expedition 323. *Paleoceanography* 30: 1641–1656. doi:10.1002/2015PA002866

THERIOT E. & SERIEYSSOL K. 1994. Phylogenetic systematics as a guide to understanding features and potential morphological characters of the centric diatom family Thalassiosiraceae. *Diatom Research* 9: 429–450. doi:10.1080/0269249X.1994.9705318

TREGUER P., NELSON D.M., VAN BENNEKOM A.J. & DEMASTER D.J. 1995. The silica balance in the world ocean: a reestimate. *Science* 268: 375–379.

TRULL T., BRAY S., MANGANINI S., HONJO S. & FRANÇOIS R. 2001a. Moored sediment trap measurements of carbon export in the Subantarctic and Polar Frontal Zones of the Southern Ocean, south of Australia. *Journal of Geophysical Research: Oceans* 106: 31489–31509.

TRULL T., SEDWICK P., GRIFFITHS F. & RINTOUL S. 2001b. Introduction to special section: SAZ project. *Journal of Geophysical Research: Oceans* 106: 31425–31429.

WILKS J.V., RIGUAL-HERNÁNDEZ A.S., TRULL T.W., BRAY S.G., FLORES J-A. & ARMAND L.K. 2017. Biogeochemical flux and phytoplankton succession: a year-long sediment trap record in the Australian sector of the Subantarctic Zone. *Deep Sea Research Part I: Oceanographic Research Papers* 121: 143–159. doi:10.1016/j.dsr.2017.01.001

ZIELINSKI U. & GERSONDE R. 1997. Diatom distribution in Southern Ocean surface sediments (Atlantic sector): implications for paleoenvironmental reconstructions. *Palaeogeography, Palaeoclimatology, Palaeoecology* 129: 213–250. doi:10.1016/S0031-0182(96)00130-7

Chapter Six

Conclusions
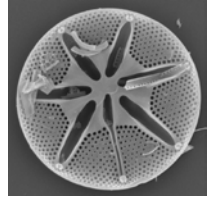
This thesis undertook to satisfy three principal aims (Fig. 1), and to concurrently help fill critical knowledge gaps in Australian and New Zealand phytoplankton fluxes and assemblages, and their significance to the wider Southern Ocean region. The aims of this thesis, the manner in which they were addressed, and the significance of the findings are discussed in the sections below.
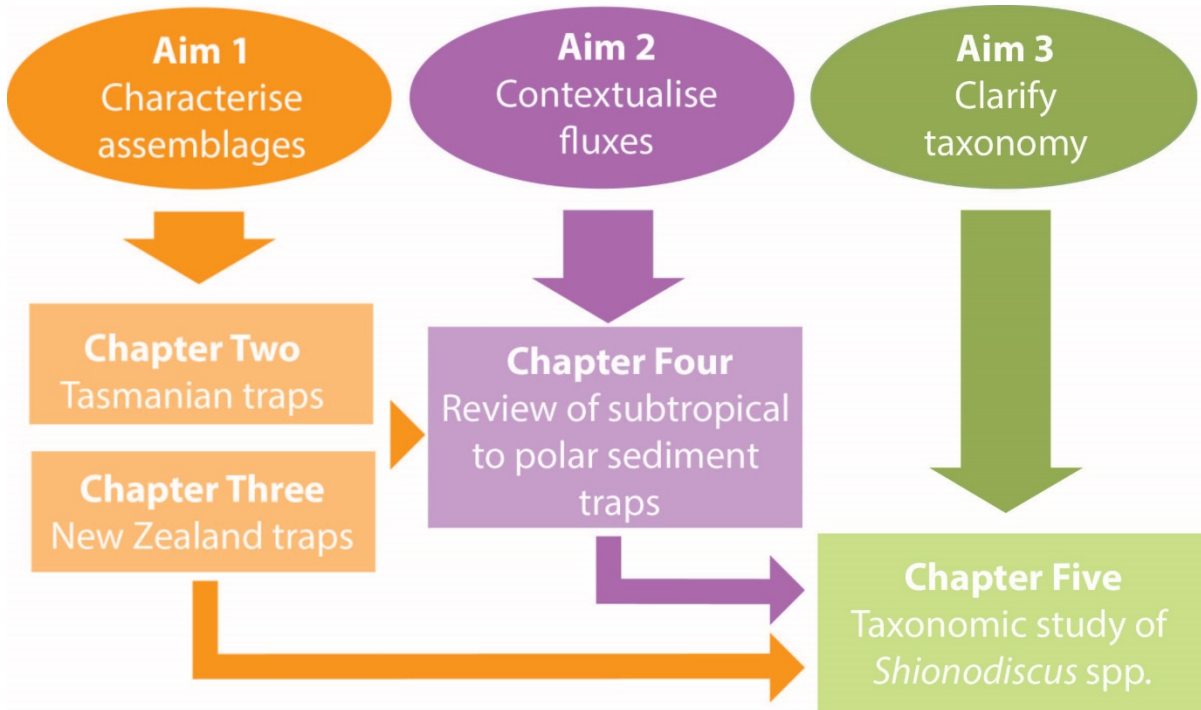

Figure 1. Schematic conclusion of this thesis, summarising the aims and relationships between the aims and chapters.

Aim One- Characterise phytoplankton assemblages

The first aim of this thesis was to characterise the diversity, abundance and seasonality of two major phytoplankton groups, diatoms and coccolithophores, from sediment trap records in two hydrologically distinct regions of the Southern Ocean. This was addressed in Chapters Two and Three.

Carbon dioxide uptake by the ocean, and subsequently carbon sequestration via export, has regulated global climate in the past, and continues to do so (Honjo et al. 2008; Landschützer et al. 2015; Gottschalk et al. 2016). Oceanic carbon export hinges upon the balance between three key pumps. These are the biological pump (exemplified by diatoms and other phytoplankton), the carbonate counter-pump (driven by calcifying phyto- and zooplankton, such as coccolithophores and foraminifera) (Riebesell et al. 2009), and the solubility pump (the movement of dissolved CO_2

in water due to physical processes) (Volk and Hoffert 1985). Knowledge of the composition and volume of export in a system is alone insufficient because:

1. different phytoplankton species are known to export varying volumes of carbon (Lam et al. 2011; Maiti et al. 2013; Leblanc et al. 2018), and

2. the assemblage composition and seasonality of phytoplankton is projected to shift in the future due to climate change (Law et al. 2017), so

3. only by comprehensive knowledge of key exporter assemblages and seasonality can we make projections about how export regimes may change, and the flow-on effects this may have on human livelihoods.

Chapter Two- The Australian sector sediment traps

Chapter Two used sediment trap data from two sediment trap depths (500 and 2000 m) south of Tasmania, obtained from 2003 to 2004. Diatoms and coccoliths were identified and counted for an annual cycle at both depths, adding value to existing data (published for the first time in this chapter) on annual bulk compound fluxes. The assemblage compositions of both diatoms and coccolithophores were characterised for both depths for the entire sample period. These data constitute three novel outcomes:

(a) these data represent the first sediment trap data in the Subantarctic Zone for which *both* diatom and coccolithophore assemblages and flux were characterised,

(b) the first seasonal record of coccolithophores in this sector, and

(c) the first seasonal record of diatoms just below the mixed layer in this sector.

Outcome (a) represents a significant and globally rare undertaking, the magnitude of which is made apparent in Chapter Five. Seasonal records of phytoplankton assemblage export are highly valuable, and even more so when from the same trap deployment. This is because phytoplankton assemblages and seasonality is highly variable both between years and on very small spatial scales (Little et al. 2018), especially at high latitudes (e.g. the Southern Ocean) (Harrison et al. 2018). Hence, even two sediment traps deployed under identical conditions in different years may capture significantly different volumes of material (Nodder et al. 2016) and assemblages (Abelmann and Gersonde 1991). For this reason, having phytoplankton and bulk compound fluxes from the same trap facilitates a more accurate way to estimate the role of different phytoplankton species in export processes during a season. In this record, coccoliths were three orders of magnitude more numerous than diatoms and, coupled with high particulate inorganic carbon flux in the same traps, indicate a strong carbonate counter-pump in the sample year.

Chapter Two also provided a valuable record of coccolithophore seasonality and flux assemblages in the Tasmanian sector (outcome b). This was, at the time of publication, only the fourth such dataset in the subtropical to polar southern hemisphere (the first three being in the Indian ocean sector near Kerguelen Island (Ternois et al. 1998), the Humboldt Current System off Chile (González et al. 2004), and the Namibia Upwelling system west of Africa (Romero and Hensen 2002)). Coccolith flux seasonality is poorly understood in the Southern Ocean, even though export is carbonate-related (i.e. the "Carbonate Ocean") in waters north of the Polar Front (Honjo et al. 2008). Thus outcome (b) also allowed a preliminary assessment of coccolithophore ecological succession, revealing two seasonal ecological groupings throughout the sample period: those species associated with day length, and those taxa with high abundances year-round or outside of the main productive season. Such data is crucial for developing a taxon-specific scheme of coccolithophore succession comparable to existing schemes for diatoms.

Regarding outcome (c), the mixed layer is the surface of the upper layers of the ocean that is considered homogenous in nutrients, temperature and salinity due to turbulence (Mellor and Durbin 1975). Particles are not considered "exported" until they have passed through the mixed layer (at minimum, though many studies extend export definitions to the base of the twilight zone), and so are unlikely to be mixed back to the surface (Ducklow et al. 2001; Buesseler and Boyd 2009). At the Tasmanian trap site, the mixed layer was particularly deep, up to 600 m in winter (Rintoul and Trull 2001), and thus shallow sediment traps may not reflect true export processes. The deployment of traps just below, or within the base of the mixed layer, and deeper traps at 2000 m (this study), and 1000 m (Rigual-Hernández et al. 2015) allow for a comprehensive comparison of particle flux attenuation at various depths.

Chapter Three- The New Zealand sector sediment traps

Chapter Three followed a similar model to Chapter Two, whereby diatoms and coccolithophores were identified and counted for an annual record (1996-1997), this time at two sites in different water masses east of New Zealand. The North Chatham Rise site (NCR) sampled subtropical waters, while the South Chatham Rise site (SCR) was moored in Subantarctic waters. Both moorings contained traps at 300 and 1000 m depths, and diatom flux was calculated for all four records, but coccolith flux was calculated for the 300 m traps only due to time constraints. The key outcomes of this chapter were as follows. These data represent:

(a) first sediment trap data of diatom and coccolith flux and assemblage seasonality north and south of the productive Chatham Rise, and first record of coccolith fluxes from sediment traps in the New Zealand sector,

(b) substantiating evidence for significant coastal and benthic input to the North Chatham Rise, and

(c) identification of a short, monogeneric "pulse" bloom event as a major particle flux source South of Chatham Rise.

The samples used in Chapter Three were archival, and the bulk compound fluxes were calculated and published by Nodder and Northcote (2001). Additionally, alkenone fluxes (temperature markers, and indicators for some phytoplankton) (Sikes et al. 2005), and current dynamics (Chiswell 2001) were published. However, phytoplankton fluxes had not yet been calculated, and the good preservation of these samples, despite gaps in the record, made it feasible to do so (outcome a).

The Chatham Rise supports several key New Zealand fisheries (Clark 2001). Characterisation of phytoplankton fluxes (as the base of the marine food web) is of importance to fisheries management. In addition, this research provides the first record of coccolith fluxes and seasonality in New Zealand waters, and represents only the fifth publication on coccolith fluxes in the southern hemisphere south of 30° S. The New Zealand and Tasmanian traps employed similar trap designs, deployment and processing methods, and occupied roughly the same latitude, but spanned different hydrological zones. This allowed for some novel comparisons of fluxes in the two sectors.

A key result of Chapter Three was persuasive evidence corroborating previous reports of the advection of coastal waters to the Chatham Rise (outcome b), as demonstrated by oceanographic observations (Chiswell et al. 2015), trace metal circulation (Ellwood et al. 2014), seafloor sediment contents (Cochran and Neil 2009), and terrigenous material captured by nearby sediment trap deployments (Nodder et al. 2005; Nodder et al. 2016). Prior to the results of this research, the presence of coastal and benthic taxa, and importantly, the seasonality of their input, had not been directly observed from sediment trap records. Considering the importance of the region to carbon export (Currie and Hunter 1998), knowledge of the sources of export fluxes in this region will be crucial to deciphering how export may change.

Analysis of diatom assemblages revealed the overwhelming bulk of diatom export at the South Chatham Rise site was contributed by a transitory *Pseudo-nitzschia* spp. pulse event, associated with a spike in silica flux; outcome (c). *Pseudo-nitzschia* spp. are well documented in New Zealand waters, but primarily in their capacity as contributors to harmful algal blooms (Rhodes et al. 2013). *Pseudo-nitzschia* bloom events may go unnoticed as these diatoms can preferentially grow at the base of the mixed layer (Seegers et al. 2015), and escape remote observations of oceanic chlorophyll-*a* concentration. Circumstantial evidence of the significance of sub-surface blooming

phytoplankton is offered by a long-term, 11-year sediment trap record, in which several years' flux capture appeared uncoupled to remote chlorophyll-*a* observations (Nodder et al. 2016). This study provides a compelling argument for the characterisation of phytoplankton fluxes, in order to identify key export taxa that may be underrepresented using other sampling methods.

Aim Two- Contextualise phytoplankton fluxes

In attempting to place the outcomes of Chapters Two and Three into the wider context of the Southern Ocean (Aim Three), it became clear that a synthesis of sediment trap deployments, and an analysis of all current data on diatom and coccolith fluxes in this region had not been previously undertaken. Since phytoplankton flux varies over small spatial scales and between years, a sediment trap in isolation yields limited information about typical export regimes or seasonal succession. When placed into the context of sediment trap results elsewhere, patterns may emerge to give insights into the main drivers of flux in different oceanic systems. Indeed, Chapter Five reveals some interesting patterns in diatom flux in the Southern Hemisphere not previously been visualised. The outcomes of Chapter Five were:

(a) the first synthesis of diatom and coccolith fluxes from published sediment trap records between the subtropics and Antarctica,

(b) the first attempt to model diatom flux data with remotely-sensed environmental parameters to derive drivers of flux, and

(c) commentary on sediment trapping with recommendations towards improving comparability of future trap data.

In Chapter Five, all available data on diatom flux (44 sediment trap moorings) and coccolith flux (six sediment trap moorings) from 30° S to Antarctica were compiled. The data were normalized to flux m^{-2} y^{-1} and/or maximum spring flux m^{-2} d^{-1}, depending on availability and length of deployment, $\log_{10}$ transformed, and mapped; outcome (a). In doing so, a trend of increasing diatom flux south of the Polar Front, the mixing point of subantarctic and Antarctic water masses, was revealed. This trend is nearly universal for the Southern Ocean, with some exceptions in the Ross and Weddell Seas that are potentially the result of differences in methodologies or preservability of diatom assemblages.

Outcome (b) attempted to identify which environmental features were driving the trend in diatom fluxes in this dataset. To do this, satellite-derived environmental data were obtained for every mooring site, and were grouped according to their potential influence on diatom fluxes. Nutrient concentrations (nitrate, phosphate, silicate and iron) control the amount of primary production, and hence the volume of production exported. Sea Surface Temperature and oxygen concentration

were chosen as variables controlling the speed of remineralization in the water column, which is inversely related to export (Laufkötter et al. 2017). Chlorophyll-a concentration was included as a measure of actual mean primary production (excluding sub-surface production). Finally, Particulate Inorganic Carbon concentration was used as a proxy for the abundance of calcifying phytoplankton, as well as ballast availability, a key export efficiency-related variable (Weber et al., 2016). Nitrate and phosphate, followed by temperature and oxygen, were identified as key indicators of diatom flux in this dataset. These results are of great interest for several reasons, not least of which being that millions of dollars' worth of sediment trap deployments had never been compiled and analysed in this manner before. In the past two or three years there have been several reviews and modelling efforts to try and decipher particle flux patterns in different oceans, although they have exclusively focused on bulk fluxes (e.g. organic carbon flux), not phytoplankton fluxes. Thus the impending publication of this Chapter is timely, serving to elucidate regional drivers of flux, and identify where further collecting efforts are needed.

The compilation and modelling of diatom fluxes was a deceptively difficult task, given that many of the deployments employed very different methodologies, and often presented the flux data in different formats. Methodologically, phytoplankton fluxes recorded can be influenced by the type of sediment trap used (e.g. conical, funnel shaped, moored or drifting) (Gust et al. 1994; Buesseler et al. 2000), poisoning method (Hedges et al. 1993), deployment depth (Buesseler et al. 2007), and post-collection processing (e.g. sieving, hand-picking) (Chiarini et al. 2013). Given the multitude of considerations in methodology, those studies that used consistent trap and processing techniques were particularly valuable, as were the rarer multi-year sediment trap studies. Sediment trap deployments of several years' duration, particularly in poorly sampled regions, is suggested as the ultimate aim of all future Southern Ocean trapping efforts to better constrain and understand phytoplankton fluxes in the southern hemisphere; outcome (c).

Aim Three- Clarify diatom taxonomy

Sediment trap records reveal that it is not the total volume of production but the phytoplankton assemblages involved that control the quantity of carbon export (Lam et al. 2011; Maiti et al. 2013; Leblanc et al. 2018). Diatom assemblage composition, for example, may influence whether a bloom primarily exports carbon or silica (Tréguer et al. 2018), which may also be seasonal, as silica- and carbon-sinking diatoms appear to display ecological succession both in the Southern Ocean and elsewhere (Margalef 1978; Quéguiner 2013). Accurate identification of diatom taxa in sediment traps is essential to the understanding of the contribution of different species to total flux. Further research is required to differentiate diatom species, and their functional roles in export using

traditional taxonomic techniques because the nature of sediment trapping frequently precludes the preservation of genetic material.

During microscopic analysis of data documented in Chapter Two, some taxa were not distinguishable using light microscopy. To determine which taxa were present, some samples were imaged using scanning electron microscopy, which revealed the genus *Shionodiscus* as a common taxon in the samples. Several *Shionodiscus* spp. are not reliably distinguishable under light microscopy due to overlapping morphological characteristics. To remedy this, the second aim of this thesis was to provide a description of the poorly-known diatom genus *Shionodiscus* from the Australian sector, with a clarification of its taxonomic status. The key outcomes were:

(a) the diversity of *Shionodiscus* spp. in Australian waters was characterised for the first time,

(b) a key to *Shionodiscus* was produced, distinguishing between features visible using different imaging techniques, and

(c) recommendations for a systematic method of grouping *Shionodiscus* species for counting when species-level identification is impossible or infeasible.

Chapter Two revealed that *Shionodiscus* diatoms comprised, together, ~10% of sinking diatom assemblages, suggesting a significant role in export. Because of outcome (a), the diversity of *Shionodiscus* in this sector was illuminated, with four *Shionodiscus* species or varieties observed, including two species, *Shionodiscus frenguellii* (A.J. Alverson, S.H. Kang & E.C. Theriot, 2006) and *Shionodiscus trifultus* ((G. Fryxell) A.J. Alverson, S.H. Kang & E.C. Theriot, 2006) that are rarely distinguished from one another in assemblage analyses due to similarity of morphology.

To aid future studies, including identifying *Shionodiscus* specimens encountered in Chapter Three, a new key was created for Australian sector *Shionodiscus* diatoms, including those not encountered in this study, but often considered morphologically similar. *Shionodiscus* spp. captured in sediment traps represented smaller size classes, and in some cases, minimum cell diameter was less than that reported in some key taxonomic texts (such as Tomas 1997). Outcomes (a) and (b) are thus valuable for taxonomists and will aid future attempts to calculate fluxes.

Due to difficulties in identifying *Shionodiscus*, most studies using light microscopy placed morphologically similar, or specimens too small to visualise, into broad groupings (e.g. "Frenguellii group"- those *Shionodiscus* species with features overlapping with*,* but not necessarily actually *S. frenguellii*). However, there is was standardised convention on grouping species. Further, publications were found employing different nomenclatural methods (Onodera et al. 2014; Stroynowski et al. 2015). Thus, outcome (c) created a standard and logical naming convention,

allowing comparability between future taxonomic studies, whether employing light or scanning electron microscopy.

Future Directions

With atmospheric CO_2 concentrations increasing, the need for a thorough understanding of carbon cycling in the global ocean is pressing. Sediment traps provide a well-tested means to quantify oceanic carbon flux via the biological pump, as well as determining flux timing and composition. They are, however, costly to deploy and retrieve, and analyses of phytoplankton fluxes require significant taxonomic expertise and time. Perhaps consequent to this, and as demonstrated in the compilation of such studies undertaken in Chapter Five, it appears that the height of sediment trap usage in the Southern Ocean was in the late 1990s and that their popularity as a tool has declined (Fig. 2). The year 1997 saw 16 sediment trap new or continuing multi-year deployments in the Southern Ocean, but there have been no new or continued deployments published since 2013.
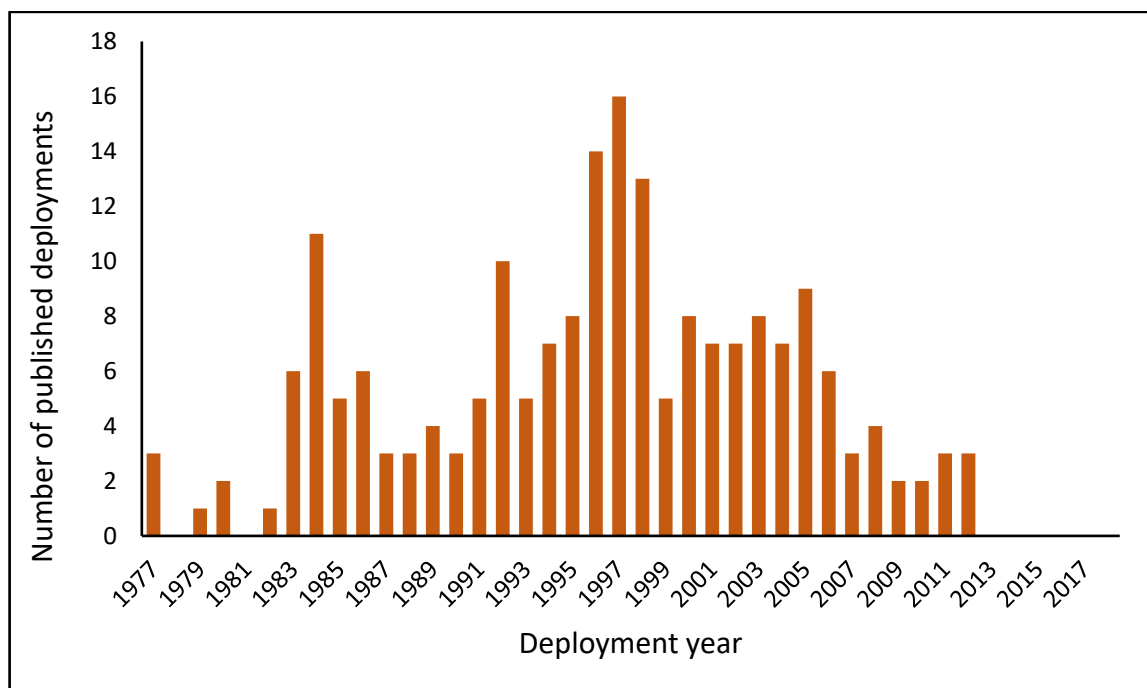
Figure 2. Number of sediment trap deployments, new or continuing and reported in publications, in the Southern Ocean between the earliest recorded trap (1977) and the present (2018). It is noted that there is at least one continuing sediment trap record in the Southern Ocean, of about 20-years duration, and the longest in the southern hemisphere at the Southern Ocean Time Series station (SOTS). However, not yet published, it is not included in the figure.

Despite declining use, there is much to be gained from sediment trap records, particularly in the under-sampled regions of the Southern Ocean. Current uncertainties over the future of the Southern Ocean biological pump under elevated CO_2 and temperature indicate that increased

understanding of the processes involved in carbon export would be highly valuable. In particular, future efforts should:

1. Systematically span hydrological zones and target under-sampled regions.
2. Consistently employ current best practice standard methodologies.
3. Include surface-to-seafloor characterisation of water column.
4. Attempt to quantify the influence of zooplankton grazing on cell carbon export.

Recommendation 1:

Chapter Five revealed that approximately 30% of the Southern Ocean has never been subject to sediment trap sampling in either open-ocean or coastal systems (e.g. the central Pacific and central Indian sectors). Instead, most sediment trap deployments have been undertaken near the coast and in areas known to be high in productivity. However, since most of the Southern Ocean exhibits low phytoplankton biomass accumulation (data via satellite; Chapter Five, Fig. 1), representative sampling of the Southern Ocean necessitates sampling in low-productivity, open-ocean systems in addition to the coast/shelf. Sediment trap deployments in the central Pacific and south-central Indian sector should be considered a priority. Further, deployments spanning several hydrological zones, particularly multi-year records, will be of greatest value, such as the AESOPS trap deployments in the New Zealand sector (Honjo et al. 2000).

Recommendation 2:

The most recent sediment trap deployments in the Southern Ocean have been undertaken using similar methodologies, and are thus highly comparable (e.g. AESOPS, SOTS, KERFIX). This is in large part thanks to the efforts of the Joint Global Ocean Flux Study (JGOFS), which, at the height of interest in sediment traps (in the late 1980s to 1990s), attempted to institute certain standardised protocols for sediment trap deployments and processing (US GOFS, 1989; Knap et al., 1996). As a result of JGOFS, it was demonstrated that the oceanic carbon cycle is more complex than was known or expected (Denman and Pena 2000). Future deployments in the Southern Ocean would benefit from the direction of a similar governing body to ensure systematic efforts, to derive the greatest possible value from each deployment.

Recommendation 3:

Particle fluxes attenuate between the surface and seafloor due to particle remineralization and consumption in the water column (Buesseler and Boyd 2009). Consequently, surface, water column and seafloor assemblages are not the same: and sediment traps and seafloor sediment are often enriched with taxa that are most resistant to consumption, breakage or dissolution (Grigorov

et al. 2014; Rigual-Hernández et al. 2016). This is well illustrated by Rembauville et al. (2016), who compared surface, sediment trap and seafloor abundances of key diatom taxa, demonstrating the increasing dominance of the more robust frustules from surface to seafloor. Future studies will ideally attempt to characterise export and sedimentation from the surface to the seafloor combining various methodological approaches. This could be achieved by combining sediment trap flux records at several depths with phytoplankton and zooplankton standing stock community characterisation and cell density, and seafloor assemblage analysis.

Recommendation 4:

One key outcome of JGOFS was the identification that zooplankton exert considerable control over phytoplankton fluxes. The role of zooplankton in controlling phytoplankton fluxes and preserved assemblages should not be overlooked: this was emphasised by Honjo et al. (2008) in their review. Analyses of the ratio of full:empty cells from sediment trap material may be used to estimate the influence of zooplankton grazing, and, combined with knowledge of cell volumes, to calculate actual carbon exported by taxa (Assmy et al. 2013; Rembauville et al. 2016). This is a realistic goal, particularly in the Australian sector, where considerable efforts have been made to characterise diatom diversity and cell biomass in a comprehensive database (Davies et al. 2017). In older samples, however, this may not always be possible. For example, samples stored in unbuffered formalin may see significant dissolution of both carbonate and silicate fractions (Hedges et al. 1993), making both bulk compound and phytoplankton flux estimates impossible. In the case of older studies, traps were often deployed without preservatives (McMinn 1996; Schloss et al. 1999), leading to sample degradation, and rendering estimates of full:empty cells infeasible. Further, carbon-destructive processing methods (such as were employed in this thesis) also preclude such analyses. Where possible, analyses of full:empty cells in existing archival or future trap records is highly recommended.

Concluding remarks

Even in the absence of new deployments, in fridges and freezers spanning the globe there are bottles and boxes of archival sediment trap material suitable for phytoplankton flux analyses which have lain untouched for years or even decades. Each sediment trap record retrieved is the result of great cost, effort and planning on the part of researchers. From this perspective, sediment tap records should be utilized to their utmost value.

In this thesis, significant value was derived from 15 and 20-year-old archival sediment trap material. By analysing diatom and coccolithophore assemblages, insights were gained on particle sources, succession, and export whereas these samples would otherwise have languished, unused. This

thesis demonstrates that both sediment trapping and phytoplankton assemblage analyses are worthwhile and relevant, and will remain a useful investment of research resources and funds in the future.

References

Abelmann A, Gersonde R (1991) Biosiliceous particle flux in the Southern Ocean. Marine
    Chemistry **35**:503-536.

Assmy P, Smetacek V, Montresor M, Klaas C, Henjes J, Strass VH, Arrieta JM, Bathmann U, Berg
    GM, Breitbarth E (2013) Thick-shelled, grazer-protected diatoms decouple ocean carbon
    and silicon cycles in the iron-limited Antarctic Circumpolar Current. Proceedings of the
    National Academy of Sciences **110**:20633-20638.

Balch WM, Bates NR, Lam PJ, Twining BS, Rosengard SZ, Bowler BC, Drapeau DT, Garley R,
    Lubelczyk LC, Mitchell C, Rauschenberg S (2016) Factors regulating the Great Calcite Belt
    in the Southern Ocean and its biogeochemical significance. Global Biogeochemical Cycles
    30:1124-1144. doi:10.1002/2016GB005414

Buesseler KO, Antia AN, Chen M, Fowler SW, Gardner WD, Gustafsson O, Harada K, Michaels AF,
    Rutgers van der Loeff M, Sarin M (2007) An assessment of the use of sediment traps for
    estimating upper ocean particle fluxes. Journal of Marine Research **65**:345-416.

Buesseler KO, Boyd PW (2009) Shedding light on processes that control particle export and flux
    attenuation in the twilight zone of the open ocean. Limnology and Oceanography
    54:1210-1232. doi:10.4319/lo.2009.54.4.1210

Buesseler KO, Steinberg DK, Michaels AF, Johnson RJ, Andrews JE, Valdes JR, Price JF (2000) A
    comparison of the quantity and composition of material caught in a neutrally buoyant
    versus surface-tethered sediment trap. Deep Sea Research Part I: Oceanographic
    Research Papers **47**:277-294.

Chiarini F, Capotondi L, Dunbar RB, Giglio F, Mammì I, Mucciarone DA, Ravaioli M, Tesi T,
    Langone L (2013) A revised sediment trap splitting procedure for samples collected in the
    Antarctic sea. Methods in Oceanography **8**:13-22.
    doi:https://doi.org/10.1016/j.mio.2014.05.003

Chiswell SM (2001) Eddy energetics in the subtropical front over the Chatham Rise, New Zealand.
    New Zealand Journal of Marine and Freshwater Research **35**:1-15.
    doi:10.1080/00288330.2001.9516975

Chiswell SM, Bostock HC, Sutton PJH, Williams MJM (2015) Physical oceanography of the deep
    seas around New Zealand: a review. New Zealand Journal of Marine and Freshwater
    Research **49**:286-317. doi:10.1080/00288330.2014.992918

Clark M (2001) Are deepwater fisheries sustainable?—the example of orange roughy (*Hoplostethus atlanticus*) in New Zealand. Fisheries Research **51**:123-135.

Cochran U, Neil H (2009) Diatom (< 63μm) distribution offshore of eastern New Zealand: Surface sediment record and temperature transfer function. Marine Geology **270**:257-271.

Currie KI, Hunter KA (1998) Surface water carbon dioxide in the waters associated with the subtropical convergence, east of New Zealand. Deep Sea Research Part I: Oceanographic Research Papers **45**:1765-1777.

Denman K, Pena M (2000) Beyond JGOFS. The changing ocean carbon cycle: a midterm synthesis of the Joint Global Ocean Flux Study **5**:469-490.

Ducklow HW, Steinberg DK, Buesseler KO (2001) Upper ocean carbon export and the biological pump. Oceanography **14**:50-58.

Ellwood MJ, Nodder SD, King AL, Hutchins DA, Wilhelm SW, Boyd PW (2014) Pelagic iron cycling during the subtropical spring bloom, east of New Zealand. Marine Chemistry **160**:18-33. doi:https://doi.org/10.1016/j.marchem.2014.01.004

GOFS, Global Ocean Flux Study (1989) Sediment Trap Technology and Sampling, In: Wilford D. Gardner (ed) Report of the U.S. GOFS Working Group on Sediment Trap Technology and Sampling. U.S. GOFS Planning Report No. 10.

González HE, Hebbeln D, Iriarte JL, Marchant M (2004) Downward fluxes of faecal material and microplankton at 2300m depth in the oceanic area off Coquimbo (30 S), Chile, during 1993–1995. Deep Sea Research Part II: Topical Studies in Oceanography **51**:2457-2474.

Gottschalk J, Skinner LC, Lippold J, Vogel H, Frank N, Jaccard SL, Waelbroeck C (2016) Biological and physical controls in the Southern Ocean on past millennial-scale atmospheric CO2 changes. Nature Communications **7**:11539. doi:10.1038/ncomms11539

Grigorov I, Rigual-Hernandez AS, Honjo S, Kemp AE, Armand LK (2014) Settling fluxes of diatoms to the interior of the Antarctic circumpolar current along 170 W. Deep Sea Research Part I: Oceanographic Research Papers **93**:1-13.

Gust G, Michaels AF, Johnson R, Deuser WG, Bowles W (1994) Mooring line motions and sediment trap hydromechanics: in situ intercomparison of three common deployment designs. Deep Sea Research Part I: Oceanographic Research Papers **41**:831-857. doi:https://doi.org/10.1016/0967-0637(94)90079-5

Harrison CS, Long MC, Lovenduski NS, Moore JK (2018) Mesoscale Effects on Carbon Export: A Global Perspective. Global Biogeochemical Cycles **32**:680-703. doi:10.1002/2017GB005751

Hedges JI, Lee C, Wakeham SG, Hernes PJ, Peterson ML (1993) Effects of poisons and preservatives on the fluxes and elemental compositions of sediment trap materials. Journal of Marine Research **51**:651-668.

Honjo S, Francois R, Manganini S, Dymond J, Collier R (2000) Particle fluxes to the interior of the Southern Ocean in the Western Pacific sector along 170°W. Deep Sea Research Part II: Topical Studies in Oceanography **47**:3521-3548. doi:http://dx.doi.org/10.1016/S0967-0645(00)00077-1

Honjo S, Manganini SJ, Krishfield RA, Francois R (2008) Particulate organic carbon fluxes to the ocean interior and factors controlling the biological pump: A synthesis of global sediment trap programs since 1983. Progress in Oceanography **76**:217-285. doi:https://doi.org/10.1016/j.pocean.2007.11.003

Knap A, Michaels A, Close A, Ducklow H, Dickson A (1996) Protocols for the joint global ocean flux study (JGOFS) core measurements. In: JGOFS Report No. 19. Reprint of the IOC Manuals and Guides No. **29**:155–162.

Lam PJ, Doney SC, Bishop JK (2011) The dynamic ocean biological pump: Insights from a global compilation of particulate organic carbon, CaCO3, and opal concentration profiles from the mesopelagic. Global Biogeochemical Cycles **25**:GB3009, doi:10.1029/2010GB003868.

Landschützer P, Gruber N, Haumann FA, Rödenbeck C, Bakker DCE, van Heuven S, Hoppema M, Metzl N, Sweeney C, Takahashi T, Tilbrook B, Wanninkhof R (2015) The reinvigoration of the Southern Ocean carbon sink. Science **349**:1221-1224. doi:10.1126/science.aab2620

Laufkötter C, John J, Stock C, Dunne J (2017) Temperature-dependent remineralization of organic matter-small impacts on the carbon cycle. In: EGU General Assembly Conference Abstracts, 13769.

Law CS, Rickard GJ, Mikaloff-Fletcher SE, Pinkerton MH, Behrens E, Chiswell SM, Currie K (2017) Climate change projections for the surface ocean around New Zealand. New Zealand Journal of Marine and Freshwater Research:1-27. doi:10.1080/00288330.2017.1390772

Leblanc K, Quéguiner B, Diaz F, Cornet V, Michel-Rodriguez M, de Madron XD, Bowler C, Malviya S, Thyssen M, Grégori G (2018) Nanoplanktonic diatoms are globally overlooked but play a role in spring blooms and carbon export. Nature Communications **9**:953.

Little HJ, Vichi M, Thomalla SJ, Swart S (2018) Spatial and temporal scales of chlorophyll variability using high-resolution glider data. Journal of Marine Systems **187**:1-12. doi:https://doi.org/10.1016/j.jmarsys.2018.06.011

Maiti K, Charette MA, Buesseler KO, Kahru M (2013) An inverse relationship between production and export efficiency in the Southern Ocean. Geophysical Research Letters **40**:1557-1561. doi:10.1002/grl.50219

Margalef R (1978) Life-forms of phytoplankton as survival alternatives in an unstable environment. Oceanologica acta **1**:493-509.

McMinn A (1996) Preliminary investigation of the contribution of fast-ice algae to the spring phytoplankton bloom in Ellis Fjord, eastern Antarctica. Polar Biology **16**:301-307.

Mellor G, Durbin P (1975) The structure and dynamics of the ocean surface mixed layer. Journal of Physical Oceanography **5**:718-728

Nodder SD, Boyd PW, Chiswell SM, Pinkerton MH, Bradford-Grieve JM, Greig MJ (2005) Temporal coupling between surface and deep ocean biogeochemical processes in contrasting subtropical and subantarctic water masses, southwest Pacific Ocean. Journal of Geophysical Research: Oceans **110:** C12017, doi:10.1029/2004JC002833

Nodder SD, Chiswell SM, Northcote LC (2016) Annual cycles of deep-ocean biogeochemical export fluxes in subtropical and subantarctic waters, southwest Pacific Ocean. Journal of Geophysical Research: Oceans **121**:2405-2424. doi:10.1002/2015JC011243

Nodder SD, Northcote LC (2001) Episodic particulate fluxes at southern temperate mid-latitudes (42–45°S) in the Subtropical Front region, east of New Zealand. Deep Sea Research Part I: Oceanographic Research Papers **48**:833-864. doi:http://dx.doi.org/10.1016/S0967-0637(00)00062-5

Onodera J, Ohashi A, Takahashi K, C. Honda M (2014) Time-series variation of diatom valve fluxes at Station K2 in the western Subarctic Pacific. Diatom **30**:104-121. doi:10.11464/diatom.30.104

Quéguiner B (2013) Iron fertilization and the structure of planktonic communities in high nutrient regions of the Southern Ocean. Deep Sea Research Part II: Topical Studies in Oceanography **90**:43-54. doi:http://dx.doi.org/10.1016/j.dsr2.2012.07.024

Rembauville M, Manno C, Tarling GA, Blain S, Salter I (2016) Strong contribution of diatom resting spores to deep-sea carbon transfer in naturally iron-fertilized waters downstream of

South Georgia. Deep Sea Research Part I: Oceanographic Research Papers **115**:22-35. doi:https://doi.org/10.1016/j.dsr.2016.05.002

Rhodes L, Jiang W, Knight B, Adamson J, Smith K, Langi V, Edgar M (2013) The genus *Pseudo-nitzschia* (Bacillariophyceae) in New Zealand: analysis of the last decade's monitoring data. New Zealand Journal of Marine and Freshwater Research **47**:490-503.

Riebesell U, Körtzinger A, Oschlies A (2009) Sensitivities of marine carbon fluxes to ocean change. Proceedings of the National Academy of Sciences **106**:20602-20609. doi:10.1073/pnas.0813291106

Rigual-Hernández A, Trull T, Bray S, Cortina A, Armand L (2015) Latitudinal and temporal distributions of diatom populations in the pelagic waters of the Subantarctic and Polar Frontal Zones of the Southern Ocean and their role in the biological pump. Biogeosciences **12**:5309-5337. doi:10.5194/bg-12-5309-2015

Rigual-Hernández AS, Trull TW, Bray SG, Armand LK (2016) The fate of diatom valves in the Subantarctic and Polar Frontal Zones of the Southern Ocean: Sediment trap versus surface sediment assemblages. Palaeogeography, Palaeoclimatology, Palaeoecology **457**:129-143. doi:http://dx.doi.org/10.1016/j.palaeo.2016.06.004

Rintoul SR, Trull TW (2001) Seasonal evolution of the mixed layer in the Subantarctic Zone south of Australia. Journal of Geophysical Research: Oceans **106**:31447-31462.

Romero O, Hensen C (2002) Oceanographic control of biogenic opal and diatoms in surface sediments of the Southwestern Atlantic. Marine Geology **186**:263-280. doi:http://dx.doi.org/10.1016/S0025-3227(02)00210-4

Schloss IR, Ferreyra GA, Mercuri G, Kowalke J (1999) Particle flux in an Antarctic shallow coastal environment: a sediment trap study. Scientia Marina **63**:99-111.

Seegers BN, Birch JM, Marin R, Scholin CA, Caron DA, Seubert EL, Howard MDA, Robertson GL, Jones BH (2015) Subsurface seeding of surface harmful algal blooms observed through the integration of autonomous gliders, moored environmental sample processors, and satellite remote sensing in southern California. Limnology and Oceanography **60**:754-764. doi:10.1002/lno.10082

Sikes EL, O'Leary T, Nodder SD, Volkman JK (2005) Alkenone temperature records and biomarker flux at the subtropical front on the Chatham Rise, SW Pacific Ocean. Deep Sea Research Part I: Oceanographic Research Papers **52**:721-748.

Stroynowski Z, Ravelo AC, Andreasen D (2015) A Pliocene to recent history of the Bering Sea at Site U1340A, IODP Expedition 323. Paleoceanography **30**:1641-1656. doi:10.1002/2015PA002866

Ternois Y, Sicre M-A, Boireau A, Beaufort L, Miquel J-C, Jeandel C (1998) Hydrocarbons, sterols and alkenones in sinking particles in the Indian Ocean sector of the Southern Ocean. Organic Geochemistry **28**:489-501.

Tomas CR (1997) Identifying marine phytoplankton. Academic press, San Diego.

Tréguer P, Bowler C, Moriceau B, Dutkiewicz S, Gehlen M, Aumont O, Bittner L, Dugdale R, Finkel Z, Iudicone D, Jahn O, Guidi L, Lasbleiz M, Leblanc K, Levy M, Pondaven P (2018) Influence of diatom diversity on the ocean biological carbon pump. Nature Geoscience **11**:27-37. doi:10.1038/s41561-017-0028-x

Volk T, Hoffert MI (1985) Ocean carbon pumps: Analysis of relative strengths and efficiencies in ocean-driven atmospheric CO_2 changes. In: E. Sundquist and W. Broecker (eds) The Carbon Cycle and Atmospheric CO: Natural Variations Archean to Present, American Geophysical Union, Washington DC.

Appendix One

Appendix of diatom occurrence and plates
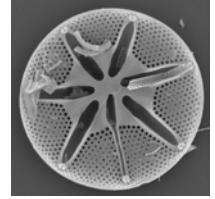
During the diatom counts undertaken for each sediment trap record, more than 80 diatom taxonomic groups were identified (mainly to species or subspecies level). In this appendix, the occurrence of each of these species at the three sediment traps is listed, along with light microscopy and/or scanning electron microscopy plates where possible.

Table A1. List of diatom taxa observed in this thesis with authority, presence in each trap (indicated with asterisk), and plate (if applicable).

Species	Authority	Present in 47°S	NCR	SCR	Plate
Actinocyclus curvulatus	Janisch, 1874	*			1.1
Actinocyclus spp.	C.G. Ehrenberg, 1837	*	*	*	1.2-1.3
Achtinoptichus senarius	(Ehrenberg) Ehrenberg, 1843		*	*	1.4
Achtinoptichus spp.	(Ehrenberg) Ehrenberg, 1844		*	*	1.5
Asteromphalus parvulus	Karsten, 1905	*	*	*	2.1
Asteromphalus hookeri	C.G. Ehrenberg, 1844	*			2.2-2.4
Azpeitia tabularis	(Grunow) G.Fryxell & P.A.Sims, 1986	*	*	*	2.5-2.6
Azpeitia spp.	M. Peragallo in J. Tempère & H. Peragallo, 1912	*	*	*	n/a
Bacteriastrum c.f. *deliculatum*	G. Shadbolt, 1854		*	*	3.1
Chaetoceros c.f. *peruvianus*	Brightwell, 1856	*			n/a
Chaetoceros Hyalochaete taxa	C.G. Ehrenberg, 1844		*		3.2
Chaetoceros Phaeoceros taxa	C.G. Ehrenberg, 1844		*	*	3.3
Chaetoceros resting spore	C.G. Ehrenberg, 1844	*		*	3.4-3.6
Cocconeis spp.	C.G. Ehrenberg, 1837	*			3.7-3.8
Corethron cryophilum	Castracane, 1886	*	*		4.1
Coscinodiscus spp.	C.G. Ehrenberg, 1839		*		4.2-4.3
Cyclotella stelligera	Cleve & Grunow, 1882		*		4.4
Dactyliosolen antarcticus	Castracane, 1886	*		*	4.5
Delphineis minutissima	(Hustedt) Simonsen, 1987		*	*	5.1
Delphineis spp.	G.W. Andrews, 1977		*		5.2
Diploneis bombus	(Ehrenberg) Ehrenberg, 1853		*	*	5.3
Diploneis stigmosa	Heiden & Kolbe, 1928	*			5.4
Ditylum brightwellii	(T. West) Grunow, 1885		*		5.5
Eucampia antarctica	(Castracane) Mangin, 1915	*			5.6
Fragilariopsis doliolus	(Wallich) Medlin & P.A. Sims, 1993	*	*		5.7-5.8
Fragilariopsis kerguelensis	(O'Meara) Hustedt, 1952	*	*	*	6.1
Fragilariopsis pseudonana	(Hasle) Hasle, 1993	*			n/a
Fragilariopsis rhombica	(O'Meara) Hustedt, 1952	*	*	*	6.2-6.3
Fragilariopsis ritscherii	Hustedt, 1958	*			6.4
Fragilariopsis separanda	Hustedt, 1958		*		n/a
Hemidiscus cuneiformis	Wallich, 1860	*	*	*	6.5
Lauderia annulata	Cleve, 1873		*		7.1
Melosira spp.	C.A. Agardh, 1824	*	*	*	7.2

Navicula directa	(W.Smith) Ralfs, 1861		*	*	7.3
Navicula spp.	J.B.M. Bory de Saint-Vincent, 1822	*	*	*	7.4
Nitzschia bicapitata	Cleve, 1901	*	*	*	7.5-7.6
Nitzschia braarudii	G.R. Hasle, 1960	*	*	*	7.7-7.8
Nitzschia kolaczekii	Grunow, 1867	*	*	*	8.1-8.2
Nitzschia longissima	(Brébisson) Ralfs, 1861		*		n/a
Nitzschia sicula	(Castracane) Hustedt	*	*	*	8.3
Odontella c.f. aurita	C.A. Agardh, 1832		*		8.4
Odontella mobilensis	(J. W. Bailey) Grunow, 1884		*	*	8.5
Pleurosigma sp.	W. Smith, 1852		*		9.1
Porosira glacialis	(Grunow) Jörgensen, 1905	*			n/a
Psammodictyon panduriforme	(W.Gregory) D.G. Mann, 1990	*	*	*	9.2
Pseudonitzschia c.f. australis	H. Peragallo in H. Peragallo & M. Peragallo, 1900		*		9.3
Pseudonitzschia c.f. pungens	H. Peragallo in H. Peragallo & M. Peragallo, 1900		*		9.4
Pseudo-nitzschia spp.	H. Peragallo in H. Peragallo & M. Peragallo, 1900	*	*	*	9.5
Pseudo-nitzschia prolongatoides	(G.R.Hasle) G.R. Hasle, 1993	*			n/a
Rhizosolenia antennata	(Ehrenberg) N.E. Brown, 1920	*	*	*	10.1
Rhizosolenia bergonii	H. Peragallo, 1892	*			10.2
Rhizosolenia setigera	Brightwell, 1858		*		10.3
Roperia tessalata	(Roper) Grunow ex Pelletan, 1889	*	*	*	10.4
Shionodiscus frenguellii group	(Kozlova) A.J. Alverson, S.H. Kang & E.C. Theriot, 2006	*	*	*	10.5
Shionodiscus gracilis var. *expectus*	(Karsten) A.J. Alverson, S.H. Kang & E.C. Theriot, 2006	*		*	10.6
Shionodiscus gracilis var. *gracilis*	(Karsten) A.J. Alverson, S.H. Kang & E.C. Theriot, 2007	*	*	*	10.7-10.8
Shionodiscus oestrupii var. *oestrupii*	(G. Fryxell & Hasle) A.J. Alverson, S.H. Kang & E.C. Theriot, 2006	*	*	*	11.1
Shionodiscus oestrupii var. *venrickae*	(G. Fryxell & Hasle) A.J. Alverson, S.H. Kang & E.C. Theriot, 2006	*	*	*	11.2-11.3
Shionodiscus poroseriatus	(Ramsfjell) A.J. Alverson, S.H. Kang & E.C. Theriot, 2006	*	*	*	11.4
Shionodiscus trifultus	(G. Fryxell) A.J. Alverson, S.H. Kang & E.C. Theriot, 2006	*			11.5
Stellarima microtrias	(Ehrenberg) G.R. Hasle & P.A. Sims, 1986	*	*	*	11.6
Stellarima stellaris	(Roper) G.R. Hasle & P.A. Sims, 1986	*			11.7-11.8
Stephenopyxis orbicularis	Wood, Crosby & Cassie, 1959		*	*	12.1
Thalassionema nitzschioides var. *capitulata*	(Castracane) Moreno-Ruiz in Moreno-Ruiz & Licea, 1995	*			n/a

Species	Authority				Figure
Thalassionema nitzschioides var. *lanceolata*	(Grunow in Van Heurck) Peragallo & Peragallo, 1901	*	*	*	12.2-12.3
Thalassionema nitzschioides var. *nitzschioides*	(Grunow) Mereschkowsky, 1902	*	*	*	12.4
Thalassionema nitzschioides var. *parva*	Heiden & Kolbe, 1928	*	*		n/a
Thalassiosira c.f. *aestivalis*	P.T. Cleve, 1873 emend. Hasle, 1973		*		12.5-12.6
Thalassiosira decipiens	(Grunow) E.G. Jørgensen, 1905		*	*	12.7
Thalassiosira eccentrica	(Ehrenberg) Cleve, 1904	*	*	*	12.8
Thalassiosira ferelineata	Hasle & G.A. Fryxell, 1977	*	*	*	13.1
Thalassiosira c.f. *gravida*	P.T. Cleve, 1896			*	13.2
Thalassiosira lentiginosa	(Janisch) Fryxell, 1977	*		*	13.3-13.4
Thalassiosira lineata	Jousé, 1968	*	*	*	13.5-13.6
Thalassiosira maculata	G.A. Fryxell & J.R.Johansen, 1985	*	*	*	13.7-13.8
Thalassiosira c.f. *punctigera*	P.T. Cleve, 1873 emend. Hasle, 1973		*		14.1
Thalassiosira rotula	Meunier, 1910		*		n/a
Thalassiosira symmetrica	G.A. Fryxell & Hasle, 1973	*	*	*	14.2-14.3
Thalassiosira tumida	(Janisch) Hasle, 1971	*			15.1
Thalassiothrix antarctica	A. Schimper ex G.Karsten, 1905	*	*	*	15.2-15.3
Trachyneis aspera	(Ehrenberg) Cleve, 1894		*		15.4-15.5
Trichotoxon c.f. spp.	F.M. Reid & F.E. Round, 1988				n/a
Trigonium alternans	(Bailey) A. Mann, 1907		*		15.6

Plate 1

Plate 2

Plate 3

Plate 4

4.1

50 μm

Jessica Wilks

4.2

4.3

Creation from Unicel
with Helicon Focus software
(www.heliconsoft.com)

4.4

4.5

20 μm
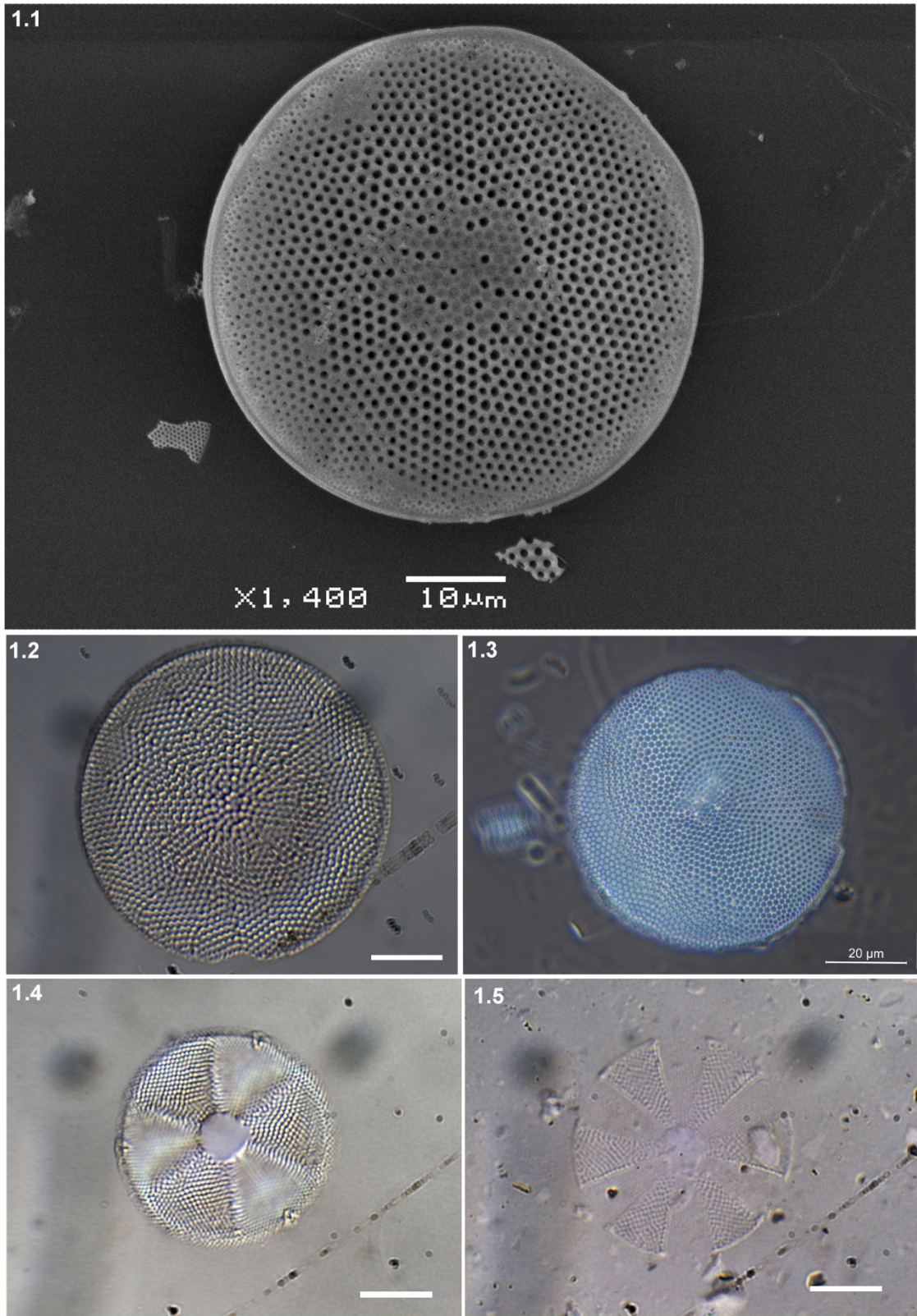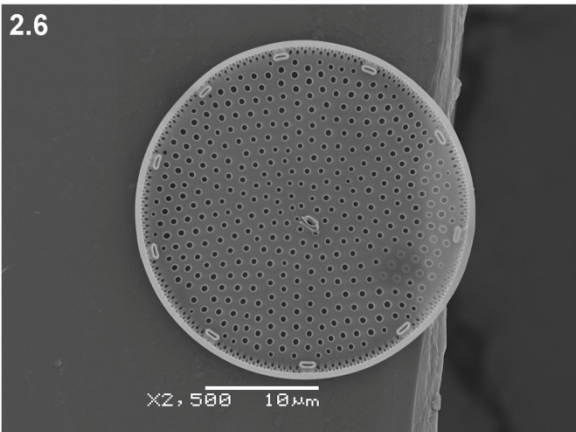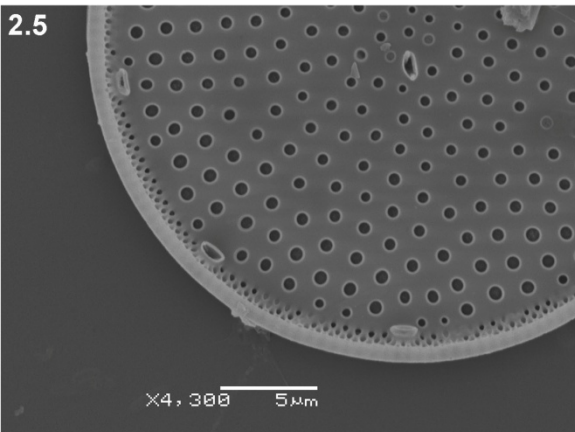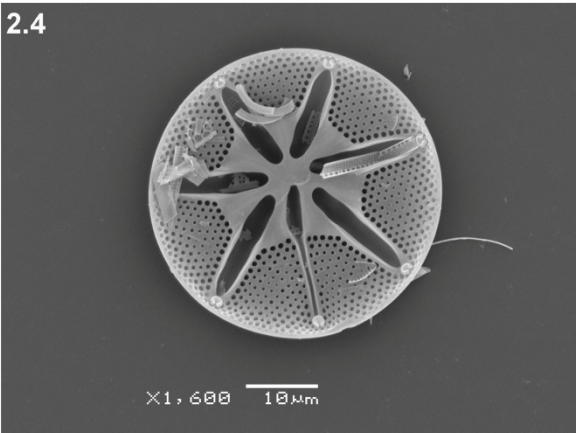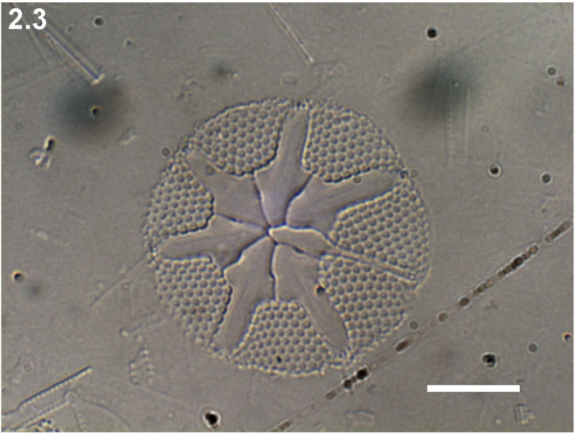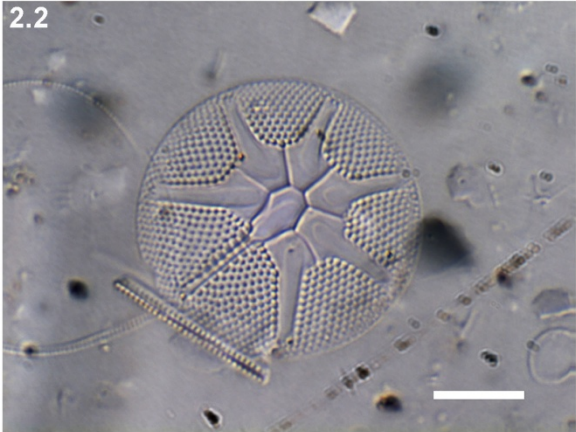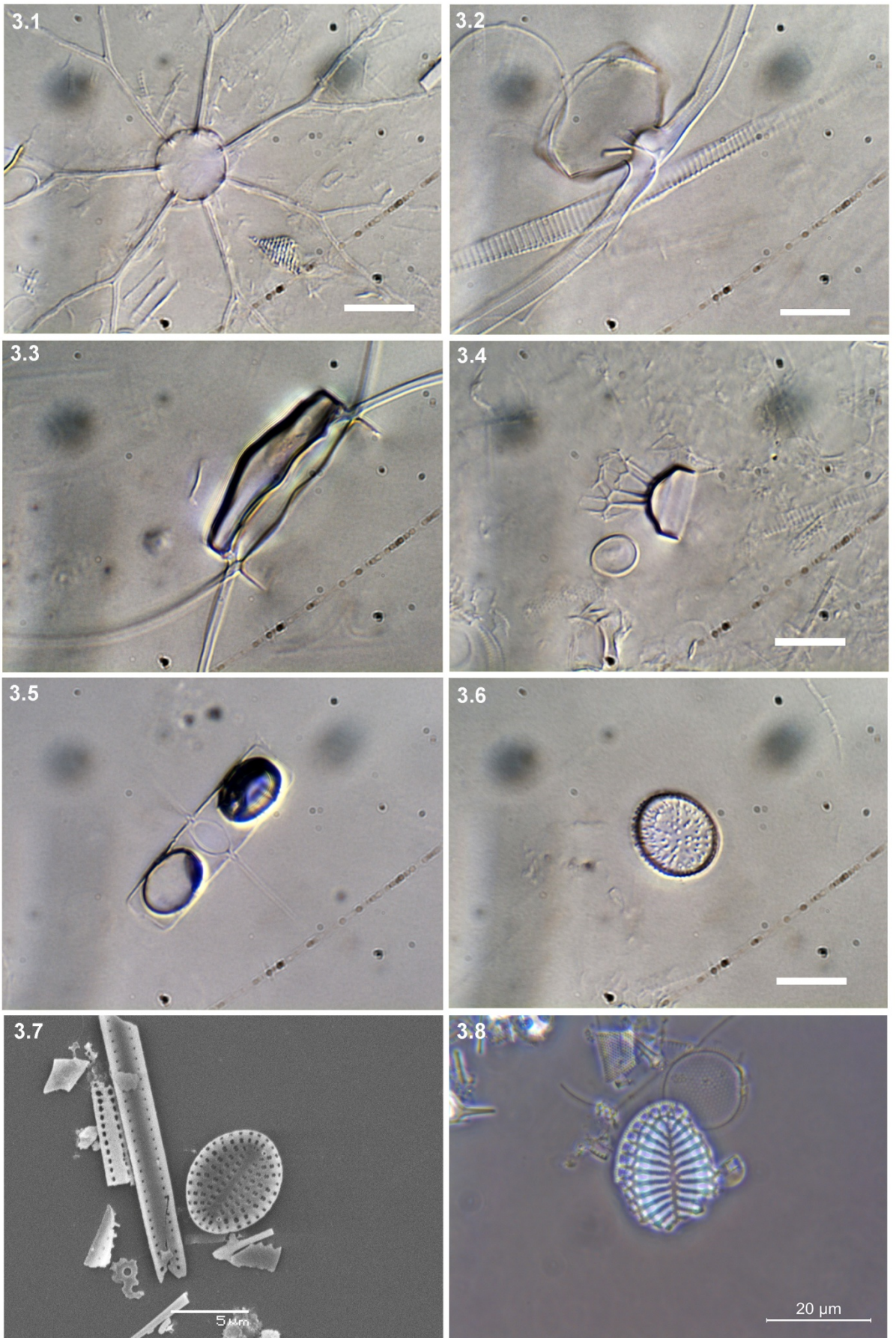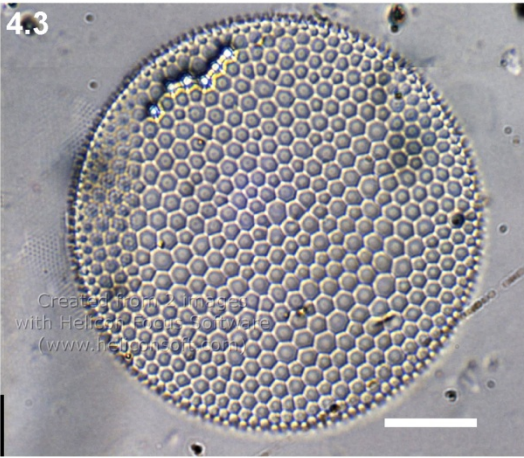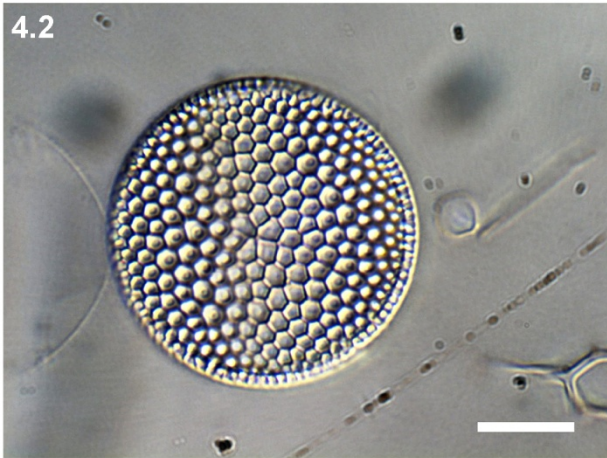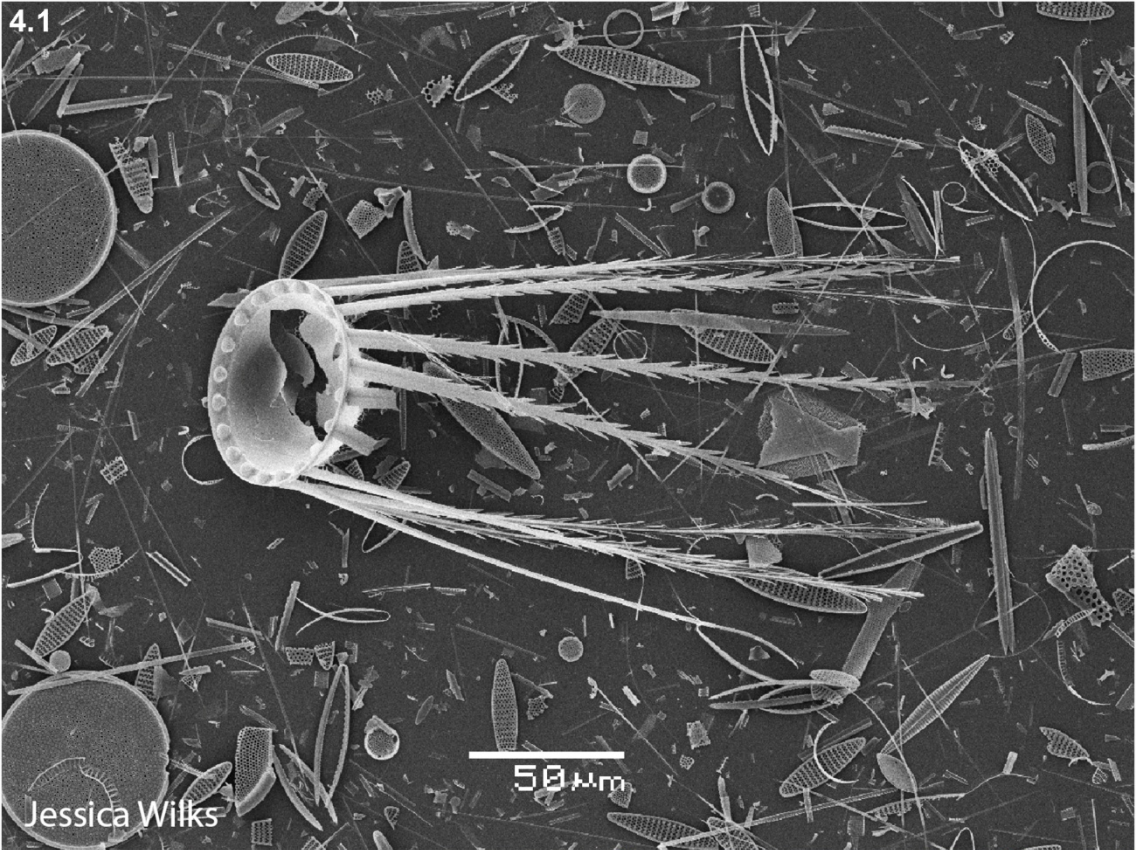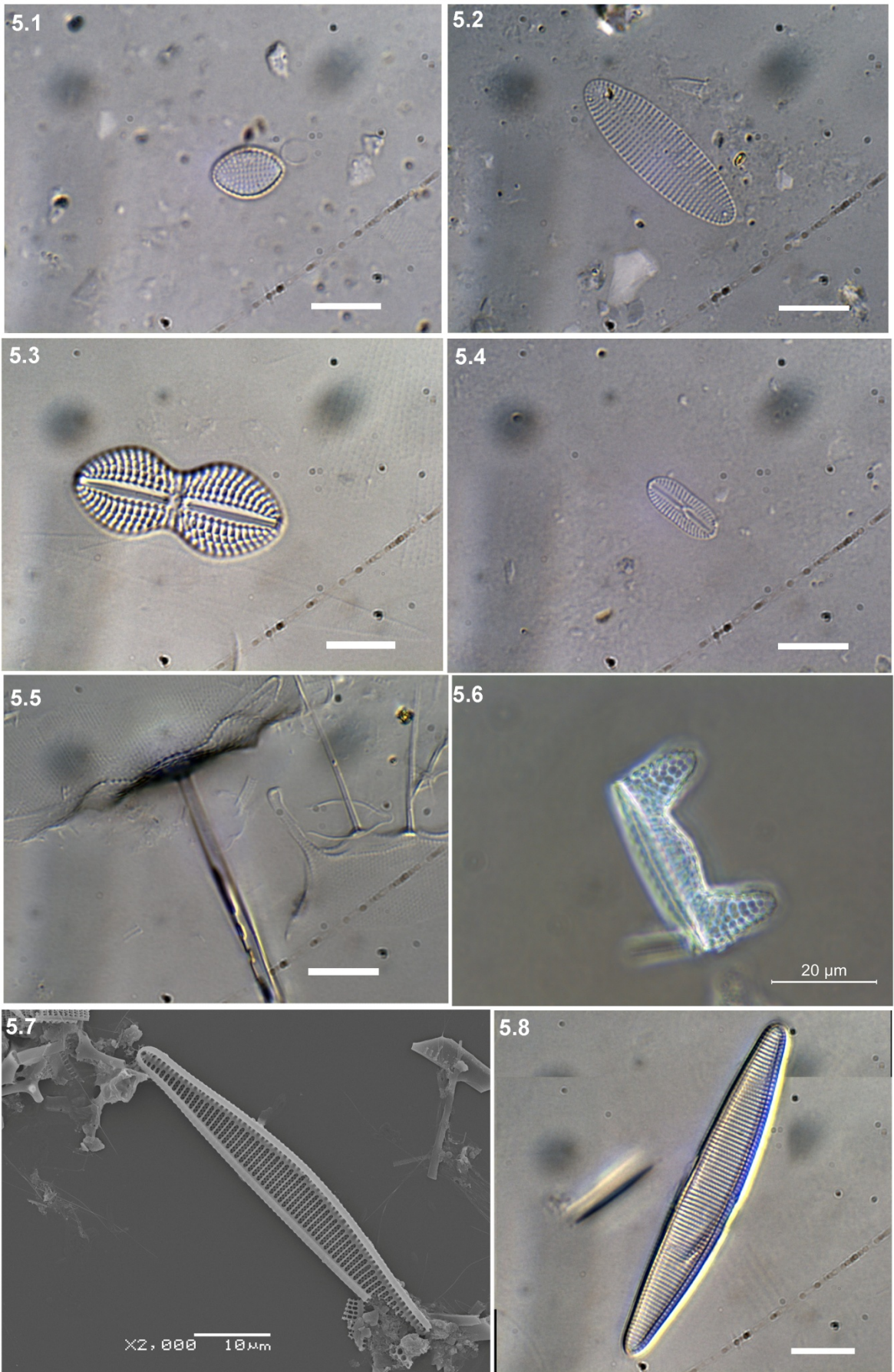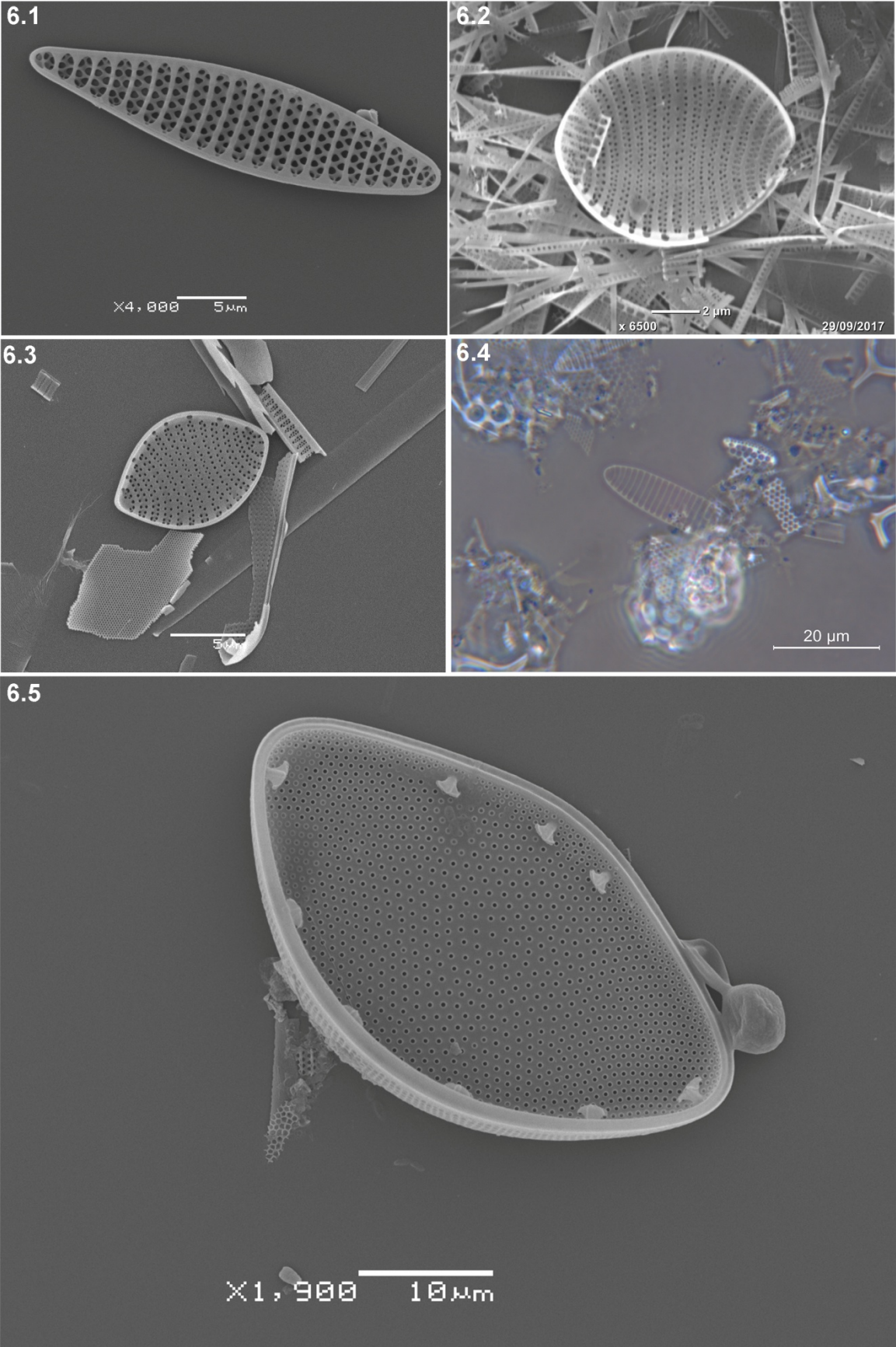
Plate 5
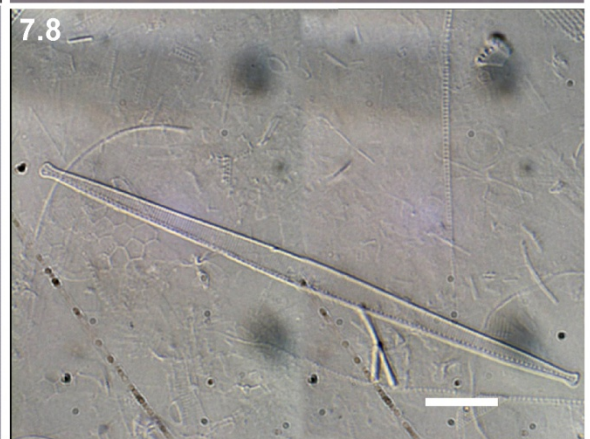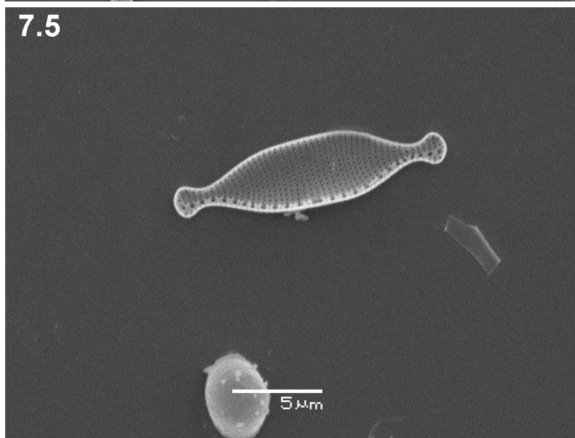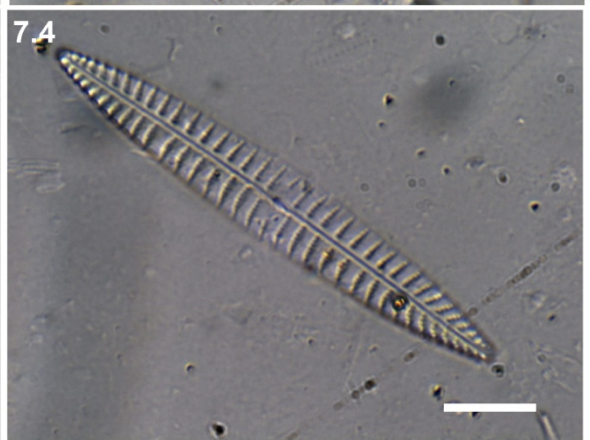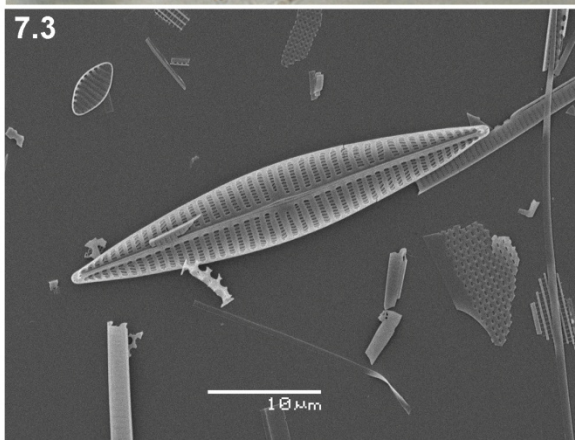
Plate 6

Plate 7

Plate 8
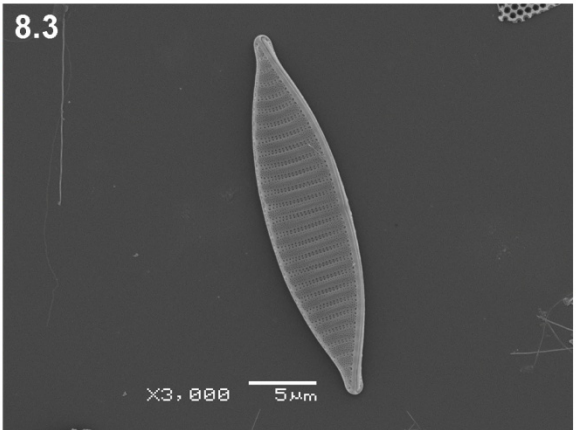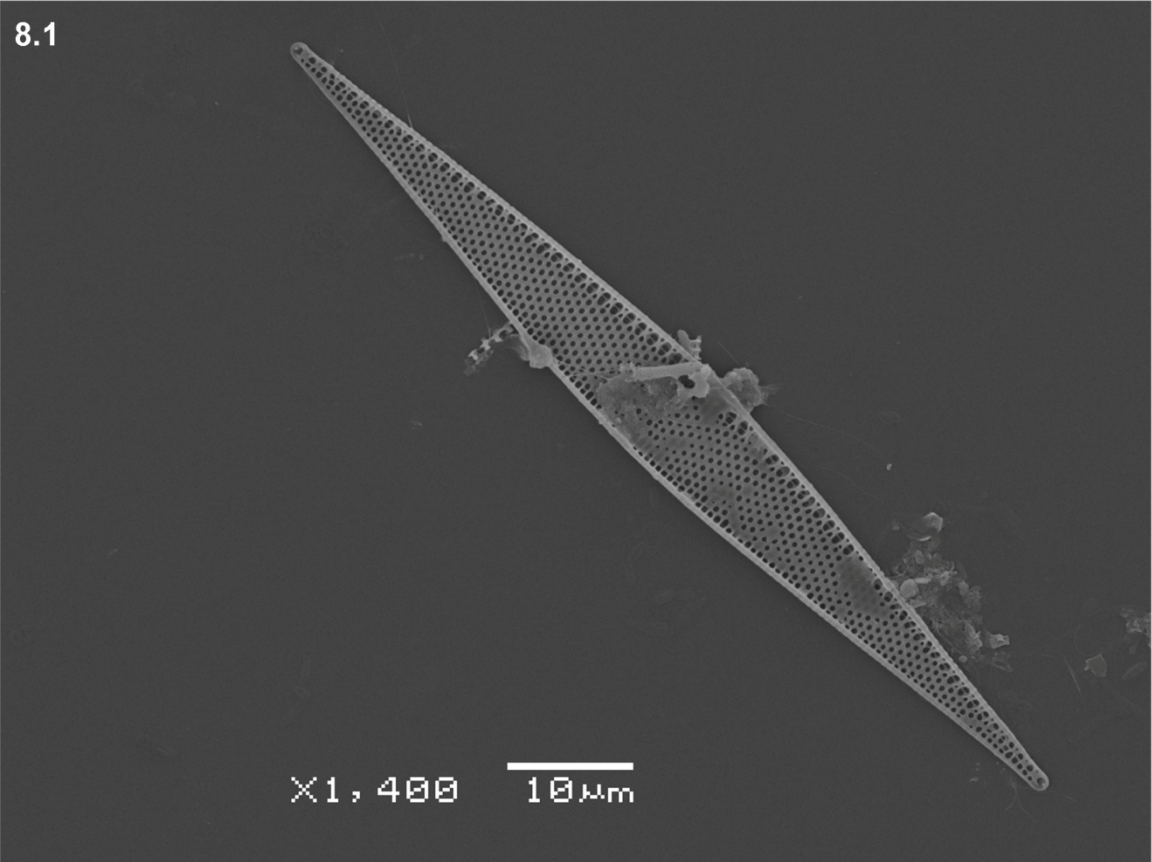
Plate 9
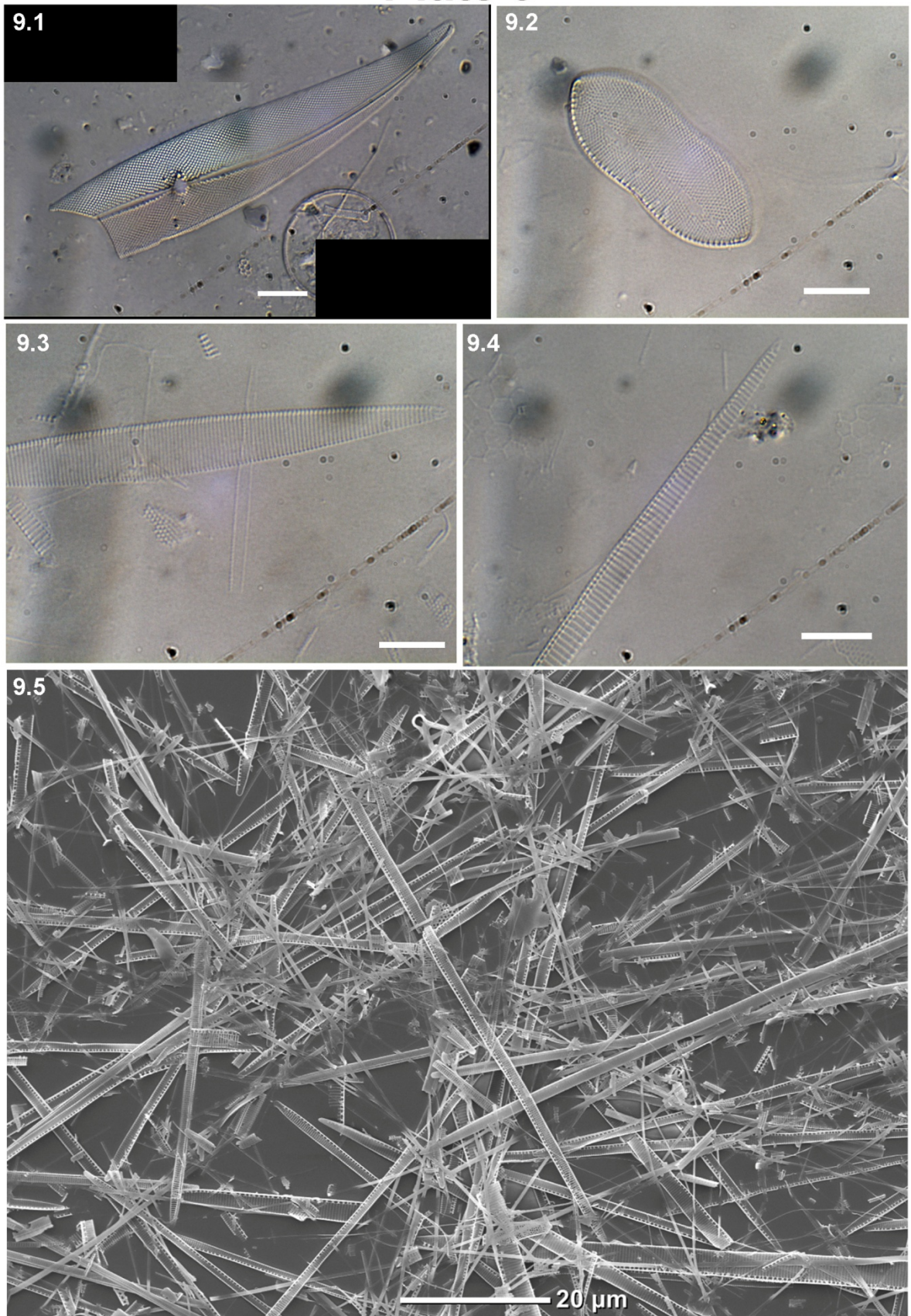
Plate 10
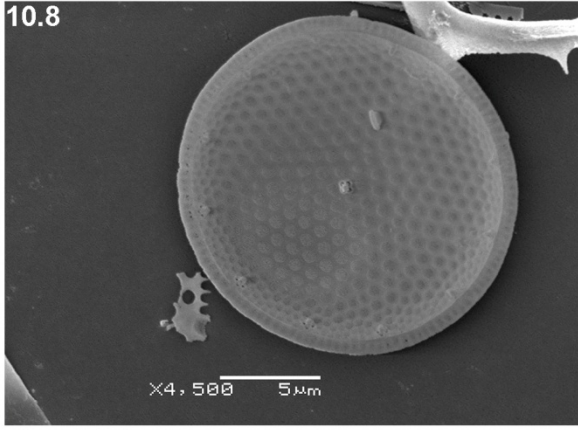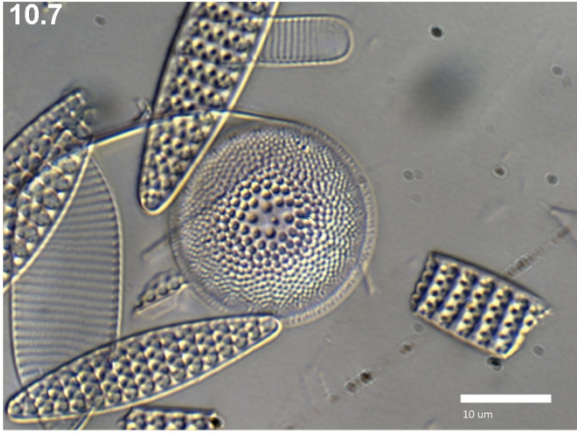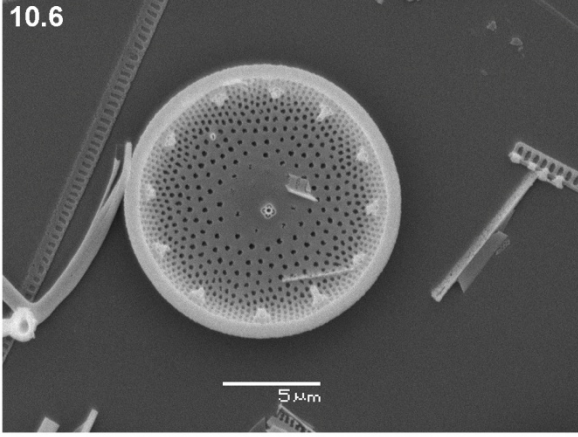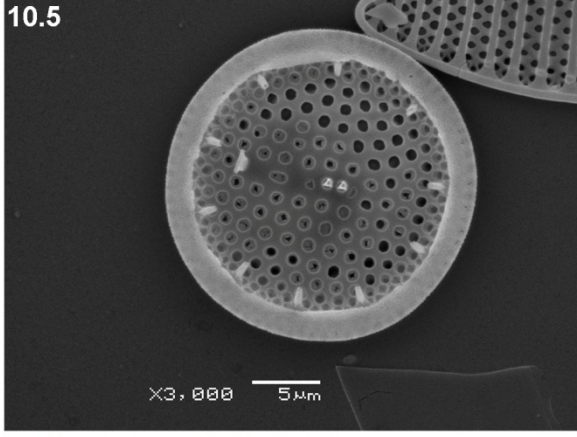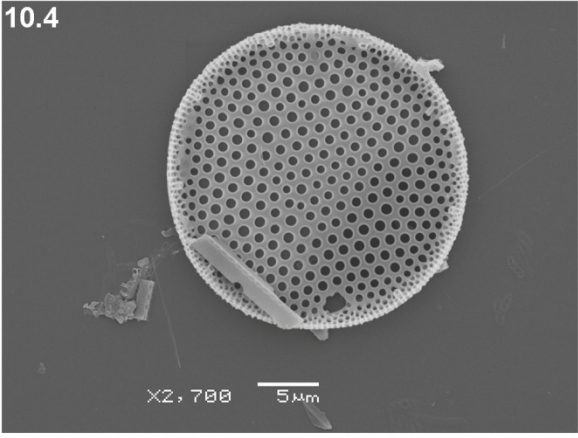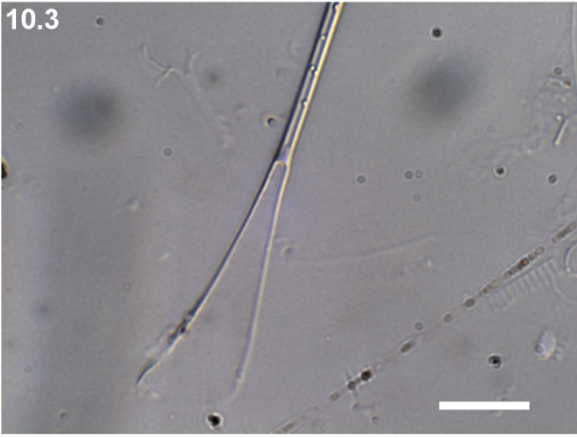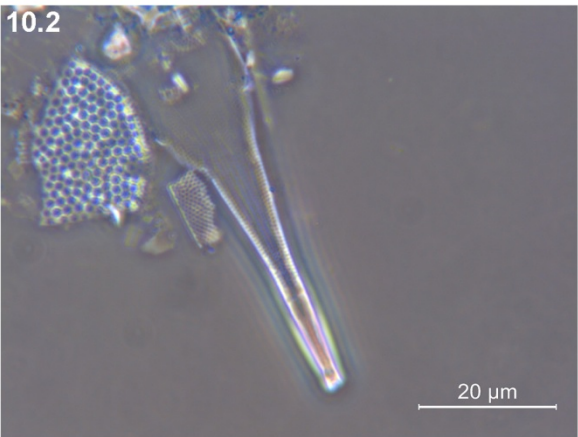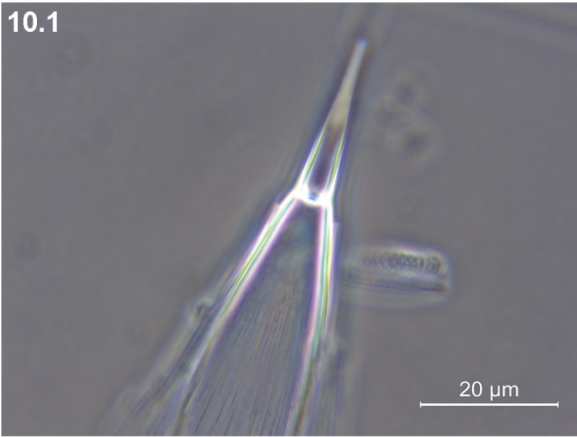
Plate 11

Plate 12

Plate 13

13.1

13.2

13.3

13.4

13.5

13.6

13.7

13.8

Plate 14

14.1

14.2

X3,000 5μm

14.3

20 μm

Plate 15

15.1 20 µm

15.2 X3,300 5 µm

**15.3** X7,500 2 µm

15.4

15.5 20 µm

15.6
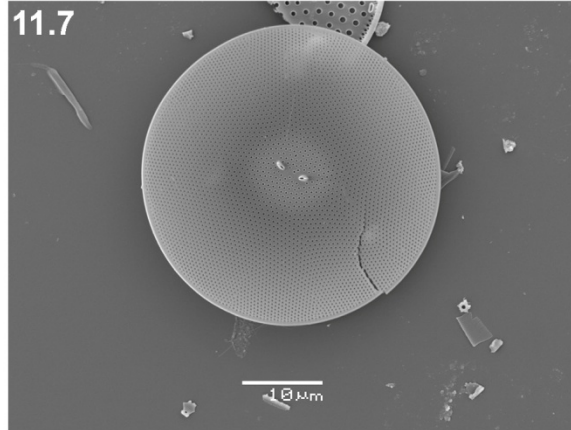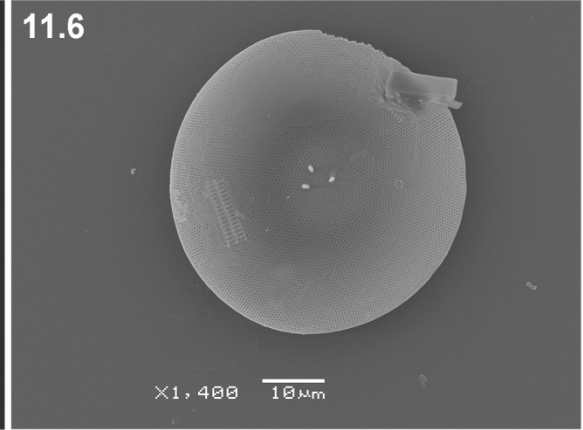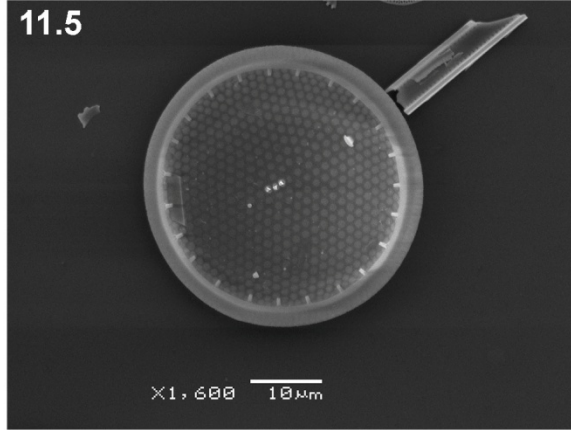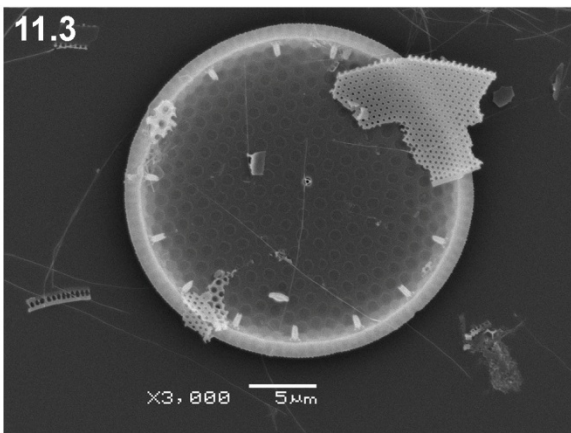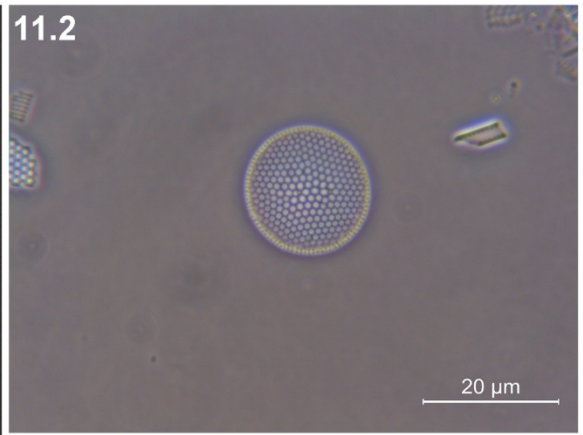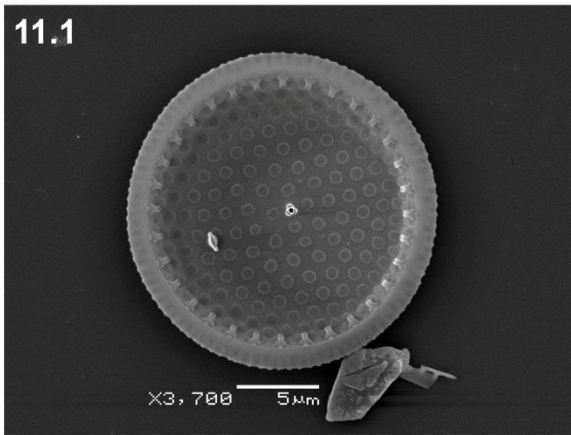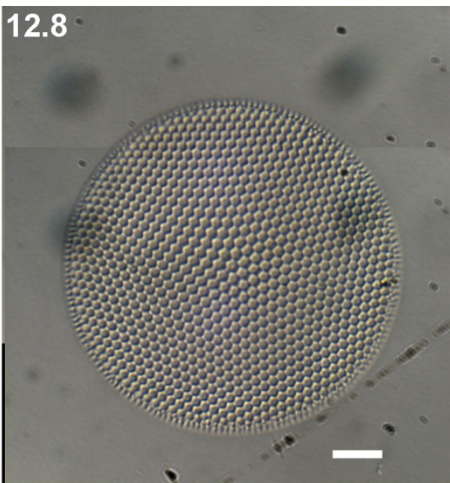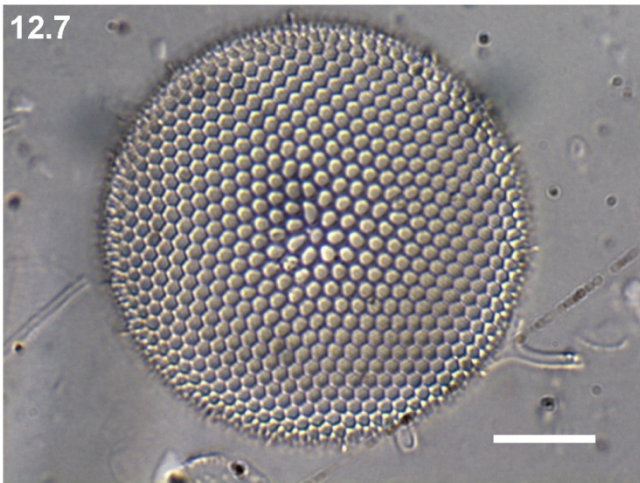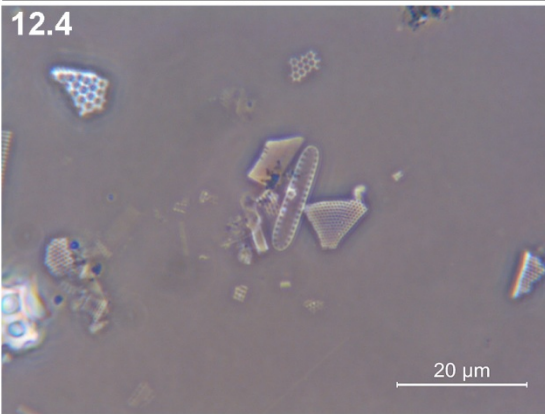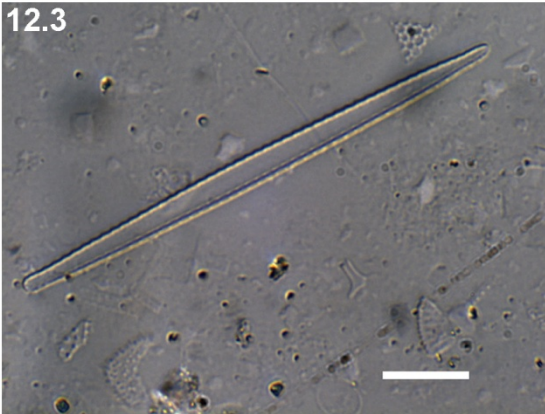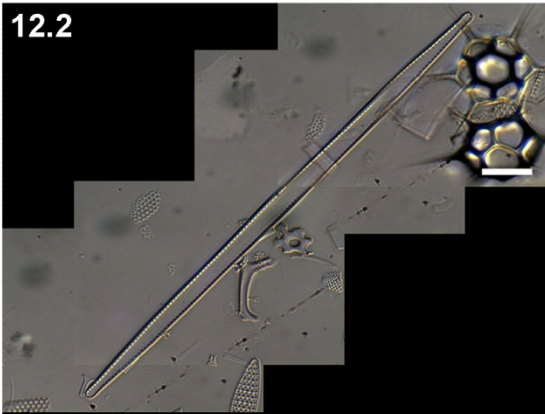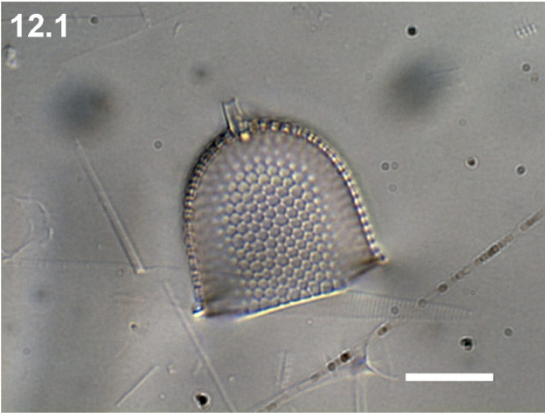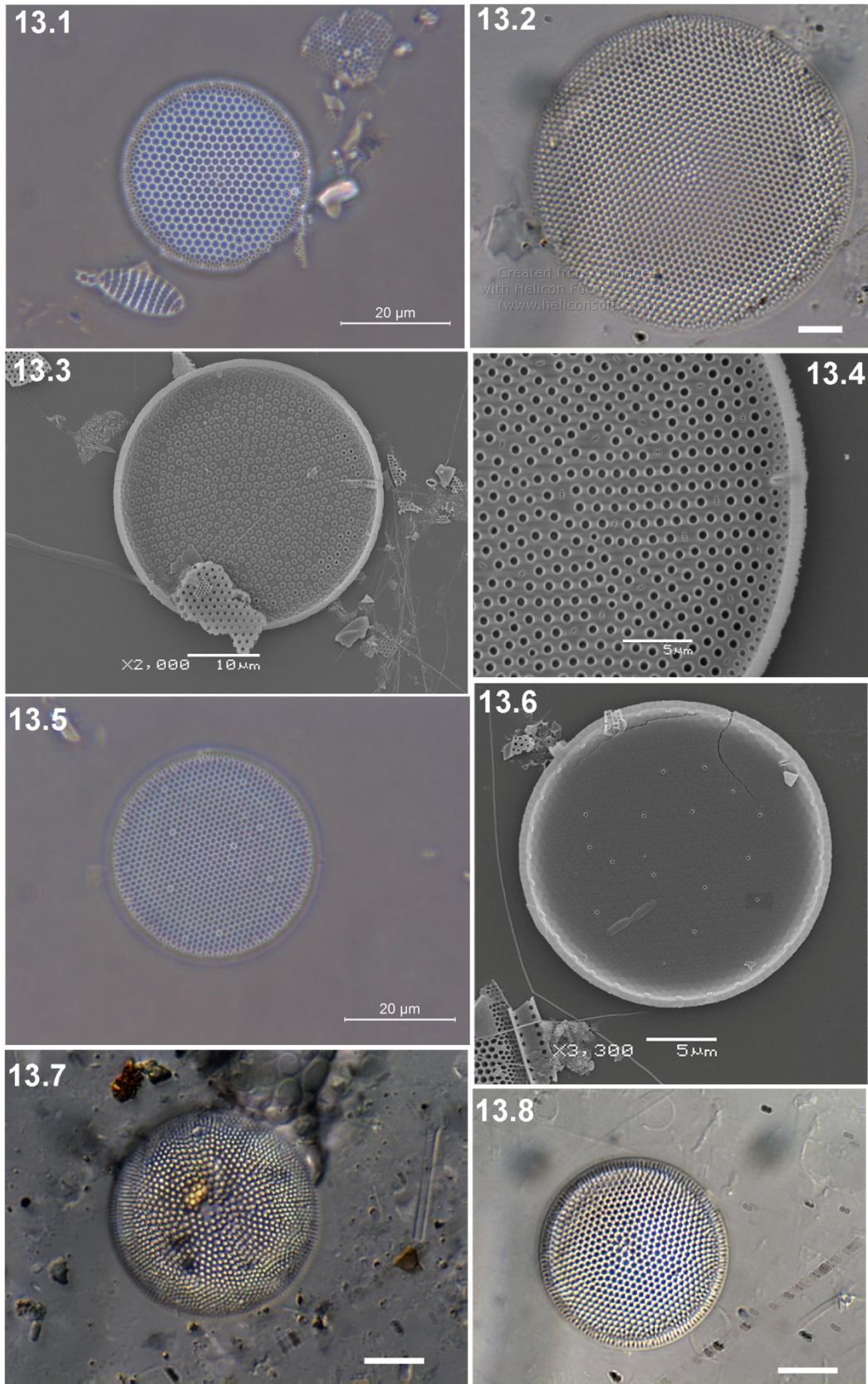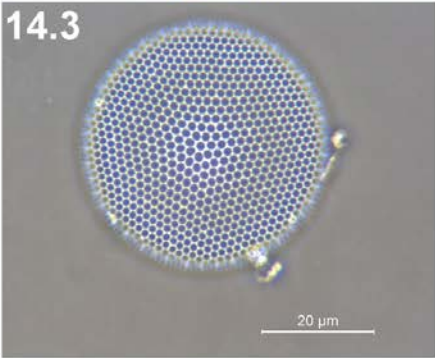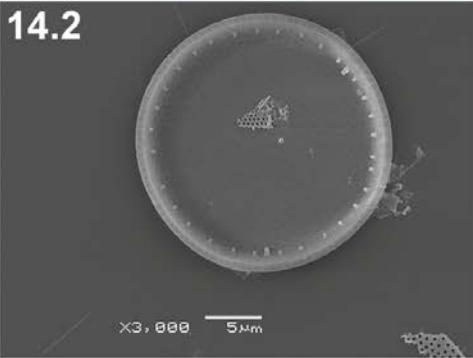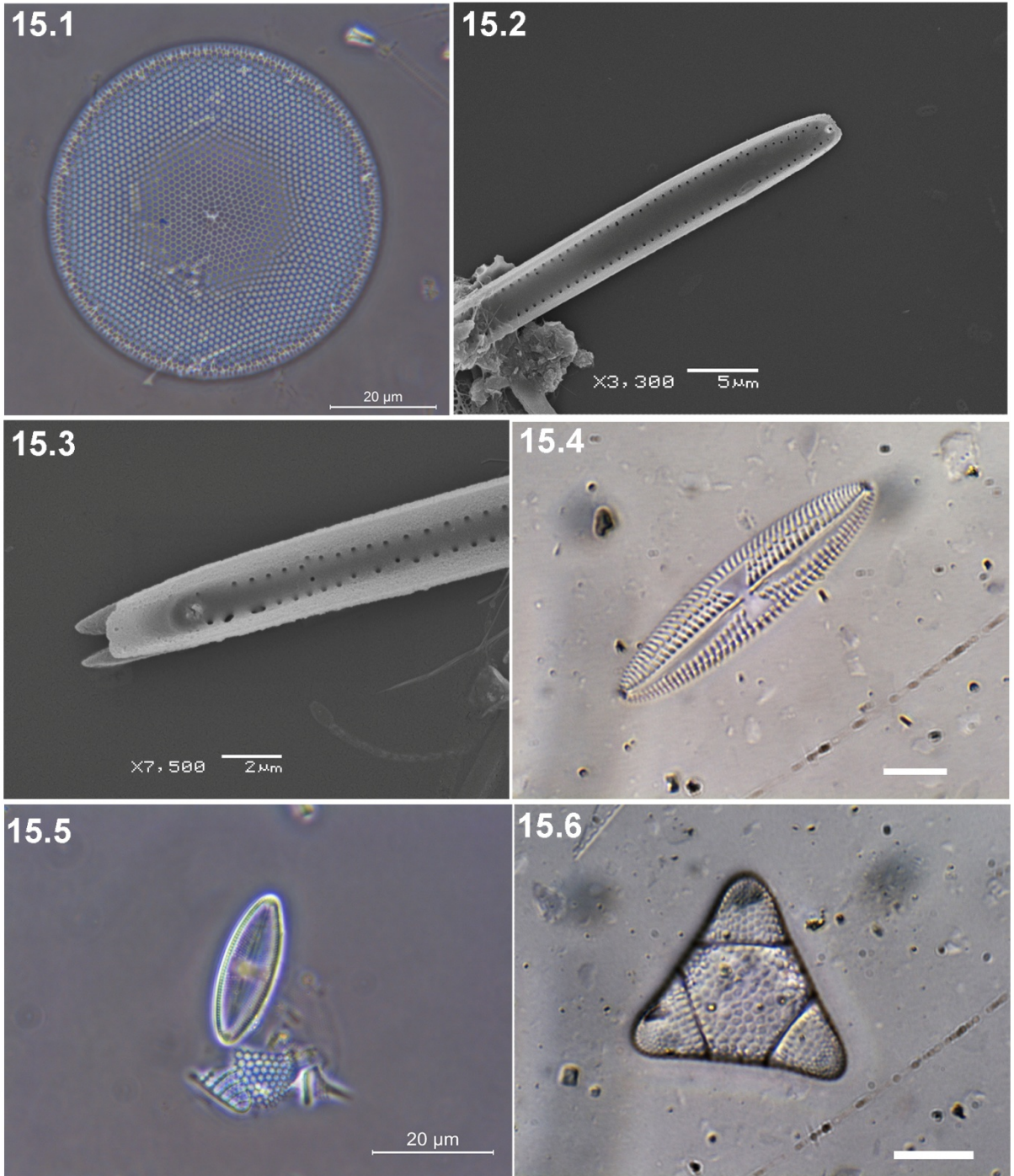
"Diatoms really are the grasses of the sea!"

Gustaaf Hallegraeff